

2012

## Investigating the impact of CD147 and its expression on neurodegeneration and Alzheimer's disease (AD)

Limbikani J. Kanyenda  
*Edith Cowan University*

Follow this and additional works at: <https://ro.ecu.edu.au/theses>



Part of the [Medical Pathology Commons](#), [Nervous System Diseases Commons](#), and the [Neurology Commons](#)

---

### Recommended Citation

Kanyenda, L. J. (2012). *Investigating the impact of CD147 and its expression on neurodegeneration and Alzheimer's disease (AD)*. Edith Cowan University. Retrieved from <https://ro.ecu.edu.au/theses/499>

This Thesis is posted at Research Online.  
<https://ro.ecu.edu.au/theses/499>

# Edith Cowan University

## Copyright Warning

You may print or download ONE copy of this document for the purpose of your own research or study.

The University does not authorize you to copy, communicate or otherwise make available electronically to any other person any copyright material contained on this site.

You are reminded of the following:

- Copyright owners are entitled to take legal action against persons who infringe their copyright.
- A reproduction of material that is protected by copyright may be a copyright infringement. Where the reproduction of such material is done without attribution of authorship, with false attribution of authorship or the authorship is treated in a derogatory manner, this may be a breach of the author's moral rights contained in Part IX of the Copyright Act 1968 (Cth).
- Courts have the power to impose a wide range of civil and criminal sanctions for infringement of copyright, infringement of moral rights and other offences under the Copyright Act 1968 (Cth). Higher penalties may apply, and higher damages may be awarded, for offences and infringements involving the conversion of material into digital or electronic form.

**Investigating the impact of CD147 and its expression on  
neurodegeneration and Alzheimer's disease AD**

**Limbikani Jetex Thangato Kanyenda  
Dip.MLT; B.Sc.; M.Sc. Human Biology**

**This thesis is presented in fulfilment of the requirements for  
the degree of Doctor of Philosophy - Human Biology**

**Faculty of Computing Health and Science; School of Medical  
Sciences**

**Edith Cowan University**

**Student Number: 2025800**

**May 2012**

## USE OF THESIS

The Use of Thesis statement is not included in this version of the thesis.

## ABSTRACT

CD147, also known as basigin, extracellular matrix metalloproteinase inducer, neurothelin, tumour cell-derived collagenase stimulatory factor, M6, HT7, OX47 or gp42, is a transmembrane glycoprotein of the immunoglobulin super-family. It is expressed in many neuronal and non-neuronal tissues with high expression in the hippocampus, pre-frontal cortex, thyroid, heart, early erythroid, amygdala and placenta. This protein is involved in various cellular and biological functions such as lymphocyte migration and maturation, tissue repair, cancer progression, T and B lymphocyte activation and induction of extracellular matrix metalloproteinase. The CD147 protein interacts with cyclophilin A, cyclophilin B, sterol carrier protein, caveolin-1 and integrins, and can influence beta amyloid peptide levels, a protein that is central to Alzheimer's disease pathology.

Mechanisms through which CD147 regulates beta amyloid levels still remain unclear, thus the current study investigated the impact of high cholesterol and beta amyloid 42 loading on CD147 expression in rat primary cortical neuronal cultures. Its expression in human brain tissue from Alzheimer's disease and non-Alzheimer's disease dementias and APPswe transgenic mice fed on a high fat/high cholesterol diet were also determined. CD147 over expression experiments in rat primary cortical neuronal and SH-SY5Y cultures using recombinant adenoviruses (AdRSV-CD147 and AdRSV-Empty) in the presence and/or absence of cyclophilin A were employed to determine level of protection against oxidative stress and toxicity. Finally sequencing of the CD147 promoter region (-392 to -242 nucleotides) was performed to identify possible single nucleotide polymorphisms that may be linked to Alzheimer's disease pathology.

The *in vitro* experiments conducted in this study have shown that cholesterol and beta amyloid loading and oxidative stress result in increased CD147 expression in rat primary cortical neuronal cultures and that CD147 protects neuronal cultures from beta amyloid toxicity only in the presence of cylophilin A. However *in vivo* experiments in animal model have shown that a high fat/high cholesterol diet does not affect brain CD147 levels as evidenced by unchanged expression levels in APPswe mice.

Human studies have revealed a correlation between CD147 and  $\gamma$ -secretase complex components (nicastrin and presenilin 1) in the hippocampus. However, there is no difference in CD147 protein expression between hippocampus and frontal cortex from Alzheimer's disease patients. Sequencing of the CD147 promoter region, where sterol carrier protein binds to initiate CD147 transcription, has identified two novel single nucleotide polymorphisms (-61A>G and 37C>G). However, single nucleotide polymorphisms within this region are not associated with Alzheimer's disease pathology.

## **ABBREVIATIONS**

A $\beta$	Amyloid beta peptide
AD	Alzheimer's disease
ADAM	A disintegrin and a metalloproteinase
ANOVA	Analysis of variance
APH1	Anterior pharynx defective homolog-1
<i>APOE</i>	Apolipoprotein E (gene)
ApoE	Apolipoprotein E (protein)
APS	Ammonium persulphate
APP	Amyloid precursor protein
APP-CTF	Amyloid precursor protein C-terminal fragment
APH	Anterior pharynx defective
ARC	Animal resources centre
3 $\beta$ -HSD	3 $\beta$ -hydroxysteroid dehydrogenase
$\beta$ -CTF	$\beta$ C-terminal fragment
BACE	Beta amyloid cleaving enzyme
BBB	Blood-brain barrier
CA1	Corn ammonis 1
CAA	Congophilic amyloid angiopathy
CyPA	Cyclophilin A
CyPB	Cyclophilin B
°C	Degrees Celsius
CSF	Cerebrospinal fluid
CNS	Central nervous system
CT	Computed tomography

CTF	C-terminal fragment
DDW	Double de-ionised water
df	Degrees of freedom
DHEA	Dehydroepiandrosterone
DMEM	Dulbecco's modified Eagles medium
DFCS	Dialysed foetal calf serum
DMSO	Dimethyl sulphoxide
DNA	Deoxyribose Nucleic Acid
DTT	Dithiotreitol
ECL	Enhanced chemiluminescence
EDTA	Ethylenediamine tetra-acetic acid
ELISA	Enzyme-linked immunosorbent assay
EMSA	Electrophoretic mobility shift assay
EMMPRIN	Extracellular Matrix Metalloproteinase-Inducer
EOAD	Early-onset Alzheimer's disease
ERK1/2	Extracellular-regulated kinase 1/2
FAD	Familial Alzheimer's disease
FCS	Foetal calf serum
FL-APP	Full length amyloid precursor protein
HBSS	Hanks balanced salt solution
HDL	High density lipoprotein
HRP	Horse radish peroxide
Ig	Immunoglobulin
IgSF	Immunoglobulin super-family
IMAC	immobilized metal ion affinity chromatography
KDa	Kilo Dalton
KPI	Kunitz protease inhibitor



LDH	Lactate dehydrogenase
LDL	Low density lipoprotein
LOAD	Late-onset Alzheimer's disease
LRP	Low density lipoprotein receptor related protein
MAPK	mitogen-activated protein kinase
MCI	Mild cognitive impairment
MCT	Monocarboxylate transporter
MLR	Multiple linear regression
MMP	Matrix metalloproteinase
MMSE	Mini-Mental State Examination
MRI	Magnetic resonance imaging
mRNA	Messenger ribonucleic acid
MRS	Magnetic resonance spectroscopy
MW	Molecular weight
NATs	Natural anti-sense transcripts
NCT	Nicestrin
NFT	Neurofibrillary tangles
NINCDS	National Institute of Neurological Disorders and Communitive Disorders and Stroke
NGF	Nerve growth factor
NP40	Ethylphenyl-polyethylene glycol
PBS	Phosphate buffered saline
PMSF	Pheynlmethyle-sulfonyl fluoride
PBST	Phosphate buffered saline with 0.05% Tween 20
PCR	Polymerase chain reaction
PEN-2	Presenilin enhancer 2
PET	Positron emission tomography

Pg	Pico gram
PHF	Paired helical filaments
PS1	Presenilin 1
PS2	Presenilin 2
RIP	Regulate intramembrane proteolysis
RNA	Ribonucleic acid
RNAi	Ribonucleic acid inhibition
ROS	Reactive oxygen species
RPM	Revolutions per minute
RT	Room temperature
SCP	Sterol carrier protein
SD	Standard deviation
SDS	Sodium dodecylsulfate
SE	Standard error
SEM	Standard error of mean
SLE	Systemic lupus erythematosus
SPE	Sperm integral membrane proteins
StAR	Steroidogenic acute regulatory protein
TACE	Tumour factor- $\alpha$ converting enzyme
TBS	Tris buffered saline
TBST	Tris buffered saline with 0.05% Tween 20
TCSF	Tumour cell-derived collagenase stimulatory factor
TEMED	N-Tetra-methylethylenediamine
TG	Triglycerides
TGF $\beta$	Transforming growth factor beta
TM	Transmembrane
TMB	Tetramethyl-benzidine

TMP	Transmembrane protein
Tween 20	Polyoxyethylene (20) sorbitan monolaurate
µg	Microgram
µM	Micromolar
V/V	Volume divided by volume
VEGF	Vascular endothelial growth factor
WFI	Water for injection
WHI	Women's Health Initiative

## LIST OF PUBLICATIONS

- Kanyenda L J, Verdile G, Boulos S, Krishnaswamy S, Taddie K, Meloni B, Mastaglia F, and Martins RN (2011). The Dynamics of CD147 in Alzheimer's disease (AD) development and pathology. *Journal of Alzheimer's disease*.
- Krishnaswamy S, Verdile G, Groth D, Kanyenda L J and Martins RN (2009). The structure and function of Alzheimer's gamma secretase enzyme complex. *Critical Reviews in Clinical Laboratory Sciences*.

## **LIST OF FIGURES**

Figure 1.1: Representation of *post-mortem* brain cross-section (A) healthy control and (B) AD patient.

Figure 1.2: Neurofibrillary tangles (NFT) and senile plaque (SP).

Figure 1.3: Congophilic amyloid angiopathy.

Figure 1.4: Amyloid Precursor Protein.

Figure 1.5: Proteolytic Processing of Amyloid Precursor Protein (APP).

Figure 1.6: Assembly of  $\gamma$ -secretase enzyme component to form the active enzyme.

Figure 1.7: Human CD147 protein.

Figure 1.8: The  $\gamma$ -secretase complex proteins.

Figure 3.1: Cholesterol increases CD147 expression in primary cortical neuronal cultures.

Figure 3.2: Cholesterol decreases FL-APP expression in primary cortical neuronal cultures.

Figure 3.3: Cholesterol treatment increases LDH release in primary neuronal cultures.

Figure 3.4: Hydrogen peroxide ( $H_2O_2$ ) treatment of rat primary neuronal cultures increases CD147 levels and LDH release.

Figure 3.5: A $\beta$ 42 treatment of rat primary neuronal cultures increased LDH release

Figure 3.6: Differential CD147 expression in neuronal cultures following treatment with A $\beta$ 42 peptide.

Figure 3:7: Differential FL-APP expression in neuronal cultures following treatment with A $\beta$ 42 peptide.

Figure 3.8: Recombinant adenoviral transduction of neuronal cultures.

Figure 3.9: CD147, FL-APP and LDH levels in recombinant adenoviral transduced neuronal cultures.

Figure 3.10: Rat primary cortical neuronal cultures transduced with recombinant adenoviruses and exposed to A $\beta$ 42 in the presence and absence of CyPA.

Figure 3.11: A $\beta$ 42 toxicity in neuronal cultures transduced with recombinant adenoviruses

Figure 3.12: SH-SY5Y cultures transduced with recombinant adenoviruses

Fig. 3.13: A $\beta$ 42 Toxicity in SH-SY5Y human neuroblastoma cultures transduced with recombinant adenoviruses.

Figure.4.1: Allocation of APP<sup>swe</sup> mice into experimental groups.

Figure 4.2: Body weights of APP<sup>swe</sup> mice fed on a normal chow and high fat/high cholesterol diets.

Figure 4.3: Total plasma cholesterol levels in APP<sup>swe</sup> mice following 10 weeks feeding with experimental diets.

Figure 4.4: Immunodetection of CD147 using rodent EMMPRINE SC-9753 antibody.

Figure 4.5: Brain CD147 levels in brain tissue from APP<sup>swe</sup> mice following 10 weeks feeding with experimental diets.

Figure 4.6: CD147 levels in kidney tissue from APP<sup>swe</sup> mice following 10 weeks feeding with experimental diets.

Figure 4.7: CD147 levels in liver tissue from APP<sup>swe</sup> mice following 10 weeks feeding with experimental diets.

Figure 4.8: Amplification of SCP-2 mRNA by RT-PCR in brain tissue from APP<sup>swe</sup> mice fed the experimental diets.

Figure 4.9: SCP-2 mRNA levels in brain tissue from APP<sup>swe</sup> mice fed normal chow or high fat high cholesterol diets.

Figure 4.10: FL-APP levels in brain tissue homogenate from APP<sup>swe</sup> mice fed normal chow or high fat high cholesterol diets.

Figure 4.11 Brain APP-C99 levels in APP<sup>swe</sup> mice after 10 weeks.

Figure 4.12 Brain APP-C83 levels in APP<sup>swe</sup> mice after 10 weeks.

Figure 4.13: Brain A $\beta$ 42/40 ratio in APP<sup>swe</sup> mice fed on a high fat/high cholesterol diet compared to controls after 10 weeks.

Figure 4.14: Plasma A $\beta$ 42/40 ratios in APP<sup>swe</sup> mice fed on a high fat/high cholesterol diet compared to controls after 10 weeks.

Figure 5.1: Immunostaining for CD147 in melanoma, glioma and brain tissue.

Figure 5.2: CD147 immunostaining in the hippocampus from control, LBD, FTD and AD brain tissue.

Figure 5.3: Quantitation of CD147 immunostaining from hippocampus of control, LBD, FTD and AD cases.

Figure 5.4: CD147 immunostaining in the frontal cortex from control, LBD, FTD and AD brain tissue.

Figure 5.5: Quantitation of CD147 immunostaining from hippocampus of control, LBD, FTD and AD cases.

Figure 5.6: A comparison of CD147 expression in hippocampus and frontal cortex from control, LBD, FTD and AD cases.

Figure 5.7: CD147 levels in hippocampus and frontal cortex.

Figure 5.8: A $\beta$ 42 levels in hippocampus.

Figure 5.9: A $\beta$ 42 levels in frontal cortex.

Figure 5.10: Comparison of A $\beta$ 42 levels between hippocampus and frontal cortex.

Figure 5.11: Nicastrin levels in hippocampus and frontal cortex.

Figure 5.12: Presenilin 1/2 levels in hippocampus and frontal cortex.

Figure 5.13: PEN2 levels in hippocampus and frontal cortex.

Fig.6.1: The Schematic view of the 5'-Untranslated region of CD147.

Figure 6.2: Purified SCP-2 protein and electrophoretic mobility shift assay of SCP protein.

Figure 6.3: Sequence of the CD147 promoter region.

Figure 6.4: Slowdown PCR amplification of the CD147 promoter region.

Figure 6.5: Linkage disequilibrium for CD147 Single Nucleotide Polymorphisms in the AIBL cohort sample.

## **LIST OF TABLES**

**Table 1.1:** CD147 nomenclature.

Table 2.1: Commonly used chemicals.

Table 2.2: Preparation of buffers/solutions and reagents.

Table 2.3: Special equipment list.

Table 2.4: Reagents for mammalian cell culture.

Table 2.5: Bacterial culture media.

Table 2.6: PCR Reagents.

Table 2.7: Test Kits.

Table 2.8: List of antibodies.

Table 5.1: List of sample IDs, pathology, age and sex of test samples.

Table 5.2: CD147 correlations with senile plaques, nicastrin, presenilin1/2 and presenilin enhancer 2 in hippocampus and frontal cortex from AD, LBD and FTD brains.

Table 6.1: Comparison of minor allele frequencies reported in European populations from NCBI and in the current study.

Table 6.2: Allelic Frequencies.

Table 6.3: Genotype association.

Table 6.4: Manual Haplotype Associations.

Table 6.5: SNPs association with A $\beta$ , cholesterol and ApoE Levels.

Table 6.6: Genotype association with SUVR.





## DECLARATION

I certify that this thesis does not, to the best of my knowledge and belief:

- (i) Incorporate without acknowledgment any material previously submitted for a degree or diploma in any institution of higher education.
- (ii) Contain any material previously published or written by another person except where due reference is made in the text; or
- (iii) Contain any defamatory material.

I also grant permission for the Library at Edith Cowan University to make duplicate copies of my thesis as required.

Signature: .....

Date: .....

## ACKNOWLEDGEMENTS

My heartfelt thanks to my supervisors, Prof Ralph Martins, and Dr. Giuseppe Verdile (Edith Cowan University), Prof. Frank Mastaglia and Dr. Sheriff Boulos (Australia Neuromuscular Research Institute) for the support, encouragement and assurance during my course of study. Thank you for instilling in me the confidence and courage to undertake this study and allowing my intellectual integrity and capability to grow.

I am also indebted to Assoc/Prof. Simon Laws, Assoc. Prof Bruno Meloni, Tammy Esmail and Dr Angus Stewart for your advice and assistance throughout my studies. You have been there for me when I very much needed guiding light during my time of study at ECU and ANRI. I enjoyed working with you and have been a source of inspiration. My heartfelt thanks also go to Jude Newberry and Kathy Lucas who were always there for administrative support.

BIG thanks to **all** laboratory staff both at ECU and ANRI for making my life easy and happy when I really needed support and encouragement. In particular I would like to acknowledge the support and assistance received from and Joane Cheing (ANRI). Your support, advice and most importantly friendship made it possible for me to achieve my objective.

Finally (and most importantly) my heartfelt thanks to my wife Eleanor and children Elizabeth, Chikondi and Emmanuel for their unconditional emotional, financial, intellectual and spiritual support. To my parents, Elizabeth and Jemitala for all the good things done for me all my life, you are really wonderful people I have ever known in my life. My thanks also go to McCusker Foundation for Alzheimer's disease Research Inc (MFARI), Edith Cowan University (ECU) and Australian Neuromuscular Research Institute (ANRI) for financial and material support towards my PhD.

## Table of Contents

<b>USE OF THESIS</b>	<b>ii</b>
<b>ABSTRACT</b>	<b>iii</b>
<b>ABBREVIATIONS</b>	<b>v</b>
<b>ACKNOWLEDGEMENTS</b>	<b>xvii</b>
<b>CHAPTER 1 Introduction</b>	<b>22</b>
1.1: Alzheimer's disease (AD).....	22
1.2: Neuropathological Characteristics of Alzheimer's disease (AD).....	24
1.2.1: Neurofibrillary tangles (NFT).....	26
1.2.2: Senile plaques (SP) .....	26
1.2.3: Cerebral amyloid angiopathy (CAA).....	29
1.3: Risk factors of AD .....	30
1.4: Beta Amyloid protein (A $\beta$ ) .....	35
1.4.1: A $\beta$ mediated toxicity .....	36
1.4.2: Mitochondrial dysfunction.....	37
1.4.3: Oxidative stress .....	38
1.4.4: Synaptic toxicity.....	39
1.5: The Amyloid Precursor Protein (APP) and its proteolytic processing .....	40
1.5.1: Amyloid precursor protein (APP) processing .....	42
1.6: The $\gamma$ -secretase complex components.....	47
1.6.1: Presenilins .....	48
1.6.2: Nicastrin (NCT) .....	52
1.6.3: Anterior Pharynx defective homolog-1 (APH-1).....	52
1.6.4: Presenilin Enhancer 2 (PEN-2) .....	54
1.7: CD147 is a multifunctional protein that modulates A $\beta$ levels.....	57
1.7.1: Protein structure and expression. ....	59
1.7.2: Functions of CD147 .....	61
1.7.3: Non neuronal functions of CD147 .....	62
1.7.4: Neuronal functions of CD147 .....	65
1.7.5: CD147 interactions with $\gamma$ -secretase and modulating beta amyloid levels 66	
1.7.6: CD147 expression in AD. ....	70
1.8: Regulating CD147 expression. ....	73
1.8.2: Regulation of SCP and $\gamma$ -secretase activity by cholesterol.....	74
1.12: Hypothesis.....	75
1.13: Aims.....	76
<b>CHAPTER 2</b>	<b>77</b>
<b>Materials and Methods</b>	<b>77</b>
2.1: Materials .....	77
2.2: Methods.....	90
2.2.1: Cell Cultures.....	90
2.2.2: Cell viability assessment .....	90
2.2.3: Cholesterol Treatment of Rat Primary Cortical Neuronal Cultures.....	91
2.2.4: A $\beta$ Treatment of Rat Primary Cortical Neuronal Cultures .....	91
2.3: <i>In vivo</i> Experiments .....	91
2.3.1: APP <sup>swe</sup> mice .....	91
2.3.2: Human Subjects .....	92
2.3.3: Homogenisation of Tissues .....	92
2.4: Protein Procedures .....	93
2.4.1: Protein Extraction from Cultures .....	93
2.4.2: SCP-2 Protein Generation .....	93

2.4.3: Cytoplasmic Protein Purification .....	94
2.4.4: Determination of Protein Concentration .....	95
2.5: Immunoblotting.....	95
2.6: Enzyme Linked Immunosorbent Assay (ELISA) .....	96
2.6.1: A $\beta$ 1-40/1-42 ELISA.....	96
2.6.2: Plasma Cholesterol ELISA .....	97
2.6.3: CytoTox 96® Non-Radioactive Cytotoxic Assay (LDH Assay) .....	98
2.7: Maintenance of bacterial cells.....	98
2.8: Competent Cells.....	98
2.8.1: Preparation of Chemically Competent KRX Cells .....	98
2.8.2: Assessment of Chemically Competent KRX Cells.....	99
2.8.3: Transformation of Chemically Competent KRX Cells.....	100
2.9: Preparation of Recombinant Adenovirus.....	100
2.10: RNA/DNA methods.....	101
2.10.1: General handling .....	101
2.10.2: RNA extraction .....	101
2.10.3: Genomic DNA extraction.....	101
2.10.4: Plasmid extractions .....	101
2.11: Cloning of the PCR Products and Cell Transformation.....	102
2.12: Restriction enzyme digestion .....	103
2.13: Ligations .....	103
2.14: Quantitation of DNA.....	103
2.15: Agarose gel electrophoresis .....	104
2.16: DNA sequencing .....	104
2.17: Human CD147 promoter amplification and sequencing.....	105
2.17.1: Slowdown PCR for amplifying GC-rich sequences.....	105
2.17.2: Amplification of the CD147 promoter .....	105
2.17.3: Sequencing of the CD147 promoter.....	106
2.18: Immunohistochemistry of Human Brain Tissue – Paraffin Embedded Sections	107
2.19: Statistical Methods.....	107
2.19.1: Linkage, allelic and haplotypic analysis .....	107
2.19.2: Additional statistical analysis.....	108
<b>CHAPTER 3</b>	<b>109</b>
Cholesterol modulates CD147 expression <i>in vitro</i> . .....	109
3.1: Introduction.....	109
3.2: Aims .....	111
3.3: Material and methods.....	111
3.3.1: Neuronal cultures .....	111
3.3.2 Cholesterol and A $\beta$ treatment of primary cultures .....	112
3.3.3: Preparation of pRSV-shuttle vectors encoding human CD147.....	112
3.3.4: Adenoviral vector construction .....	113
3.3.5: Hydrogen peroxide treatment.....	113
3.3.6: Western blot analysis .....	114
3.4: Results.....	114
3.4.1: Cholesterol treatment increases CD147 expression in primary neuronal cultures in a dose dependent manner.....	114
3.4.2: Cholesterol increases LDH release in rat primary cortical neuronal cultures	117
3.4.3: Oxidative stress induces CD147 expression and affects cell viability in rat primary cortical neuronal cultures in a dose dependent manner .....	119

3.4.4: Adenoviral mediated CD147 over expression does not affect cell viability in rat primary neuronal cultures. ....	125
3.4.5: Adenoviral mediated CD147 expression protected rat primary cortical neuronal cultures against A $\beta$ 42 toxicity only in the presence of cyclophilin A (CypA) 128	
3.4.6: Adenoviral mediated CD147 expression protected SH-SY5Y cell cultures against A $\beta$ 42 toxicity only in the presence of cyclophilin A (CypA).....	131
3.5: Summary of results .....	134
3.6: Discussion .....	134
3.7: Conclusion Taken together, the findings of the present chapter identify potentially important relationships between cholesterol loading, CD147 expression, A $\beta$ toxicity and the putative involvement of CYPA protein in neuroprotection, and possibly in A $\beta$ clearance in AD. ....	138
<b>CHAPTER 4</b>	<b>139</b>
<b>A high fat/ high cholesterol diet does not affect CD147 levels in APPswe transgenic mice</b>	<b>139</b>
4.1: Introduction.....	139
4.2: Aims.....	142
4.3: Materials and methods .....	143
4.3.1: Experimental animals and diets .....	143
4.3.2: Western blot and ELISA analyses.....	143
4.3.3: SCP-2 analysis .....	144
4.4: Results.....	146
4.4.1: Impact of a high fat/high cholesterol diet on body weight and plasma cholesterol levels. ....	146
4.4.2: Cerebral CD147 protein levels are not significantly altered in APPswe mice fed a high fat/high cholesterol diet .....	149
4.4.4: Effects of the high fat/high cholesterol diet on APP and some of its metabolites. ....	164
4.4.5: Ratio of A $\beta$ 42/A $\beta$ 40 peptides in the brain and periphery of APPswe mice after 10 weeks on a high fat/high cholesterol diet or normal chow diet. ....	171
4.5: Summary of results .....	175
4.6: Discussion .....	175
4.6.1: High fat/high cholesterol diet influences plasma cholesterol levels ..	176
4.6.3: Increased cholesterol levels do not alter brain CD147 levels in vivo.	179
4.6.4: A high fat/high cholesterol diet does not appear to affect SCP-2 transcript levels 180	
4.6.5: CD147 influences on A $\beta$ production .....	182
4.7: Conclusions.....	185
<b>CHAPTER 5</b>	<b>186</b>
<b>CD147 protein expression and localisation in AD brain tissue.</b>	<b>186</b>
5.1: Introduction.....	186
5.2: Aims.....	187
5.3: Materials and methods .....	188
5.3.1: Sourcing and preparation of tissues .....	188
5.3.2: Western blot analysis .....	190
5.3.3: Immunohistochemistry analysis.....	190
5.4: Results.....	191
5.4.1: CD147 protein expression levels are not altered in brain tissue from Alzheimer's disease (AD) cases.....	191
5.4.2: Associations of CD147 protein expression with levels of A $\beta$ 42 and core protein components of $\gamma$ -secretase. ....	203

5.5: Summary of results: .....	217
5.6: Discussion .....	217
5.6.3: PEN2 are increased in Alzheimer's disease (AD) .....	220
5.7: Conclusion .....	223
<b>CHAPTER 6</b> .....	<b>225</b>
<b>Polymorphisms in the CD147 promoter region may influence Alzheimer's disease (AD) pathology.</b> .....	<b>225</b>
6.1: Introduction .....	225
6.2: Aims .....	227
6.3: Material and methods .....	227
6.4: Results .....	231
6.4.1: SCP-x and pro-SCP bind CD147 DNA in vitro .....	231
6.4.2: CD147 promoter is a GC-rich region requiring special PCR technique to amplify. ....	234
6.4.3: CD147 promoter contains two novel SNPs not previously reported. ....	237
6.4.4: CD147 promoter SNPs are not associated with AD. ....	241
6.4.5: CD147 promoter SNPs are not associated with A $\beta$ , cholesterol and ApoE levels. ....	245
6.4.5: CD147 promoter SNP rs11551906 is associated with AD pathology. ....	247
6.5: Summary of results .....	249
6.6: Discussion .....	249
6.6.1: SNPs association with AD .....	249
6.6.2: SUVR is associated with rs11551906 .....	251
6.6.3: Novel SNPs within the CD147 promoter .....	252
6.7: Conclusion .....	253
<b>CHAPTER 7</b> .....	<b>254</b>
<b>General discussion</b> .....	<b>254</b>
7.1: The link between CD147 protein and AD pathology. ....	254
7.2: Cholesterol and A $\beta$ 42 loading increases CD147 protein expression <i>in vitro</i> .....	259
7.3: A $\beta$ 42 induced oxidative stress increases CD147 protein expression <i>in vitro</i> .....	262
7.4: Adenoviral mediated CD147 over expression protects neuronal cell against A $\beta$ 42 induced oxidative stress only in the presence of CyPA <i>in vitro</i> .....	263
7.5: CD147 levels are not altered by high fat/high cholesterol diet <i>in vivo</i> .....	266
7.6: High fat/high cholesterol diet did not affect SCP-2 levels <i>in vivo</i> .....	268
7.7: CD147 protein levels are not altered in Alzheimer's disease (AD) .....	270
7.8: Incidence of known CD147 SNPs and discovery of 2 novel CD147 SNPs .....	272
7.9: Future directions .....	273
7.10: Conclusions .....	274
<b>Chapter 8</b> .....	<b>275</b>
<b>References</b> .....	<b>275</b>

# CHAPTER 1

## Introduction

### 1.1: Alzheimer's disease (AD)

In November 1901, a woman called Auguste Deter was admitted to a mental hospital by a German neuropathologist/psychiatrist Alois Alzheimer because of impaired memory, paranoia and disorientation complaints. Her condition deteriorated after a few years leading to language deficits, hallucinations and aggressive behaviour. Her physical and mental condition deteriorated considerably, consequently resulting in her death in 1906. After Auguste's death, Alzheimer performed an autopsy on her brain and identified unusual formations which are now known as the characteristic hallmarks of Alzheimer's disease, namely neurofibrillary tangles and amyloid plaques.

Currently, dementia, of which Alzheimer's disease (AD) is the most common form, is posing escalating social and financial burdens especially with the ageing population. Globally, it is estimated that there are about 26.6 million dementia cases with approximately 245,000 cases being in Australia, and of these, 50 – 70 % are AD cases. This is expected to rise to approximately 1.1 million by 2050 with an annual financial impact on the Australian community already exceeding \$6.6 billion annually (Access Economic Report, 2003). The disease is a progressive neurodegenerative disorder resulting in atrophy of the brain due to neuronal loss (**Fig. 1.1B**) and clinically, is characterised by memory impairment and behavioural changes. To date, *post-mortem* examination is still the most affirmative determination of AD, based on the presence of the pathological hallmarks. With advances in brain imaging technology such as magnetic resonance imaging (MRI), computed tomography (CT) and positron emission



tomography (PET), there is now an opportunity to diagnose and differentiate AD ante-mortem from various other dementias. Over the past several years there has also been intensive research to identify biomarkers that can be used to diagnose AD with high sensitivity and specificity, prior to onset of symptoms.

Although pathological hallmarks of AD (**Fig.1.2** and **1.3**) have been known for over a century, there is still no consensus on the chain of events that result in the onset and progression of AD. A number of hypotheses have been postulated to account for neuronal dysfunction/loss in the AD brain. Of these, the most widely studied and accepted is the “amyloid hypothesis” which postulates that the aggregation and accumulation of a small peptide, termed amyloid- $\beta$  ( $A\beta$ ), triggers a cascade of events that include the generation of free radicals, oxidative damage and inflammatory processes, resulting in neurodegeneration. The  $A\beta$  protein is a small 4-kDa peptide that is generated from the proteolytic processing of its parent molecule, the amyloid precursor protein (APP) (see below and **Fig.1.5**) (Yu et al., 2000, Jankowsky et al., 2004, Krishnaswamy et al., 2009, Ionov and Pushinskaya, 2010, Perez et al., 2010, Guo et al., 2011, Kim et al., 2011).

Dysregulated proteolytic processing of APP or impaired  $A\beta$  clearance are primary events that lead to the accumulation of  $A\beta$  within the AD brain. In familial cases, where genetic mutations are inherited in an autosomal dominant manner, the dysregulated proteolytic processing of APP is thought to lead to the accumulation of  $A\beta$ , whereas in the more common sporadic cases, the impaired clearance of  $A\beta$  from the CNS is thought to be a major contributor to AD pathogenesis. One protein that has been implicated in both the production and clearance/degradation of  $A\beta$  is CD147. The CD147 protein is a transmembrane glycoprotein originally described for its ability to

activate metalloproteases and amongst its many functions has been recently thought to modulate A $\beta$  levels. Discussed below is a general overview of AD pathogenesis and the implications for CD147 in modulating A $\beta$  accumulation and neuronal functions that may be compromised in AD.

## **1.2: Neuropathological Characteristics of Alzheimer's disease (AD)**

As AD progresses, gross morphological changes occur, such as the widening of the sulci, narrowing of the gyri and enlargement of the ventricles of the brain, in the frontotemporal areas (**Fig.1.1**) (Wu et al., 2003, Wu et al., 2010). During the early stages of AD there is atrophy of the medial temporal lobe, hippocampus, and the amygdala (Cahill and McGaugh, 1998). Loss in brain mass due to degeneration is generalised. The progression of brain atrophy starts from the temporal lobe and spreads to the frontal lobe and cerebral cortices (Baum et al., 1995). Measurement of the medial temporal lobe has been used in diagnosis and in the monitoring of disease progression (Denihan et al., 2000).

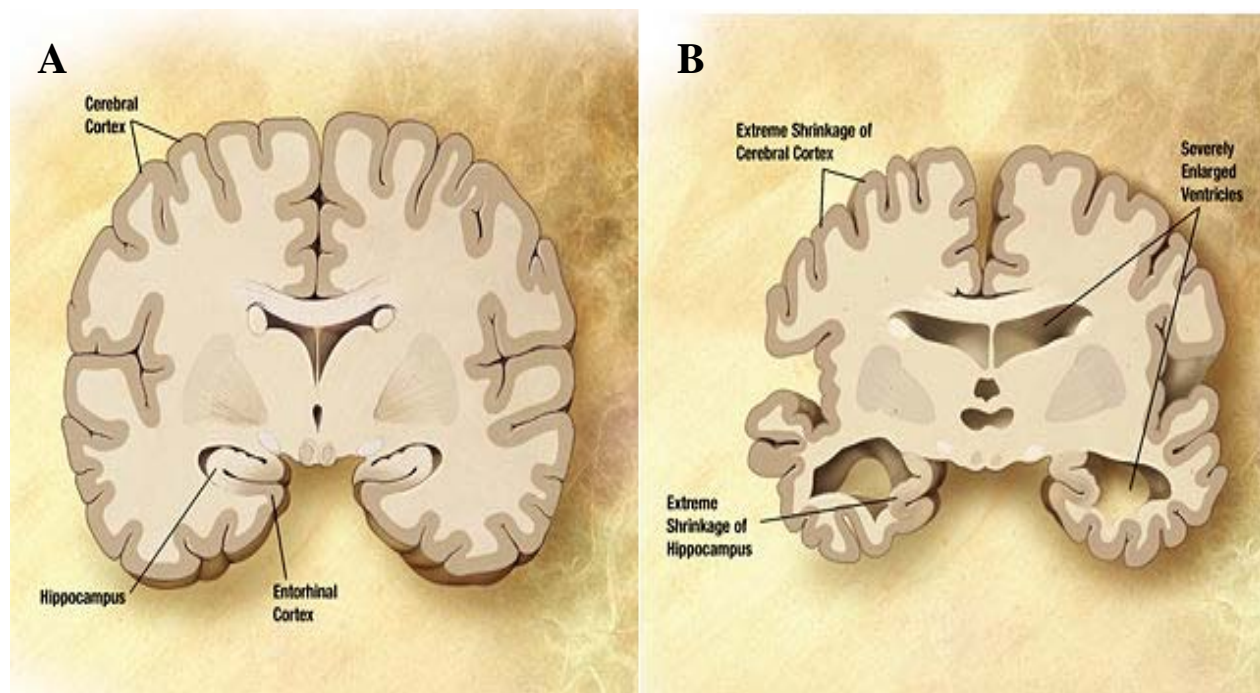


**Figure 1.1: Representative schematic diagram of *post-mortem* brain cross-sections.**

Differential characteristics of health control brain (A) and Alzheimer's disease patient (B). The AD brain is featured by severely enlarged ventricles and shrinkage of the cerebral cortical and hippocampal regions, which are responsible for memory and cognitive functions.

(Image courtesy:<http://knol.google.com/k/lara/alzheimer-s-disease/Ing3X-E/g1JpHQ>).

The histopathological hallmarks of AD are senile plaques (SP), neurofibrillary tangles (NFTs) and congophilic amyloid angiopathy (CAA) (Vinters and Gilbert, 1983). The early NFT and SP deposits are concentrated in regions of the brain mostly associated with memory and learning such as the hippocampus (Masters and Beyreuther, 1995, Gilman, 1997).

### **1.2.1: Neurofibrillary tangles (NFT)**

A key characteristic of AD is the pattern of NFT lesions in the brain that is symmetrical in both hemispheres (Braak and Braak, 1997). In healthy neurons, microtubules are parallel structures involved in cell motility, transport, shape and mitosis that are supported by tau proteins (Goedert, 1993, Avila et al., 2004). The equilibrium between phosphorylation and de-phosphorylation of tau modulates the cytoskeleton influencing the morphology of the axon (Maccioni et al., 2001). The hyper-phosphorylation of tau protein reduces the binding of tau to microtubules resulting in the formation of filamentous structures called paired helical filaments (PHF) which are the basic constituents of NFT (**Fig. 3**) (Goedert, 1993, Gilman, 1997).

### **1.2.2: Senile plaques (SP)**

Senile plaques consist of a central core of radiating amyloid fibrils surrounded by dystrophic neurites and activated glial cells. Plaques may also appear as a diffuse amorphous deposition of A $\beta$  (Eikelenboom et al., 2010, Hurtado et al., 2010, Perl, 2010). Silver staining reveals a central core of A $\beta$  surrounded by swollen abnormal neurites (**Fig. 1.2**) (Anderton, 2002, Mathis et al., 2004). Congo red staining reveals a characteristic birefringence seen under polarised light indicating the anti-parallel beta-

sheet conformation of A $\beta$ ; this is the characteristic that makes it “amyloid”. Transmission electron microscopy reveals the fibrillary nature of the plaque cores that reflects the distinguishing pattern of A $\beta$  aggregation (Morris, 1997). The number of SP are greatly increased in AD (Mathis et al., 2004), compared to what can be found in an apparently normal person – it is thought that the presence of significant numbers of SP and NFT indicate pre-clinical AD, since by the time AD symptoms arise, neurodegeneration has been occurring for years.

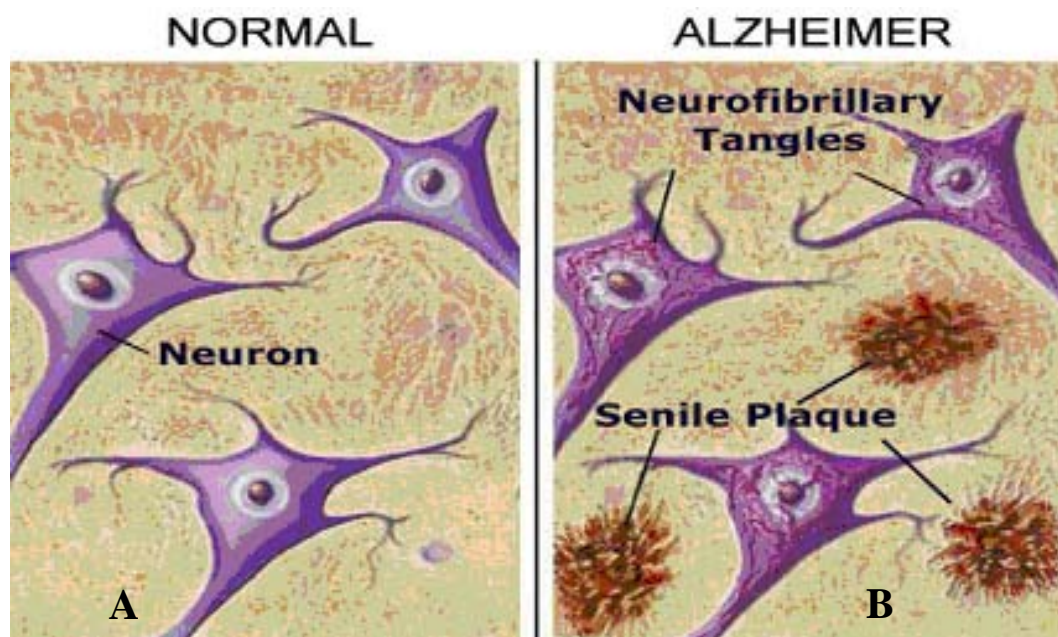


**Figure 1.2: Neurofibrillary tangles (NFT) and senile plaque (SP)**

Comparison of a normal brain (A) and pathological hallmarks of AD (B) showing NFT described as filamentous structures arranged in bundles within affected neurons and SP with the characteristic dense core of beta amyloid. (*Image courtesy: <http://www.spice-of-life.com>*).

### 1.2.3: Cerebral amyloid angiopathy (CAA)

Congophilic amyloid angiopathy (CAA) is due to A $\beta$  peptide accumulation in blood vessel walls within the brain (**Fig.1.3**) (Weller et al., 2000). CAA increases the frequency of intracerebral haemorrhage as a result of vessel wall weakness. Smooth muscle tissue is replaced by A $\beta$  in the blood vessels. This results in hindrance of arterial elasticity which plays a significant role in the clinical pathology of AD (Weller et al., 2000).

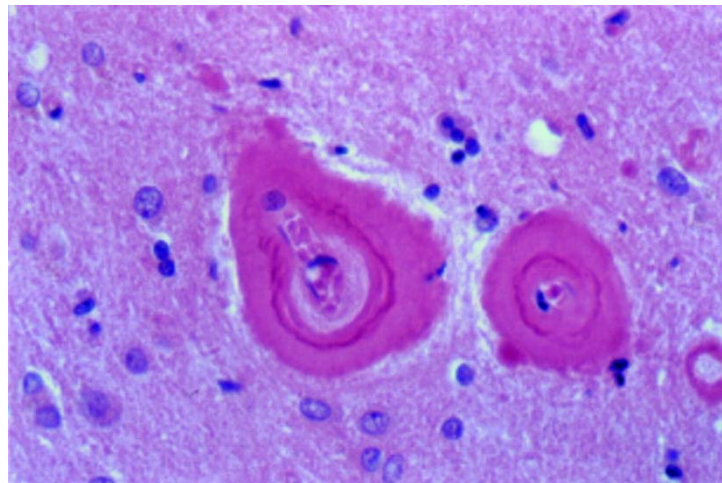


**Figure 1.3: Congophilic amyloid angiopathy**

Concentric cellular, eosinophilic thickening of penetrating cortical vessels with severe luminal narrowing, typical of advanced amyloid angiopathy (haematoxylin and eosin) (Weller et al., 2000)

### 1.3: Risk factors of AD

Alzheimer's disease can be classified broadly into two groups, late-onset AD (LOAD, occurring >65 yrs) and early onset AD (EOAD, occurring < 65 yrs). The more common sporadic late-onset cases are associated with many risk factors. Of these age and possession of the  $\epsilon 4$  allele of the APOLIPOPROTEIN gene (APOE  $\epsilon 4$ ) are the major risk factors for most populations globally (Roses, 1994, Martins et al., 1995, Roses, 1997, Martins et al., 2006). Many other potential risk factors for AD have been described which include, low levels of sex steroids (Pericak-Vance et al., 1991, Poirier et al., 1993, Strittmatter et al., 1993, Haskell et al., 1997, Lambert et al., 1998, Short et al., 2001), increased levels of gonadotropins (Smith et al., 1998, Bowen et al., 2000, Short et al., 2001), head injury, physical inactivity, stroke, diabetes, hypertension, and hypercholesterolemia. In addition to APOE  $\epsilon 4$ , recent genome-wide association studies in humans have identified a number of possible additional loci associated with increased risk for LOAD (Caselli et al., 2009). These have revealed associations of specific genes such as TOMM40, APOC1, CLU, CRI, PI-CALM, EXOC3L2, BIN1 and APOC2 with LOAD (Bertram et al., 2007, Harold et al., 2009, Lambert et al., 2009, Seshadri et al., 2010). Although these genes have had various, significant associations with LOAD, APOE $\epsilon 4$  is still by far the strongest genetic risk factor of AD.

The human APOE gene is located on the long arm of chromosome 19 (19q13.2) (Olaisen et al., 1982, Das et al., 1985). It is 3.7 kb in length containing three exons and introns and encodes a 34kDa protein. There are three major polymorphisms of APOE ( $\epsilon 2$ ,  $\epsilon 3$ , and  $\epsilon 4$ ), which result from a single amino acid substitution at residues 112 and/or 158 (Utermann et al., 1980, Rall et al., 1982, Weisgraber et al., 1982). Of these APOE alleles, the  $\epsilon 4$  form is associated with an increased risk of developing AD with approximately 40-60% of sporadic cases carrying this allele. The APOE  $\epsilon 4$  allele is



associated with a rapid decline in memory in individuals without dementia and in individuals considered to have mild cognitive impairment (Boyle et al., 2010). Further, the risk of developing AD markedly increases in individuals with increasing copy number of the  $\epsilon 4$  allele. Risk increases from 3.5 times when carrying one copy of  $\epsilon 4$  (heterozygous) to almost 15 times when carrying two copies of  $\epsilon 4$  (homozygous) compared to those lacking  $\epsilon 4$  (Breitner et al., 1998, Davidson et al., 2006). Individuals who have AD and have two copies of the  $\epsilon 4$  gene develop the disease earlier compared to those that do not possess this gene or have only one copy of this gene. Similarly, individuals with two copies of *APOE*  $\epsilon 4$  also appear to have a more severe pathology. The *APOE*  $\epsilon 2$  allele, on the other hand, associated with a reduced frequency in the AD population, is associated with a delayed age of onset of AD and is associated with a less severe pathology than that observed with AD patients harbouring *APOE*  $\epsilon 4$ . Thus the presence of the *APOE*  $\epsilon 2$  allele is thought to exert a protective effect.

The combination of *APOE*  $\epsilon 4$  and other environmental or dietary risk factors for AD can increase the risk of developing the disease further. The presence of the *APOE*  $\epsilon 4$  allele in western society also increases the risk of other disorders associated with high fat/ high cholesterol intake, including type-2 diabetes, hypertension (high blood pressure), hypercholesterolemia (high cholesterol levels) and cardiovascular disease, all of which are also AD risk factors (Simons et al., 1998a). Research reports have also shown evidence that a higher intake of calories and saturated fat may be associated with increased risk of AD in individuals with the *APOE*  $\epsilon 4$  allele (Kalmijn et al., 1997, Refolo et al., 2000a, Mihovilovic et al., 2007, Torreggiani et al., 2009). Furthermore, individuals with type-2 diabetes possessing the *APOE*  $\epsilon 4$  allele are at twice the risk of developing AD compared to  $\epsilon 4$  carriers who do not have diabetes (Martins et al., 2006).

These studies provide evidence in support of an interaction between *APOE*  $\epsilon$ 4 and dietary factors enhancing the risk of AD.

The major function of apoE is to mediate the clearance of lipoproteins by interacting with the low-density lipoprotein (LDL) family on receptors in liver cells (Beisiegel et al., 1989). ApoE-containing lipoproteins initially bind to cell surface heparin-sulphate proteoglycans, and are subsequently transferred to the LDL receptor-like protein (LRP) or LDL receptor for endocytosis via clathrin coated vesicles (Ji et al., 1993, Havel, 1998). Studies also suggest an important role for apoE in the uptake and redistribution of cholesterol within the CNS (Roheim et al., 1979, Pitas et al., 1987, Holtzman et al., 1995).

Several mechanisms of action of apoE have been proposed that may account for its association with AD. These include modulating the metabolism of A $\beta$  by influencing its clearance and aggregation rates (Bales et al., 2002). In animal models, apoE has been associated with brain cholesterol such that high cholesterol levels increase A $\beta$  accumulation within the brain (Refolo et al., 2000a). A study by Naslund *et. al.*, (Naslund et al., 2000) showed that ApoE co-localised with A $\beta$  in SP within brain tissue from AD cases. ApoE has also been shown to enhance the aggregation of A $\beta$ 1-40 (Sanan et al., 1994). Conflicting results from various studies exist on the influence of the apoE  $\epsilon$ 4 isoform on cellular uptake of A $\beta$ 1-40 with some studies showing this isoform to be correlated with increased A $\beta$ 40 uptake. Conversely other groups have shown that A $\beta$  uptake is reduced in the presence of the apoE  $\epsilon$ 4 isoform compared to the other apoE isoforms (Yang et al., 1995, Cole et al., 1999). These discrepancies have been explained by the fact that earlier studies showing enhanced aggregation of A $\beta$ 1-40

with apoE  $\epsilon$ 4 isoform used poorly lipidated apoE which compromised its function (Yang et al., 1995).

Recent studies have shown that apoE binds to A $\beta$  and may modify its biological activities. Wilhelmus and colleagues (Wilhelmus et al., 2005) evaluated the effect of apoE on A $\beta$ -mediated toxicity of cerebrovascular cells. Their results showed that cultured cells with  $\epsilon$ 4/ $\epsilon$ 4 genotype were more vulnerable to A $\beta$  toxicity than those with  $\epsilon$ 3/ $\epsilon$ 3 or  $\epsilon$ 3/ $\epsilon$ 4 genotype (Wilhelmus et al., 2005). Taken together, these outcomes suggest that apoE plays a direct isoform specific role in A $\beta$  deposition. This notion is supported by the findings in mouse models where differences in isoform specific action on A $\beta$  aggregation and clearance by apoE  $\epsilon$ 4 and apoE  $\epsilon$ 2 respectively were identified (Smith et al., 1998).

Increased levels of apoE have a detrimental influence on the neuronal cell system promoting cytotoxicity or neurite degeneration (Hashimoto et al., 2000). However, low levels of plasma apoE are found in AD subjects (Veer et al., 2011). Current data suggest that one mechanism by which apoE may alter the risk for AD is isoform-dependent regulation of A $\beta$  cytotoxicity. It is thought that extracellular apoE binds to A $\beta$  and thereby modifying A $\beta$  -mediated cell toxicity (Wilhelmus et al., 2005). This however changes with each apoE isoform where apoE  $\epsilon$ 2 is most protective and apoE $\epsilon$ 4 is least protective due to isoform specific differences in binding to A $\beta$  (Mahley et al., 1996). ApoE is also thought to have isoform specific effects on microglia activation in AD brains (Egensperger et al., 1998) or an inhibitory effect on activation of cultured glial cells by A $\beta$  peptides (Hu et al., 1998).

A role for apoE in the clearance of A $\beta$  has also received attention. There are two major A $\beta$  clearance mechanisms in the brain – firstly there is receptor mediated clearance by cells in brain parenchyma (microglia, astrocytes, neurons), along the interstitial fluid (ISF) drainage pathway, or through the blood brain barrier (BBB). Secondly A $\beta$  can be cleaved by endopeptidases such as insulin degrading enzyme (IDE) and neprilysin which are both expressed in neurons and vascular cells, as well as other enzymes such as endothelin converting enzymes (Bu, 2009). A $\beta$  peptide clearance in the periphery has been shown to be mediated by apoE. For example, Hone et al. demonstrated that A $\beta$  is rapidly removed from plasma by murine peripheral tissues and that the rate of clearance is affected by apoE (Hone et al., 2003). In this study, C57 BL/6J and APOE knockout mice were intravenously injected with A $\beta$ 40 peptide and blood was taken from the retro-orbital sinus at various time-points. In the C57 BL/6J mice, it was observed that the liver had removed a large proportion (40.8%) of the injected A $\beta$  followed by the kidney (4.4%) by 90 minutes, whereas these tissues had undetectable levels of A $\beta$  in the APOE knockout animals (Hone et al., 2003). Recent findings have extended this work and have shown that the presence of apoE  $\epsilon$ 4 led to a reduced plasma clearance of A $\beta$  and reduced uptake by two major peripheral organs that clear A $\beta$  from the periphery, the liver and kidney (Sharman et al., 2010). It was also found that levels of the A $\beta$  degradation enzyme, insulin degradation enzyme (IDE) were reduced in brain and kidney from mice harbouring the APOE  $\epsilon$ 4 allele. The decreased capacity of apoE  $\epsilon$ 4 to clear/degrade A $\beta$  from the periphery and the associated lower levels of IDE, particularly in the brain, suggest an explanation for the greater brain A $\beta$  accumulation and higher risk of AD in APOE  $\epsilon$ 4 carriers. Individuals carrying the APOE  $\epsilon$ 4 allele also bear some risk of developing the early-onset form of AD. However there are also some familial AD subjects that are not associated with either APP, PS1 or PS2 mutations or APOE $\epsilon$ 4

inheritance that suggests that other underlying factors may be responsible for such familial forms of AD.

Overall, EOAD accounts for only a small percentage of AD cases but is the most severe form of the disease. The majority of EOAD cases are familial forms of AD showing autosomal dominant inheritance. Familial AD (FAD) is typically associated with an early age of onset (reviewed by (Martins et al., 2009)). Most of our knowledge of the molecular events underlying the development of AD comes from FAD since we can use genetic analysis to identify the genes and proteins involved. Mutations at only three loci are known to cause FAD although other loci may yet be found (Caselli et al., 2009). One locus hosts the gene for the Amyloid Precursor Protein (APP) from which A $\beta$  is cleaved by the action of two “secretases”;  $\beta$ -secretase and  $\gamma$ -secretase (see section 1.5.1). Mutations in APP alter these cleavages so that A $\beta$  production is increased or more aggregation-prone forms of A $\beta$  are formed (reviewed by (Martins et al., 2009)). The remaining two loci host the presenilin genes PSEN1 and PSEN2 with mutations in these genes accounting for 50-70% of EOFAD cases (Zhang et al., 2010a, Stevens et al., 2011). The presenilin proteins form the catalytic core of protein complexes with  $\gamma$ -secretase activity (see section 1.6). Mutations in the presenilins also appear to alter the rate of A $\beta$  production (see section 1.6.1). The role of A $\beta$  in AD pathogenesis and its production are described in detail below.

#### **1.4: Beta Amyloid protein (A $\beta$ )**

As described before in section 1.2.2.2 SPs containing amyloid deposits are neuropathological hallmarks of the AD brain. The accumulation and aggregation of A $\beta$  is central to the amyloid hypothesis and has a major role in AD pathogenesis (Maccioni et al., 2001). The A $\beta$  protein is a proteolytic fragment of the amyloid precursor protein

(APP) (**Fig.1.6**) (Hartmann et al., 1996). There are two major forms of A $\beta$ , A $\beta_{40}$  which terminates at Val40 of the A $\beta$  sequence and the longer and more pathogenic form A $\beta_{42}$ , which terminates at Ala42 of the A $\beta$  sequence. A $\beta_{42}$  forms aggregates more quickly resulting in the formation of senile plaques (SP) (Iwatsubo et al., 1994). Immunochemical studies suggest that the deposition of A $\beta_{42}$  precedes A $\beta_{40}$  (Iwatsubo et al., 1994, Lippa et al., 1998). It is estimated that approximately 90% of A $\beta$  found in the sporadic AD brain is A $\beta_{40}$ , with the remaining 10 % A $\beta_{42}$  (Chapman et al., 2001). A $\beta$  in cerebrospinal fluid (CSF) and blood is secreted by neuronal/glial cells and accumulates in cerebral capillaries, arterioles and venules. Furthermore, blood platelets are key contributors of secreted A $\beta$  in the periphery (Maccioni et al., 2001, Borroni et al., 2002). Increased levels of soluble form of A $\beta_{40}$  are more strongly correlated with AD than amyloid plaque load (Fonte et al., 2001, Hemar and Mulle, 2011, Lewczuk et al., 2011). Furthermore, recent evidence has shown that small aggregates of A $\beta$ , termed oligomers or protofibrils are the major neurotoxic species rather than the amyloid fibrils or the senile plaques themselves (Goedert and Spillantini, 2006a, b, Spillantini et al., 2006). These aggregated forms of A $\beta$  in the brain parenchyma trigger a cascade of pathological events that lead to AD pathology, neuronal loss and the associated cognitive decline (Hardy and Higgins, 1992, Small et al., 2001). Several factors are involved in the process of A $\beta$  aggregation and toxicity that contribute to AD pathology some of which are discussed below.

#### **1.4.1: A $\beta$ mediated toxicity**

The soluble forms of A $\beta$  aggregates have been implicated in disruption of several cellular functions including mitochondrial activity (Dyrks et al., 1992, Butterfield et al., 2001, Palmblad et al., 2002, Lustbader et al., 2004a), oxidative stress (Martins et al.,

1986, Butterfield et al., 2001 ), receptor mediated functions (Yaar et al., 1997, Wei et al., 2002 , Fuentealba et al., 2004, Pereira et al., 2004, Bhaskar et al., 2009), disruption of  $\text{Ca}^{2+}$  homeostasis (Mattson et al., 1993, Hartmann et al., 1994), membrane depolarization and disorder (Muller et al., 2001, Verdier et al., 2004) and microglia activation (Giulian et al., 1996). Most studied mechanisms of  $\text{A}\beta$  induced toxicity are described below.

#### **1.4.2: Mitochondrial dysfunction**

Neurons are highly differentiated cells that need large amounts of Adenosine triphosphate (ATP) and depend on mitochondrial function and oxygen supply to survive (Ames, 2000, Erecinska et al., 2004). As a result neuronal function and survival are very sensitive to mitochondrial dysfunction (Fiskum et al., 1999, Nicholls and Budd, 2000). Neuronal death and loss in AD may be attributed to an intracellular interaction between  $\text{A}\beta$  and  $\text{A}\beta$  binding alcohol dehydrogenase (ABAD) which in turn alters the enzyme's active site and prevents native dehydrogenase activity (Lustbader et al., 2004b, Caspersen et al., 2005). This is evidence of the presence of a mitochondrial pool of  $\text{A}\beta$  within the AD brain that disrupts normal mitochondrial function. This is supported by the finding of  $\text{A}\beta$  accumulation within mitochondria from brains of AD patients, rodent models, and neuronal cells over expressing APP (Caspersen et al., 2005, Crouch et al., 2005, Manczak et al., 2006). Since APP and  $\gamma$ -secretase components are present in mitochondria,  $\text{A}\beta$  could be generated within mitochondria (Anandatheerthavarada et al., 2003, Hansson et al., 2004, Devi et al., 2006) which may in turn significantly impact the functions of the mitochondrial electron transport chain which is essential for the cell's energy requirement (Casley et al., 2002, Crouch et al., 2005) leading to neuronal death due to oxidative stress.

### 1.4.3: Oxidative stress

Oxidative stress is a major contributor to neuronal cell loss in a number of neurodegenerative disorders including AD, and there is strong evidence linking oxidative stress to A $\beta$ . Oxidative stress occurs due to over and/or under production of reactive oxygen species (ROS) via oxidative phosphorylation within the mitochondria that exceeds antioxidant defence systems, leading to oxidative damage of cellular components. ROS are by-products of ATP generation as the CNS consumes 20% of the total oxygen supply. This notion is supported by the findings of Martins et al (Martins et al., 1986) who reported an increase in activity of enzymes from the hexose monophosphate pathways in *post-mortem* AD brain samples compared to age-matched controls. This increased activity of the hexose monophosphate enzymes reflected the increased oxidative stress in the AD brain. Several subsequent reports have also confirmed the original finding and have shown extensive oxidative damage in AD, including lipid peroxidation (Sayre et al., 1997, Butterfield et al., 2002), oxidized proteins (Bisette et al., 1991, Smith et al., 1991) nucleic acid damage (Gabbita et al., 1998, Lovell et al., 1999) and advanced glycation end-products (AGE) (Markesbery and Lovell, 1998, Perry et al., 2003). Oxidative damage in AD may be a direct result of A $\beta$  peptide accumulation which cause neurotoxicity by production of ROS (Behl et al., 1994) through interaction with metals, mainly copper (Cu) (Curtain et al., 2001, Dong et al., 2003). A $\beta$ -Cu combination generates hydrogen peroxide (H<sub>2</sub>O<sub>2</sub>) that has been shown to cause oxidative damage of lipids and intracellular proteins. These findings clearly show that A $\beta$  mediated generation of ROS contributes to neuronal cell death in AD.



#### **1.4.4: Synaptic toxicity**

Cognitive impairment in AD is often attributed to synaptic dysfunction and neuronal cell loss in the hippocampus which is one region of the brain crucial for memory (Hyman et al., 1984, Davies et al., 1987 ). Depleted neurotransmitters and synaptic connections are indicators of synaptic loss ((Whitehouse et al., 1982, Small et al., 2001) and impact learning and memory skills by affecting signal transmission between neurons. There is now evidence that naturally secreted low molecular weight A $\beta$  oligomers and synthetically derived oligomeric A $\beta$ 42 disrupt signal transmission in the hippocampus leading to loss of hippocampal plasticity (Nagerl et al., 2004, Zhou et al., 2004). The biochemical mechanism by which soluble oligomers bind to synaptic plasma membranes and interfere with signalling molecules that are required for synaptic plasticity is unclear. Studies show that A $\beta$  oligomers can interact with membranes to induce a cascade of structural changes such as opening of ion pores, enhancing membrane permeability or ion conductance by modulating a wide array of ion channels and affecting osmotic flux (Mattson and Chan, 2003, Demuro et al., 2010). Disrupted cellular homeostasis affects neuritic dystrophia and blockage of intra-neuronal signalling essential for cognitive functions that may consequently lead to synaptic dysfunction (De Fusco et al., 2003, Lingrel et al., 2007, Moseley et al., 2007). There is also data that has shown that intracellular A $\beta$  accumulation and soluble A $\beta$  oligomers can induce synaptic dysfunction and dendrite loss. However, the molecular mechanisms that underline the loss of synapses and ensuing decline in memory related functions caused by A $\beta$  are complex. Neurodegeneration in AD is specific to particular regions of the brain, but it is still not clear what makes the particular subset of neurons and their processes more vulnerable to the effects A $\beta$  toxicity.

### **1.5: The Amyloid Precursor Protein (APP) and its proteolytic processing**

The amyloid precursor protein (APP) is highly expressed primarily in the brain but is also found in non-neural cells from many different tissues such as liver, kidney and muscle though the level of expression in most peripheral tissues is markedly lower (Turner et al., 2003). The function(s) of APP is still not fully understood but there is evidence to indicate that it plays an important role in an intricate protein signalling network and associated with the regulation of non-neuronal cell mitosis (Nishimoto et al., 1993, Popp et al., 1996). APP is thought to maintain nerve cell growth, morphology and functional plasticity and plays a role in learning and memory (Janus et al., 2000, Morgan et al., 2000, Bayer et al., 2001). The localisation of APP within synapses suggests that APP plays a role in neuronal communication (Chapman et al., 2001). The non-neuronal isoform of APP which contains the Kunitz protease inhibitor domain (KPI) may be involved in cellular adhesion and inhibition of serine proteases (Festoff et al., 2001). The major neuronal form of APP is a glycoprotein comprised of 695 amino acids, characterized by a large ectodomain, a transmembrane domain and a small endodomain (reviewed in (Sisodia and Price, 1995). The APP gene is encoded on chromosome 21. Six different APP isoforms have been identified and are generated from the alternative splicing of exons 7, 8 and 12. These APP isoforms are broadly divided into two groups, either containing KPI (KPI-APP) or lacking KPI (non KPI-APP) (Hook et al., 1999). The KPI-APP group include APP<sub>563</sub>, APP<sub>751</sub>, and APP<sub>770</sub>. The non KPI-APP includes APP<sub>695</sub>, APP<sub>365</sub>, and APP<sub>714</sub> and dominates in neuronal cells. The latter group lacks the KPI domain due to splicing out of exon 7 during transcription (Ponte et al., 1988).

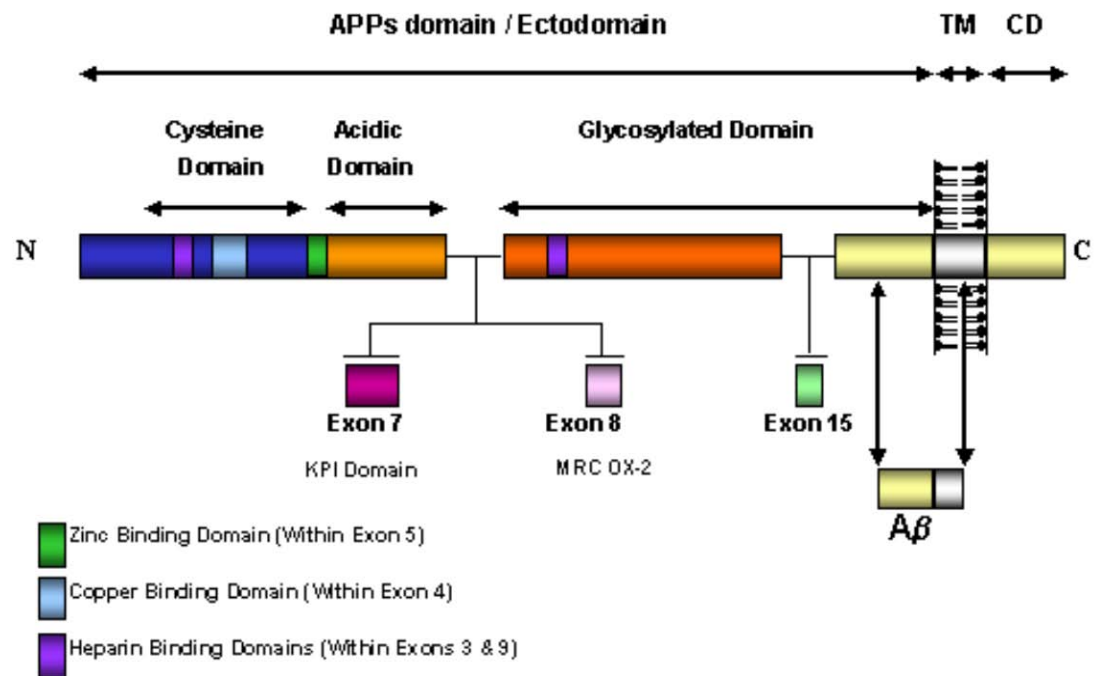


**Figure 1.4: Amyloid Precursor Protein.**

Schematic diagram of APP showing the three main sections: ectodomain, transmembrane and cytoplasmic domain.

### **1.5.1: Amyloid precursor protein (APP) processing**

The APP protein undergoes proteolytic cleavage by enzymes termed BACE,  $\alpha$ , and  $\gamma$ -secretases which act via two competing pathways (reviewed in Krishnaswamy et al., 2009). The non-amyloidogenic pathway involves the cleavage of APP by  $\alpha$ -secretase which precludes A $\beta$  formation whereas the alternative amyloidogenic pathway involves APP cleavage by  $\beta$  and  $\gamma$ -secretase resulting in the A $\beta$  production. These two competing pathways are discussed below.

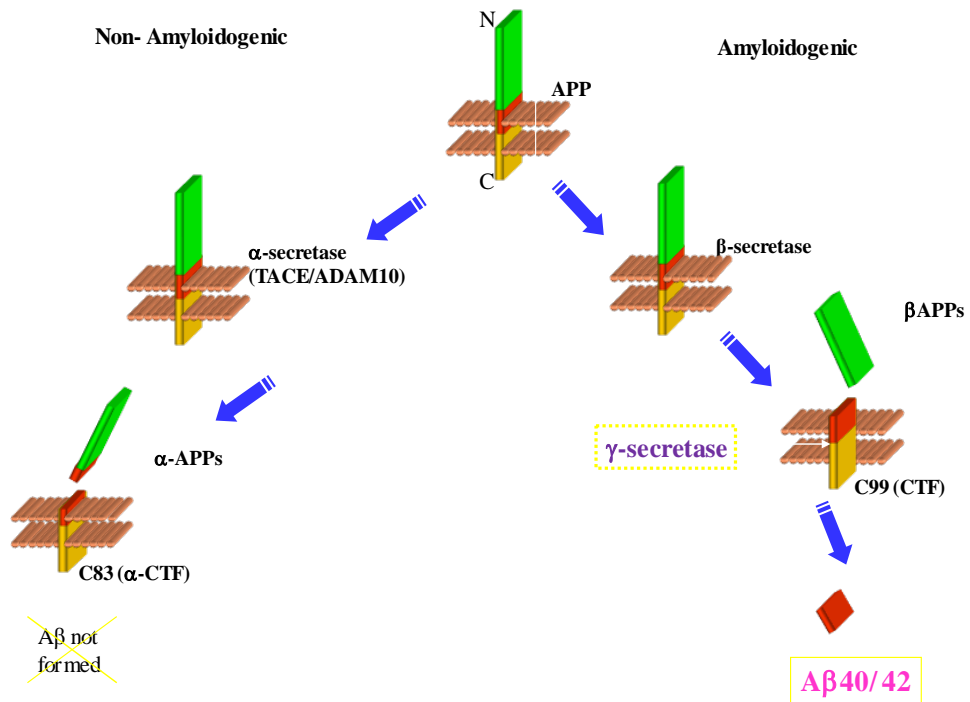


**Figure 1.5: Proteolytic Processing of Amyloid Precursor Protein (APP).**

The two competing APP pathways and the enzymes involved in each pathway. Non-amyloidogenic and Amyloidogenic pathways (*adapted from (Barron et al., 2006)*).

### 1.5.1.1: $\alpha$ -secretase cleavage of APP

The non-amyloidogenic pathway involves the cleavage of APP by  $\alpha$ -secretase between residues 16 and 17 of the A $\beta$  sequence thus precluding A $\beta$  formation. Cleavage by  $\alpha$ -secretase results in the liberation of a secreted form of APP ( $\alpha$ -APPs) and a membrane bound C-terminal fragment of APP which contain residues 18-42 of the A $\beta$  domain (Sisodia and Price, 1995). The membrane bound C-terminal fragment is further cleaved by  $\gamma$ -secretase, at the C-terminal end of A $\beta$ , to liberate non-amyloidogenic fragments. Cleavage of APP by  $\alpha$ -secretase is regulated by protein kinase C or other factors such as hormones (Buxbaum et al., 1993, Bayer et al., 2001).

Tumour necrosis factor- $\alpha$  converting enzyme (TACE), a disintegrin and a metalloproteinase, which belong to The ADAM family of type-1 transmembrane glycoproteins, (ADAM9, ADAM 17 and ADAM 10) have all been shown to have  $\alpha$ -secretase activity. These metallo-proteases are involved in cellular activities such as cellular adhesion and membrane protein shedding (Black et al., 1997). These metallo-proteases have been shown to process APP in a number of *in vitro* and *in vivo* studies. *In vitro* co-expression of ADAM9 with APP resulted in increased production of  $\alpha$ APPs (Koike et al., 1999). Its activity has also been demonstrated in the plasma membranes and the protein secretory pathway (Kuentzel et al., 1993, Refolo et al., 1995, De Strooper, 2007). Over-expression of ADAM10 has been shown to facilitate  $\alpha$ -cleavage of APP whereas knock down precludes endogenous  $\alpha$ -cleavage activity in cell lines including primary neurons (Lammich et al., 1999, Lopez-Perez et al., 2001, Kuhn et al., 2010). There is data that suggest that ADAM10 is the constitutive  $\alpha$ -secretase that is active at the cell surface as evidenced by reduced ADM10 protein levels in platelets of sporadic AD patients which correlate with reduced sAPP $\alpha$  levels (Colciaghi et al.,

2002). This has also been confirmed in neurons from mice with neural ADAM10 knock-out which resulted in significant reduction of sAPP $\alpha$  production to negligible levels (Jorissen et al., 2010).

#### **1.5.1.2: $\beta$ -site APP cleaving enzyme**

Beta site APP cleaving enzyme (BACE), formerly known as  $\beta$ -secretase, is a 501 amino acid trans-membrane protein consisting of signal, trans-membrane, luminal and cytosolic domains (Vassar et al., 1999). Two isoforms of  $\beta$ -secretase (BACE 1 and 2) which belong to the aspartyl-protease family have been identified (Vassar, 2004). In the amyloidogenic pathway BACE cleaves APP at the N- terminus of the A $\beta$  domain to release a  $\beta$ -APPs product and a membrane bound C-terminal fragment ( $\beta$ -CTF). Subsequent cleavage by  $\gamma$ -secretase releases A $\beta_{40}$  or A $\beta_{42}$  and the APP intracellular domain (AICD). (Naslund et al., 2000). The BACE gene is located on chromosome 11q23.3, near a region recently identified as having increased lode scores for AD (Hussain et al., 1999, Vassar et al., 1999). The biological functional and genetic association studies indicate that polymorphisms in the BACE1 gene might be a genetic risk factor for late-onset AD (Kan et al., 2005).

Unlike BACE2, which is highly expressed in heart, kidney and placenta tissue (Yang et al., 1995), BACE1 is highly expressed in the brain with relatively low amounts in most peripheral tissues with the exception of the pancreas (Vassar et al., 1999). Over-expression of BACE correlates with increased cleavage of APP and its activity increases with age (Li et al., 2000b). Furthermore BACE1 levels are elevated in AD brain especially in regions vulnerable to neurodegeneration (Li et al., 2000b, Holsinger et al., 2002). In addition BACE1 knockout mice crossed with APP transgenic mice have low

cerebral A $\beta$  levels (Luo et al., 2001), providing further evidence that BACE1 accounts for the majority of  $\beta$ -secretase activity in the brain.

#### **1.5.1.3: $\gamma$ -Secretase cleavage of APP**

Following APP cleavage by BACE, the last step in A $\beta$  generation is the cleavage of the  $\beta$ -CTF by  $\gamma$ -secretase at the C-terminal end of the A $\beta$  region. This final cleavage by  $\gamma$ -secretase releases A $\beta_{40}$  or A $\beta_{42}$  (Naslund et al., 2000). The complete structure of the  $\gamma$ -secretase enzyme has not yet been fully identified but it is well established that the presenilins together with anterior pharynx defective (APH-1), nicastrin, and presenilin enhancer (PEN-2) are the core members of the enzyme complex. (Xia et al., 1997, Zhou et al., 2005). It has been originally proposed that two different  $\gamma$ -secretases termed  $\gamma_{40}$ -secretase and  $\gamma_{42}$ -secretase exist which are responsible for the generation of A $\beta_{40}$  and A $\beta_{42}$  respectively (Citron et al., 1996). However, more recently a model has been proposed to suggest a single  $\gamma$ -secretase enzyme with a broad range of activity, performing multiple cleavages sequentially along the APP-C99 fragment. The “successive cleavage” model, originally proposed by Ihara and colleagues (Qi-Takahara et al., 2005, Takami et al., 2009) provides a sequence of cleavage events by  $\gamma$ -secretase that occurs within the C-terminal fragment of APP (C99) to generate A $\beta_{40}$  and A $\beta_{42}$ . In this model, after BACE cleavage of APP (to form the N-terminal of A $\beta$ ) the remaining C-terminal part of APP-C99 is first cleaved within the transmembrane domain at the epsilon ( $\epsilon$ )-site nearest the cytosol to release the AICD. Cleavage proceeds progressively in increments towards the N-terminal of A $\beta$  at zeta ( $\zeta$ ) and  $\gamma$  sites respectively. This model also proposes that A $\beta_{40}$  and A $\beta_{42}$  are generated from a different cleavage process and depends on the initial position of  $\epsilon$ -cleavage



The  $\gamma$ -secretase enzyme is a high molecular weight aspartyl protease that cleaves type I transmembrane proteins within the hydrophobic environment of the lipid bi-layer. In addition to cleaving APP to release A $\beta$ ,  $\gamma$ -secretase also cleaves other substrates such as Notch to release the notch intracellular domain (NICD) fragment (Esler and Wolfe, 2001, Lee et al., 2002). Notch is a type I transmembrane protein which is first acted upon by a disintegrin and metalloprotease within the extra-cellular region, followed by  $\gamma$ -secretase mediated cleavage within the trans-membrane domain to liberate NICD. This fragment translocates to the nucleus where it co-activates the transcription of the genes involved in many developmental pathways (Ray et al., 1999). The  $\gamma$ -secretase enzyme also cleaves sterol regulatory element binding protein (SREBP), an integral membrane protein located in the endoplasmic reticulum consisting of N- and C-terminal domains after being acted upon by sterol sensitive protease in the luminal loop (Sakai et al., 1996). SREBP plays a significant role in cholesterol homeostasis by stimulating transcription of sterol-regulated genes and plays a role in the activation of proteins involved in cholesterol biosynthesis (Leonard et al., 1986, Wang et al., 1994, Brown and Goldstein, 1997). There are several other  $\gamma$ -secretase substrates. Examples include epithelial (E) and neural (N) cadherins, involved in cell adhesion, CD44 that acts as a signal transduction molecule and activates transcription in the nucleus, and Erb-B4, which plays a significant role in neuronal development by regulating cell proliferation and differentiation (Okamoto et al., 2001, Yarden and Sliwkowski, 2001, Marambaud et al., 2003). Due to the large number of substrates  $\gamma$ -secretase has been a difficult target to develop inhibitors and/or modulators of its activity.

### **1.6: The $\gamma$ -secretase complex components**

The  $\gamma$ -secretase complex is a multimeric protein complex composed of Presenilin 1 (PS1), Nicastrin (NCT), anterior pharynx defective-1a (APH-1a), and Presenilin

enhancer-2 (PEN-2) (Kimberly et al., 2003) (**Fig.1.6**). Its molecular weight has been reported to be different in some studies. One study reported it to be ~2MDa, whereas others reported it to be ~250KDa and ~500KDa (Li et al., 2000a, Edbauer et al., 2002, Farmery et al., 2003, Kimberly et al., 2003, Li et al., 2003b). PS1/2 which is the catalytic components of the  $\gamma$ -secretase share 67% of the overall protein sequence (reviewed in (Krishnaswamy et al., 2009). There is also evidence of the existence of distinct PS1 and PS2 complexes where PS1 containing complexes produce both A $\beta$ 40 and A $\beta$ 42 whereas PS2 containing complexes only produce A $\beta$ 42 (Lai et al., 2003, Mastrangelo et al., 2005). Other proteins that are involved in modulating A $\beta$  levels such as CD147 (**Fig.1.6**) but do not appear to be core components of the complex have also been identified (Winkler et al., 2009).

### **1.6.1: Presenilins**

The Presenilins (PS1 and PS2) are transmembrane proteins consisting of 8-10 hydrophobic domains (Sherrington et al., 1995, Lehmann et al., 1997). The gene spans more than 50 to 75kb and is organized into 12 exons, the first two corresponding to 5' untranslated regions (Alzheimer's Disease Collaborative Group, 1995; (Mitsuda et al., 1997). Two presenilin genes have been identified; presenilin 1 (PS1) located on the short and long arms of chromosome 14 and presenilin 2 (PS2) found on the long arm of chromosome 1. The PS1-holoprotein is composed of 467 amino acids with a molecular weight of 45 kDa (Sherrington et al., 1996, Lehmann et al., 1997). PSI is similar in structure to sperm integral membrane proteins (SPE) which play a role in membrane trafficking in the organelles within the Golgi (L'Hernault and Arduengo, 1992, Levitan and Petersen, 1995). The similarity to SPE may suggest that PS1 is also involved in protein trafficking. Other roles for PS1 include signal transduction during development, apoptosis and cellular calcium ion homeostasis (Marjaux et al., 2004). However, its role

in APP metabolism and processing has received the most attention. Initial evidence comes from many *in vivo* and *in vitro* studies which have shown that mutations in PS1 increase the production of the longer more pathological A $\beta$  species (Martins et al., 1995, Guo et al., 1997, Xia et al., 1997, Jankowsky et al., 2004). A subsequent study provided evidence that presenilins may have  $\gamma$ -secretase activity and represents the core catalytic subunit of the enzyme. Many reports have shown that presenilin ablation or mutagenesis of two highly conserved aspartate residues within transmembrane domains 6 and 7 result in a reduction in A $\beta$  levels *in vitro* and *in vivo* (De Strooper et al., 1999, Steiner et al., 1999, Wolfe et al., 1999, Esler et al., 2000). Furthermore, aspartyl protease inhibitors and transition state analogue inhibitors designed to target the active site of the protease, all reduce A $\beta$ 40 and A $\beta$ 42 levels and have been shown to have affinity label and bind to PS1 (Esler et al., 2000, Li et al., 2000a, Seiffert et al., 2000). In addition, physical interactions between presenilins and  $\gamma$ -secretase substrates have been identified (reviewed in (Verdile et al., 2004)). Although initial evidence strongly implicated presenilins in  $\gamma$ -secretase catalytic activity they do not exhibit typical aspartyl protease structural characteristics, in particular they lack the typical D(T/S)G motif required for the active site of an aspartyl protease. However, presenilins do contain the two aspartyl residues (e.g.: D257 and D385 for PS1) which are either critical for the active site on the  $\gamma$ -secretase complex or constitute the active site. The formation of this aspartyl catalytic site could result from one or multiple presenilin molecules. The full length PS1 protein is rapidly endoproteolytically cleaved within its characteristic large hydrophilic loop into amino- and carboxyl-terminal fragments (NTF/CTF) of ~27 and ~17 kDa, respectively (Borchelt et al., 1996, Thinakaran et al., 1996, Podlisny et al., 1997). These fragments are thought to interact with each other to form the catalytic component of  $\gamma$ -secretase (Levitan et al., 2001, Laudon et al., 2004a, Laudon et al., 2004b). The stoichiometry and the nature of the interaction between these fragments

remain unclear. It has also been shown by many studies that the NTF:CTF form a heterodimer in mammalian cells (Seeger et al., 1997, Grunberg et al., 1998, Yu et al., 1998, Beher et al., 1999) leading to suggestions that this heterodimer is the active  $\gamma$ -secretase. However, Cervantes and colleagues 2001 (Cervantes et al., 2001) provided evidence that the presenilin fragments can form a tetramer by identifying heterodimers as well as NTF and CTF homodimers in yeast. Evidence for heterodimer and NTF homodimer (but not CTF homodimer) formation has been provided by photo affinity labelled cross linking studies (Schroeter et al., 2003). This formation provides a core of aspartyl residues required for aspartyl protease activity. However, it has yet to be established whether the hypothetical “core” is formed between fragments from one PS1 molecule or multiple molecules within the complex.

The PS proteins (PS1 and PS2) share 62% amino acid identity and several lines of evidence suggest that these proteins have quite distinct functions. Mice lacking PS1 die before birth and the embryos display severe skeletal and brain deformities, whilst mice lacking PS2 develop mild pulmonary fibrosis and haemorrhages with age (Shen et al., 1997, Steiner et al., 1999, Rozmahel et al., 2002). Neuronal cultures isolated from PS1 ablated mice, when compared to those isolated from PS2 knockout mice, exhibit higher A $\beta$  production and are less sensitive to  $\gamma$ -secretase inhibitors (Lai et al., 2003). Lai and colleagues also provided evidence suggesting the existence of distinct PS1 and PS2 containing complexes (Lai et al., 2003). Evidence exists that these complexes may have a differential capacity to generate A $\beta$ , whereby PS1 containing complexes produce both A $\beta$ 40 and A $\beta$ 42, and PS2 containing complexes are involved in A $\beta$ 42 (but not A $\beta$ 40) generation (Mastrangelo et al., 2005). Placanica et al., (Placanica et al., 2009) provided further evidence for distinct PS1 and PS2  $\gamma$ -secretase complexes in the generation of A $\beta$  where they are in dynamic equilibrium, possibly under control of pen-2 expression. It

has also been suggested that PS2 is less efficient at generating A $\beta$  peptide than PS1 (Bentahir et al., 2006, Placanica et al., 2009).

Evidence for different capacities for PS1 and PS2 to process other  $\gamma$ -secretase substrates comes from a study that has shown that notch defects in PS1 null mice can be rescued with wild-type PS2, but fails to rescue APP processing (Mastroangelo et al., 2005). These findings suggest that PS2 is capable of facilitating Notch processing but is associated with only very low levels of A $\beta$  production. Although the presenilins share some sequence identity (67%), there are domains within these proteins that show sequence divergence, where transmembrane (TM) 3 and 4 and the large cytoplasmic domains show 38% and 68% sequence divergence. This information could be used to identify critical areas between these two proteins responsible for their activities.

A very large number of missense mutations have been isolated in the human presenilin genes from families with EOAD (>190 mutations in PS1, and 23 in PS2, <http://www.molgen.ua.ac.be/ADMutations>). A large number of these mutations are missense mutations involving substitution of a single amino acid. Others include small deletions, insertions or splice mutations (De Strooper, 2007). The I4Sev5 and Glu318GLY mutations are exceptions because they exhibit incomplete penetrance (Rossor et al., 1996, Helisalmi et al., 2000). Mutations in the presenilins are known to be scattered throughout these proteins and it has been proposed that these mutations may all be hypomorphic – i.e. they decrease  $\gamma$ -secretase activity (Wolfe, 2007). The decreased presenilin/ $\gamma$ -secretase activity as a result of mutations might shift the ratio of A $\beta$  production from shorter forms (e.g. A $\beta$ 40) that are less toxic (or possibly even protective) towards production of longer forms (predominantly A $\beta$ 42) that have a greater tendency to form toxic oligomers .

### **1.6.2: Nicastrin (NCT)**

Nicastrin is a type 1 transmembrane glycoprotein which was identified as a component of the  $\gamma$ -secretase enzyme complex when it was found to co-immunoprecipitate with PS1 and APP (Yu et al., 2000). It is comprised of a 670 amino acid long hydrophilic N-terminal domain, a trans-membrane domain, and a relatively short cytoplasmic C-terminus of 20 amino acid residues (Yu et al., 2000). The protein is synthesized as an endoglycosidase-H-sensitive glycosylated precursor protein which is an immature form. It is then modified by complex glycosylation in the Golgi apparatus and by sialylation in the trans-Golgi network to generate the mature nicastrin molecule (Yu et al., 2000). NCT is physically associated with presenilin and has a major role in stabilization and proper localization of presenilin to the membrane-bound  $\gamma$ -secretase complex (Kopan and Goate, 2002). NCT plays a role as a scaffold for the assembly of the  $\gamma$ -secretase enzyme complex that binds APH-1 to form the first sub-complex (Morais et al., 2003, Periz and Fortini, 2004). It is also thought that NCT plays a role in the assembly of the  $\gamma$ -secretase complex within the endoplasmic reticulum and intracellular trafficking of the complex to the cell surface (Shah et al., 2005, Zhang et al., 2005). Evidence has also been provided to suggest that NCT is essential for the interaction between the  $\gamma$ -secretase complex and APP-C99 (Shah et al., 2005).

### **1.6.3: Anterior Pharynx defective homolog-1 (APH-1)**

The Aph-1 molecule is a 30 kDa transmembrane protein comprising 308 amino acids (Goutte et al., 2002). Two human homologues of APH-1 genes exist, APH-1a and APH-1b located on chromosome 1 and 15 respectively. APH-1a exhibits isoforms, APH-1aS and APH-1aL, generated through alternative splicing of a single transcript

(Lee et al., 2002, Gu et al., 2003, Saito and Araki, 2005). APH-1a and APH-1b are expressed in certain human and mice tissues such as hippocampus, cortex, medulla, testes, lung and the large intestines (Saito and Araki, 2005, Coolen et al., 2006), whereas APH-1aS is expressed more than APH-1aL (Saito and Araki, 2005). Both APH-1a and APH-1b are multi-pass membrane proteins with seven transmembrane domains (Fortna et al., 2004) whereas APH-1aS and APH-1aL have different C-terminal sequences (Lee et al., 2002, Gu et al., 2003). *In vitro* evidence has shown that down-regulation of APH-1a and APH-1b alters the formation of the multimeric complex and strongly reduces the production of A $\beta$  (Luo et al., 2003). Knock down experiments of APH-1a result in impaired maturation of NCT and decreased expression of PS1, PS2, and PEN-2 proteins (Saito and Araki, 2005). *In vivo* experiments have provided evidence that complexes containing different isoforms of aph-1 may also have different functionality. Mice lacking APH-1a are embryonic lethal whilst those lacking APH-1b appear to be normal phenotypically (Ma et al., 2005, Serneels et al., 2005, Serneels et al., 2009), suggesting that aph1a complexes are essential for Notch signalling during embryogenesis. In the absence of APH-1a an active  $\gamma$ -secretase complex formation is disrupted (Ma et al., 2010). Collectively these data suggest that complexes containing aph-1a are active and those containing aph-1b maybe redundant.

However, aph-1b complexes have been shown to have a role in neuregulin-1 (Nrg-1) signalling. Aph-1b knockout mice show signs of schizophrenia including hypersensitivity to psychiatric drugs, sensory motor gating abnormalities and working memory deficits (Dejaegere et al., 2008). In addition, subsequent findings show that inactivation of aph-1b  $\gamma$ -secretase complexes led to a reduction in AD pathology without altering Notch related signalling (Serneels et al., 2009), suggesting the existence of different complexes that selectively process certain substrates.

Apart from the scaffolding function it shares with nicastrin, aph1 also interacts with the mature forms of PS1, nicastrin and pen-2 (Lee et al., 2002, Hansson et al., 2004, Hansson et al., 2005) on the cell surface where it binds the  $\gamma$ -secretase substrates and facilitates cleavage (Hansson et al., 2005). Structural and functional similarities between aph-1 and other proteases that possess the ability for intra-membranous cleavage such as rhomboid, (Urban et al., 2001, Lee et al., 2003a) suggests that it may also have catalytic activity, though there is yet no direct evidence for this.

#### **1.6.4: Presenilin Enhancer 2 (PEN-2)**

The Presenilin Enhancer 2 (PEN-2) is a ~12 kDa protein with 101 amino acids and consists of two trans-membrane domains with its N- and C- terminus facing the lumen of the endoplasmic reticulum (Crystal et al., 2003). Interaction of PEN-2 with other proteins aids the stability of the  $\gamma$ -secretase complex which is otherwise degraded by the proteasome in the absence of this interaction (Crystal et al., 2003, Prokop et al., 2004). PEN-2 is required for stabilization of the presenilin N- and C-terminal fragments within the  $\gamma$ -secretase complex and also contributes to the maturation of nicastrin. Further, PEN-2 is thought to contribute to the endo-proteolysis of the presenilin holoproteins into N- and C-terminal fragments (Prokop et al., 2004). Interaction of PEN-2 with APH-1 and NCT in drosophila increases the formation of presenilin fragments and promotes  $\gamma$ -secretase activity (Takasugi et al., 2003). Knockout and knockdown experiments of PEN-2 expression have shown a marked decrease in PS1 endo-proteolysis and A $\beta$  production, suggesting that PEN-2 is essential for both PS1 fragment formation and  $\gamma$ -secretase activity, (Steiner et al., 2002, Takasugi et al., 2003). PEN-2 has been shown to bind to PS1 and the “DYLSF” domain of PEN-2 and a “NF” motif on trans-membrane 4 of PS1 have been shown to be critical for this interaction



(Hasegawa et al., 2004, Kim and Sisodia, 2005). The C-terminal fragment of PEN-2 has been shown to be critical for  $\gamma$ -secretase activity, where altering the length of the PEN-2 CTF (Naruhashi et al., 1997) or introducing loss of function mutations into the CTF (Hasegawa et al., 2004, Prokop et al., 2004) reduces A $\beta$ <sub>40</sub> and A $\beta$ <sub>42</sub> levels.

Although PS, NCT, aph1 and Pen2 are known to be the core-components of  $\gamma$ -secretase there are a number of other proteins that interact with components of the  $\gamma$ -secretase enzyme or APP to modulate A $\beta$  production (Zhou et al., 2005, Chen et al., 2006). One such protein is CD147. As a major focus in this study the sections below will describe the structure, function and roles in neuronal homeostasis and in regulating A $\beta$  levels

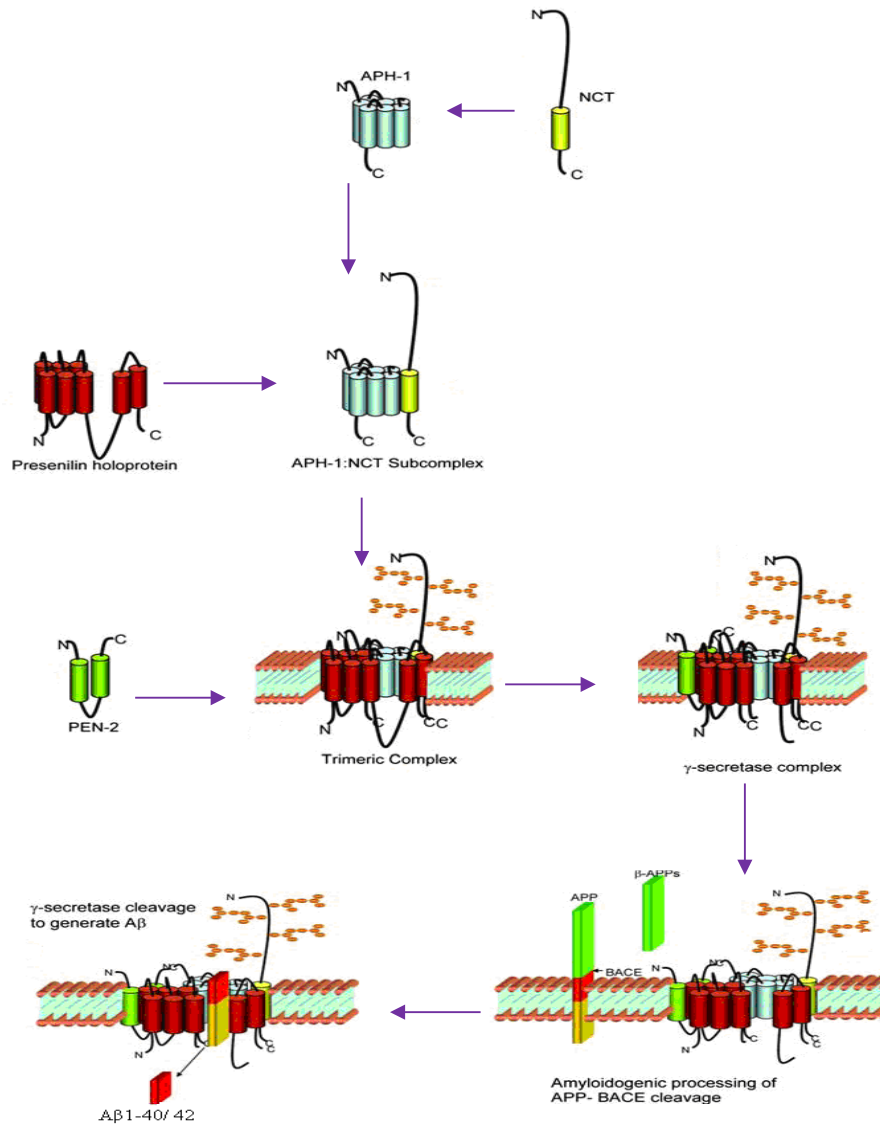


**Figure 1.6: Assembly of  $\gamma$ -secretase enzyme complex to form the active enzyme.**

NCT and APh-1 binds to form NCT: APh -1 sub complex, presenilin binds to this sub complex forming a trimeric complex that is transported to the cell surface after the post-translational modification of NCT, wherein PEN-2 attaches to the complex. Following the BACE cleavage of APP molecule,  $\gamma$ -secretase cleaves APP-C99 releasing A $\beta$ 1-40 or A $\beta$ 1-42 (adapted from (Verdile et al., 2007)).

### **1.7:CD147 is a multifunctional protein that modulates A $\beta$ levels**

The CD147 protein has been identified in various species and assigned different names (**Table 1.1**). Initially termed tumour cell-derived collagenase stimulatory factor (TCSF) because of its ability to induce matrix metalloproteinase (MMP) expression in fibroblasts, the CD147 cell membrane receptor protein is now classified as a trans-membrane glycoprotein belonging to the immunoglobulin super-family (IgSF) (Biswas and Vonderhaar, 1987, Fossum et al., 1991, Miyauchi et al., 1991, Kasinrerker et al., 1992, Biswas et al., 1995), that has been shown to induce the production of several MMPs (Kataoka et al., 1993, Biswas et al., 1995, Guo et al., 1997). It has been classified as a member of a small family of related proteins, including the teratocarcinoma antigen GP70 and the synaptic glycoprotein SDR1, that share the features of two Ig-like extracellular domains, a short cytoplasmic tail, and a single trans-membrane domain (Fossum et al., 1991, Shirozu et al., 1996). In addition to playing a vital role in foetal development, CD147 is critical to the development of the nervous system, spatial learning and memory, sensory inputs and retinal functions (Naruhashi et al., 1997, Muramatsu and Miyauchi, 2003, Zhou et al., 2005). The CD147 protein has been linked to cancer, tumour progression and arthritis. More recently this protein has been implicated in AD pathogenesis (Nabeshima et al., 2006a, Winkler, 2008, Nahalkova et al., 2010), in particular regulating A $\beta$  levels (Zhou et al., 2005, Vetrivel et al., 2008b). The following sections provides a detailed discussion on CD147 protein structure, expression and function with particular focus on neuronal functions and its role in neurodegenerative diseases such as AD.

**Table 1.1: CD147 nomenclature**

<b>Designated name</b>	<b>Species</b>	<b>Reference</b>
Extracellular Matrix Metalloproteinase-Inducer (EMMPRIN) and M6	Human	(Kasinrerk et al., 1992)
Neurothelin, 5A11 and HT7	Chicken	(Seulberger et al., 1990, Fadool and Linser, 1993, Schlosshauer et al., 1995)
OX47 and CE9	Rat	(Fossum et al., 1991, Nehme et al., 1995)
CD147, gp42	Human and Mouse	(Altruda et al., 1989, Miyauchi et al., 1991, Miyauchi et al., 1995)

### **1.7.1: Protein structure and expression.**

CD147 is composed of an extracellular domain of 187 residues, a 24-residue trans-membrane domain and a 40 amino acid cytoplasmic region (Biswas et al., 1995). Its extracellular region has two Ig domains (Domain1 and Domain 2) and an N-terminal domain with several enzyme catalytic sites. The trans-membrane (TM) domain contains a glutamic acid residue thought to be important in protein-protein association (**Fig.1.7**) (Miyauchi et al., 1990, Fossum et al., 1991).

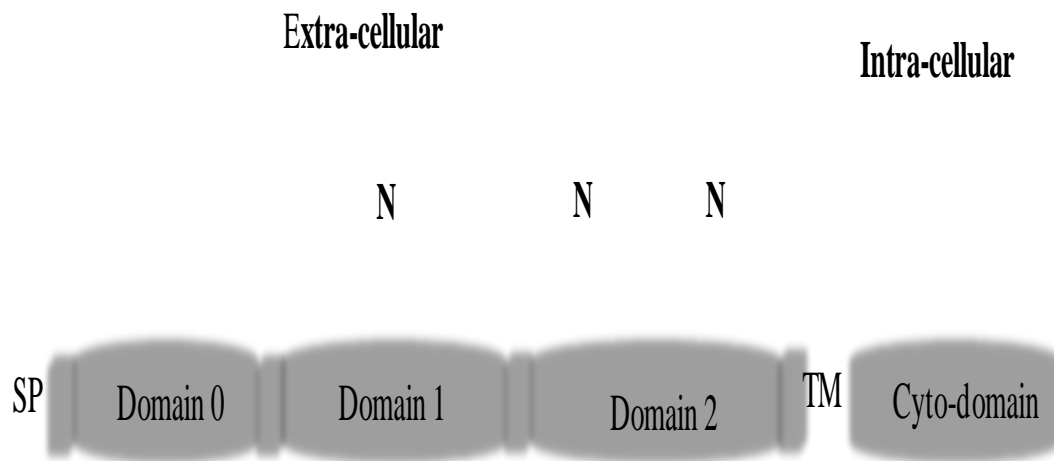


**Figure 1.7: Human CD147 protein.**

Structure showing the signal peptide sequence (SP), consensus asparagines-linked glycosylation sites (N), extracellular domains (0, 1 and 2), transmembrane domain (TM), and cytoplasmic domain (Cyto-domain) (adapted from (Belton et al., 2008)).

Although, the CD147 protein is expressed in most tissues, it is relatively highly expressed in tumours where it has been demonstrated to participate in tumour invasion and metastasis (Reimers et al., 2004, Tang et al., 2004, Tang et al., 2005, Nabeshima et al., 2006b). It is also highly expressed on activated T and B lymphocytes, dendritic cells, monocytes, macrophages, heart, early erythroid, thyroid, pre-frontal cortex and placenta (Kasinrerk et al., 1992, Kochi and Ushio, 1999, Liang et al., 2005). Patients with systemic lupus erythematosus (SLE) exhibit elevated CD147 levels in activated CD3+ T Cells compared to healthy donor, suggesting its involvement in the progression of SLE (Pistol et al., 2007). In the brain CD147 is highly expressed in neurons within the cornu ammonis (CA) region and dentate of the hippocampus (Fan et al., 1998). Other brain areas that express CD147 include the upper layers of the cortex, with the CA region of the hippocampus and neuronal processes showing weak expression (Vetrivel et al., 2008b).

CD147 can also be detected in conditioned media from tumour cell cultures (Biswas, 1984, Tang et al., 2004, Hanata et al., 2007), in supernatant of lipid loaded macrophages (Yue et al., 2009) and more recently detected in human serum (Moonsom et al., 2010) indicating that CD147 can be secreted and is present in a soluble form. The function(s) of soluble CD147 remain unclear, however, it has been shown to stimulate stromal fibroblast cells to express metalloproteases (MMPs), facilitating matrix degradation, tumour invasion and metastasis (Tang et al., 2004). Similar functions have been suggested for soluble CD147 in atherosclerotic plaque destabilization (Yue et al., 2009).

### **1.7.2: Functions of CD147**

In non-diseased tissue CD147, has been shown to interact/associate with several proteins. Its trans-membrane and cytoplasmic domains play a critical role in protein-

protein interactions associated with the plasma membrane (Kirk et al., 2000). In pathology, CD147 is implicated in some diseases such as cancer where it facilitates its metastasis through MMPs induction and systemic lupus erythematosus (SLE) (Biswas, 1984) that is characterized by activated T Lymphocytes. The CD147 protein also has important roles in the central nervous system and more recently has been implicated in neurodegenerative diseases such as AD (Nahalkova et al., 2010). The following sections will discuss some of the more established neuronal and non-neuronal roles for CD147.

### **1.7.3: Non neuronal functions of CD147**

A number of functions for CD147 appear to be due to its ability to regulate metalloproteinases (MMPs), a family of proteolytic enzymes which are capable of degrading molecules of the extracellular matrix (Sanderson et al., 2005). In reproduction, degradation of the endometrium after embryo implantation is facilitated by MMPs, which is influenced by CD147 expression in fibroblasts (Li et al., 2001, Chen et al., 2007). Induction of MMPs by CD147 in human placenta promotes parturition by inducing foetal membrane rupture and detachment from the uterus. Roles for CD147 in reproduction also appear to extend to fertilization where CD147 knock-out mice are infertile, due to deficiencies in spermatogenesis (Igakura et al., 1998) and roles in sperm-egg interaction (Sexena et al., 2001).

CD147 facilitated induction of MMPs also appears to have a role in stromal cells of cancer tumours where it maintains extracellular matrix integrity and cell communication through association with integrins (Curtin et al., 2005). Integrins are cell surface receptors composed of alpha and beta chain heterocomplexes that serve as bi-directional transducers of extracellular and intracellular signals during cell adhesion, proliferation, differentiation and tumour progression. The structural and functional properties of both



integrins and CD147 provide a conducive environment for the interaction of the two proteins.

Tumorigenic cells expressing CD147 induce MMP expression by neighbouring fibroblasts facilitating cancer cell migration (Biswas, 1982, Kataoka et al., 1993, Biswas et al., 1995, Heppner et al., 1996). Further evidence that CD147 regulates MMP expression during cancer metastasis is provided by studies in human breast cancer and glioblastoma cell lines where suppression of CD147 by antisense RNA decreased MMP-2, MMP-9 and also down-regulated vascular endothelial growth factor (VEGF) (Liang et al., 2005, Tang et al., 2005). The consequences of CD147 induction of MMP extends to tissue repair where diseased eye corneas have elevated levels of CD147 localized to those areas of greatest MMP expression (Gabison et al., 2005). The mechanism by which CD147 regulates MMP production is largely unclear, although its glycosylation is necessary for its action as de-glycosylated CD147 induces MMP secretion from a breast cancer cell line (Sun and Hemler, 2001, Tang et al., 2004). One possible mechanism is through the mitogen-activated protein kinase (MAPK) signalling pathway which is known to regulate MMP production. Knock-down of CD147 by siRNA has been shown to inhibit phosphorylation of the MAPK signalling molecules SAPK/JNK, suggesting a possible mechanism by which CD147 regulates MMP levels (Qian et al., 2008).

Evidence also exists that CD147 has a role in transport of products from the glycolytic pathway. The monocarboxylate transporter (MCT) protein catalyses the protein linked monocarboxylates including lactate and pyruvate, glucose metabolites necessary for the maintenance of metabolic homeostasis within most cells (Halestrap and Price, 1999, Kirk et al., 2000). Of the four isoforms, only MCT1 and MCT4 interact with CD147

and this association facilitates the expression of both MCTs and CD147 (Kirk et al., 2000). These two isoforms require direct interaction with CD147 for their transport to the plasma membrane (Kirk et al., 2000) in order to mediate lactate transport across the plasma membrane (Wilson et al., 2002). Deficiency in MCT 1 and MCT 4 in the retina affects the photoreceptor cells due to reduced lactate transport resulting in blindness. Similarly CD147 absence or depletion leads to impaired surface expression of MCT1, which results in the death of photoreceptor cells due to lack of lactate transport (Philips et al., 2003). Taken together these findings indicate that CD147 acts as a chaperone for MCT1 and MCT4 translocation to the plasma membrane.

The identification that CD147 is a signalling receptor for cyclophilin A (CyPA) provided a novel function for this transmembrane glycoprotein (Yurchenko et al., 2002). CyPA is an ubiquitously expressed intracellular protein belonging to the immunophilin family, and is known to function as a ligand for the immunosuppressive drug, cyclosporine (Liu et al., 1991, Colgan et al., 2005) and shown to also regulate protein trafficking in cells (Brown et al., 2001, Chklovskaya et al., 2001, Ansari et al., 2002, Huang et al., 2002). Elevated cyclophilins levels have been reported in several inflammatory conditions including severe sepsis (Tegeder et al., 1997), vascular smooth muscle cell disease (Jin et al., 2000), and rheumatoid arthritis (Billich et al., 1997). These inflammatory effects may be mediated by cyclophilins-CD147 interactions which initiate/progress the recruitment of leucocytes, which express CD147 receptor, (Yurchenko et al., 2001, Yurchenko et al., 2005) into inflamed tissues (Sherry et al., 1992, Xu et al., 1992, Allain et al., 2002).

The roles of CD147 in cell development, tumour progression, cell metabolism and signalling have been well studied. However, its role in the CNS has received less

attention. Cell signalling and its ability to interact with a number of proteins, including cyclophilins, has suggested roles for CD147 in neuroprotection and in the pathogenesis of neurodegenerative diseases such as AD. These roles are discussed further below.

#### **1.7.4: Neuronal functions of CD147**

Expression of CD147 (*Basigin*) has been shown to be extensively expressed in a number of regions of the mouse CNS (Fan et al., 1998). The regions include: mitral cells in the olfactory bulb; limbic system including the amygdala and piriform cortex; hypothalamus including the paraventricular nucleus and the ventromedial nucleus, the Purkinje cells in the cerebellum; the pontine nucleus in the pons; thalamus; retina including the outer and inner granular layers and ganglion cells (Fan et al., 1998). Such extensive expression in many regions of the CNS suggests a number of functions and particularly the relatively high expression in the limbic system (Fan et al., 1998), would suggest functions in memory and behaviour. This was addressed by Naruhashi and colleagues (Naruhashi et al., 1997) where a number of behavioural tasks were carried out in mice lacking CD147. Compared to wild-type and heterogeneous (*Basigin* +/-) mice, the CD147 null mice (*Basigin* -/-) performed worse in memory and learning tasks (e.g. Y-maze and water finding tasks). In addition CD147 null mice were less sensitive to light, pain, and induced electric shock, reflecting the importance of CD147 in sensory functions.

Through its interaction, the CD147 receptor has been proposed to mediate neuroprotection mediated by CyPA (Boulos et al., 2007) which is abundantly expressed in the brain, primarily localized to neurons (Goldner and Patrick, 1996) and co-localises with neuronal CD147 receptor in the hippocampus and cortex of rodents (Lad et al., 1991, Goldner and Patrick, 1996, Fan et al., 1998). Although its role in the CNS is undefined,

CyPA has been implicated in neuronal differentiation (Hovland et al., 1999, Chiu et al., 2003, Song et al., 2004), cortical plasticity (Arckens et al., 2003) and embryonic neuronal growth and development (Nahreini et al., 2001). CyPA is also up-regulated in neuronal cultures following pre-conditioning treatments (Meloni et al., 2005). Over-expression of CyPA in primary cortical neuronal culture has been shown to attenuate neuronal death induced by oxidative stress or ischemic insults (Boulos et al., 2007). Similar protection was also achieved with the addition of exogenous human CyPA protein to neuronal cultures. Activation of the CD147 receptor by CyPA was shown to stimulate the phosphorylation of ERK1/2, which activates the anti-apoptotic proteins Bcl-2 (Riccio et al., 1999) and Bag-1 (Perkins et al., 2003) and phosphorylation-mediated inactivation of pro-apoptotic proteins such as Bim (Biswas and Greene, 2002) and Bad (Bonni et al., 1999, Zhu et al., 2002). These downstream pro-survival signalling events may be one mechanism through which CyPA/CD147 interaction protects neurons from toxic insults. Although a role for CD147 in neuronal protection has been reported, its involvement in neurodegenerative diseases has been directed at AD, where it appears to control levels of A $\beta$ .

#### **1.7.5: CD147 interactions with $\gamma$ -secretase and modulating beta amyloid levels.**

A role for CD147 in modulating A $\beta$  levels came about following the observation that knock-down of CD147 resulted in increased levels of secreted A $\beta$ 40 and A $\beta$ 42 from cells (Zhou et al., 2005, Vetrivel et al., 2008b) (**Fig.1.8B**). The mechanism by which CD147 modulates A $\beta$  accumulation is unclear, with two studies proposing different mechanisms of action. Zhou and colleagues (Zhou et al., 2005) showed that CD147 is possibly a regulatory component of the  $\gamma$ -secretase complex. In their study it was

observed that CD147 depletion using RNAi resulted in elevated A $\beta$ 40/42 production, without affecting expression levels of NCT, pen-2, aph-1 and PS1 (Zhou et al., 2005). However, Vetrivel and colleagues (Vetrivel et al., 2008b) showed that CD147 did not interact with the other  $\gamma$ -secretase complex components and concluded that it was not an integral part of the complex. Instead, the authors showed that CD147 mediates the degradation of A $\beta$  possibly via stimulating the production of the MMPs, which have previously been shown to degrade A $\beta$  (Backstrom et al., 1996, Nalivaeva et al., 2008, Kong et al., 2010). The discrepancies between these two studies could be due to methodological differences and it is possible that CD147 may have varying functions in different cell lines. Vetrivel and colleagues used HEK-293 (compared to CHO cells used in the Zhou et al study) in over-expressing CD147. Nahalkova and colleagues (Nahalkova et al., 2010) recently provided further evidence that CD147 interacts with  $\gamma$ -secretase components and may influence A $\beta$  production. The authors showed that the sub-cellular distribution of CD147 was altered from a cell surface localisation in PSwt and PS1-/- cells, to a peri-nuclear localisation in PS2-/- cells. This study not only indicated that specific components of  $\gamma$ -secretase interact with CD147, but also implied that CD147- $\gamma$ -secretase interaction may occur in mitochondria-associated membranes (MAM), the cellular fraction where the majority of  $\gamma$ -secretase activity is proposed to be localized (Area-Gomez et al., 2009, Schon and Area-Gomez, 2010).

Purification and biochemical characterization of interactors of endogenous  $\gamma$ -secretase in HEK-293 cells showed that CD147, together with TMP21 a member of the p24 cargo-protein family, which functions in quality control and protein transport in the ER and Golgi (Li et al., 2000a), co-purified in a high molecular complex with  $\gamma$ -secretase (Winkler et al., 2009). However, these proteins could not be affinity captured with  $\gamma$ -secretase inhibitors, indicating that they are not part of the active  $\gamma$ -secretase complex.

These findings support the notion that both CD147 and TMP21 may act to control A $\beta$  levels (**Fig.1.8A**) within the cell but they most likely are not part of the core components of the  $\gamma$ -secretase complex, thereby affecting A $\beta$  levels indirectly.

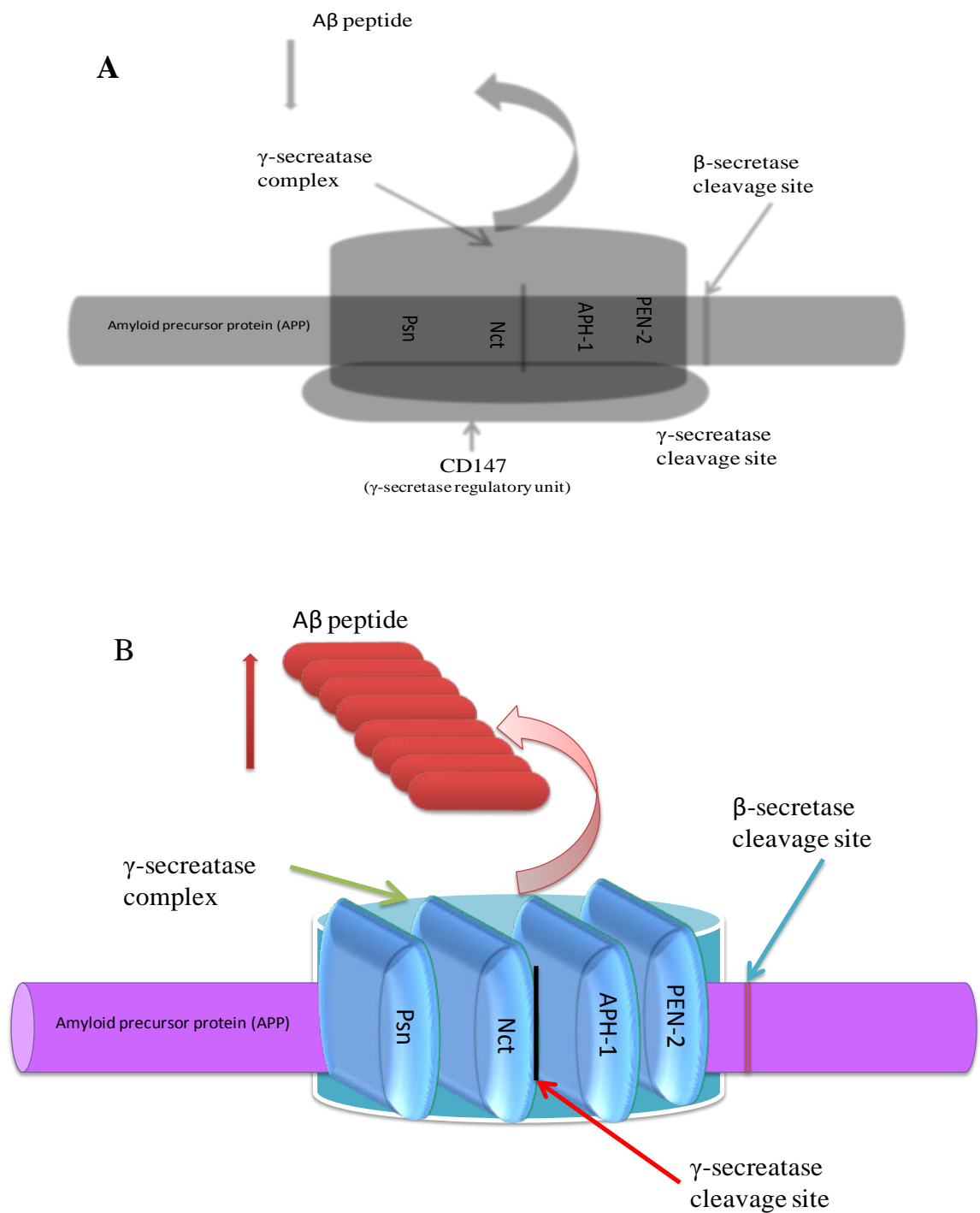


**Figure 1.8: The  $\gamma$ -secretase complex proteins.**

Proteins of the  $\gamma$ -secretase complex (Psn, Nct, APH-1 and PEN-2) with CD147 as a regulatory subunit of the  $\gamma$ -secretase complex showing reduced generation of A $\beta$  peptides (A) and without CD147 showing increased generation of A $\beta$  peptides (B).

### **1.7.6: CD147 expression in AD.**

Considering the roles of CD147 in neuro-protection and modulating A $\beta$  levels, it would be conceivable that modulating CD147 transcription or its expression would impact on its activity. Apart from *in vitro* over-expression and knock-down studies in proof-of-concept studies, the effects of modulating CD147 transcription/expression on AD pathology have not been explored. Indeed, whether CD147 transcription or protein expression is altered in AD has not been fully examined. Only one study has investigated CD147 protein expression levels in different brain regions in a small number of control and AD brain samples (Nahalkova et al., 2010). The numbers used (n=3/group) were too small to show significant differences in CD147 levels, however qualitative analysis of immunostained tissue sections revealed that CD147 staining was more intensive in the neurons and capillaries in both frontal cortex and thalamus of AD compared to control brain. More detailed, quantitative analysis in a larger number of tissue samples is required to determine if CD147 protein expression is significantly altered in AD. In addition, correlations with plaques and NFTs would be required to determine if CD147 expression is significantly associated with AD pathology.

Evidence also exists that CD147 may be modulated at the transcription level. One study investigated the presence of natural anti-sense transcripts (NATs) in AD associated genes including PRESNILINS, BACE1/2, APP, APOE, TAU, NICAISTRIN, PEN2, APH1A/B as well as CD147 (Guo et al., 2006). The exact function of NATs remain unclear, however they are thought to play a role in suppressing gene expression (Yelin et al., 2003, Alfano and Poli, 2005). The authors showed that NATs were present in CD147 and 3 other genes, namely APP, BACE2, and APH1A critical for A $\beta$  production. These results suggest that NATs may have a role in modulating A $\beta$



production, by controlling expression of genes important in APP metabolism including *APP* itself, components of A $\beta$  generating enzymes and CD147. Polymorphisms or other genetic variations in the CD147 gene and associations with AD have yet to be investigated; however if such variations exist, particularly in the promoter, they may impact on A $\beta$  accumulation. Such variations may alter binding of transcription factors such as sterol carrier protein 2 (SCP-2), which is known to control CD147 expression by binding its promoter region, in turn altering  $\gamma$ -secretase activity (Ko and Puglielli, 2007). Accumulated evidence presented above, indicates a role for the multifunctional CD147 receptor in AD pathogenesis, possibly by modulating A $\beta$  levels through altering production or clearance. However, its involvement in AD pathogenesis may not be limited to A $\beta$ .

Many pathological conditions involving inflammation are associated with increased CD147 expression in tissues and cells. These include lung inflammatory diseases (Foda et al., 2001, Hasaneen et al., 2005), rheumatoid arthritis (Kontinen et al., 2000, Tomita et al., 2002, Zhu et al., 2006, Yang et al., 2008, Damsker et al., 2009), systemic lupus erythematosus (SLE) (Pistol et al., 2007), chronic liver diseases induced by hepatitis C virus (HCV) (Shackel et al., 2002), atherosclerosis (Spinale et al., 2000, Choi et al., 2002, Yoon et al., 2005, Siwik et al., 2008) and ischemia (Boulos et al., 2007, Waldow et al., 2009). Inflammatory mediated increases in CD147 levels are thought to be a mechanism by which MMPs are activated and potentiate tissue repair and or remodelling, for example in instances of myocardial infarction (Spinale et al., 2000, Siwik et al., 2008, Nie et al., 2009) or destabilization of atherosclerotic plaques (Yoon et al., 2005). CyPA- CD147 interactions also appear to play important roles in inflammation. The up-regulation of CD147 expression observed in most inflammatory diseases, overlap with an up-regulation of CyPA. This is thought to contribute to the

recruitment of immune cells to sites of inflammation via a chemokine-like activity (Yurchenko et al., 2005). Pro-inflammatory leucocytes have been reported to have increased expression of CD147, compared to non-inflammatory cells (Zhu et al., 2005). This may facilitate the interaction between leucocytes and thereby further promoting leukocyte recruitment. Recent evidence for this was shown by Damsker and colleagues (Damsker et al., 2009), where activated CD4<sup>+</sup> T cells showed enhanced CD147 expression. The CyPA- CD147 interaction may also contribute to MMP production. In an apoE deficient mouse model of atherosclerosis, knock-down of CD147 and the presence of cyclophilin inhibitor during cell differentiation, hindered up-regulation of MMPs. Whereas the presence of CyPA up-regulated MMPs and both CD147 and CyPA were found in atherosclerotic plaques in these mice. The results suggested that CyPA/CD147 pathway may have a role in atherosclerotic plaque pathology.

The presence of CD147 mRNA transcripts in microglia (Inoue et al., 1999) and astrocytes (Meeuwssen et al., 2003) suggests a potential role for this protein in inflammatory processes mediated by these cells. Indeed, it may have a similar role as it has in the periphery where it could facilitate chemokine-mediated recruitment of inflammatory cells. However, at present there is no evidence that CD147 can mediate release of cytokines from astrocytes or microglia. The presence of CD147 in astrocytes may also mediate other functions. Since CD147 is up-regulated in astrocytes in a mouse model of permanent focal cerebral ischemia and co-localises with MMP-9 suggests its participation in neurovascular remodelling (Kleene et al., 2007) through ATPase in astrocytes which bound to CD147 and facilitated lactate transport via the astroglial monocarboxylate transporter 1 (MCT1) (Maekawa et al., 2008). Astrocytic lactic transport facilitated by MCT and activated by CD147 has important implications in maintaining glucose metabolism “glycolytic flux” in the brain (Gandhi et al., 2009).

This has implications in AD, as brain glucose metabolism is impaired in AD individuals with mild cognitive decline (MCI) and transgenic mouse models of AD (Bigi et al., 2003, Hooijmans et al., 2007).

## **1.8: Regulating CD147 expression.**

### **1.8.1 Control of CD147 expression by Sterol carrier protein (SCP)**

The expression of CD147 is controlled by sterol carrier protein 2 (SCP-2), a protein that is involved in trafficking and intracellular utilization of cholesterol and other lipids. The SCP protein plays a key role in cholesterol metabolism as it facilitates in cholesterol uptake (Hirai et al., 1994, Colles et al., 1995, Lipka et al., 1995, Moncecchi et al., 1996, Schroeder et al., 1998, Atshaves et al., 1999), intracellular transport (Puglielli et al., 1995), esterification (Murphy and Schroeder, 1997) and oxidation (Chanderbhan et al., 1986, Yamamoto et al., 1991). In addition it has been shown to remodel lipid composition, structure and function of lipid rafts (Schroeder et al., 2007). The levels of SCP are altered in a number of diseases where lipid metabolism is abnormal, including diabetes and Zellweger syndrome, where patients lack SCP-2 and are deficient in fatty acid oxidation and normal lipid metabolism (reviewed in (van Heusden et al., 1990, Wirtz, 1997)). In the neurodegenerative disease, Niemann-Pick Type C disease, where there is failure of cholesterol trafficking within the endosomal-lysosomal pathway caused by mutation in the NPC protein (Nixon, 2004, Lo et al., 2010, Gallala et al., 2011), there is a marked reduction in levels of the 13KDa SCP-2 protein and accumulation of lipids in the lysosomes and Golgi (Roff et al., 1992). Interestingly, some intriguing parallels exist with NPC and AD, such as NFT formation, lysosomes dysfunction and accumulation of A $\beta$  (reviewed in (Nixon, 2004).

The SCP-2 gene is part of a fusion gene that contains two initiation sites encoding a 15.4 kDa (pro-SCP-2) and a 58.9 kDa (SCP-x) protein (Ohba et al., 1994, Ohba et al., 1995). The 58.9 kDa SCP-x protein undergoes a post-translational cleavage process to yield a mature 12.9 kDa SCP-2 where it has been shown to translocate to the nucleus and activate CD147 transcription (Ko and Puglielli, 2007). In contrast, expression of pro-SCP-2 has been shown to abolish activity of 12.9 kDa SCP-2 and inhibit CD147 transcription, resulting in an increase in A $\beta$  production. SCPx/SCP-2 expression and synthesis has been shown to be regulated by hormones (McLean et al., 1989, Mendis-Handagama et al., 1998), hypolipidemic drugs, lipid rich conditions (Kraemer et al., 1995) and during development. (Trzeciak et al., 1987, Baun, 1993, Mori et al., 2009). Although over-expression and knockdown studies have revealed that SCP-2 can regulate CD147 levels, impacting on A $\beta$  production, whether regulating SCP-2 levels impacts on CD147 expression has yet to be determined.

### **1.8.2: Regulation of SCP and $\gamma$ -secretase activity by cholesterol**

The largest pool and concentration of cholesterol in the body exists in the brain where it is a constituent of cell membranes and myelin. Cholesterol is important for normal brain function and defects in cholesterol metabolism are associated with serious neurological and mental dysfunctions (Tint et al., 1994). Brain cholesterol is efficiently protected from exchange with circulating lipoproteins by the blood-brain barrier (BBB) and thus most of the cholesterol found in the brain is synthesized locally, although at a low rate. Alterations in cholesterol metabolism occur with age and have been implicated in both increased AD risk and progression of this disease (Jarvik et al., 1995, Igbavboa et al., 1996). Cardiovascular risk factors such as hypercholesterolemia, increased LDL and

reduced HDL levels, hypertension, obesity and type II diabetes make important contributions to the risk of developing AD. These risk factors also impact on disease pathogenesis and are known to modulate the levels of key AD associated proteins including A $\beta$ . In neurons and other cell lines cholesterol levels modulate APP metabolism modulating secretase activity (Racchi et al., 1997, Simons et al., 1998b, Galbete et al., 2000a, Kojro et al., 2001, Runz et al., 2002). Evidence exists that cellular sites that are rich in cholesterol and sphingolipid-rich membranes microdomains (so called lipid rafts; (Lee et al., 1998, Wahrle et al., 2002), contain BACE1 and the  $\gamma$ -secretase complex, promoting A $\beta$  production at these sites (reviewed in (Cheng et al., 2007)). Knowing that SCP has a role in nearly all aspects of cholesterol metabolism and also facilitates CD147 transcription, it is conceivable that changes in cholesterol homeostasis (i.e. under cholesterol loading) will alter levels of SCP, thereby impacting on CD147 levels. Indeed cholesterol enrichment in rat aortic smooth muscle cells resulted in an increased SCP mRNA and protein levels of SCPx and SCP-2 protein (Kraemer et al., 1995), providing evidence that cholesterol and its derivatives can regulate SCP expression. Whether this results in changes in CD147 levels, thereby impacting on A $\beta$  levels remains to be determined. Given the apparent relationship between cholesterol and A $\beta$  it is important to investigate factors involved in cholesterol transport and metabolism such as sterol carrier protein (SCP).

### **1.12: Hypothesis**

Alzheimer's disease is a very heterogeneous and a multifactorial ageing disorder of the nervous system. Accumulation and toxicity of the A $\beta$  protein are key mediators of neurodegeneration in AD and its levels can be modulated through altering its production and clearance. A number of factors and cellular pathways (and proteins within these

pathways) are known to influence the production and or clearance of A $\beta$ . The CD147 protein has recently been implicated in AD pathogenesis, in particular regulating A $\beta$  levels. The roles of CD147 in cell development, tumour progression, cell metabolism and signalling have been well studied. However, its role in the CNS has received less attention. Cell signalling and its ability to interact with a number of proteins, including cyclophilins, has suggested roles for CD147 in neuroprotection and in pathology of neurodegenerative diseases such as AD. Considering the roles of CD147 in neuroprotection and modulating A $\beta$  levels, it would be conceivable that modulating CD147 transcription or its expression would impact on its activity. Apart from *in vitro* overexpression and knock-down experiments in proof-of-concept studies, the effects of modulating CD147 transcription/expression on AD pathology have not been explored. Indeed, whether CD147 transcription or protein expression is altered in AD or in the presence of risk factors has not been fully examined. One such factor is cholesterol metabolism, which could impact on CD147 expression through regulating one of its major transcription regulators, Sterol Carrier Protein (SCP-2).

### **1.13: Aims**

This thesis explores the effects of modulating CD147 expression on neurodegeneration and AD pathogenesis and addresses the following specific aims:

1. To determine if cholesterol and A $\beta$  accumulation alters CD147 protein levels *in vitro* and alter neuronal toxicity.
2. To determine if cholesterol alters CD147 levels in a mouse model of AD.
3. To determine if CD147 protein levels are altered in AD brain.
4. To determine if polymorphisms within the promoter region of CD147 are associated with AD and correlate with A $\beta$  accumulation.

## CHAPTER 2

### Materials and Methods

#### 2.1: Materials

**Table 2.1:** Commonly used chemicals

CHEMICAL	SUPPLIER
Ammonium persulphate (APS)	Bio-Rad Irvine, CA.- USA
Acrylamide	Bio-Rad Irvine, CA.- USA
Aprotonin	Sigma Saint Lous, MO - USA
Ammonium chloride (NH <sub>4</sub> CL)	Sigma Saint Lous, MO - USA
Adenosine triphosphate (ATP)	Sigma
Agarose (Biotechnology grade)	Ameresco
Ampicillin (sodium salt)	Sigma
Agar	Amresco
Bacto-tryptone	Difco
Bacto-Yeast extract	Difco
Bis-tris	Bio-Rad Irvine, CA.- USA
Bicine	Bio-Rad Irvine, CA.- USA
Bradford reagent	Bio-Rad
Calcium chloride	BDH
Dithiotreitol (DTT)	Sigma Saint Lous, MO - USA
D-(+)-Glucose	BDH

Dimethylsulphoxide (DMSO)	Sigma
Di-sodium hydrogen orthophosphate	Sigma
DNA molecular weight marker standard (1.0 kb ladder)	Promega
DNA molecular weight marker standard (Lambda HindIII digest)	Promega
Deoxynucleotide triphosphates (dNTPs)	Promega
Ethylenediaminetetra acetic acid (EDTA)	BDH chemicals Pty. Ltd., Vic. - Australia
Ethylphenyl-polyethylene glycol (NP40)	ICN Biomedicals, Inc. Aurora, Ohio - USA
Ethanol	BDH chemicals Pty. Ltd., Vic. - Australia
Ethidium bromide	Sigma
Glacial acetic acid	BDH
Glycine	Bio-Rad Irvine, CA.- USA
Glycerol	Sigma
Human recombinant cyclophilin A (hrCyPA)	Biomol
Hydrochloric acid	BDH
Isopropyl alcohol	BDH
Isopropylthio- $\beta$ -D-galactoside (IPTG)	Boehringer Mannheim
Kanamycin sulphate	Sigma
Leupeptin	Sigma Saint Lous, MO - USA
Methanol	BDH chemicals Pty. Ltd., Vic. - Australia
Magnesium chloride	BDH



M-MLV Reverse transcriptase, RNase H minus Point mutant	Promega
N,N,N,N,N'-Tetra-methyl thylenediamine (TEMED)	Bio-Rad Irvine, CA.- USA
N <sub>1</sub> N-dimethylformamide	BDH
Phenylmethyl-sulfonyl fluoride (PMSF)	Sigma Saint Lous, MO - USA
Phosphate buffered saline (PBS)	Fisher Biotech International Ltd., Perth - Australia
Potassium chloride	BDH
Protein molecular weight marker	Invitrogen
Protease inhibitors	Roche
<i>Pfu</i> DNA polymerase	Promega
RNasin ribonuclease Inhibitor	Promega
Sodium dodecylsulfate (SDS)	Bio-Rad Irvine, CA.- USA
Restriction enzymes	Promega, New England (NEB) Biolabs
Sodium acetate	BDH
Sodium dihydrogen orthophosphate	Sigma
Sodium dodecyl sulphate (SDS)	Sigma
Sodium hydroxide	BDH
Trizol reagent	Invitrogen
Trizma base	Sigma
Tween20	Sigma
<i>T4</i> DNA ligase	Promega

**Table 2.2:** Preparation of buffers/solutions and reagents

<b>SOLUTION</b>	<b>PREPARATION</b>
Acrylamide/bis (49.5%/3%)	A stock solution was made by dissolving 96g of acrylamide and 6g of bis-acrylamide in double distilled water (DDW) making up to 2 litres and the stock solution stored at 4 °C.
Ammonium persulfate (10% w/v APS)	A stock solution was made by dissolving 1g APS powder in DDW making the final volume to 10 ml, Aliquoted (1ml) and stored at -20°C
Anode Buffer (10x stock solution)	A stock solution was made by dissolving 242.2g Tris-chloride in DDW making up to 1 litre
Ampicillin	A stock solution was made by dissolving 50 mg/ml stock in WFI, sterilised by microfiltration (0.2 µm) and stored at -20°C
Aβ42	Aβ42 was prepared by dissolving 1mg in 180µl 20mM NaOH, 630µl Baxter water and 90µl 10x PBS pH7.4 and sonicate for 5 minutes. Centrifuge and transfer supernatant into a new tube. Measure absorbance on a Shimadzu UV/VIS Spectrophotometer at 214nm (1:24 dil.). Calculate concentration by multiplying OD by the correction (15.45) and dilution (25) factors.
Cholesterol (5mg/ml)	Cholesterol working solution was prepared by dissolving 40mg/ml cholesterol stock in 6 ml sterile Baxter water

Cathode Buffer (10x stock solution)	A stock solution was made by dissolving 121.1g of Tris, 179.2g tricine and 10g SDS in DDW, making the final volume to 1 litre.
Carbonate/Bicarbonate Buffer (50mM)	50mM carbonate/bicarbonate buffer consisted of 0.26g of Na <sub>2</sub> CO <sub>3</sub> , 0.21g of NaHCO <sub>3</sub> , with addition of DDW made up to 50ml and adjusted to pH 9.6 using HCl.
DNA loading dye	6x stock prepared in 1 x TAE buffer and containing bromophenol blue (0.25%), xylene cyanol ff (0.25%) and 30% glycerol
dNTPs (10 mM stock solution)	A stock solution was made by mixing 100 µl of each constituent (dATP, dTTP, dCTP and dGTP each at 100 mM) with 600 µl of WFI, dispensing 100 µl aliquots and stored at -20°C
Ethidium bromide	Prepared as 10 mg/ml stock with WFI. Stored in the dark, at 4°C
ELISA Blocking Buffer	Blocking Buffer was prepared by dissolving 0.25g of bovine serum albumin (BSA: Sigma Chemical Co., USA) into 25ml of PBST.
ELISA Standards (Aβ40)	Standards were prepared by diluting 1mg/ml Aβ40 stock with PBST to concentrations ranging from 15.625 pg/ml to 1µg/ml
ELISA	Detection antibody solution were prepared by diluting 0.125g BSA in 12.5ml of PBST and 12.5µl of secondary antibodies (R208) (1:1000) for each

	plate. The Neutravidin HRP solution was prepared by the addition of 1.25µl of nHRP and 12.5ml of PBST (1:10000).
MgCl <sub>2</sub> (1M)	MgCl <sub>2</sub> (1M) was prepared by dissolving in WFI and sterilised by microfiltration/0.2 µm
MgSO <sub>4</sub> (1M)	MgSO <sub>4</sub> (1M) was prepared by dissolving in WFI and sterilised by microfiltration/0.2 µm
MOPS SDS running buffer	Supplied as 20x stock (Invitrogen) and composed of MOPS (1 M); Tris Base (1 M); SDS (69.3 mM); EDTA (20.5 mM) made up in ultrapure water.  Unadjusted 1x buffer is pH 7.7
NuPAGE lauryl dodecyl sulphate (LDS) sample buffer	Supplied as 4x stock (Invitrogen) and composed of glycerol (4 g); Tris-Base (0.682 g); Tris HCl (0.666 g); LDS (0.8 g); EDTA (0.006 g); Serva Blue G250 (0.75 ml of 1% solution); phenol red (0.25 ml of 1% solution) made up in 10ml of ultrapure water.  Unadjusted 1x buffer is pH 8.5
NuPAGE transfer buffer	Supplied as 20x stock (Invitrogen) and composed of bicine (500 mM); Bis-Tris (500 mM); EDTA (20.5 mM); chlorobutanol (1 mM) made up in ultrapure water. Unadjusted 1x buffer is pH 7.2
Oligonucleotides (Custom)	Synthetic oligonucleotides were ordered as 250ng/ml solutions from Proligo (USA) and stored at -20°C
Phosphate buffered saline (PBS)	10x stock was prepared by dissolving 11.5 g of di-

pH7.5	sodium hydrogen orthophosphate anhydrous (80 mM), 2.96 g sodium dihydrogen orthophosphate (20 mM), 5.84 g sodium chloride (100 mM) in Milli-Q water to 1000 ml
Sodium acetate	Prepared as 3 M solution (pH 5.2) in Milli-Q, adjusted with glacial acetic acid and autoclaved
TAE	A one litre, 50x stock solution was prepared by combining Trizma base (242 g), 57.1 ml of glacial acetic acid and 100 ml of 0.5 M EDTA (pH 8.0) with Milli-Q water
TB Buffer	HEPES (10 mM), CaCl <sub>2</sub> (15 mM), KCl (250 mM) were dissolved in WFI and the pH adjusted to 6.7 with KOH, prior to adding MnCl <sub>2</sub> (55 mM). The solution was sterilised by microfiltration/0.2 µm and stored at -4°C

**Table 2.3:** Special equipment list

<b>EQUIPMENT</b>	<b>COMPANY</b>
Dry Block Heater	Ratek Instruments Australia
Electrophoresis Power Supply	Amersham Pharmacia Biotech
FLUOstar Optima Spectrophotometer	BMG Labtech
Florescent Microscope	Olympus
Gene Pulser Xcell	Bio-Rad
IBlot	Invitrogen
Mastercycler Gradient	Eppendorf
Qp RT-PCR (BioRad)	Bio Rad – South Africa
Scanner, UMAX 1220S	UMAX Technologies Inc., CA.- USA
Sonifier 450	Branson
UVmini-12 Spectrophotometer	Shimadzu – Japan
VI-Cell™ XR Cell Viability Analyser	Beckam Coulter- USA

**Table 2.4:** Reagents for mammalian cell culture

<b>REAGENT</b>	<b>SUPPLIER</b>
B27 supplement	Invitrogen Carlsbad, CA - USA
$\beta$ -mercaptoethanol	Sigma
D-Glucose	Sigma
Dulbecco's modified Eagles medium (DMEM)	ICN Biomedical, Costa Mesa, CA - USA
Foetal calf serum (FCS)	JRH Biosciences Lexan, KS - USA
Gentamycin	Invitrogen
Glutamax	Invitrogen
Hanks balanced salt solution (HBSS)	Invitrogen
Hibernate E media	Brain Bits, Springfield IL - USA
L-glutamine	Sigma
Neurobasal medium without L-glutamate	Invitrogen
OPTI-MEM and DMEM	ICN Biomedical,
Poly-D-Lysine	Sigma
Penicillin	Sigma-Aldrich Pty. Ltd., Sydney-Australia
Streptomycin	Sigma
Trypsin, 0.25% (1X) with EDTA 4Na	Trace Biosciences Pty Ltd., Vic.-Australia

**Table 2.5:** Bacterial culture media

<b>MEDIA</b>	<b>PREPARATION</b>
F-12 Medium	Dissolve 1 packet of media in a litter of dH <sub>2</sub> O, add 2.4g sodium bicarbonate and 2g D-glucose and adjust pH to 7.2. Filter sterilized and add 5%FCS.
2x YT Medium	Dissolve 16g bacto-tryptone, 10g bacto-yeast extract and 5g sodium chloride in 900 ml deionised H <sub>2</sub> O, make up to 1000ml and sterilize at 15 lb.sq.in on liquid cycle
SOB++	Bacto-tryptone (20 g), Bacto-yeast (5 g), NaCl (0.5 g) and KCl (0.186 g) dissolved in WFI to a final one litre volume and sterilised. Prior to use, 20 ml of MgCl <sub>2</sub> (1 M stock) and MgSO <sub>4</sub> (1 M stock) was added to a final concentration of 10 mM
Terrific Broth	Dissolve 12g bacto-tryptone, 24g bacto-yeast extract and 4ml glycerol in 900ml-deionised water. Add 0.17M KH <sub>2</sub> PO <sub>4</sub> and 0.72M K <sub>2</sub> HPO <sub>4</sub> solution prepared by dissolving 2.31g KH <sub>2</sub> PO <sub>4</sub> and 12.54g K <sub>2</sub> HPO <sub>4</sub> in 90ml dH <sub>2</sub> O adjusted to 100ml.



**Table 2.6:** PCR Reagents

<b>REAGENT</b>	<b>SUPPLIER</b>
DNA and Gel purification systems	Promega Corporation, Madison, WI - USA
DNA loading dye	Promega
<i>dNTPs</i>	Qaigen ,Victoria – Australia
KAPA SYBR FAST RT-PCR master mix	BioRad, Cape Town - South Africa
<i>KpnI</i>	Promega
<i>XhoI</i>	Promega
<i>1kb</i> DNA ladder	Promega
<i>T4</i> ligase	Bio-Labs, - New England
<i>T4</i> ligase buffer	Bio-Labs, - New England

**Table 2.7:** Test Kits

<b>KIT</b>	<b>SUPPLIER</b>
Amyloid Beta Assay Kit	Covance- USA
Cholesterol Assay Kit	Cayman Chemical company, MI- USA
LDH Cytotoxicity Assay Kit	Cayman Chemical company, MI – USA
Micro BCA Pierce Protein Assay Kit	Pierce, Rockford, IL., USA
Light Shift Chemiluminescent EMSA Kit	Pierce, Rockford, IL., USA
7-Deaza-2'-Deoxy-Guanosine Kit	Jena Bioscience, Jena - Germany

**Table 2.8:** List of antibodies

ANTIBODY	USE	DILUTION	SOURCE	SUPPLIER
Anti-EMMPRIN (Allain et al.) MAB2623	Immunohistochemistry	1:200	Mouse monoclonal	Chemicon, California – USA
Anti-Human $\beta$ amyloid 1-40/42 polyclonal antibody (AB-5076)	Immunohistochemistry	1:200	Rabbit polyclonal	Millipore, New South Wales – Australia
Biotinylated Rabbit Anti-Mouse	Immunohistochemistry	1:200	Mouse monoclonal	DAKO, Glostrup – Denmark
$\beta$ -Actin (AB8229)	Western blot	1:5000	Mouse monoclonal	Abcam, Waterloo – Australia
C1/1.6	Western blot	1:5000	Mouse polyclonal	Kindly provided by Dr Paul Mathews, NYU
Donkey anti-Rabbit HRP	Western blot	1:10000	Donkey	Amersham, Buckinghamshire – UK.
Donkey anti-Goat (HRP)	Western blot	1:20000	Goat	Santa Cruz – USA
Donkey anti-Mouse (HRP)	Western blot	1:5000	Mouse	Chemicon – USA
M42 – A $\beta$ 42	ELISA	1:1000	Mouse	kindly provided by Pankaj Mehta, NY- USA

M40-A $\beta$ 40	ELISA	1:1000	Rat	kindly provided by Pankaj Mehta, NY- USA
Nicastrin	Western blot	1:500	Rabbit polyclonal	Sigma
Presenilin	Western blot	1:2000	Mouse monoclonal	Kindly provided by Dr Paul Mathews, NYU
PEN 2	Western blot	1:2000	Rabbit polyclonal	Sigma
SC-9754 (Human)	Western blot	1:5000	Goat polyclonal	Santa Cruz biotechnology Inc – USA
SC-9757 (Rat)	Western blot	1:5000	Goat polyclonal	Santa Cruz biotechnology Inc – USA
Sheep anti- Mouse HRP	Western blot	1:10000	Mouse	Amersham, Buckinghamshire – UK.
SCP-2 (NB100-93459)	Western blot	1:5000	Goat monoclonal	Novus Biologicals, CO - USA
WO2	Western blot	1:2500	Mouse polyclonal	Kindly provided by Dr Colin Masters, University of Melbourne
4G8 Rodent A $\beta$	ELISA	1:1000	Mouse monoclonal	Sigma, Sydney – Australia
6E10 Human/pig A $\beta$	ELISA	1:400	Mouse monoclonal	Covance- USA

## **2.2: Methods**

### **2.2.1: Cell Cultures**

#### **2.2.1.1: Culturing Primary Rat Neurons**

All animal experiments were approved by the University of Western Australia (UWA) and Edith Cowan University (ECU) Animal ethics committees. Establishment of cortical cultures was as previously described (Meloni et al., 2005). Briefly, cortical tissue from E18 to E19 Sprague-Dawley rats were dissociated in Dulbecco's modified Eagle medium (DMEM; Invitrogen supplemented with 1.3mM L-cysteine, 0.9mM NaHCO<sub>3</sub>, 10U/ml papain (Sigma , USA) and 50U/ml DNase (Sigma) and washed in cold DMEM/10% horse serum. Culture plates (6-well) were coated with poly-D-Lysine (50µg/ml; 70-150K; Sigma) and incubated overnight at room temperature. The poly-D-Lysine was removed and replaced with Neurobasal Media (containing 2% B27; 4% FCS; 1% horse serum; 62.5µM glutamate; 25µM 2-mercaptoethanol and 30µg/ml penicillin). Neurons were plated at a density of  $3 \times 10^6$  cells per well and cultures were maintained in a CO<sub>2</sub> incubator (5% CO<sub>2</sub>; 95% air balance and 98% humidity) at 37°C. On DIV 4 half the media was removed and replaced with fresh NB/2% B27 containing the mitotic inhibitor cytosine arabinofuranoside (Cara), one third of the culture media was removed and replaced with fresh NB2° on day *in vitro* (DIV) 9, and the cultures were maintained at 37°C in 5% CO<sub>2</sub>.

#### **2.2.2: Cell viability assessment**

Cell viability was assessed by measuring lactate dehydrogenase (LDH) release using the Cayman Chemicals test kit (Cayman Chemical Company, MI – USA) according to manufacturer's instructions. Differences between groups were determined by ANOVA

with  $p < 0.05$  considered statistically significant. Unless otherwise stated, all experiments were conducted at least three times.

### **2.2.3: Cholesterol Treatment of Rat Primary Cortical Neuronal Cultures**

Rat primary cortical neuronal cultures were seeded in 6-well plates in NB2 media (4ml/well). Prior to treatment, 2ml media was removed and treatment prepared in the equal volume and added back to the respective wells. Cholesterol concentration of 0, 5, 10, 15, 20 and 30 $\mu$ g/ml water soluble-cholesterol (5mg/ml stock) were used to treat the neurons at DIV12 and used at DIV14 and DIV14 for western blot and LDH analysis (see section 2.6.3., below)

### **2.2.4: A $\beta$ Treatment of Rat Primary Cortical Neuronal Cultures**

Freshly prepared A $\beta$ 42 peptide (10 $\mu$ M) was added to appropriate wells in neuronal cultures at DIV 7 for the CD147 over expression experiments. Neuronal cultures were treated with 0, 1, 2.5, 10 and 15  $\mu$ M A $\beta$ 42 at DIV14 at 37°C for 48 hours.

## **2.3: *In vivo* Experiments**

### **2.3.1: APP<sup>swe</sup> mice**

The APP<sup>swe</sup> mice were purchased from Animal Resources Centre (ARC) (WA, Australia). Two groups of APP<sup>swe</sup> mice were fed on normal or high fat/high cholesterol diet for 60 days. Animals were weighed once a week. The experiment group (18 animals) comprising 9 males and 9 females were fed on a high fat/high cholesterol diet

SF08-033 (comprised of 10% fat, 0.75% cholesterol, 0.3% cholate and additional vitamins). The control group (18 animals, 9 males and 9 females) were maintained on normal chow. Animals were sacrificed at 90 days and tissue samples (liver, kidney and half of the brain) were collected and snap frozen in liquid nitrogen and stored at – 80°C. The other half of the brain was fixed in 10% formal-saline and kept at RT whereas the plasma was kept at -80°C until further processing. Tissues were homogenized in PBS cocktail containing protease inhibitor (Roche) prior to protein determination and western blot analysis. The levels of CD147, FL-APP, and APP-CTF were measured in all tissue homogenates whereas A $\beta$ 40/42 levels were only measured in plasma and brain samples.

### **2.3.2: Human Subjects**

Brain samples (frozen and 10% formal-saline fixed) of AD, Lewy body disease, frontotemporal dementia and controls were obtained from the West Australian Brain Bank Network (WABBN). Frozen tissues were homogenized as described in section 3.3.3 and used for protein determination and western blot analysis. Paraffin-embedded tissue section (0.5 $\mu$ ) were prepared from fixed tissues and used for immunohistochemistry analysis.

### **2.3.3: Homogenisation of Tissues**

Frozen human hippocampal and frontal cortex tissues and rat brain, kidney and liver tissue were kept on dry ice prior to being homogenized. Tissue fragments (approx. 100 mg) were homogenised in 300 $\mu$ l of tissue homogenising buffer containing protease

inhibitor (Roche) using a hand-held Kinematica polytron homogeniser (KPH). Samples were aliquoted (25  $\mu$ l) and stored at -80°C for further analysis.

## **2.4: Protein Procedures**

### **2.4.1: Protein Extraction from Cultures**

Culture media was removed from 6-well plates and 150 $\mu$ l of RIPA lysis buffer (1M Tris-HCl pH7.5, 5M NaCl, 0.5M EDTA, 0.5ml of 10% SDS and 125 $\mu$ l Igepal) containing protease inhibitor (20 $\mu$ l of protease inhibitor in 1ml of lysis buffer) was added to each well and the resulting lysate transferred to a new eppendorf tube, vortexed, and centrifuged at 14000 rpm at 4°C for 30 minutes. The supernatant was collected, aliquoted and stored at -80°C until further analysis.

### **2.4.2: SCP-2 Protein Generation**

SCP-2 protein was generated using KRX E.coli cell line. The cells were transformed with pro-SCP and SCP-x DNA (1 $\mu$ l) and subcultured on Kanamycin agar plates over night. Following the transformation of chemically competent KRX cells with expression vectors, colonies were inoculated into 2ml tubes containing 2x YT media; fitted with Eppendorf LidBac membrane filters and incubated overnight at 37°C with shaking (1400rpm). Two hundred millilitres of Terrific Broth (containing 50 $\mu$ g/ml kanamycin) was inoculated with 2ml of the overnight culture. The flask of KRX cells containing the required plasmid vector was incubated at 37°C in a conical flask (2L) with shaking (275rpm), until OD600 reached 0.8-1.0. The flask was transferred to room temperature with shaking (275rpm) until the OD600 reached approximately 1.3 (1.2 - 1.5). Protein

expression was induced by the addition of 1mM IPTG and 0.1% Rhamnose. The cultures were incubated at room temperature with shaking (275rpm) for approximately 18 hours.

Cultures were transferred to a 250ml pre-cooled centrifuge bucket and centrifuged at 10000g for 10 minutes at 4°C. The supernatant was discarded and the pellet was stored at -20°C. Pellets were re-suspended in 25ml Lysis buffer. The cell suspension was subjected to three passages of homogenization using a French press, followed by centrifugation at 10000g for 10 minutes. Inclusion bodies containing the desired protein were recovered from the homogenate as a pellet. The lysate was retained and further processed to recover recombinant proteins localized to the cytoplasm.

#### **2.4.3: Cytoplasmic Protein Purification**

The purification of pro-SCP and SCP-x cytoplasmic protein was achieved through Immobilized Metal Ion Affinity Chromatography (IMAC). The lysate was treated with 1ml of Ni-NTA agarose beads (Qiagen) and gently mixed at 4°C for 1 hour. The combined solution was centrifuged at 2000g for 5 minutes, and the supernatant removed. Four millilitres of wash solution was then mixed with the remaining beads, followed by centrifugation at 2000g for 5 minutes. This step was repeated 4 times. To elute the protein, 1ml of elution buffer was added to the beads, centrifuged for 5 minutes at 2000g and the supernatant collected. This step was repeated using 1ml, followed by 0.5ml of elution buffer. In total approximately 2.5ml of protein solution was collected using this method.



The protein solution was transferred to dialysis tubing and dialysed against three 2 litre volumes of dialysis buffer solution at 4°C, over a 24 hour period. The protein solution was then removed from the cellulose tubing, combined with glycerol (10%), filter sterilised (0.2µM) and stored at -80°C.

#### **2.4.4: Determination of Protein Concentration**

The Micro BCA Pierce protein assay kit (Pierce) was used to determine the protein concentration in each sample. Sample blanks (PBS), samples and standards (100µl) were transferred to a 96-microplate wells and 100µl of detection reagent (prepared according to the manufacturer's instructions) was added and incubated at 56°C for 15 minutes. Absorbance was measured at 595nm using a microplate reader (Bio-Rad Model 3550) and protein concentration (µg/ml) were extrapolated from a standard curve.

#### **2.5: Immunoblotting**

Protein (25µg/ml) was separated by SDS-PAGE, transferred to nitrocellulose membranes and analysed by immunoblotting (Peano et al., 2011). Membranes were incubated in blocking buffer (TBS containing skim milk 5% w/v) at RT for 1 hour then incubated with primary antibody in TBST (containing skim milk 0.5% w/v) (SC-9753 and SC-9754 for mouse and human EMMPRIN respectively, C1/1.6 for FL-APP and CTF, NT1 for PS1, ant-PEN2, β-actin and ant-nicastrin) RT for a further 2 hours. Membranes were washed three times for 10 minutes in TBST and incubated with secondary antibodies at RT for a further one hour. Membranes were washed three times for 10 minutes in TBST with a final wash with TBS to remove the Tween 20. Following

treatment with luminal enhancer solution diluted 1:1 with stable peroxidase solution (Pierce, Rockford, IL., USA) at RT for 2 minutes; membranes were exposed on Amersham Hyperfilm-ECL film at RT for up to 10 minutes until the desired signal intensity was attained.

Films of western immunoblots were scanned and optical density determined through the Bio-rad, Quantity-One software (GS-800 Calibrated Densitometer – BioRad). Specifically film backgrounds were subtracted from optical density of individual protein bands. An internal control was run on each gel for inter-gel normalisation. Levels for the proteins of interest were represented as a ratio of to the  $\beta$ -actin, to control for inter sample loading differences and presented in scatter plots. Western blots for all individual data points are presented in next to their corresponding scatter plots.

## **2.6: Enzyme Linked Immunosorbent Assay (ELISA)**

### **2.6.1: A $\beta$ 1-40/1-42 ELISA**

Brain homogenates were prepared in Paul Mathew's homogenisation buffer (250mM sucrose, 20mM Tris-HCL, 1mM EDTA, and 1mM EGTA pH 7.4). In brief homogenized brain tissues were centrifuged at 4°C (100,000g) for one hour and the supernatants were again centrifuged at 4°C (30,000g) for one hour and stored at -80°C. A $\beta$  levels were measured in supernatants using ELISA method. In brief, primary antibody (6E10; 1:400; Covance- USA) was incubated in 96-well plate at 4°C overnight and washed with phosphate buffered saline with PBST. Plates were incubated in blocking buffer at RT for 1 hour and washed with PBST. Samples and standards (250 $\mu$ l/well in duplicates) were loaded and incubated at RT for 2 hours followed by an overnight incubation at 4°C. Plates were washed with 100 $\mu$ l/well PBST and 100 $\mu$ l/well

of detection antibody solution (containing antibody R306; 1:1000; Covance- USA) was added and incubated at RT for 1.5 hours and unbound detection antibody was removed by washing with PBST. Thereafter 100µl/well neutravidin-HRP solution (nHRP; 1:10,000 in PBST) was added and incubated at RT for 1 hour before washing with PBST followed by addition of 100µl TMB/KGP reagent to each well and incubated at RT in the dark for 10 – 15 minutes. The reaction was stopped by addition of 100µl stop solution 1M (H<sub>3</sub>PO<sub>4</sub>) to each well and the absorbance read at 450nm on a Bio-Rad Model 3550 Microplate reader.

### **2.6.2: Plasma Cholesterol ELISA**

Total plasma cholesterol was measured using the cholesterol assay kit (Cayman Chemical Company, MI- USA) according to the manufacturer's instructions. In brief, 50ul of plasma and standards were added to appropriate wells in a 96-well plate followed by the addition of 50 µl assay cocktail (containing 4.745ml assay buffer, 150µl cholesterol detector, 50µl HRP, 50µl cholesterol oxidase and 5µl cholesterol esterase) incubated for 30 minutes at RT and the fluorescence measured at excitation 580nm and emission 595nm wavelengths using a FLUOstar Optima spectrophotometer (BMG Labtech). Cholesterol concentration (mM) was calculated using the formula below:

$$\left[ \frac{\text{Sample adjusted fluorescence} - (y - \text{intercept})}{\text{slope}} \right] \times \text{sample dilution} \times 0.001$$

### **2.6.3: CytoTox 96® Non-Radioactive Cytotoxic Assay (LDH Assay)**

Lactate dehydrogenase (LDH) is a stable cytosolic enzyme released from dead cells following plasma membrane degradation. The CytoTox 96® Non-Radioactive Cytotoxic Assay (Promega) is a colorimetric assay which quantitatively measures LDH. In brief, lactate dehydrogenase released by cells is measured following the enzymatic LDH mediated conversion of the tetrazolium salt (INT) substrate into its red formazan product, which is detected spectrophotometrically at 490nm. The amount of formazan produced is proportional to the number of lysed cells in culture. Differences between groups were determined by ANOVA where  $p < 0.05$  was considered statistically significant. Unless otherwise stated, all experiments were conducted at least three times.

### **2.7: Maintenance of bacterial cells**

For long-term storage, both recombinant and non-recombinant bacterial cells were resuspended in 2xYT medium containing 15% glycerol, aliquoted out into sterile 2 ml cryotubes (Nunc), snap frozen in liquid nitrogen and stored at -70°C. Cells were recovered from slightly thawed frozen aliquots using sterile loops or micropipette tips and used to inoculate agar or liquid culture media.

### **2.8: Competent Cells**

#### **2.8.1: Preparation of Chemically Competent KRX Cells**

KRX cells were thawed slowly on ice, and 5µl was inoculated into 1 ml of 2x YT media, and incubated on Thermo mixer Comfort (Eppendorf) incubator at 37°C for 1 hour with shaking (300rpm). A 100µl aliquot of the broth mixture was plated onto a

pre-dried 2x YT agar plate, and incubated at 37°C overnight. Two colonies were inoculated into two 2ml tubes containing 2x YT media; fitted with Eppendorf LidBac membrane filters and incubated overnight at 37°C with shaking (1400rpm).

Three millilitres of overnight KRX broth was inoculated into 500ml of fresh SOB medium, and incubated at 28°C with shaking at 225rpm. Once the OD600 of KRX broth reached 0.4, the culture was transferred to nice slurry for 10 minutes, and then centrifuged at 3,000g in a pre-cooled bucket rotor for 10 minutes. The cell pellet was gently resuspended in 100ml of ice cold TB, incubated on ice a further 10 minutes, and re-pelleted by centrifugation at 3,000g for 10 minutes. The cell pellet was gently resuspended in 18.6ml of TB, mixed with 1.4ml of DMSO, and incubated on ice a further 10 minutes. Aliquots of the cell mixture (0.6ml) were transferred to 1.5ml microfuge tubes, snap frozen in liquid nitrogen and stored at -80°C.

### **2.8.2: Assessment of Chemically Competent KRX Cells**

Freshly prepared competent cells were assessed for their competency in the following manner. Two microlitres of freshly thawed competent cells were transformed with 0.1ng of pGEM 3Z plasmid DNA. A 100µl aliquot of the transformation mix was plated onto agar plates (containing ampicillin; 50µg/ml) and incubated at 37°C overnight. The colonies were then counted and the transformation efficiency was calculated according to the following formulation.

$$\frac{90\text{cfu}}{0.01\text{ng}} \times 10^3 = 9 \times 10^6 \text{ colony forming units (CFUs)/}\mu\text{g of plasmid DNA}$$

### **2.8.3: Transformation of Chemically Competent KRX Cells**

An aliquot of KRX cells was thawed on ice. Eight microlitres of DNA was added to 1.5ml microfuge tubes containing 50µl of competent cells, gently mixed and incubated on ice slurry for 10-30 minutes. The transformation mix was heat shocked at 42°C for 30-45 seconds; returned to ice for 2 minutes, and 900µl of pre-warmed 2x YT was added, followed by incubation at 37°C for 1 hour with gentle shaking (300rpm). Transformation mixes were plated on 2x YT agar plates (containing the appropriate antibiotic) and incubated at 37°C overnight.

### **2.9: Preparation of Recombinant Adenovirus**

Recombinant RSV-Empty and RSV-CD147 viruses were prepared according to the method of (He et al., 1998), with some modifications. Briefly pShuttle plasmid DNA was linearized by *PmeI* digestion and introduced into E.coli strain BJ5183 carrying pAdeasy (Zeng et al., 2001) by electroporation (Gene Pulser II, Biorad). Recombinants were selected on media containing 50µg/ml kanamycin, and their plasmid DNA checked by *PacI* digestion. HEK-293 cells grown to 90% confluence in 25cm<sup>2</sup> flasks were transfected with 3µg of *PacI* linearized recombinant plasmid DNA using Lipofectamine2000 (Invitrogen, USA). Viral plaques appeared within 5 – 10 days and viral material used to for subsequent amplification of the virus in HEK-293 before purification and concentration using the Adeno-X virus purification kit (BD Biosciences, USA). Viral titres were determined by end-point dilution assay, as indicated by EGFP reporter expression

## **2.10: RNA/DNA methods**

### **2.10.1: General handling**

All plastic ware, solutions and buffers used in conjunction with DNA or RNA were either certified free of DNases or RNases as supplied by the manufacturer or prepared in-house and sterilised appropriately. In general, preparations of oligonucleotides, DNA and RNA were reconstituted in sterile WFI and stored at -20°C. For analytical or preparative work, oligonucleotides, DNA or RNA samples were handled aseptically, and were thawed and maintained on ice when in use.

### **2.10.2: RNA extraction**

Total RNA was extracted from tissue cultures or animal tissue samples using TRIZOL® Reagent, a mono-phasic solution of phenol and isothiocyanate and used according to the manufacturer's instructions. Total RNA was resuspended in sterile water for injection (WFI) at 0.2 to 1.0 µg/ml and stored at -80°C

### **2.10.3: Genomic DNA extraction**

Total genomic DNA was extracted from cells grown in culture using the MasterPure™ Complete DNA and RNA Purification Kit from Epicentre Technologies. Total genomic DNA was resuspended in sterile WFI and stored at -20°C.

### **2.10.4: Plasmid extractions**

Small-scale isolation of purified plasmid DNA from *E.coli* was performed with the Wizard® Plus SV Minipreps DNA Purification System Kit (Promega). Single colonies

were inoculated into 1.8 ml of 2xYT medium (containing an appropriate antibiotic) in microfuge tubes fitted with a PTFE membrane lid (Lid<sub>Bac</sub>Eppendorf) and grown 16-18 hours at 37°C with shaking at 1400 rpm. Cells were pelleted by centrifugation and plasmid DNA was recovered by following the manufacturer's instructions. Plasmid DNA was eluted from the mini-column in 80-100 µl sterile WFI.

## **2.11: Cloning of the PCR Products and Cell Transformation**

Cloning was performed by adding 0.5 - 4µl PCR product, 1µl salt solution, 1µl sterile water and 1µl TOPO vector in a final volume of 6µl. The mixture was then incubated at room temperature for 5 minutes and placed on ice ready for transformation.

KRX cells were thawed on ice for 5 minutes or till completely thawed and 200µl of cells transferred to chilled tubes on ice. DNA (8µl) was added to the cells and incubated for 15 minutes. The cells were heat shocked on Thermo mixer Comfort (Eppendorf) for 45-50 seconds at 42°C and immediately placed on ice for 2 minutes. 2YT medium (900µl) was added to each tube and incubated on Thermo mixer Comfort (Eppendorf) at 37°C for 60 minutes with shaking at 225rpm. Tubes were centrifuged for 1 minute at 14000rpm and pellet suspended in 100µl media. Cells were cultured on Kanamycin agar plates and incubated at 37°C overnight. The following day colonies (one colony per tube) were suspended in 1.800ml 2YT medium with Kanamycin and incubated overnight on Thermo mixer Comfort (Eppendorf) incubator with shaking speed set at 14000rpm.



## **2.12: Restriction enzyme digestion**

Restriction enzyme reactions were performed on plasmid DNA for both preparative and analytical purposes. In general, restriction digests comprised DNA (0.2-3.0 µg) in sterile WFI and combined in a 20-80 µl reaction volume with 1x restriction enzyme buffer (supplied as a 10x stock by the enzyme manufacturer) and at least 4 Units of enzyme per µg of DNA. Reactions were allowed to proceed for at least 2 hours at the temperature specified by the manufacturer. For double or triple digests, reactions were either conducted separately followed by purification (as described in section 2.3.2.6) or simultaneously if enzyme buffer conditions were compatible. Linearization of plasmid vector DNA by restriction digestion was performed for 12-18 hours using excess restriction enzyme. For directional cloning into expression vectors, whereby the use of two different restriction enzymes was necessary, digests were always performed sequentially.

## **2.13: Ligations**

For ligation reactions, insert DNA (100-250 ng) was combined with sterile WFI in a volume of 25 µl with: 1x *T4 DNA* ligase ligation buffer (supplied as a 10x stock by the enzyme manufacturer, Promega); linearised plasmid vector DNA (25-50 ng) and *T4 DNA* ligase 4.5 Units. Ligation mixtures were incubated at room temperature for 12-18 hours and stored at -20°C. Insert to plasmid DNA ratios were kept at a minimum of 3:1.

## **2.14: Quantitation of DNA**

Where necessary, DNA and RNA samples were quantified spectrophotometrically by measuring absorbance at two wavelengths, 260 nm and 280 nm. The instrument used

for this purpose was the NanoDrop (Analytical Technologies) and the protocols followed were described by the manufacturer. The concentration and purity of nucleic acid in the sample is automatically calculated by the instrument, and whilst concentrations were dependent on the quantity of starting material, pure preparations of RNA and DNA routinely gave OD<sub>260</sub>/OD<sub>280</sub> ratios of approximately 1.8.

### **2.15: Agarose gel electrophoresis**

Plasmid DNA, RNA, restriction enzyme fragments and PCR products were mixed with DNA loading dye and electrophoresed in agarose gels (0.7-2.5% w/v) using a TAE buffer system. Gels were pre-stained with ethidium bromide (0.5 µg/ml) and bands were visualised by UV transillumination (Foto/UV21, Fotodyne transilluminator), sized against DNA molecular weight markers and imaged/digitised following capture with a digital camera (brand, Kodak).

### **2.16: DNA sequencing**

The ABI Prism™ Big Dye Terminator version 3.1 reaction ready fluorescent labelling sequencing mix, employing Ampli Taq® DNA polymerase, was used to sequence double-stranded DNA. Briefly, 2.0 µl of stock reaction mixture was combined with: 25 ng of DNA oligonucleotide sequencing primer; 500-750 ng of purified double-stranded plasmid DNA template and made up to 10 µl with WFI. Cycling conditions used were: initial denaturation at 96°C for 1 minute, followed by 25 amplification cycles (96°C for 30 seconds, 50°C for 30 seconds and 60°C for 4 minutes) and a final 11°C hold. To precipitate the resulting DNA product, samples were mixed with 20 µl of WFI, 3 µl of sodium acetate (pH 5.2) and 75 µl of ice-cold 100% ethanol. The samples were held at

room temperature (protected from light) for 20 minutes, and centrifuged at 14000 rpm for 30 minutes. The entire supernatant was carefully aspirated and discarded. Two hundred and fifty microlitres of 75% ethanol were added to the tube containing the DNA pellet. The tube was gently inverted several times and centrifuged at 14 000 rpm for 10 minutes. The entire supernatant was carefully aspirated and the DNA pellet dried at 65°C for 2 minutes. Dried samples were submitted to the Department of Clinical Immunology (Royal Perth Hospital) or the Australian Neuromuscular Research Institute (Queen Elizabeth II Medical Centre) sequencing facilities.

## **2.17: Human CD147 promoter amplification and sequencing**

### **2.17.1: Slowdown PCR for amplifying GC-rich sequences**

Slowdown PCR was performed as described by Frey et al (Frey et al., 2008). In brief the reaction contained 2µl each primer (forward 5' *CCAGAAAGGTAACCGCCAGC* and reverse 5' *GCCATGATTTCCTATTCTCGC*; *Gene Works, AU*), 1.6µl MgCl<sub>2</sub>, 2 µl DNA, 0.2 µl Taq polymerase, 4 µl 10x PCR buffer (Phusion), 1.5 µl 7-Deaza-dGTP, 2 µl dNTPS and 9.7 µl dH<sub>2</sub>O. The thermal cycle conditions are as follows:

1 cycle of 95°C for 5min., setting heating ramp to 2.5°C<sup>-1</sup> and the cooling ramp rate for reaching annealing temperature to 1.5°C<sub>s</sub><sup>-1</sup>

48 cycles of 95°C x 30 sec denaturation. 30secannealing with a progressively lowered temperature from 70-53°C at a rate of 1°C every third cycle and a primer extension of 40 sec at 72°C. 15 cycles of 58°C, 4°C hold. The 360bp product (which covers the region of interest -392 to -242 nucleotides) was verified by agarose electrophoresis and viewed under UV on Biorad Gel doc.

### **2.17.2: Amplification of the CD147 promoter**

Human genomic DNA samples (health controls; *n*=100 and AD cases, *n*=100) were sourced from the Australian Biomarker and Lifestyle (ABIL) study (Perth and

Melbourne – Australia). Sequencing of the CD147 promoter region was done at Applied Genetic Diagnostics (APG), Department of Pathology-University of Melbourne. The ~30-50ng genomic DNA was amplified by PCR in a reaction containing 400nM each primer (forward 5' **AGGCTCTGGGAGTACAGACG** and reverse 5' **CCGGGAGGAACCTCTAGTC**), 1mM MgCl<sub>2</sub>, 200uM dNTPs, 8% DMSO and 2U of AmpliTaq Gold (Applied Biosystems). The thermal cycle conditions are as follows:

1 cycle of 94°C for 5min

35 cycles of 94°C x 45sec, 60°C x 45sec, 72°C x 45sec

1 cycle of 72°C x 10min, 4°C hold.

### **2.17.3: Sequencing of the CD147 promoter**

The 709bp product (which covers the region of interest -392 to -242 nucleotides) was verified by agarose electrophoresis before pre-sequencing cleanup using EXOSAP-IT (GE Healthcare) and a sequencing reaction with 5uM forward primer and Big Dye V3.1 terminators (Applied Biosystems). The Qiagen DyeEx kit was used to clean up the product before capillary electrophoresis on an ABI3130xl Genetic Analyser with POP7 polymer. The product was amplified by PCR and sequenced by capillary electrophoresis on an ABI 3130xl Genetic Analyser and compared to the reference sequence NG\_007468.1 using Mutation Surveyor Software. Results were confirmed by repeat PCR and sequencing.

Analysis and visualization of LD and haplotype maps was undertaken using the Haploview V4.2 software (Barrett et al., 2005). Generated data files were then analyzed in SPSS using student T-test and One Way Anova.

## **2.18: Immunohistochemistry of Human Brain Tissue – Paraffin Embedded Sections**

Frozen and formalin fixed frontal cortex and hippocampal tissues were sourced from the Western Australian Brain Bank Network (WABBN) in conjunction with the National Neural Tissue Resource Centre (NNTRC) and the Australian Brain Bank Network (ABBN). Paraffin sections were prepared in our laboratory. Paraffin sections were de-parafinized in 3 changes of xylene for 15 minutes followed by hydration in 3 changes of alcohol and distilled water for 2 minutes then rinsed in water. Antigen retrieval (EDTA pH8) was achieved by boiling sections for 20 minutes. This was followed by peroxidase blocking (3% Hydrogen Peroxide) for 30 minutes. Non-specific binding was blocked by 10% normal goat serum for 10 minutes, and exposed to anti-CD147 (Santa Cruz; 1:400) diluted in PBS for 90 minutes at room temperature. Preparations were washed three times in PBS prior to the addition of the secondary antibody and incubated for 20 minutes. Tissues were washed three times followed by the addition of Streptavidin for 20 minutes at room temperature. This was followed by counterstaining with Haematoxylin for 5 minutes, dehydrated and cleared then mounted with DPX. Slides were viewed and pictures taken using fluorescence microscopy (Olympus IX70) with Olympus DP70 digital camera.

## **2.19: Statistical Methods**

### **2.19.1: Linkage, allelic and haplotypic analysis**

Linkage Disequilibrium was estimated by  $D'$  and  $r^2$  as implemented in Haploview V4.2 software (Barrett et al., 2005). Allelic and haplotypic associations with clinical classification were undertaken using chi-squared ( $\chi^2$ ) tests as implemented in

Haploview. Corrections for multiple testing were considered if mandatory, 1000 permutations as implemented in Haploview. Genotype associations were then analyzed using IBM SPSS® Statistics version 19. Analysis of association with categorical variables (i.e. clinical classification) was undertaken using  $\chi^2$  analysis, whilst continuous variables were analyzed using either the Student's *T-test* or One Way ANOVA, where appropriate.

### **2.19.2: Additional statistical analysis**

The resulting data was analysed using the statistical analysis system software 'SPSS V17.0 for windows using One-Way ANOVA, Independent Sample T-test, and correlation analysis. The mean and standard deviation were used to report the data distribution and independent group ANOVA was used to compare differences among groups. All *p-values* reported are two-tailed and the significant level is 0.05.

## CHAPTER 3

### Cholesterol modulates CD147 expression *in vitro*.

#### 3.1: Introduction

Factors associated with an increased risk of developing Alzheimer's disease (AD), which is related to toxic A $\beta$  peptide accumulation in the brain include diet, obesity, old age, genetic profile (e.g. ApoE allele- isoform  $\epsilon$ 4), age-dependent reproductive hormone changes and head trauma (Sparks et al., 1990, Sparks, 1997). In addition, high circulating plasma cholesterol levels and pre-existing cardiovascular diseases can also increase the risk of AD (reviewed in (Martins et al., 2006)). Furthermore, epidemiological findings linking diet and AD in humans are supported by animal dietary experiments. For example, high fat/high cholesterol diets in rabbits, cynomolgus monkeys and APP<sup>swe</sup> transgenic mice leads to increased A $\beta$  brain deposition (Sparks et al., 1994b, Sparks et al., 2002, Wu et al., 2003, Schmechel et al., 2004). Taken together, these studies link high fat/high cholesterol diets with increased A $\beta$  accumulation.

A $\beta$  peptides are generated by the sequential cleavage of amyloid precursor protein (APP) by the beta amyloid cleaving enzyme (BACE) followed by the  $\gamma$ -secretase enzyme (Li et al., 2000a, Naslund et al., 2000). The  $\gamma$ -secretase enzyme occurs in a complex with presenilin-1 (PS1), A $\phi$ H-1, presenilin-2, PEN-2 and Nicastrin. Recently, the CD147 receptor was found to co-fractionate with members of the  $\gamma$ -secretase complex, and proposed to modulate A $\beta$  formation, via an as yet undescribed regulatory mechanism (Biswas et al., 1995, Zhou et al., 2005, 2007). However, follow-up studies

have indicated that instead of regulating A $\beta$  production, CD147 has a role in its degradation and clearance (Vetrivel et al., 2008b). Regardless of the mechanism, both studies support a role for CD147 negatively modulating A $\beta$  peptide levels (Zhou et al., 2005, Vetrivel et al., 2008b), where reductions result in A $\beta$  accumulation (Zhu et al., 2005).

The CD147 cell membrane receptor protein is a transmembrane glycoprotein belonging to the immunoglobulin super-family (IgSF) (Biswas and Vonderhaar, 1987, Fossum et al., 1991, Miyauchi et al., 1991, Kasinrerk et al., 1992, Biswas et al., 1995), which can induce the production of several MMPs, inducing MMP9 which is up-regulated in AD Brain (Kataoka et al., 1993, Biswas et al., 1995, Guo et al., 1997). CD147 is also a member of the small family of related proteins that includes the teratocarcinoma antigen GP70 and the synaptic glycoprotein SDR1 (Fossum et al., 1991, Shirozu et al., 1996). Cell signalling and its ability to interact with a number of proteins, including cyclophilins, has suggested roles for CD147 in neuroprotection and in pathology of neurodegenerative diseases such as AD. (Kirk et al., 2000, Yurchenko et al., 2002, Wilson et al., 2005, Ko and Puglielli, 2007).

The sterol carrier protein 2 (SCP-2) has a major role in cholesterol metabolism and trafficking (Baum et al., 1997, Zanlungo et al., 2000), where it facilitates the rapid translocation of lipids such as cholesterol between membranous organelles, into cells and tissues such as liver and blood (Baum et al., 1997, Zanlungo et al., 2000). Importantly, SCP 2 regulates CD147 transcription (Ko and Puglielli, 2007), suggesting that CD147 expression is influenced by cholesterol metabolism. Knowing that SCP has a role in nearly all aspects of cholesterol metabolism and also facilitates CD147 transcription, it is conceivable that changes in cholesterol homeostasis (i.e. under



cholesterol loading) will alter levels of SCP, thereby impacting on CD147 levels. This chapter determines whether CD147 expression in primary rat neurons is altered under conditions of cholesterol loading or accumulated A $\beta$ .

### **3.2: Aims**

#### **Specific aims:**

Determine if addition of exogenous cholesterol or A $\beta$  alters the expression of CD147 and full length APP protein in rat primary cortical neuronal cultures

- 1) Determine if cholesterol affects the viability of rat primary cortical neurons in cultures.
- 2) Determine if cholesterol affects CD147 levels in rat primary cortical neuronal cultures.
- 3) Determine if A $\beta$  treatment affects CD147 protein and FL-APP levels in rat primary cortical neuronal cultures.
- 4) Determine if adenoviral mediated CD147 protein over expression with or without CyPA can protect rat primary cortical neurons and SH-SY5Y cells against A $\beta$ 42 mediated toxicity.

### **3.3: Material and methods**

#### **3.3.1: Neuronal cultures**

Primary cortical rat neuronal cultures were established in 6 well plates from E18 embryos as described in section 2.2.1.1. Neurons were plated at a density of  $3 \times 10^6$  cells per well and cultures were maintained in a CO<sub>2</sub> incubator (5% CO<sub>2</sub>; 95% air balance and 98% humidity) at 37°C. On day *in vitro* four (DIV4) half the media was removed and replaced with fresh NB/2% B27 containing the mitotic inhibitor cytosine

arabinofuranoside (Cara), one third of the culture media was removed and replaced with fresh NB2° on DIV9, and the cultures were maintained at 37°C in 5% CO<sub>2</sub>.

### **3.3.2 Cholesterol and A $\beta$ treatment of primary cultures**

Cultures were treated on DIV12 with water soluble cholesterol (Sigma) for 48 hours. Prior to treatment, 2ml media was removed and replaced with an equal volume media containing cholesterol. Cholesterol concentration consisted of 0, 5, 10, 15, 20, and 30 $\mu$ g/ml prepared from a stock of water soluble cholesterol (5 $\mu$ g/ml).

Rat primary cortical neuronal cultures were exposed to increasing levels of A $\beta$ 42 for 48 hours and/or hydrogen peroxide (H<sub>2</sub>O<sub>2</sub>) (3 $\mu$ M). Freshly prepared A $\beta$ 42 peptide (10 $\mu$ M oligomeric A $\beta$ ) was added to neuronal cultures at DIV 7 to determine CD147 expression induction levels. Neuronal cultures were treated with 0, 1, 2.5, 10 and 15  $\mu$ M A $\beta$ 42 at DIV14 at 37°C for 48 hours. CyPA protein was prepared in house.

### **3.3.3: Preparation of pRSV-shuttle vectors encoding human CD147**

Total RNA was isolated from the human glioma cell line U251, reverse transcribed and amplified by PCR using gene specific primer pairs containing unique restriction sites (bold) and a Kozak sequence (underlined) as follows: - forward (*KpnI*) 5'**ggtaccg**ccaccatggcggctgcgctgttc3' and reverse (*XhoI*) 5'**ctcgagtc**aggaagagttcctc3'.

The resulting PCR products were gel purified, ligated into pGEM-Teasy (Promega, USA) and sequence verified. For sub cloning, the CD147 cDNA fragment was released by restriction enzyme digestion and ligated into the modified shuttle plasmid

pRSV/WPRE/CMV: EGFP (Boulos et al., 2006) to generate the pShuttle vector pRSV: CD147.

#### **3.3.4: Adenoviral vector construction**

Recombinant adenoviruses were prepared according to the method of He et al. (1998), with some modifications (Boulos, Meloni et al. 2006). Briefly, pShuttle plasmid DNA was linearized by *PmeI* digestion and introduced, by electroporation (Gene Pulser II, Biorad) into the *Escherichia coli* strain BJ5183 carrying pAdeasy (Zeng, Smith et al. 2001). Recombinants were selected on media containing 50 µg/ml kanamycin, and their plasmid DNA checked by *PacI* digestion. HEK-293 cells grown to 90% confluence in 25cm<sup>2</sup> flasks were transfected with 3µg of *PacI* linearized recombinant plasmid DNA using Lipofectamine 2000 (Invitrogen, USA). Following the appearance of viral plaques (5 – 10 days) culture lysates were used for viral amplification in HEK-293 cells. Adenoviral particles were purified and concentrated from cell lysates using the Adeno-X kit (BD Biosciences, USA). Viral titers were determined by end-point dilution assay, as indicated by enhanced green fluorescent protein (GFP) reporter expression.

#### **3.3.5: Hydrogen peroxide treatment**

Neuronal cultures were exposed to 3µM H<sub>2</sub>O<sub>2</sub> for 30 minutes, media removed and replaced with fresh NB2 and further maintained in CO<sub>2</sub> incubator at 37°C for 24 hours. Neuronal lysates were collected after 24 hours and CD147 expression determined by western blot analysis.

### 3.3.6: Western blot analysis

The levels of CD147 and full length APP (FL-APP) were determined by western blot as described in section 2.5. The EMMPRIN SC-9757 (Santa Cruz) and C1/6.1 (kindly provided by Collin Masters) primary and anti-goat and anti- mouse secondary antibodies were used to probe for CD147 and FL-APP respectively from protein collected culture lysates. Following immunoblotting, CD147 and FL-APP protein bands were quantified using the GS-800 Calibrated Densitometer (BioRad). Cell viability (in the presence and/or absence of CyPA, 100ng/ml) were determined by LDH release assay as described in section 2.2.2.

## 3.4: Results

### 3.4.1: Cholesterol treatment increases CD147 expression in primary neuronal cultures in a dose dependent manner

To determine if cholesterol influences CD147 expression in neurons, rat primary cortical neuronal cultures at DIV12 were treated with increasing doses of soluble cholesterol (0, 5, 10, 15, 20, 25, 30ug/ml). At 48 hours post-cholesterol addition, cell homogenates were collected and subjected to Western blot analysis to determine CD147 (**Fig.3.1**) and FL-APP protein levels (**Fig.3.2**). Cholesterol treatment increased CD147 protein expression in a dose dependent manner from 5 µg/ml, reaching a statistically significant peak at 20µg/ml ( $p<0.001$ ), then dropping below untreated control levels at 30µg/ml. (**Fig.3.1**; n=6 independent experiments). Western blot analysis revealed a steady, dose dependent decline in FL-APP protein levels with increasing cholesterol, which dropped below untreated control levels at 25µg/ml ( $p< 0.005$ ) and 30ug/ml ( $p<0.001$ ; **Fig.3.2**).

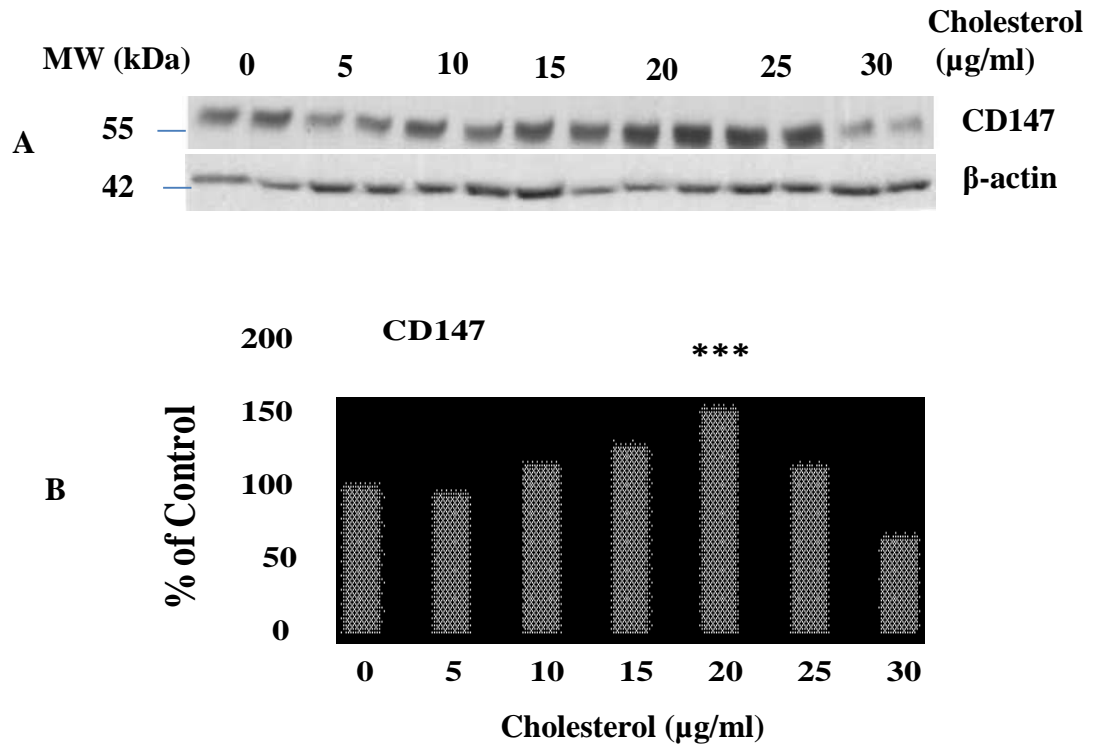


**Figure 3.1: Cholesterol increases CD147 expression in primary cortical neuronal cultures**

Representative Immunoblots (run in duplicates) from rat primary cortical neuronal culture lysates following treatment with cholesterol for 48 hours. Membranes were probed with anti-CD147 and ant-β-actin antibodies (**A**). CD147 values were normalized against beta actin and calculated as a percent of the control. Densitometry and statistical data analysis of CD147 protein levels (**B**). Values are expressed as mean  $\pm$ SD (from 6 independent experiments). \* $p < 0.001$  and \* $p < 0.05$ ). Compared to controls, neuronal cultures treated with 20μg/ml cholesterol showed significant increase of CD147 expression while those treated with 30μg/ml cholesterol showed significant decrease of CD147 expression levels.

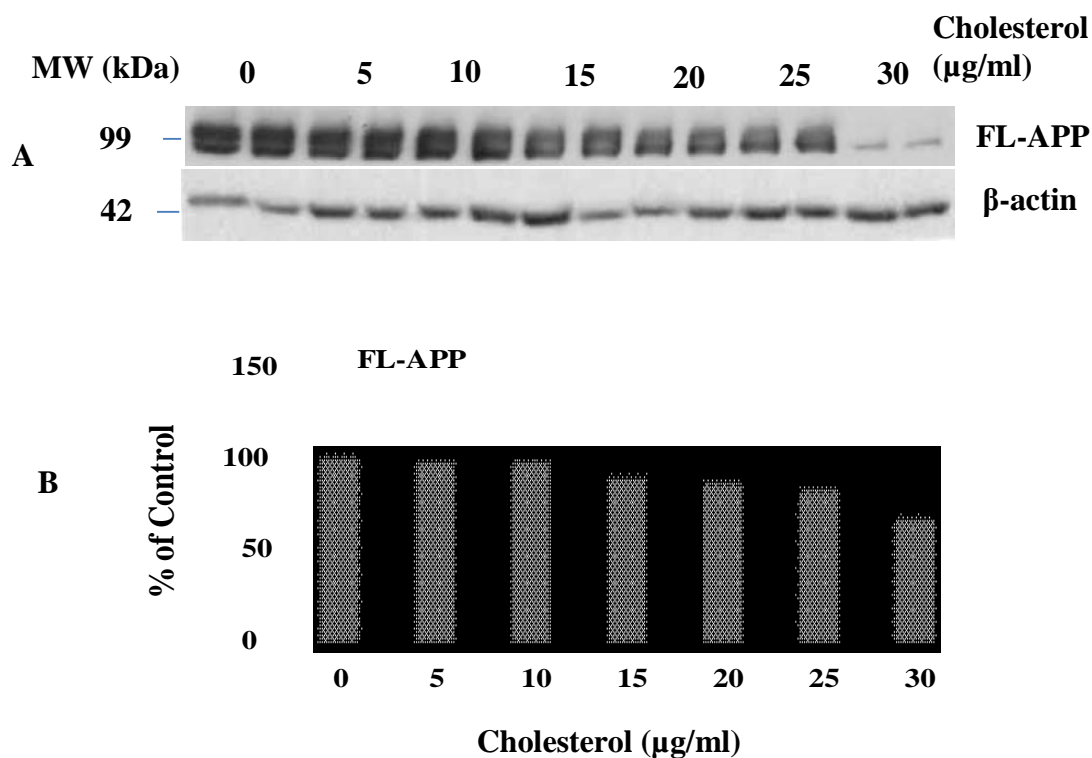


**Figure 3.2: Cholesterol decreases FL-APP expression in primary cortical neuronal cultures**

Representative Immunoblots (duplicate samples) from rat primary cortical neuronal culture lysates following treatment with cholesterol for 48 hours. Membranes were probed with anti- anti-FL-APP and ant-  $\beta$ -actin antibodies (**A**). FL-APP values were normalized against beta actin and calculated as a percent of the control. Densitometry and statistical data analysis of FL-APP (**B**). Values are expressed as mean  $\pm$ SD (from 6 independent experiments). \* $p < 0.005$  and \*\*\* $p < 0.001$ ).

### **3.4.2: Cholesterol increases LDH release in rat primary cortical neuronal cultures**

In the previous experiment (4.4.1) I observed a dramatic decline in both CD147 and FL-APP, at the two highest cholesterol concentrations, 25ug/ml and 30ug/ml. Why this occurred is not known but toxic A $\beta$  peptide accumulation (Notkola et al., 1998, Refolo et al., 2000a, Oksman et al., 2006) and free cholesterol loading is associated with widespread mitochondrial dysfunction and apoptosis (Yao and Tabas, 2001, Matsuda et al., 2002). Furthermore, protein translation can be suppressed in cells undergoing environmental stress (Hara et al., 2011, Nilsson and Sunnerhagen, 2011, Koponen et al., 2012). Thus I next investigated if cell viability was affected by cholesterol loading. In these experiments increased cholesterol levels appeared to induce cell stress as indicated by cell rounding and degeneration (data not shown). To determine if cholesterol increases cellular stress, we measured lactate dehydrogenase (LDH) release in the supernatants from cholesterol treated cultures. I chose LDH because it is a reliable marker of mitochondrial function, and hence, cellular health (Ying (Salahudeen et al., 2001, Sawane et al., 2002, Ying and Gervay-Hague, 2005, Aras et al., 2008). I found that compared to untreated cells, LDH release increased in a dose dependent manner in response to cholesterol treatment (48 hours post addition), ( $p=0.001$ ; **Fig.3.3**).

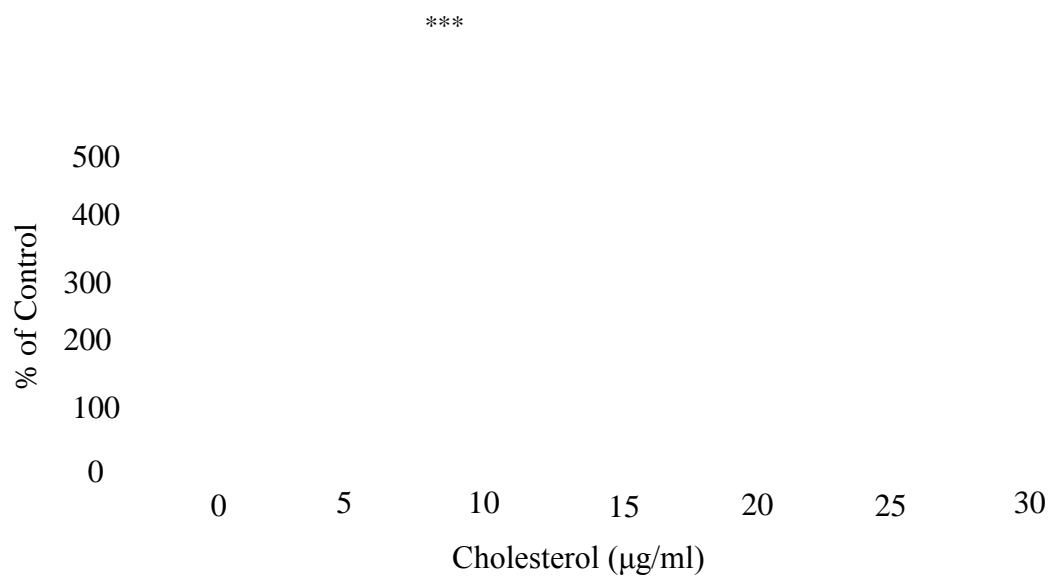


**Figure 3.3: Cholesterol treatment increases LDH release in primary neuronal cultures**

LDH release in rat primary cortical rat neuronal cultures exposed to cholesterol at DIV14 for 48 hours. The chart represents data from 6 independent experiments and values are expressed as mean  $\pm$ SD, \*\*\*  $p < 0.001$ .



### **3.4.3: Oxidative stress induces CD147 expression and affects cell viability in rat primary cortical neuronal cultures in a dose dependent manner**

Oxidative stress is an important contributing factor in a number of neurodegenerative disorders including AD, and strong evidence links A $\beta$  mediated neurotoxicity and oxidative stress. Oxidative stress occurs when reactive oxygen species (ROS), which are by-products of mitochondrial phosphorylation, exceed the cells antioxidant defence systems (Huang et al., 1999, Zhu et al., 2002, Lustbader et al., 2004b). Reactive oxygen species such as H<sub>2</sub>O<sub>2</sub> and OH<sup>-</sup> damage proteins, DNA, and cell organelles leading to cellular death.

Thus, as oxidative stress is known to induce CD147 expression in cardiac myocytes (Seko et al., 2004), I wondered if A $\beta$  treatment could similarly increase CD147 expression in neuronal cultures. As part of this study, I first confirmed that hydrogen peroxide (H<sub>2</sub>O<sub>2</sub>), an oxidative stress inducer, induces CD147 protein expression (**Fig.3.4**). Compared to control, results from these experiments have shown that cultures exposed to 3 $\mu$ M H<sub>2</sub>O<sub>2</sub> showed increased CD147 expression and LDH release (**Fig.3.4**).

Next I sought to determine if A $\beta$ 42 induces CD147 expression (**Fig.3.5**), I treated rat primary cortical neuronal cultures on DIV12 with increasing concentrations of A $\beta$ 42 peptide (0, 1, 2.5, 5, 10 and 15 $\mu$ M). I first measured LDH release and as expected, observed a significant increase in neuronal cultures exposed to higher A $\beta$ 42 ( $p < 0.001$ ) (**Fig.3.5**). Finally I measured CD147 and FL-APP levels using western blot analysis of lysates which revealed that CD147 protein levels increased in response to A $\beta$  in a dose dependent manner, reaching statistical significance at 5 - 15 $\mu$ M compared to controls

( $p < 0.001$  respectively) (**Fig 3.6**). By contrast, high A $\beta$  concentrations ( $\geq 5\mu\text{M}$ ) caused FL-APP expression to decline ( $p < 0.001$ ) compared to untreated controls (**Fig 3.7**).

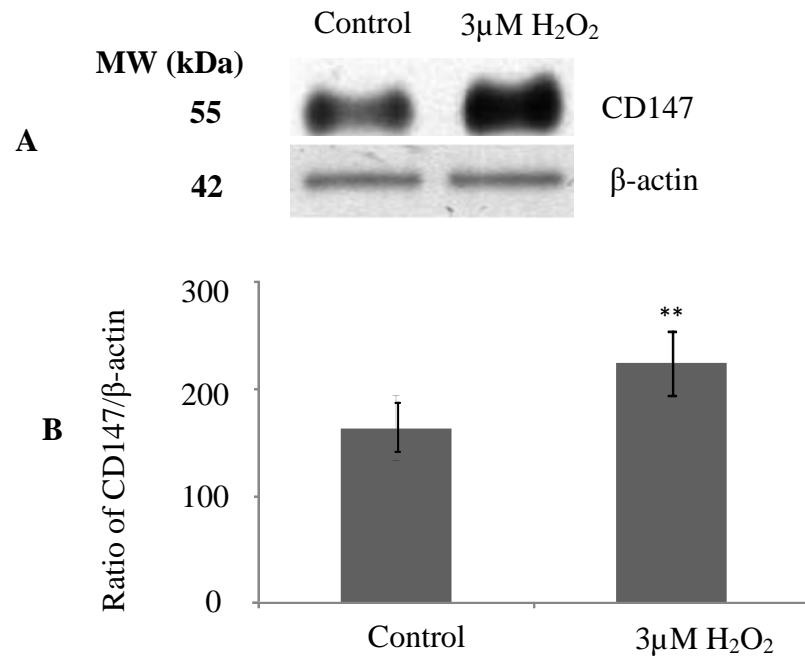


**Figure 3.4: Hydrogen peroxide (H<sub>2</sub>O<sub>2</sub>) treatment of rat primary neuronal cultures increases CD147 levels and LDH release**

Representative immunoblots from rat primary cortical neuronal culture lysates following treatment with 3μM H<sub>2</sub>O<sub>2</sub> for 24 hours. Membranes were probed with anti-anti-CD147 and anti-β-actin antibodies (**A**). Densitometry and statistical data analysis of CD147 (**B**). Values are expressed as mean ±SD (from 3 independent experiments) \*\* $p < 0.01$ ).

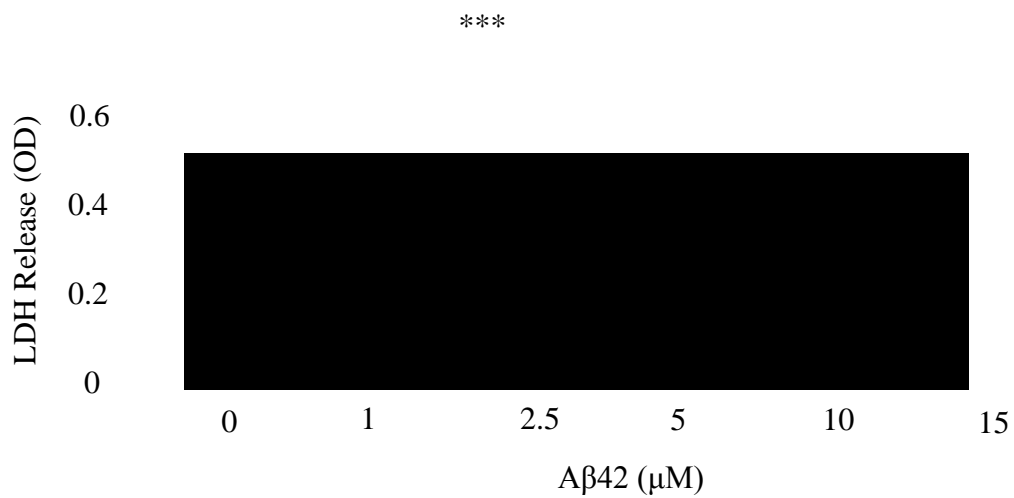


**Figure 3.5: Aβ42 treatment of rat primary neuronal cultures increases LDH release**

LDH release in rat primary cortical rat neuronal cultures exposed to Aβ42 at DIV14 for 48 hours. The chart represents data from 6 independent experiments and values are expressed as mean  $\pm$ SD, \*\*\*  $p < 0.001$ .

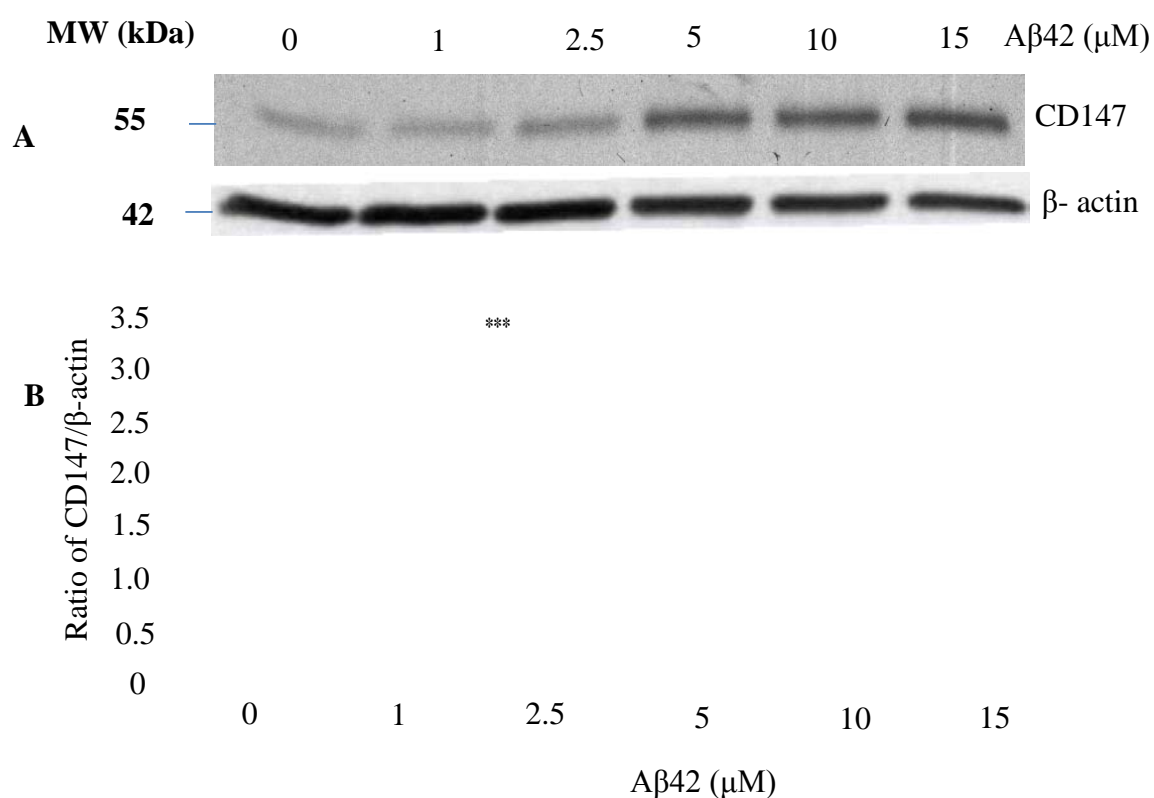


**Figure 3:6: Differential CD147 expression in neuronal cultures following treatment with Aβ42 peptide.**

Western blot analysis of rat primary cortical neuronal culture lysates harvested 48 hours after Aβ42 treatment; **A**) representative immunoblot probed with anti-CD147 and anti-β-actin antibodies. **B**) Densitometry and statistical analysis of CD147 expression. The chart represents data from 6 independent experiments and values are expressed as mean  $\pm$ SD, \*\*\*  $p < 0.001$ .

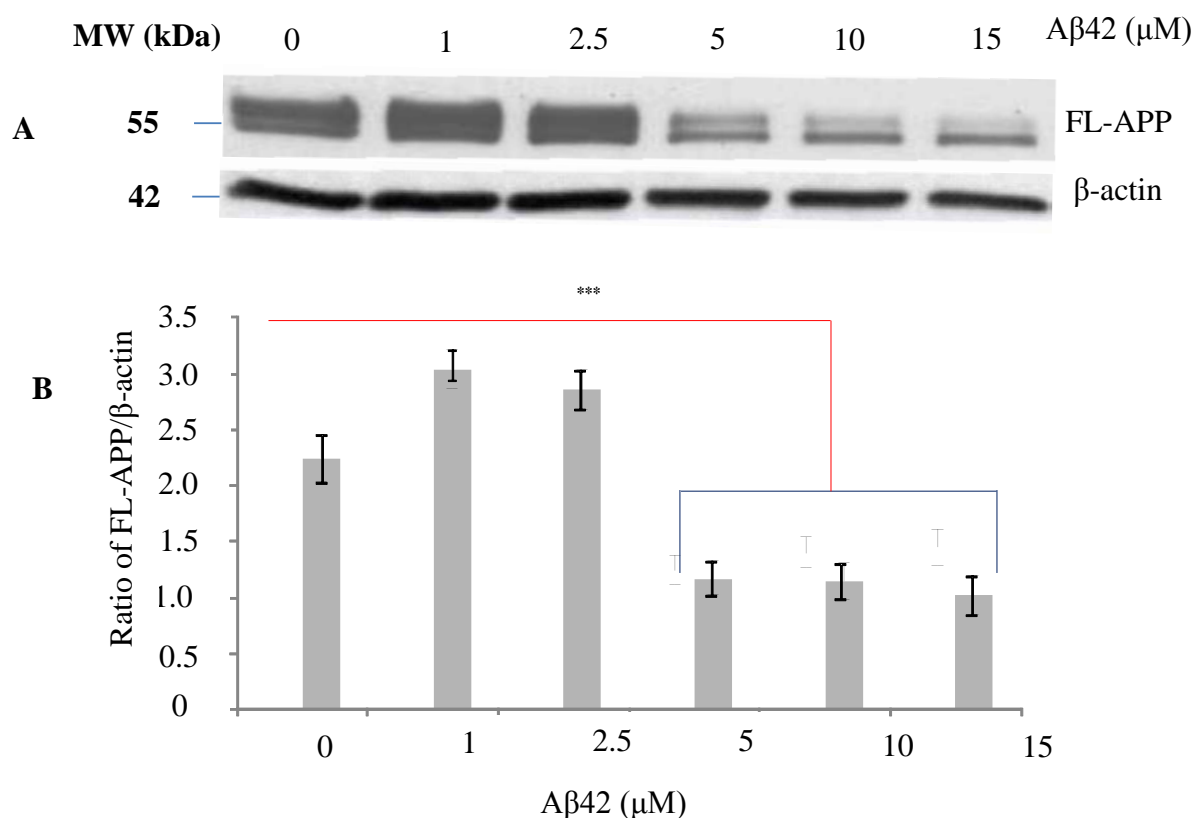


**Figure 3:7: Differential FL-APP expression in neuronal cultures following treatment with Aβ42 peptide.**

Western blot analysis of rat primary cortical neuronal culture lysates harvested 48 hours after Aβ42 treatment; **A)** representative immunoblot probed with anti-FL-APP and anti-β-actin antibodies. **B)** Densitometry and statistical analysis of FL-APP expression. The chart represents data from 6 independent experiments and values are expressed as mean  $\pm$ SD, \*\*\*  $p < 0.001$ .

#### **3.4.4: Adenoviral mediated CD147 over expression does not affect cell viability in rat primary neuronal cultures.**

To determine if elevated CD147 expression can cause cell death, I transduced rat primary cortical neuronal cultures with a recombinant adenovirus expressing human CD147 (AdRSV-CD147) and control recombinant adenovirus (AdRSV-Empty) at 100 moi. Approximately 70% of the neurons were transduced as indicated by GFP reporter expression GFP (**Fig.3.8**). CD147 levels were determined by western blot analysis using human EMMPRIN SC-9757 monoclonal antibody. As expected the results clearly show the absence of human CD147 expression in the AdRSV-Empty transduced neuronal cultures and expression of human CD147 protein in neuronal cultures transduced with AdRSV-CD147 (**Fig.3.9A**). Over expression of CD147 did not alter FL-APP levels (**Fig.3.9A**) or decrease cell viability as indicated by LDH release (**Fig.3.9B**).

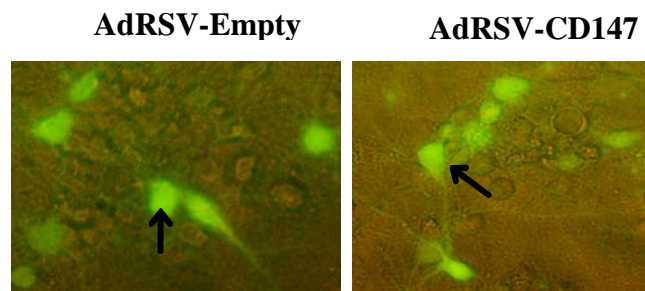


**Figure 3.8: Recombinant adenoviral transduction of neuronal cultures**

Fluorescent microscopy of rat primary cortical neuronal cultures transduced with adenoviral constructs AdRSV-Empty and AdRSV-CD147 at 100 moi for 72 hours. GFP reporter expression indicating successful adenoviral transduction of cortical neuronal cultures.



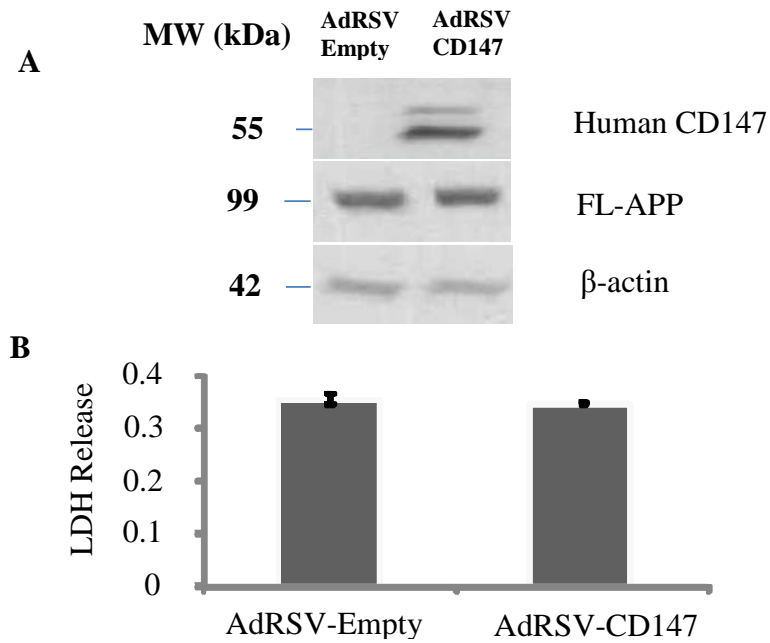


**Figure 3.9: CD147, FL-APP and LDH release levels in recombinant adenoviral transduced neuronal cultures**

Rat primary cortical neuronal cultures transduced with adenoviral constructs AdRSV-Empty and AdRSV-CD147 at 100 moi for 72 hours. Immunoblots probed for human CD147, FL-APP, and  $\beta$ -actin loading control (**A**) and corresponding LDH release in culture (**B**).

### **3.4.5: Adenoviral mediated CD147 expression protected rat primary cortical neuronal cultures against A $\beta$ 42 toxicity only in the presence of cyclophilin A (CypA)**

Studies have shown that cyclophilin A (CypA)/CD147 receptor-mediated ERK1/2 signalling protects neurons against oxidative stress and ischemic injury (Boulos et al., 2007). These findings prompted me to determine if increased CD147 expression, in the absence and/or presence of CyPA, is responsible for protecting neuronal cultures against A $\beta$ 42 toxicity. Rat primary cortical neuronal cultures were transduced with AdRSV-Empty and AdRSV-CD147 adenoviruses (**Fig.3.10**). Prior to A $\beta$ 42 (20 $\mu$ M) exposure, cultures were treated with recombinant CyPA (100ng/ml) or protein vehicle for 30 minutes. I measured LDH release in culture supernatants to determine the level of cell viability. Visual inspection of the cultures showed that CyPA provides protection against A $\beta$ 42 injury (**Fig.3.10**). However, analysis of LDH release in cultures transduced with AdRSV-CD147 and CyPA showed statistically significant protection against A $\beta$ 42 toxicity ( $p < 0.05$ ) (**Fig.3.11B**). However AdRSV-Empty transduced cultures treated with CyPA showed protection trend against A $\beta$ 42 toxicity (**Fig.3.11A**). This outcome was possibly due to low CD147 expression in AdRSV-Empty transduced cultures as cells exhibiting low level expression are reportedly unresponsive to CyPA (Trachtenberg et al., 2011).

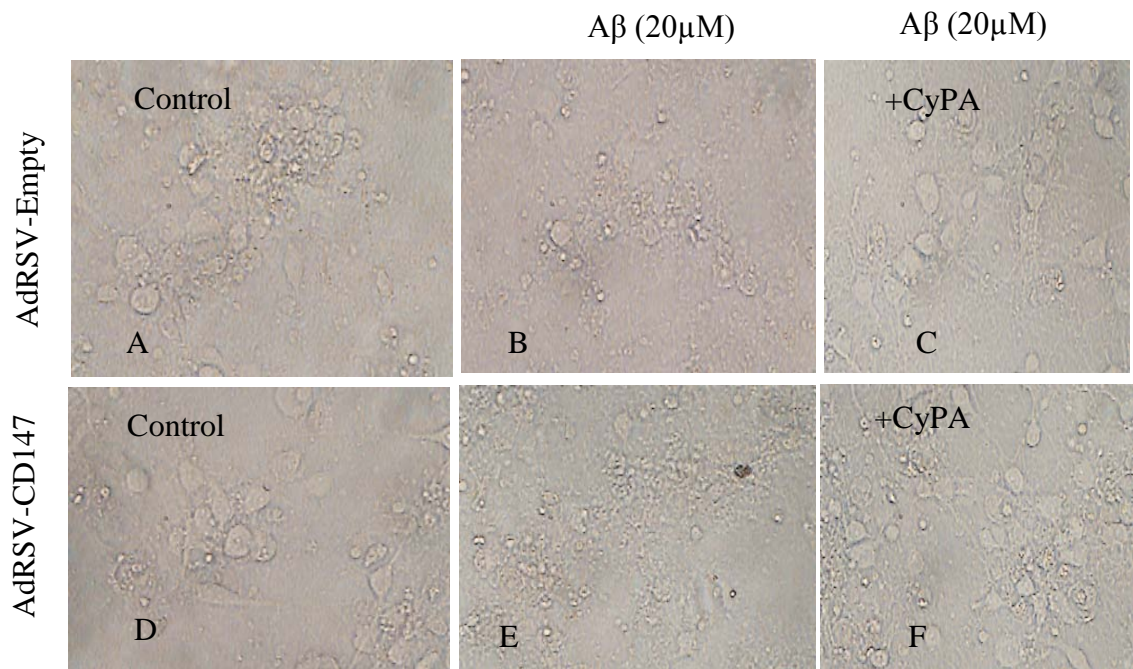


**Figure 3.10: Rat primary cortical neuronal cultures transduced with recombinant adenoviruses and exposed to A $\beta$ 42 in the presence and absence of CyPA**

Rat primary cortical neuronal cultures transduced with AdRSV-Empty (**A**, **B** and **C**) and AdRSV-CD147 (**D**, **E** and **F**) at a moi of 100. Cultures exposed to 20 $\mu$ M A $\beta$ 42 (**B**, **C**, **E** and **F**) without (**B** and **E**) and with (**C** and **F**) CypA (100ng/ml). Compared to untreated control cultures (**A** and **D**), cultures without CyPA pre-treatment (**B** and **E**) showed induced increased neuronal death compared to those pre-treated with CyPA (**C** and **F**).

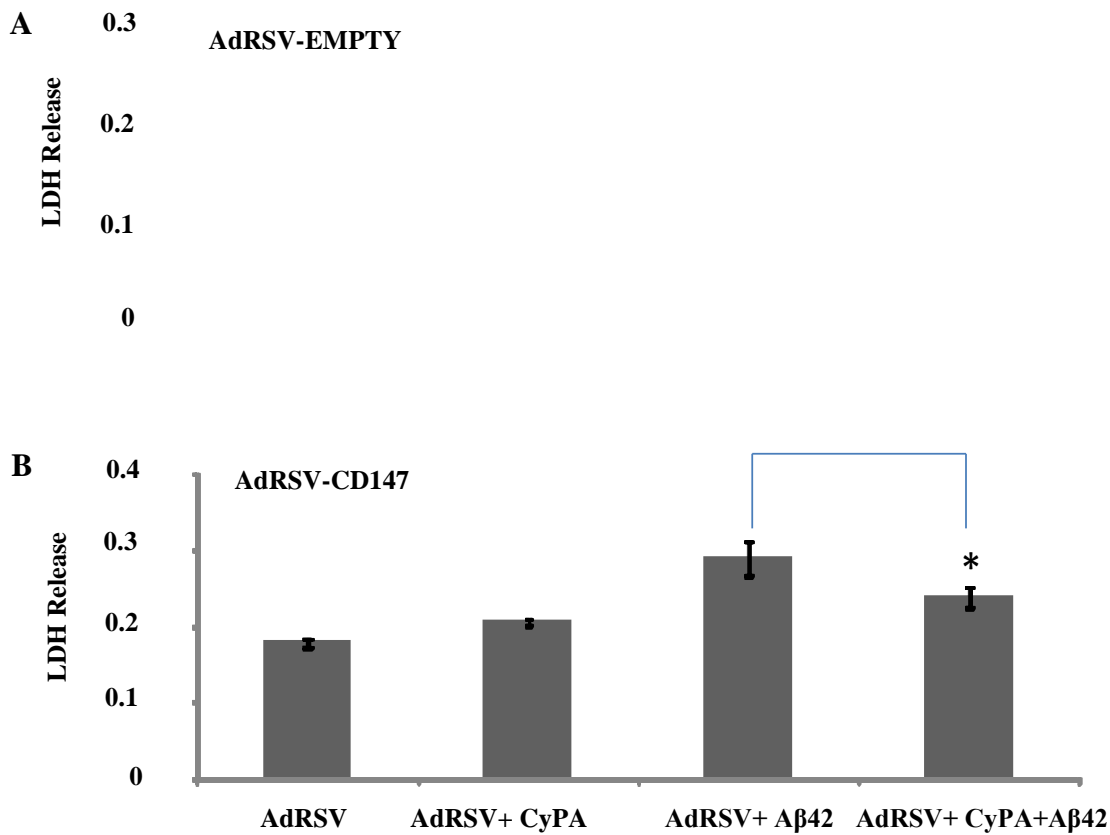


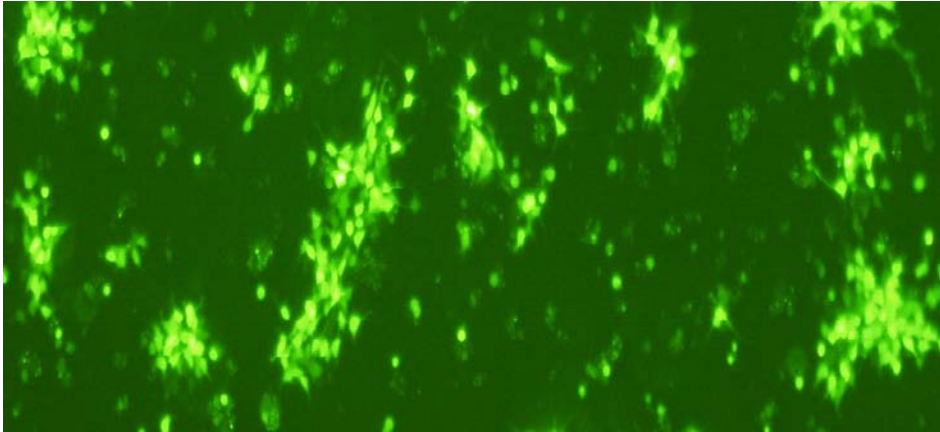
**Figure 3.11: Aβ42 toxicity in neuronal cultures transduced with recombinant adenoviruses**

LDH release in rat primary cortical neuronal cultures transduced with AdRSV-Empty (**A**) and AdRSV-CD147 (**B**) at moi of 100 and exposed to 20μM Aβ42 with and without CypA (100ng/ml) pre-treatment. Values are expressed as mean ±SE ( $n=3$ ) and indicate that CD147 protected neuronal cultures against Aβ42 toxicity in the presence of CyPA ( $p<0.05$ ).

#### **3.4.6: Adenoviral mediated CD147 expression protected SH-SY5Y cell cultures against A $\beta$ 42 toxicity only in the presence of cyclophilin A (CypA)**

In order to consolidate the findings from rat primary cortical neuronal cultures, I performed additional experiments in SH-SY5Y human neuroblastoma cell line. I chose SH-SY5Y cells because they have low CD147 expression and are of human origin, and unlike mixed neuronal cultures are more of purely neuronal cell type. This eliminates potentially indirect effects of CyPA protection to demonstrate if CyPA acts through CD147 to mediate neuroprotection that has not been confirmed in neurons. SH-SY5Y cultures were transduced with adenoviral constructs (AdRSV-Empty and AdRSV-CD147) at moi 40. Compared to controls (**Fig.3.12 B and C**) positive adenoviral transduction was confirmed by GFP reporter expression in AdRSV-Empty (**Fig.3.12B**) and AdRV-CD147 (**Fig.3.12C**) cultures. Next cultures were exposed to A $\beta$ 42, CyPA and CyPA+ A $\beta$ 42 and LDH release was measured with a cell viability marker. The results showed that AdRSV-CD147, in the presence of CyPA, protected SH-SY5Y cultures against A $\beta$ 42 toxicity ( $p < 0.001$ ) (**Fig.3.13B**). These results are similar to those from rat primary neuronal cultures, providing further confirmation that adenoviral mediated CD147 protects neurons against A $\beta$ 42 induced oxidative stress in the presence of CyPA. Just as in the rat primary neuronal culture experiments, SH-SY5Y cultures transduced with AdRSV-Empty showed protection trend against A $\beta$ 42 induced toxicity (**Fig.3.13A**).

**AdRSV-EMPTY**



**AdRSV- CD147**

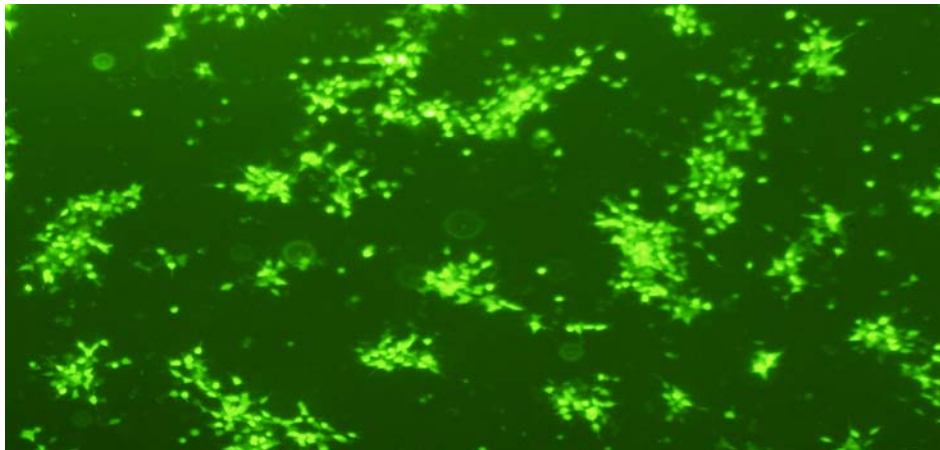


**Figure 3.12: SH-SY5Y cultures transduced with recombinant adenoviruses**

Fluorescent microscopy images of SH-SY5Y cultures transduced with AdRSV-Empty and AdRSV-CD147 at moi of 40. GFP reporter expression indicating over 80% of neurons transduced with recombinant adenoviruses.

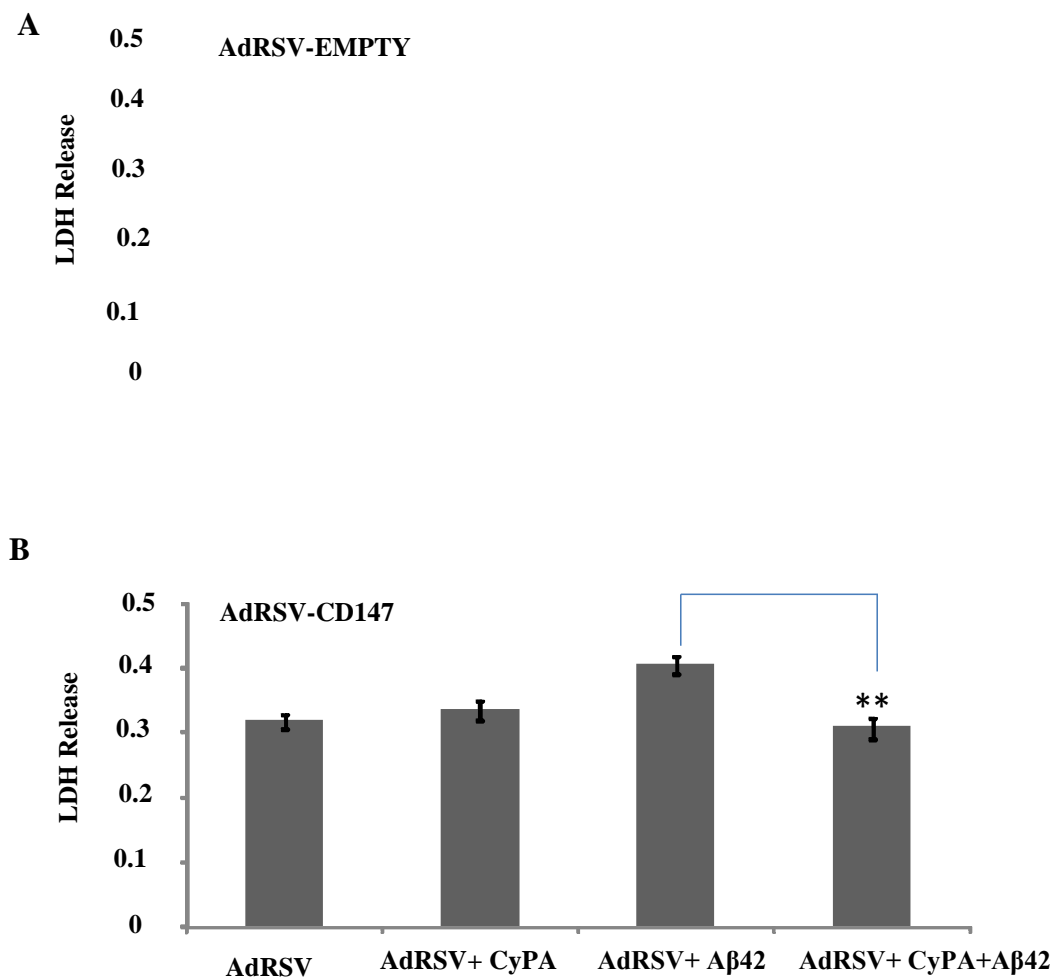


**Fig. 3.13: Aβ42 Toxicity in SH-SY5Y human neuroblastoma cultures transduced with recombinant adenoviruses**

LDH release in SH-SY5Y human neuroblastoma cultures transduced with AdRSV-Empty (**A**) and AdRSV-CD147 (**B**) at moi 40 and exposed to 20μM Aβ42 with and without CypA (100ng/ml) pre-treatment. Values are expressed as mean ±SE (n=3). Results indicate that CD147 protected SH-Y5Y human neuroblastoma cells against Aβ42 toxicity in the presence of CyPA (\*\* $p < 0.001$ ).

### **3.5: Summary of results**

Overall the *in vitro* results presented in this chapter have demonstrated for the first time that cholesterol and A $\beta$ 42 can induce CD147 expression. Finally that adenoviral mediated CD147 expression protects neuronal cultures against A $\beta$ 42 induced oxidative stress only in the presence of CyPA.

### **3.6: Discussion**

#### **3.6.1: Cholesterol loading affects CD147 levels *in vitro***

In the current study I demonstrated for the first time that cholesterol increases CD147 expression dose dependently in primary neuronal cultures. The sterol carrier protein (SCP) which is involved in cholesterol uptake (McLean et al., 1989, Moncecchi et al., 1996, Atshaves et al., 1999, Atshaves et al., 2009), intracellular transport (Kraemer et al., 1995, Ren et al., 2004), esterification (Murphy and Schroeder, 1997) and oxidation (Atshaves et al., 2009), reportedly affects CD147 expression by modulating transcription (Puglielli et al., 1995, Ko and Puglielli, 2007). This link suggests that cholesterol may influence SCP protein levels, thereby modulating CD147 expression. To investigate this relationship, I postulated that SCP protein levels change in response to cholesterol challenge. However, attempts to detect SCP protein in culture lysates by western blot analysis were unsuccessful, despite trying 4 different commercially available antibodies. Thus, I was unable to confirm or refute this hypothesis.

As part of this study, I also confirmed that neuronal degeneration increased in response to cholesterol using LDH release as a marker of mitochondrial function and cellular health (Nixon, 2004, Feng et al., 2010, Metrailler-Ruchonnet et al., 2010, Zhang et al.,



2010b). The increase in CD147 expression and LDH release suggested an association between CD147 regulation and the cells response to injury. Oxidative stress is a major contributor to neuronal cell loss in a number of neurodegenerative disorders including AD, and there is strong evidence linking oxidative stress to A $\beta$ . Oxidative stress occurs when reactive oxygen species (ROS), resulting from mitochondrial oxidative phosphorylation, exceed the cells naturally occurring antioxidant defence systems, lead to chemical damage of cellular structures and components. That this process occurs in AD is supported by the findings of Martins et al (Martins et al., 1986) who reported an increase in activity of enzymes from the hexose monophosphate pathways in post-mortem brain samples compared to age-matched controls. Several reports have also shown extensive oxidative damage in AD, including lipid peroxidation (Sayre et al., 1997, Kontush et al., 2001, Butterfield, 2002), oxidized proteins (Carney et al., 1994, Chan et al., 1999, Wang et al., 2003) nucleic acid damage and advanced glycation end products (AGE) (Torreggiani et al., 2009). Oxidative damage in AD may be a direct result of A $\beta$  peptide accumulation which causes neurotoxicity by producing reactive oxygen species (ROS) (Carney et al., 1994, Devi et al., 2006, Torreggiani et al., 2009) through interaction with metals, but mainly copper (Huang et al., 1999, Curtain et al., 2001, Dong et al., 2003, Crouch et al., 2005). Specifically, the combination of A $\beta$  and Cu ions generates hydrogen peroxide (H<sub>2</sub>O<sub>2</sub>) that causes damage to lipids and proteins. These findings clearly show that A $\beta$  mediated generation of ROS is a potentially important contributor of neuronal cell death in AD.

Thus, since elevated cholesterol is also associated with increased A $\beta$  production (Refolo et al., 2000a, Wu et al., 2003, Fitz et al., 2010), I postulated that oxidative stress/reactive oxygen species (ROS) generation, induced by A $\beta$  (Smith et al., 1998, Lin et al., 2001, Butterfield et al., 2002), might also account for the observed CD147

increase, independently of any SCP related mechanism. Specifically, CD147 expression has been linked to oxidative stress (Boulos et al., 2007). As mentioned earlier, and in support of this idea, I noted that cultures treated with increasing cholesterol levels exhibited hallmarks of degeneration, indicating cellular stress. To test this hypothesis, I also measured A $\beta$  levels in the supernatants of cholesterol treated cultures. However, despite using a highly sensitive commercial ELISA assay, I found that A $\beta$  levels were undetectable. Interestingly, Western blot analysis also revealed a steady, dose dependent decline in FL-APP protein levels with increasing cholesterol. These results are consistent with another study that previously reported a downward shift in FL-APP levels with increasing cholesterol levels (Galbete et al., 2000b), due apparently to a decrease in APP (sAPP) secretion caused by the disruption of the immature APP glycosylation by cholesterol. The disruption of FL-APP may account for the lack of detectable A $\beta$ , as reduced FL-APP levels would have limited the amount of amyloid protein available for cleavage by gamma secretase and hence A $\beta$  generation.

Cholesterol can reportedly increase oxidative stress by directly impacting on mitochondrial function (Homma et al., 2004, Oliveros et al., 2004, Lu et al., 2011, Mei et al., 2012), a process that may produce injurious levels of ROS, including hydrogen peroxide. In testing this possible association I exposed rat primary neuronal cultures to hydrogen peroxide and observed an increase in CD147 expression alongside increased LDH release. Subsequently, I tested if the human A $\beta$ 42 toxic peptide species could similarly increase CD147 levels in neuronal cultures, given that it also induces H<sub>2</sub>O<sub>2</sub>/oxidative stress (Butterfield et al., 2002). As postulated and for the first time, I demonstrated that, A $\beta$ 42 increases CD147 expression in a dose dependent manner, a potentially significant finding in AD, given that CD147 down regulation increases A $\beta$ 42 (Zhou et al., 2005, 2006, 2007). Furthermore and importantly, I demonstrated that

increased CD147 expression is not directly toxic to neurons *in vitro*.

### **3.6.2: CD147 protects neuronal cultures from A $\beta$ 42 induced toxicity only in the presence of CYPA**

As part of this study I also investigated the behaviour of extracellular CYPA protein within the context of AD and A $\beta$  toxicity and CD147 expression. Recent reports indicate that CD147 depletion and/or knock down results in elevated A $\beta$  peptide levels (Zhou et al., 2005) and that CyPA/CD147 signalling may protect neurons from oxidative and ischemic injury (Boulos et al., 2007). Furthermore, it is also reported that CD147 null mice exhibit neurological abnormalities such as spatial learning and memory deficits and that CD147 depletion affects embryonic development (Igakura et al., 1998, Muramatsu and Miyauchi, 2003, Chen et al., 2007). Taken together, these findings suggest that CD147 expression may protect against neuronal damage *in vivo*. The question arises, whether the biological effects attributable to CYPA would occur *in vivo* and additionally, if CYPA protein occurs within the extracellular compartment. Importantly, strong evidence indicates that CYPA secretion occurs in response to oxidative stress, which as alluded to earlier is a feature of the AD brain. Indeed, endothelial cells and even neurons are known to secrete CYPA at least *in vitro*.

Whilst exogenous addition of recombinant CyPA protein reportedly protects neurons against oxidative and ischemic injury (Boulos et al., 2007), no studies have conclusively determined that protection against A $\beta$  is mediated via the CD147 receptor. In the current study, I showed for the first time that recombinant CYPA protein protects primary cortical neurons and human SH-SY5Y neuroblastoma cultures against A $\beta$ 42, via a CD147 dependent mechanism. Importantly, although recombinant CYPA protein

appeared to increase the viability of cultures with basal CD147 expression, the level of protection only reached significance when CD147 was over expressed. These findings may be explained by a recent study, demonstrating that CYPA mediated biological effects require a threshold level of CD147 expression (Yang et al., 2008, Trachtenberg et al., 2011) cultures. Nevertheless, these results support the notion that CYPA mediates its neuroprotective effects through the CD147 receptor, which is presumably imparted by increasing pro-survival signalling such as ERK1/2 activation (Boulos et al., 2007), Bcl-2 up regulation (Biswas and Greene, 2002, Perkins et al., 2003, Metrailler-Ruchonnet et al., 2010) and through Bax and caspase3 inhibition (Abdi et al., 2011).

The impact of extracellular CYPA protein and CD147 signalling on AD may not just be limited to neuroprotective. CYPA/CD147 receptor signalling can also induce the production of matrix metalloproteinases (MMPs), including MMP9, which interestingly is known to be up regulated in AD brain (Backstrom et al., 1996, Lorenzl et al., 2003, Bruno et al., 2009, Romi et al., 2012). Of particular significance, Vetrivel et al, (2008) postulated that CD147 may aid A $\beta$  clearance, by somehow promoting its degradation. My findings linking A $\beta$ , CD147 expression and extracellular CYPA may provide a potential mechanism by which this could occur.

### **3.7: Conclusion**

Taken together, the findings of the present chapter identify potentially important relationships between cholesterol loading, CD147 expression, A $\beta$  toxicity and the putative involvement of CYPA protein in neuroprotection, and possibly in A $\beta$  clearance in AD.

## CHAPTER 4

### **A high fat/ high cholesterol diet does not affect CD147 levels in APPswe transgenic mice**

#### **4.1: Introduction**

The previous chapter provided evidence that cholesterol levels can modulate CD147 expression in culture as evidenced by elevated cellular CD147 levels under conditions of high cholesterol in the medium. The aims of the studies of this chapter involve extending these findings, in particular, determining the effect of increased cholesterol on CD147 levels *in vivo*.

Cholesterol, a component of cell and organelle membranes, is essential for normal brain function. The brain contains the largest single pool of cholesterol that account for 25% of total body cholesterol and its derivatives (Dietschy and Turley, 2004, Vaya and Schipper, 2007). Cholesterol levels in the brain are maintained mostly by recycling brain cholesterol, however some transfer of cholesterol from the brain to the periphery does occur across the BBB, most likely following conversion to 24-OH cholesterol. Transfer from the blood to the brain can also occur. Excessive dietary cholesterol may upset this balance in many ways, both directly and indirectly via effects on general lipid metabolism, inducing insulin resistance and cardiovascular problems. Defects in cholesterol metabolism can induce neurological dysfunctions (Tint et al., 1994, Feng et

al., 2003). Cholesterol accumulation has been shown to be toxic (Li et al., 2011) and can contribute to the development of age-related diseases (reviewed in Liu et al., 2010).

A number of studies have assessed the impact of high fat/ high cholesterol diets on AD pathology in transgenic and non-transgenic animal models. Animals fed high cholesterol diets often suffer from increased A $\beta$  deposition (Sparks et al., 1994b, Refolo et al., 2000b, Shie et al., 2002). For example, hypercholesterolemic mice (Refolo et al., 2000b) demonstrate an increase in deposit sizes of A $\beta$  (Refolo et al., 2000b), and in rabbits, a comparatively longer duration on a high cholesterol diet results in a more severe accumulation of brain A $\beta$  (Sparks et al., 1994a). In another study, higher levels of A $\beta$  deposition were observed in 12 month old TgAPPswe mice which had been fed a high fat/high cholesterol diet (HFHC) for 10 months (Shie et al., 2002), compared to TgAPPswe mice fed standard rodent chow.

As APP itself and the enzymes involved in its cleavage are associated with membranes, particularly the trans-membrane  $\gamma$ -secretase enzyme, it is not surprising that much research has centred around membrane cholesterol levels and their effect on A $\beta$  production. Cholesterol and sphingolipid-rich membranes microdomains (so called lipid rafts; (Lee et al., 1998, Wahrle et al., 2002) have been found to contain BACE1 and the  $\gamma$ -secretase complex, promoting A $\beta$  production at these sites (reviewed in Cheng et al., 2007). A $\beta$ 40 and A $\beta$ 42 have been found to accumulate in the lipid rafts of aging Tg2576 mice (Kawarabayashi et al., 2004), and interestingly, there appears to be a sequence in the appearance of APOE and phosphorylated tau with the former increasing progressively from 12 months and the latter from 18 months of age in Tg2576 mice (Kawarabayashi et al., 2004).

Membrane cholesterol content can switch APP processing from the amyloidogenic pathway to the non-amyloidogenic pathway or vice versa. Although the mechanisms remain unclear, alterations in membrane cholesterol levels may modulate lipid fluidity. Depletion of membrane cholesterol has been shown to lead to a reduction in A $\beta$  production, which is restored when cholesterol is replenished (Simons et al., 1998b, Wahrle et al., 2002). There is some controversy concerning these results however, as some researchers claim that the depletion of membrane cholesterol in many experiments is too severe for the effects to be physiologically relevant. It is thought that disorganization in the structure of the lipid bilayer could alter the  $\alpha$ -secretase processing of APP by shifting the proximity of the secretase cleavage sites to the intramembrane domain of APP, and in vitro studies have demonstrated that high levels of cholesterol affect  $\alpha$ -secretase and BACE activity and result in a decrease in soluble APP levels and an increase in A $\beta$  production. However, it is still unclear how membrane cholesterol influences  $\gamma$ -secretase activity, thought to be concentrated to lipid rafts (Dickstein et al., 2010). Some studies have shown that  $\gamma$ -secretase is dependent on lipid rafts but is not cholesterol-dependent, whereas others have shown that cholesterol can indeed modulate enzyme activity. Evidence has also been provided proposing that cholesterol plays a role in the conversion of soluble monomeric A $\beta$  into insoluble aggregates (Schneider et al., 2006).

Another mechanism that is explored in this chapter involves the regulation of some of the components of cholesterol metabolism. Many proteins have been linked to both cholesterol metabolism and AD, and one protein that is involved in both cholesterol metabolism and in CD147 function is the sterol carrier protein SCP-2. This protein plays a key role in cholesterol metabolism as it functions in cholesterol uptake (Hirai et al., 1994, Colles et al., 1995, Lipka et al., 1995, Moncecchi et al., 1996, Schroeder et al.,

1998, Atshaves et al., 1999), intracellular transport (Puglielli et al., 1995), esterification (Murphy and Schroeder, 1997) and oxidation (Chanderbhan et al., 1986, Yamamoto et al., 1991). In addition it has been shown to remodel lipid composition, structure and function of lipid rafts (Schroeder et al., 2007). As described in chapter 1 (section 1.7.6) SCP facilitates CD147 transcription; it is therefore conceivable that changes in cholesterol homeostasis (i.e. under cholesterol loading) will alter levels of SCP, thereby impacting on CD147 levels and A $\beta$  metabolism. Indeed cholesterol enrichment in rat aortic smooth muscle cells has been shown to result in an increase in SCP mRNA (Kraemer et al., 1995), providing evidence that cholesterol and its derivatives can regulate SCP expression. Whether this results in changes in CD147 levels, remains to be determined.

## **4.2: Aims**

The overall aim of the current study was to determine if dietary cholesterol loading impacts on cerebral CD147 levels *in vivo*. To assess this, AD model transgenic mice (APPswe) were fed a normal chow diet or a high fat/high cholesterol diet and the following were determined.

- 1) The impact of a high fat/high cholesterol diet on body weight and plasma cholesterol levels.
- 2) The impact of a high fat/high cholesterol diet on CD147 levels in the brain and peripheral organs. Any potential correlations between extent of changes and circulating cholesterol levels were also assessed.
- 3) The impact of a high fat/high cholesterol diet on SCP mRNA levels in the brain.



- 4) The impact of a high fat/high cholesterol diet on cerebral levels of APP and its metabolites.

### **4.3: Materials and methods**

#### **4.3.1: Experimental animals and diets**

The APP<sup>swc</sup> mice were divided into 4 different groups, and fed for 10 weeks on either standard mouse chow (control) or a high fat/high cholesterol diet containing 10% fat, 0.75% cholesterol, 0.3% cholate and additional vitamins (**Fig.4.1**). Baseline body weights were recorded, then mice were weighed once a fortnight. The average weight gain for each animal was calculated at the end of the study to determine the weight gain over the course of administering the diet. Following 10 weeks, mice were sacrificed and plasma, liver, brain and kidney tissues were collected; snap frozen and stored at – 80°C. The brains were divided into right (which were instantly snap frozen) and left (stored in RNA Later) hemispheres.

#### **4.3.2: Western blot and ELISA analyses**

Brain tissue homogenates underwent Western immunoblotting for CD147, FL-APP and the APP C-terminal fragments C-99 and C-83, whereas liver and kidney homogenates were immunoblotted for CD147 only, as described in section 2.5. Films of western immunoblots were scanned and optical density determined through the Bio-rad, Quantity One Software. Specifically film backgrounds were subtracted from optical density of individual protein bands. An internal control was run on each gel for inter-gel normalisation. Levels for the proteins of interest were represented as a ratio of the  $\beta$ -actin, to control for inter sample loading differences and presented in scatter plots.

Western blots for all individual data points are presented in next to their corresponding scatter plots.

ELISA was used for analysis of brain and plasma A $\beta$ 40 and A $\beta$ 42 levels as described in section 2.6.1. Total cholesterol levels were measured in plasma as described in section 2.6.2.

#### **4.3.3: SCP-2 analysis**

To assess whether the high fat/high cholesterol diet led to changes in SCP-2 transcript levels, SCP-2 mRNA was extracted from 100mg of APP<sup>swe</sup> mice brains fed on a normal chow or a high fat/high cholesterol diet using RNeasy Lipid Tissue Mini Kit (50) (Qiagen) according to the manufacturer's instructions. SCP-2 forward (TGCGTTGGCTATGTGTATGG) and reverse (TGCCAGTCAGTCCCAAATA) primers were designed using the Net Primer program and manufactured by Gene Works (Australia). Successful generation of the SCP-2 cDNA PCR product was confirmed by acrylamide gel electrophoresis. The cDNA amplification was performed using a 2-step cycling protocol (10 min at 95°C activation, 40 cycle of 15 sec at 95°C and 60 sec at 60°C, 60°C-95°C melt). The qRT-PCR reactions were performed using KAPA SYBR<sup>®</sup> FAST qPCR Kit Master Mix (South Africa) using the same primers on the Bio-Rad iCycler RT-PCR System using a total reaction volume of 20  $\mu$ l. The optical densities were normalized against mTB House Keeping Gene. SCP-2 expression was determined by comparing relative ratio values of mice fed on a normal chow diet against those fed on a high fat/high cholesterol diet.

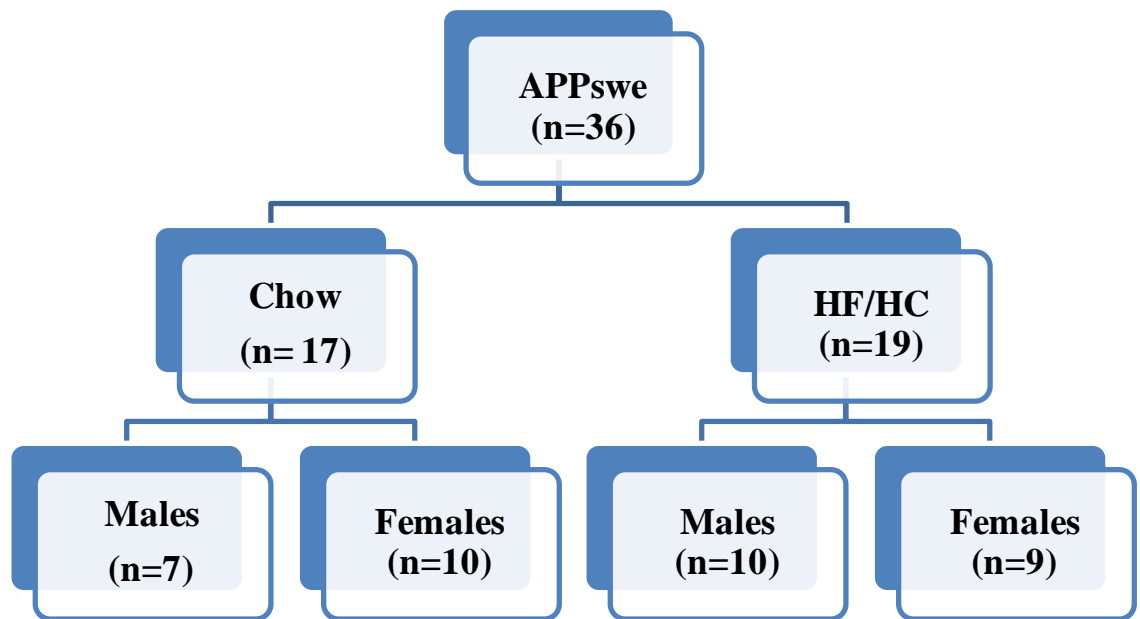


**Figure.4.1: Experimental groups**

APPswe mice ( $n=36$ ; 17 males, 19 females) were divided into two major groups. The first group ( $n=17$ ; 7 males, 10 females) were fed a normal chow diet and the other ( $n=19$ ; 10 males, 9 females) a high fat high cholesterol diet.

## 4.4: Results

### 4.4.1: Impact of a high fat/high cholesterol diet on body weight and plasma cholesterol levels.

Experimental mice were fed either a normal chow control or a high fat/high cholesterol diet for 10 weeks and weighed every fortnight. The body weight gain over the 10 week period is shown in **Figure 4.2**. As expected, all mice (either on the normal chow or high fat/ high cholesterol diet) gained weight over the treatment period, indicating that they were eating the diets provided.

Following 10 weeks of administering the diets, mice were sacrificed and tissues and plasma collected. Total plasma cholesterol was measured in all mice and levels are shown in **Fig. 4.3**. Compared to mice fed on the normal chow control diet, those fed a high fat, high cholesterol diet had significantly higher plasma cholesterol levels. Female mice on the high fat/high cholesterol diet exhibited a greater (2 fold) increase in cholesterol level, than males (compare **Fig. 4.3C** with **Fig.4.3B**). Overall, the results indicate that the high fat, high cholesterol diet consumed by the mice significantly increased plasma cholesterol levels.

To address the hypothesis that CD147 is altered in the presence of cholesterol *in vivo*, I then measured levels of this protein in the brain and peripheral organs of mice fed the different diets.

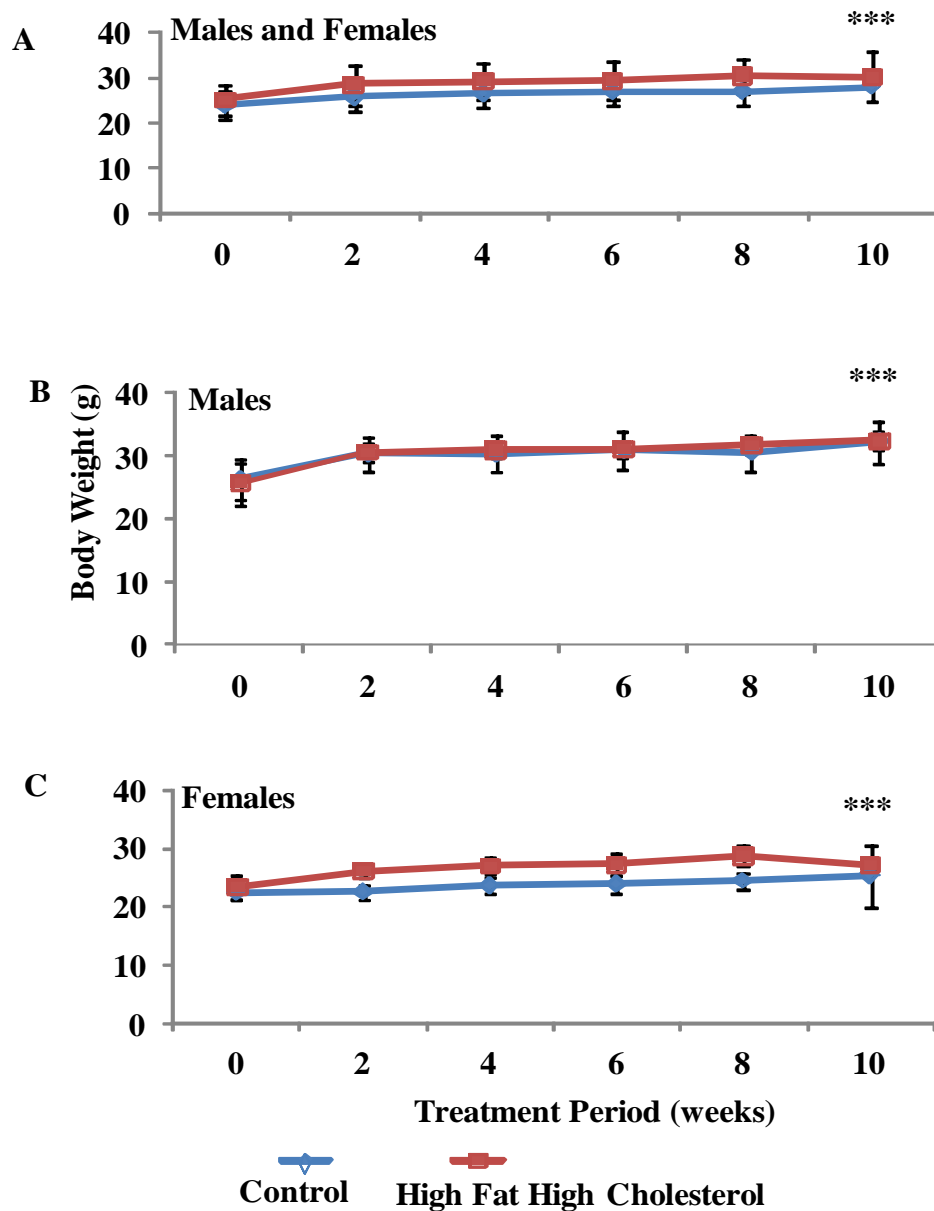


**Figure 4.2: Body weights of APPswe mice fed on a normal chow and high fat/high cholesterol diets.**

Graphs represent body weight gain in (A) all mice, n=36, (B) males, n=17 and (C) females, n=19 during the course of study. Mice were weighed at baseline (0) and every fortnight for 10 weeks after administering the diet. Data represents average body weight of mice at each of the measurement stages  $\pm$  SD. \*\*\*,  $p < 0.001$ , values significantly increased over baseline weights.

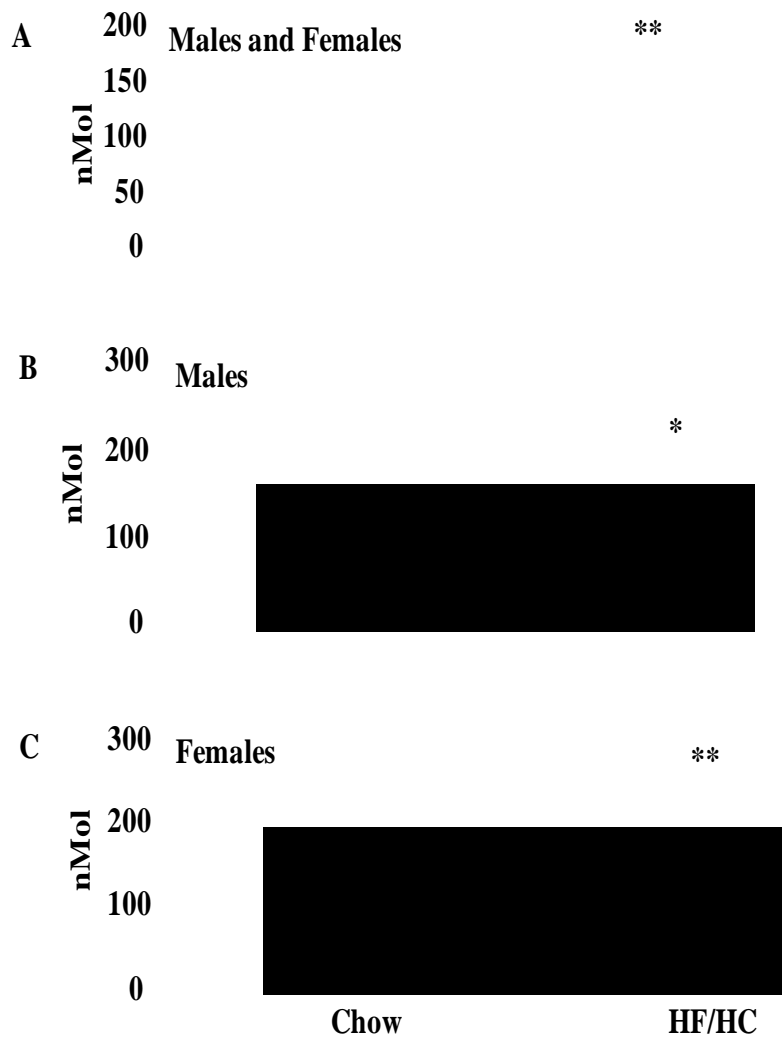


**Figure 4.3: Total plasma cholesterol levels in APPswe mice following 10 weeks feeding with experimental diets.**

Plasma cholesterol levels in (A) all experimental mice on a normal chow (n=17) or a high fat/high cholesterol diet (n=19), (B) males on a normal chow diet (n=7) or a high fat/high cholesterol diet (n=10) and (C) females on a normal chow (n=10) or a high fat/high cholesterol diet (n=9). The data represents mean  $\pm$  SE. \* $p < 0.05$ , \*\* $p < 0.01$ ; values significantly increased over those obtained from mice fed normal chow diet.

#### **4.4.2: Cerebral CD147 protein levels are not significantly altered in APP<sup>swe</sup> mice fed a high fat/high cholesterol diet**

The CD147 protein levels of tissue homogenates were measured by Western immunoblot analysis using the rodent specific antibody EMMPRINE SC-9753 as described above. Although expression of CD147 in rodent brain tissue has been widely reported (Nahalkova et al., 2010, Xie et al., 2010, Agrawal and Yong, 2011), detection of this protein in the kidneys and liver has yet to be documented. Thus preliminary analysis was performed where expression in the peripheral organs was compared to that observed in homogenates of primary rat neuronal lysate, human brain and mouse brain (**Fig 4.4**). A protein band similar to that detected in rat primary neuronal lysate, was also detected at ~58 kDa in mouse brain, liver and kidney homogenates. However this protein band was absent from the human brain homogenates, indicating EMMPRINE SC-9753 antibody specificity for rodent CD147.

Having established that CD147 can be detected in mouse brain, liver and kidneys, immunoblotting with this antibody was then performed on homogenates from all the experimental mice (**Fig.4.5**). Semi-quantitative analysis revealed no significant changes in CD147 level in either the males or the females. However, compared to mice fed on a normal chow diet, the data indicate an increasing trend in males ( $p=0.096$ ) and a decreasing trend in females ( $p=0.201$ ) fed on the high fat/high cholesterol diet (**Fig.4.5C and D**, respectively). Analysis of CD147 protein levels in the peripheral organs (kidney and liver) revealed a significant reduction in the kidney tissue levels of CD147 in the males only ( $p=0.03$ ) (**Fig. 4.6**). No significant differences in CD147 levels were observed in the liver samples (**Fig.4.7**) from either the male or the female

mice on the different diets. However, compared to mice fed the normal chow diet, a trend towards lower CD147 levels was observed in liver tissues from the male mice fed on the high fat/high cholesterol diet.



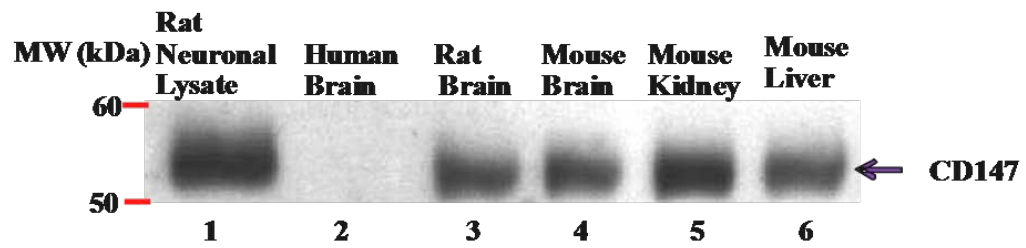


**Figure 4.4: Immunodetection of CD147 using rodent EMMPRINE SC-9753 antibody.**

Immunoblot of rat neuronal lysate (lane 1), human and mouse brain tissues (lanes 2-4) and mouse peripheral tissues (lanes 5-6). CD147 was detected in rat (lanes 1 and 3) and mouse (lanes 4-6) but not human (lane 2) tissue samples indicating the EMMPRINE SC-9753 antibody used is specific for rodent CD147.

**NOTE: THIS PAGE IS LEFT BALNK ON PURPOSE**

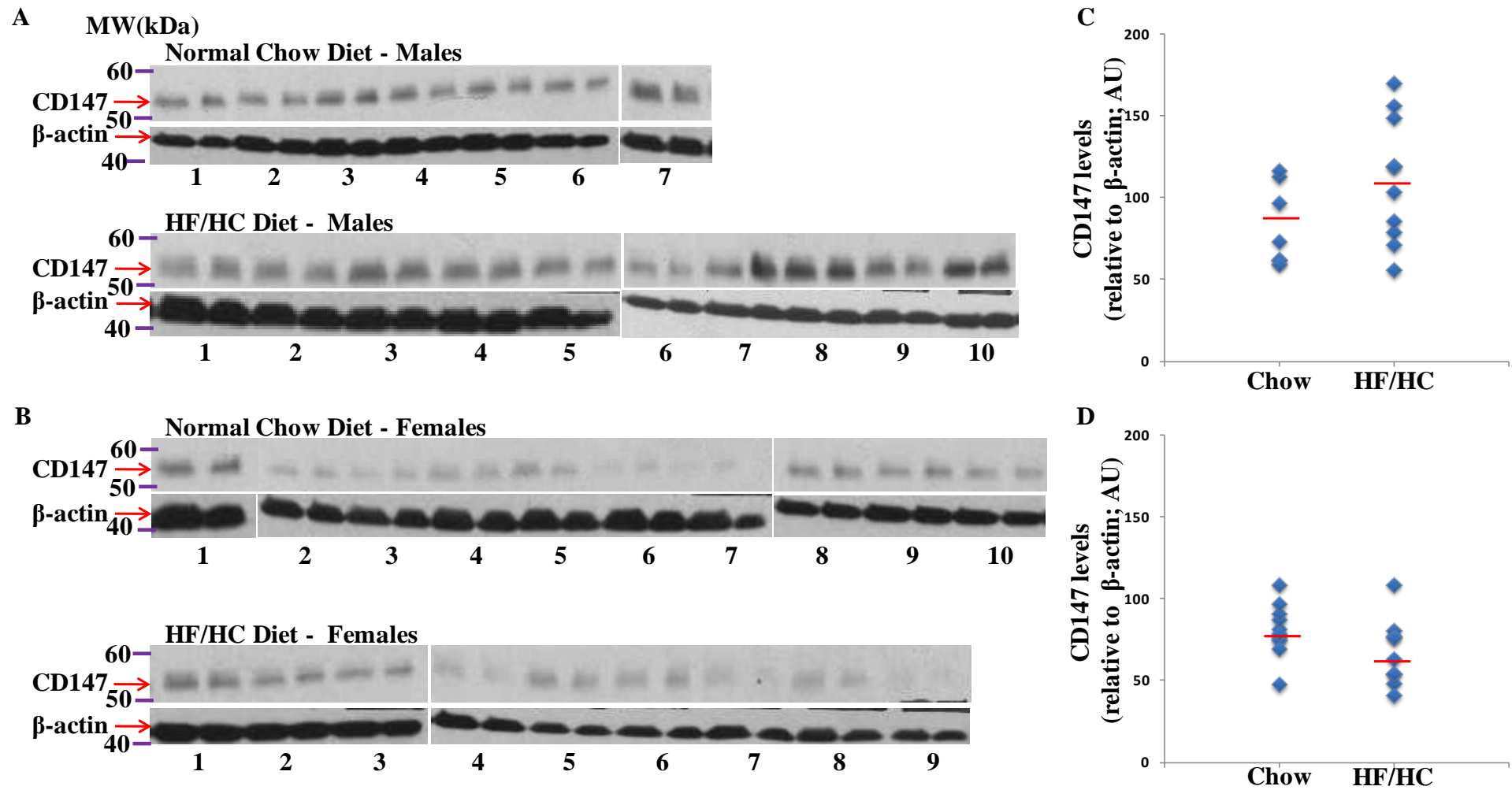


**Fig.4.5: Brain CD147 levels in brain tissue from APP<sup>swe</sup> mice following 10 weeks feeding with experimental diets.**

**Figure 4.5: Brain CD147 levels in brain tissue from APP<sup>sw</sup> mice following 10 weeks feeding with experimental diets.**

Western blot analysis of brain tissue from APP<sup>sw</sup> mice fed the normal chow diet or the high fat/high cholesterol diet for 10 weeks, males (A, C) and females (B, D). Western blots of brain homogenates run in duplicate show the 58 kDa CD147 protein levels and corresponding  $\beta$ -actin levels as a loading control in males (A) and females (B). Scatter plots of quantitated CD147 levels in males (C) and females (D) on the different diets. Individual points represent a specific mouse sample value (average of duplicate samples in adjacent lanes) with the group mean represented by a horizontal line. Compared to those fed on a normal chow diet, data indicate a trend towards higher CD147 levels in males and a trend towards lower levels in females fed the high fat/high cholesterol diets respectively.

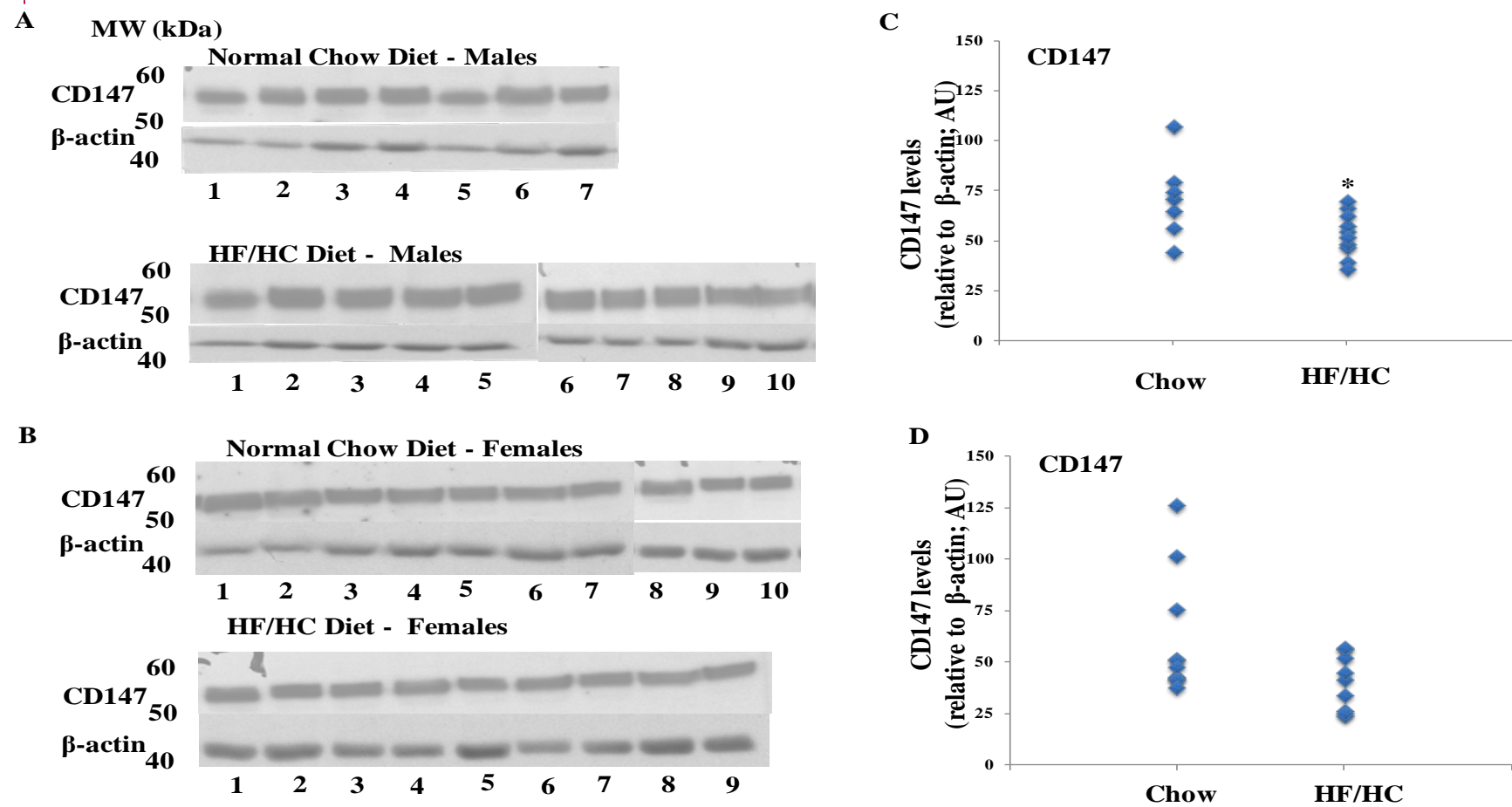


Figure 4.6: CD147 levels in kidney tissue from APP<sup>swe</sup> mice following 10 weeks feeding with the experimental diets.

**Figure 4.6: CD147 levels in kidney tissue from APP<sup>swc</sup> mice following 10 weeks feeding with the experimental diets.**

Western blot analysis of kidney tissue from APP<sup>swc</sup> mice fed the normal chow diet or the high fat/high cholesterol diet for 10 weeks, males (A, C) and females (B, D). Western blots of kidney homogenates show the ~58 kDa CD147 and corresponding  $\beta$ -actin levels as a loading control in males (A) and females (B). Scatter plots of quantitated CD147 levels from in males (C) and females (D) on the different diets. Individual points represent a specific mouse value with the group mean represented by horizontal line. Compared to mice fed the normal chow diet, data indicate a significant reduction in CD147 levels ( $*p<0.05$ ) in the male mice fed the high fat/high cholesterol diet, with a trend towards lower levels in the female mice fed the high fat/high cholesterol diet.

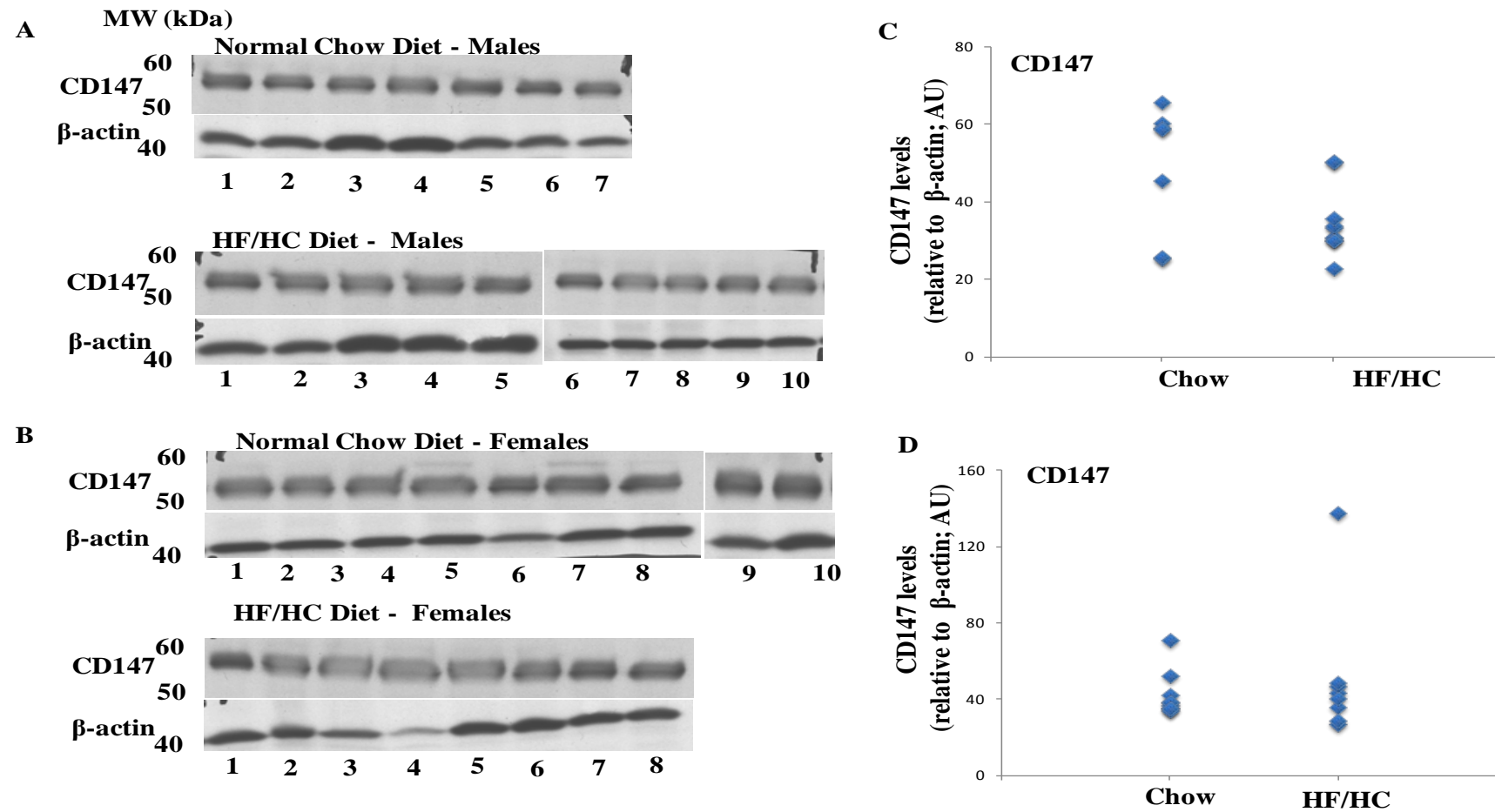


Figure 4.7: CD147 levels in liver tissue from *APP<sup>sw/e</sup>* mice following 10 weeks feeding with the experimental diets.

**Figure 4.7: CD147 levels in liver tissue from APP<sup>swc</sup> mice following 10 weeks feeding with the experimental diets.**

Western blot analysis of liver tissue from APP<sup>swc</sup> mice fed the normal chow diet or the high fat/high cholesterol diet for 10 weeks, males (A, C) and females (B, D). Western blots of liver homogenates run as single samples show the ~58 kDa CD147 levels and corresponding  $\beta$ -actin levels as a loading control in males (A) and females (B). Scatter plots of quantitated CD147 levels from males (C) and females (D) on the different diets. Individual points represent a specific mouse value (as quantitated from adjacent samples) with the group mean represented by a horizontal line. Compared to mice fed the normal chow diet, data indicate no significant change in CD147 levels. However there is a trend towards lower CD147 levels in the males fed the high fat/high cholesterol diet.



#### **4.4.3: Transcription of SCP-2 is not altered by a high fat/high cholesterol diet.**

The sterol carrier protein (SCP-2) plays a key role in a number of aspects of cholesterol metabolism (Hirai et al., 1994, Colles et al., 1995, Lipka et al., 1995, Moncecchi et al., 1996, Schroeder et al., 1998, Atshaves et al., 1999) and is a key regulator of CD147 expression (Ko and Puglielli, 2007). Evidence exists that cholesterol can regulate SCP mRNA in rat aortic smooth muscle cells (Kraemer et al., 1995). In the section above I have shown that the CD147 protein levels in the brain are not altered but increasing trend in males and decreasing trend in females were observed in mice fed on a high fat high cholesterol diet. To determine if this is associated with changes in SCP transcription, the brain tissue underwent quantitative RT-PCR analysis as described in section 4.3. The mRNA was extracted from brain tissue stored in RNA later. Forward and reverse primers were designed against SCP as well as a housekeeping gene mTB (see section 4.3) and used to amplify the transcripts for quantitative RT-PCR. PCR analysis of cDNA using the primers (**Fig. 4.8A**) shows the presence of a ~173 bp transcript representing SCP-2 (lanes 3-6, blue arrow) and a ~175 bp transcript representing mTB (lanes 8-11, red arrow). These bands were absent in the control (lanes 2 and 7), which consisted of master mix without cDNA template and indicates the absence of contaminating DNA. These results validated the use of the primers for quantitative RT-PCR analysis for amplification of the mRNA.

Amplification curves show that SCP-2 was successfully amplified starting from cycle 25 peaking at cycle 35 (**Fig. 4.8B**) with the amplification peak temperature of 80°C (**Fig. 4.8 C and D**). The relative amounts of generated SCP-2 transcript, represented as a ratio of the MTB housekeeping gene is shown in Figure 5.9. The results show that compared to mice fed normal chow control diet, SCP-2 transcript levels were not altered in brain tissue from mice fed a high fat/ high cholesterol diet (**Fig.4.9**).

**Note: This page left blank on purpose.**

DNA Ladder  
(100bp)

PCR

RT-PCR

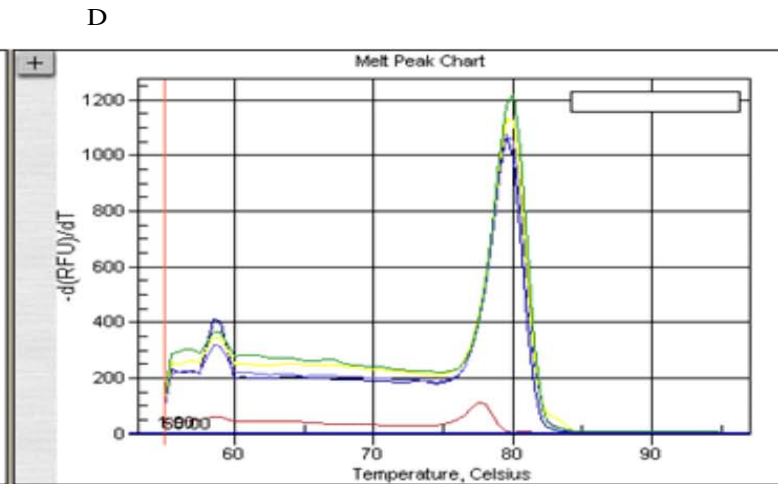
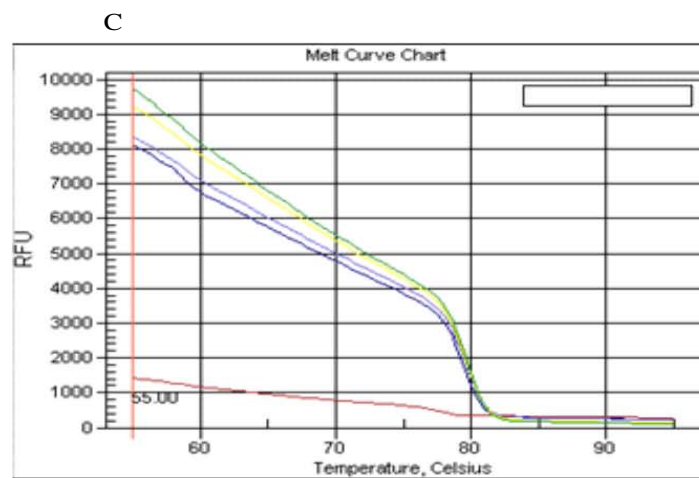
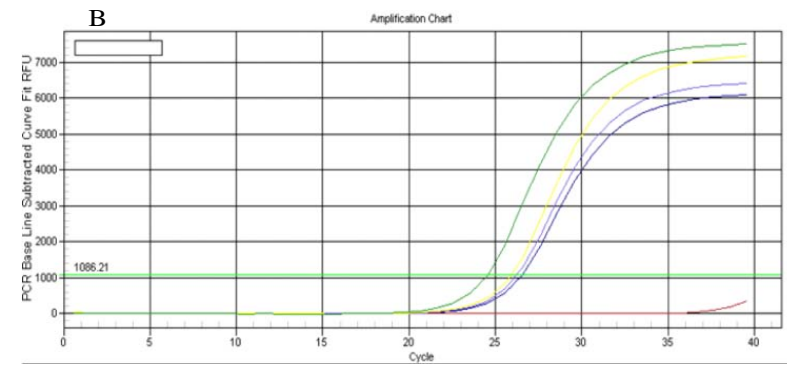
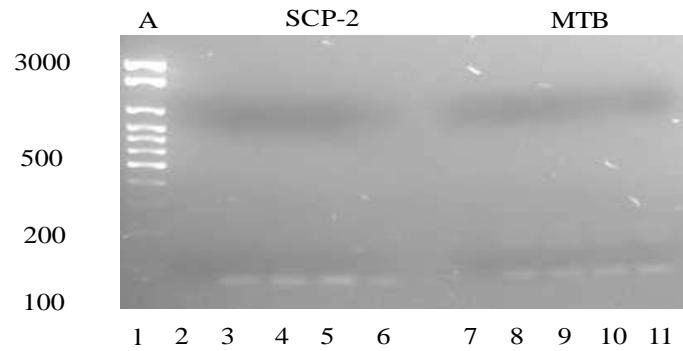


**Figure 4.8: Amplification of SCP-2 mRNA by RT-PCR in brain tissue from APP<sup>swe</sup> mice fed the experimental diets**

**Figure 4.8: Amplification of SCP-2 mRNA by RT-PCR in brain tissue from APPswe mice fed the experimental diets**

Agarose gel of PCR products of cDNA extracted from 4 samples of 100 mg brain tissue (2 from mice fed the normal chow diet and 2 from mice fed high fat/high cholesterol diet) (A). The 100 bp DNA ladder is shown in lane 1, and the master mix without cDNA (negative control) is shown in lanes 2 and 7. SCP was successfully amplified and detected as a ~173 bp band (lanes 3-6, blue arrow). The mTB housekeeping gene was also successfully amplified and can be seen as a ~175bp band (lanes 8-11, red arrow). Representative charts of (B) amplification (C), melting curve and (D) melting peak of amplified SCP-2.

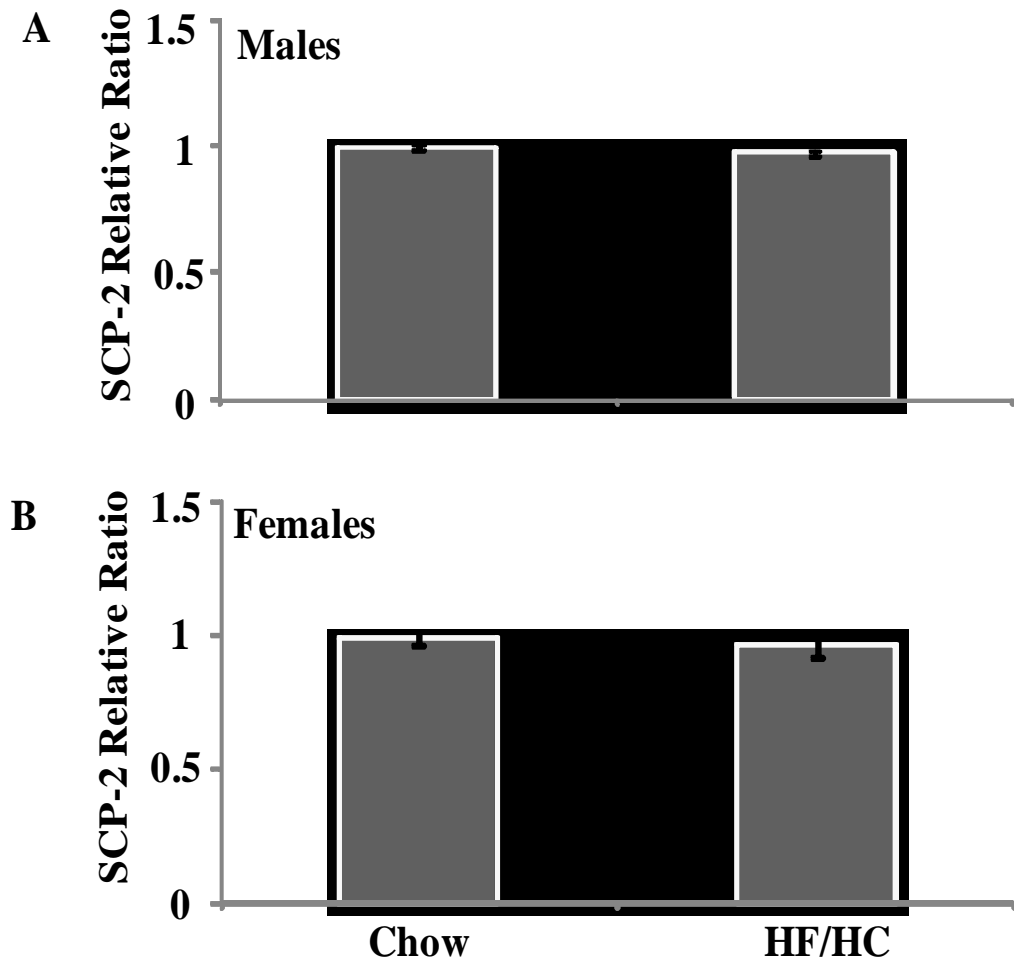


**Figure 4.9: SCP-2 mRNA levels in brain tissue from APPswe mice fed the normal chow diet or the high fat/high cholesterol diet.**

Levels of SCP-2 mRNA were measured in brain tissue from (A) Male and (B) Female mice fed a normal chow diet or high fat/high cholesterol diets. Data was normalised against the housekeeping gene *mTB* and levels are represented as a ratio of that observed in brain tissue from mice fed the normal chow diet (indicated as a “relative ratio”). Data are represented as mean  $\pm$ SD and show no difference in SCP-2 mRNA levels between mice fed on normal chow and high fat/high cholesterol diets.

#### **4.4.4: Effects of the high fat/high cholesterol diet on APP and some of its metabolites.**

Studies investigating APP metabolism in transgenic mice fed high fat and/or high cholesterol diets have shown various effects on A $\beta$  metabolism. Refolo et al. reported increases (Refolo et al., 2000a), Howland et al. reported a decrease (Howland et al., 1998) and George et al. reported no change in A $\beta$  levels (George et al., 2004). To determine if the diet used in this study impacted on levels of APP and its metabolites in mouse brain tissue, brain homogenate levels of full length APP and its C-terminal fragments (C83 and C99) were assessed by Western immunoblotting (as described in section 2.5). The C83 fragment is the C-terminal fragment of APP left in the membrane after  $\alpha$ -secretase cleavage, whereas the C99 fragment is the membrane fragment of APP that is left after  $\beta$ -secretase cleavage. The results show a significant increase in FL-APP levels in brain tissue from both the male ( $p=0.026$ ) and female ( $p=0.004$ ) mice fed the high fat high cholesterol diet (**Fig. 4.10**). Furthermore, the male mice fed the high fat/high cholesterol diet demonstrated significantly lower levels of the APP C83 fragment ( $p=0.003$ ) compared to those fed a normal chow diet (**Fig. 4.12A and C**). A trend towards lower levels of the APP C99 fragment was also observed in the brain tissue of male mice that had been fed the high fat/high cholesterol diet (**Fig.4.11A and C**), compared to those on the normal chow diet.

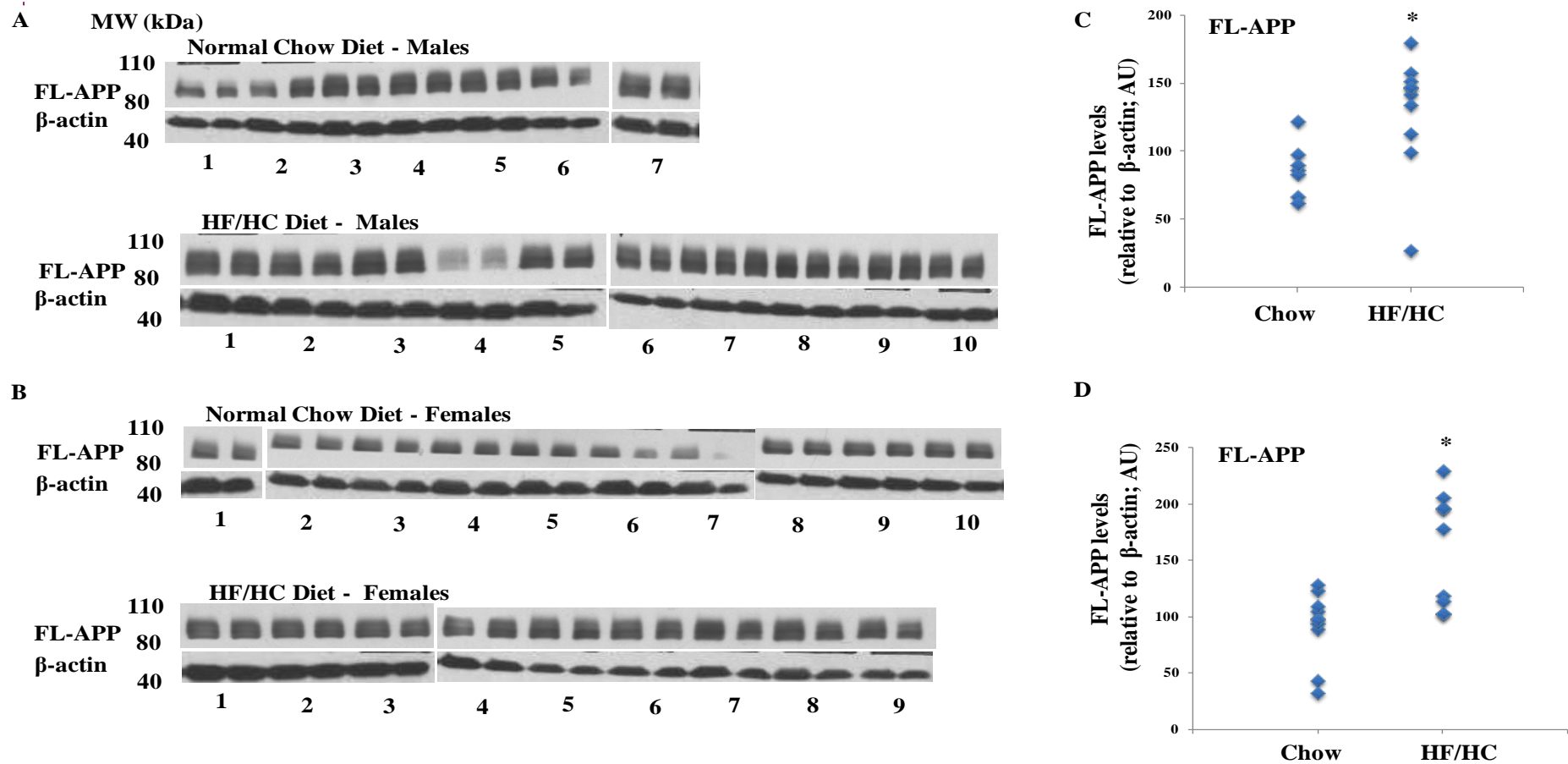


Figure 4.10: FL-APP levels in brain tissue homogenate from *APP<sup>swe</sup>* mice fed the normal chow diet or the high fat high cholesterol diet.

**Figure 4.10: FL-APP levels in brain tissue homogenate from APP<sup>swc</sup> mice fed the normal chow diet or the high fat high cholesterol diet.**

Western blot analysis of brain tissue from APP<sup>swc</sup> mice fed the normal chow diet or the high fat/high cholesterol diet for 10 weeks, males (A, C) and females (B, D). Western blots of brain homogenates run in duplicate showing the ~95-105 kDa FL-APP protein levels and corresponding  $\beta$ -actin levels as a loading control in males (A) and females (B). Scatter plots of quantitated FL-APP levels from males (C) and females (D) on the different diets. Individual points represent a specific mouse sample value (average of duplicates in adjacent lanes) with the group mean represented by a horizontal line. Compared to those fed the normal chow diet, data indicates significantly higher FL-APP levels ( $*p < 0.05$  respectively) in both males and females fed the high fat/high cholesterol diet.



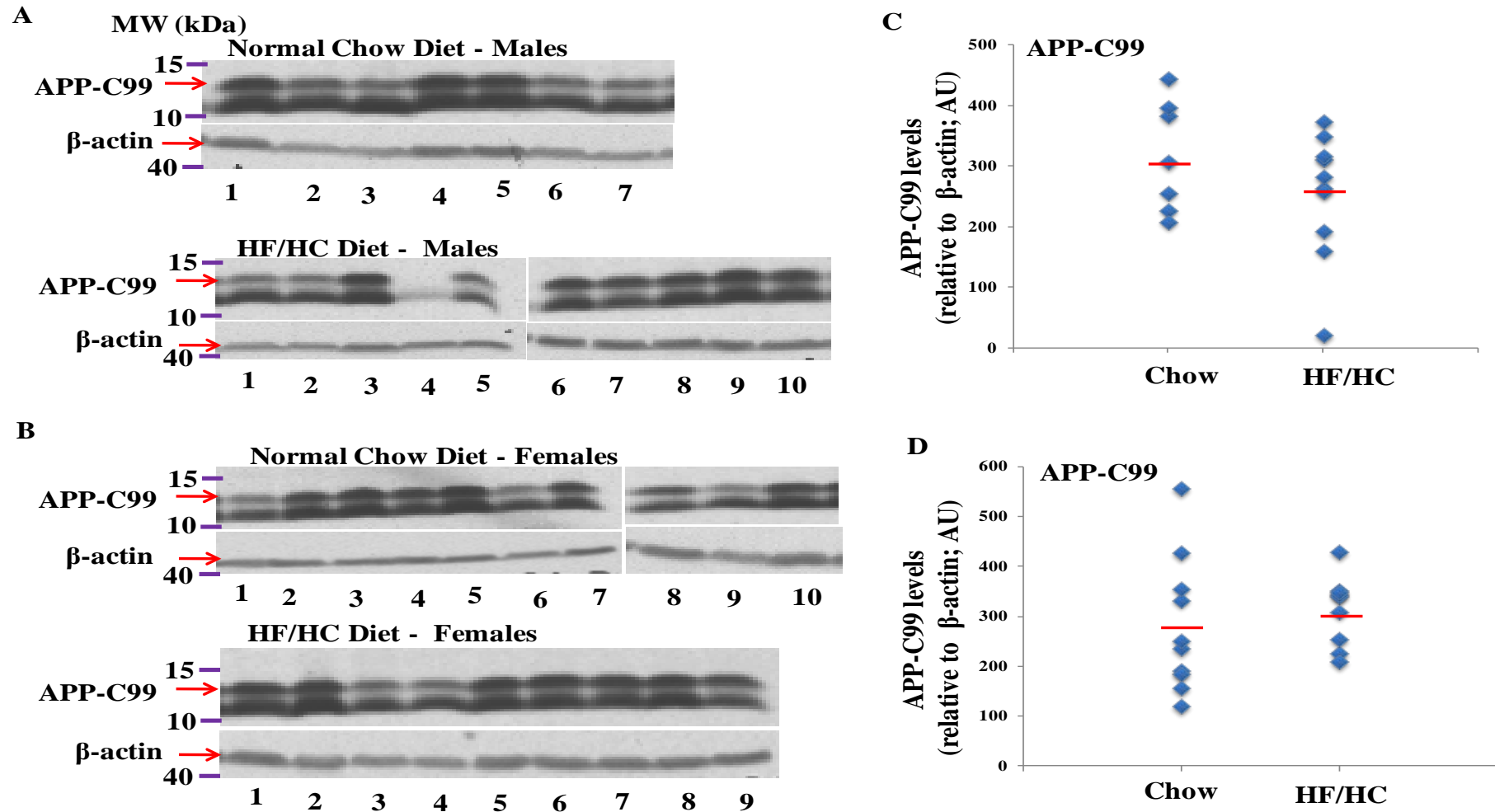


Figure 4.11 Brain APP-C99 levels in APP<sup>swe</sup> mice after 10 weeks on the different diets

**Figure 4.11 Brain APP-C99 levels in APP<sub>swe</sub> mice after 10 weeks on the different diets**

Western blot analysis of brain tissue from APP<sub>swe</sub> mice fed the normal chow diet or the high fat/high cholesterol diets for 10 weeks, males (A, C) and females (B, D). Western blots of brain homogenates showing the ~10 kDa APP-C99 protein levels and the corresponding  $\beta$ -actin levels as a loading control in males (A) and females (B). Scatter plots of quantitated APP-C99 levels from males (C) and females (D) on the different diets. Individual points represent a specific mouse sample value (as quantitated from adjacent lanes) with the group mean represented by a horizontal line. Compared to those fed the normal chow diet, the data indicate no change in APP-C99 levels in either the male or female mice fed the high fat high cholesterol diet. However a trend towards lower levels of C99 fragments can be seen in the male mice fed the high fat/high cholesterol diet.

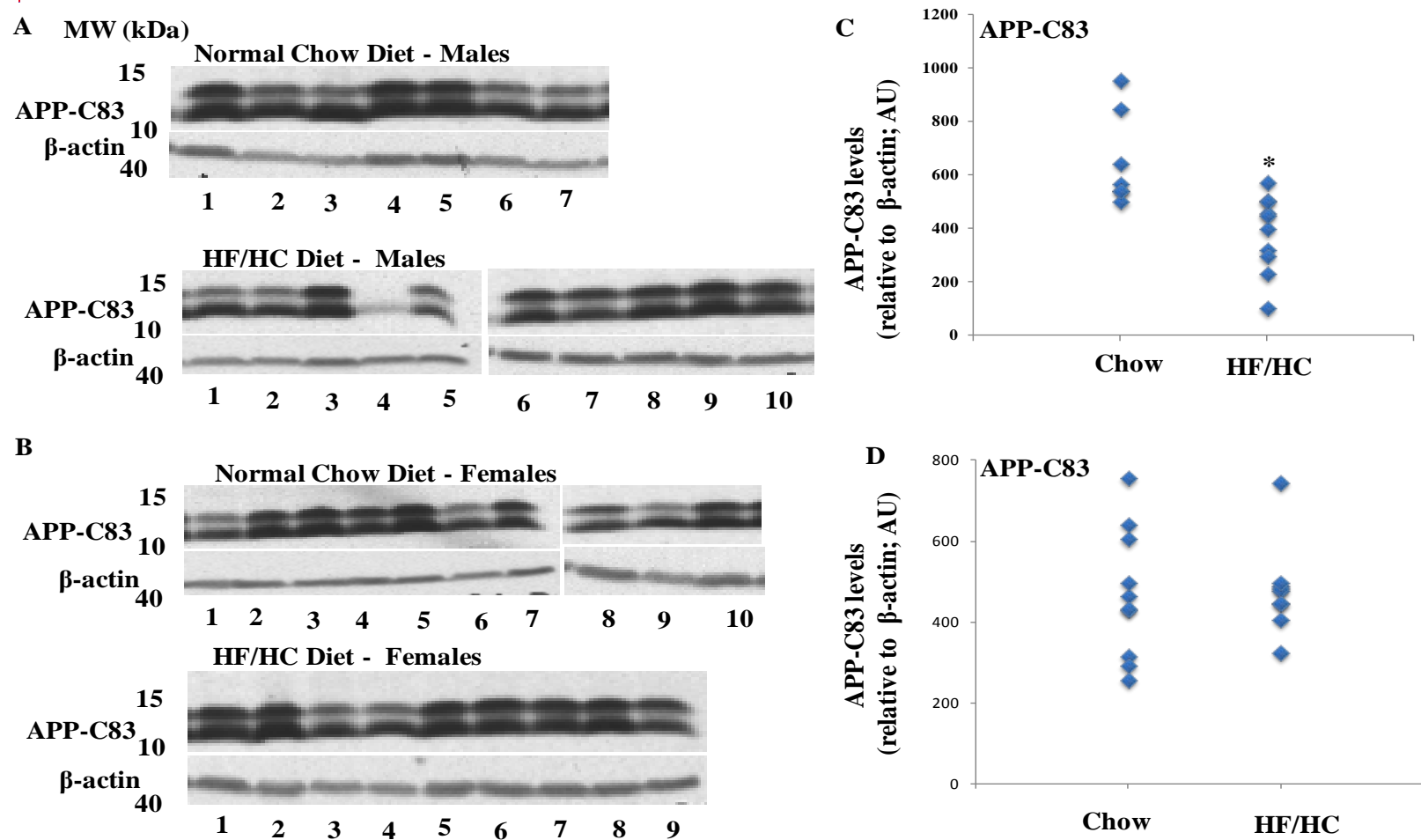


Figure 4.12 Brain APP-C83 levels in APP<sup>swe</sup> mice after 10 weeks on either the normal chow diet or the high fat/high cholesterol diet.

**Figure 4.12 Brain APP-C83 levels in APP<sup>swe</sup> mice after 10 weeks on either the normal chow diet or the high fat/high cholesterol diet.**

Western blot analysis of brain tissue from APP<sup>swe</sup> mice fed the normal chow diet or the high fat/high cholesterol diets for 10 weeks, males (A, C) and females (B, D). Western blots of brain homogenates showing the ~10 kDa APP-C83 protein levels and corresponding  $\beta$ -actin levels as a loading control in males (A) and females (B). Scatter plots of quantitated APP-C83 levels from males (C) and females (D) fed the different diets. Individual points represent a specific mouse sample value (as quantitated from adjacent lanes) with the group mean represented by a horizontal line. Compared to those fed the normal chow diet, data indicates a significantly lower levels of APP-C83 fragments ( $*p<0.01$ ) in the males after being fed the high fat/high cholesterol diet.

#### **4.4.5: Ratio of A $\beta$ 42/A $\beta$ 40 peptides in the brain and periphery of APPswe mice after 10 weeks on a high fat/high cholesterol diet or normal chow diet.**

To determine whether the high fat high cholesterol diet impacted on brain A $\beta$  accumulation, brain levels of A $\beta$ 40 and A $\beta$ 42 peptides were measured by ELISA as described in section 2.6.1. As an increase in A $\beta$ 42 is indicative of greater pathology, the data is represented as a ratio of A $\beta$ 42/A $\beta$ 40 (**Fig. 4.13**). Although not significant, a trend towards an increase in brain A $\beta$ 42/A $\beta$ 40 ratio is observed in mice fed high cholesterol/ high fat diet (**Fig. 4.13 A-C**), indicating a shift in A $\beta$  production towards the longer more amyloidogenic form of A $\beta$  (A $\beta$ 42), or perhaps indicating that less A $\beta$ 42 was being cleared. It is noted however, that there is a large variation amongst those mice fed the high fat/high cholesterol diet. In particular a few mice (2 females and 3 males) had ratios of much greater than 2, indicating more than 2-fold greater levels of A $\beta$ 42 compared to A $\beta$ 40 levels. Interestingly it should be noted that 3 of these mice had the highest levels of plasma cholesterol (>200nMol), suggesting plasma cholesterol levels can influence APP metabolism and/or A $\beta$ 42 production.

Peripheral A $\beta$  levels have been evaluated as a potential AD biomarker and have been used to assess a number of therapeutic agents including  $\gamma$ -secretase inhibitors or agents to promote amyloid clearance in preclinical studies using transgenic mice models (Kounnas et al., 2010, Wang et al., 2011, Winkler et al., 2010, Martone et al., 2009). Clinical studies have shown positive correlations between hypercholesterolaemia or body fat and peripheral A $\beta$  levels (Balakrishnan et al., 2005, Hoglund et al., 2004, Smith et al., 2001). To determine if a high fat/ high cholesterol diet can induce changes in peripheral A $\beta$  levels, plasma A $\beta$ 40 and A $\beta$ 42 levels were measured. The results are again shown as a ratio (**Fig 4.14**), and no overall significant change in plasma A $\beta$ 42/40

ratio was observed in the periphery of mice fed the high fat/ high cholesterol diet, compared to those fed the normal chow diet.

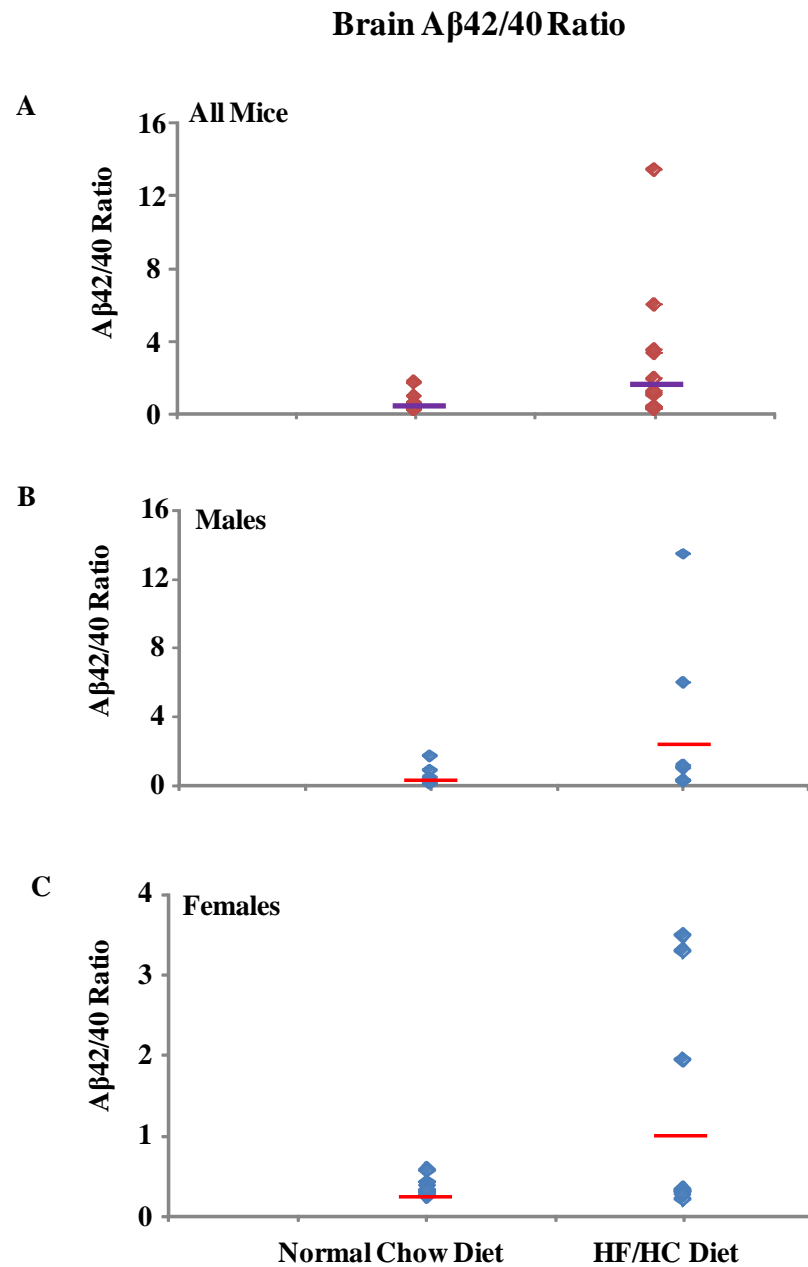


**Figure 4.13: Brain A $\beta$ 42/40 ratios in APPswe mice fed on a high fat/high cholesterol diet compared to controls after 10 weeks.** Representative scatter plots showing brain A $\beta$ 42/40 ratios: (A) all mice, (B) males and (C) females. Individual points represent a specific sample value with the sample mean represented by horizontal line. There were no significant differences however results show that there is a trend towards an increase in the mice brain A $\beta$ 42/40 ratios, after being fed the high fat/high cholesterol diet for 10 weeks.

## Plasma A $\beta$ 42/40 Ratio

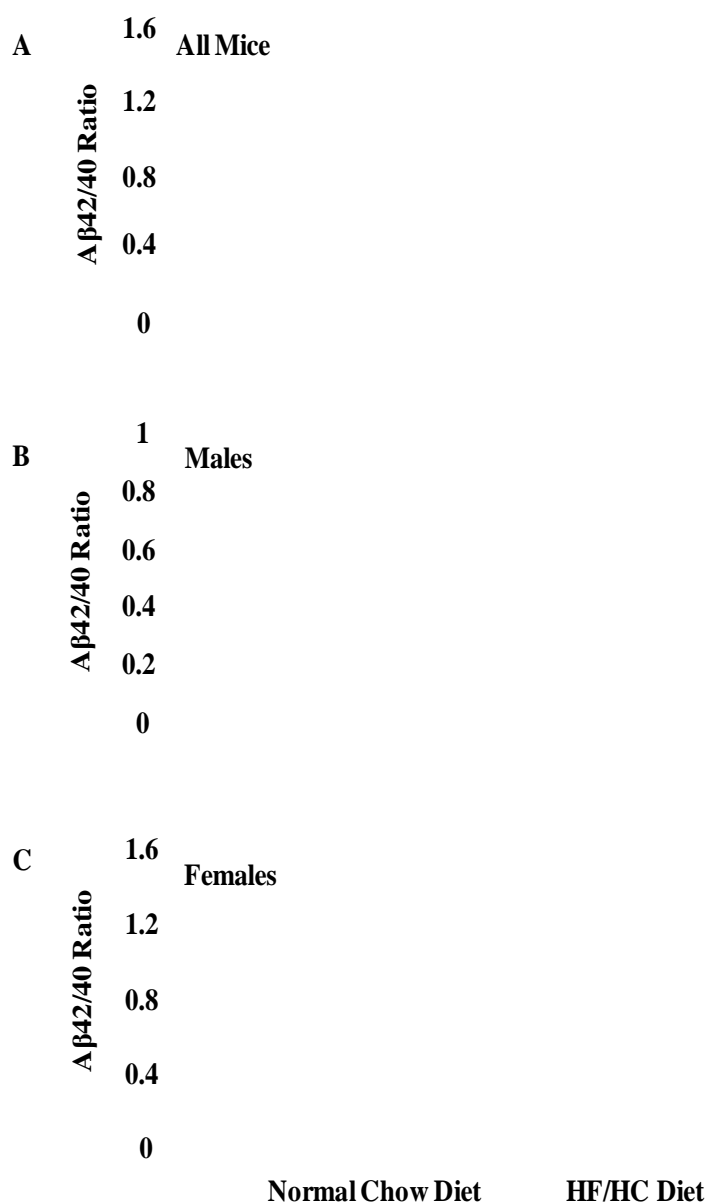


**Figure 4.14: Plasma A $\beta$ 42/40 ratios in APPswe mice fed either a high fat/high cholesterol diet or a normal chow diet for 10 weeks.**

Representative scatter plots showing plasma A $\beta$ 42/40 ratios: (A) all mice, (B) males and (C) females. Individual points represent a specific sample value with the group mean represented by a horizontal line. Results indicate that plasma A $\beta$ 42/40 ratios were not altered.



#### **4.5: Summary of results**

Overall the results presented in this chapter show associations between increases in plasma cholesterol with increases in brain FL-APP, and a trend towards a higher proportion of brain A $\beta$  being the more amyloidogenic A $\beta$ 42 peptide. No changes in cerebral CD147 levels were detected as a result of high fat/high cholesterol diet, though significantly lower levels were detected in the male mouse kidney samples, and a trend towards lower CD147 levels was detected in the female mouse kidney samples. Observed changes do not appear to be mediated by changes in SCP-2 gene expression, as the high fat/ high cholesterol diet did not alter SCP-2 transcript levels. Although not significant, a trend towards increases in cerebral A $\beta$ 42 levels was observed in those mice fed the high fat/ high cholesterol diet, and there was also a trend towards lower levels of C-terminal fragments of APP, though only in male mice.

#### **4.6: Discussion**

The expression of CD147 is known to play an important role in a number of pathological diseases/disorders. Examples include facilitating metastasis of many cancers (lung, cervical and prostate cancers) through MMP induction (Zeng et al., 2011, Wu et al., 2011, Han et al., 2011 (Zhu et al.) and facilitating chemokine-mediated recruitment of inflammatory cells in pathological conditions involving inflammation (see chapter 1, (Kanyenda et al., 2011)). Roles of CD147 expression in the CNS are less established, however it appears to be important in neurodevelopment and neuroprotection (see chapter 1, (Kanyenda et al., 2011)). With respect to AD, CD147 expression has been shown to regulate A $\beta$  levels *in vitro* and *in vivo*, for example RNAi knockdown of this gene results in A $\beta$  accumulation (Zhou et al., 2005) and over-expression results in a reduction in A $\beta$  levels (Vetrivel et al., 2008b).

Knockdown studies have shown that the sterol carrier protein is a major transcription factor that controls the expression of CD147. As shown and described in chapter 6, SCP binds CD147 within the promoter region and influences CD147 transcription. The sterol carrier protein is a key protein involved in cholesterol metabolism where it has been shown to promote cholesterol uptake (Hirai et al., 1994, Colles et al., 1995, Lipka et al., 1995, Moncecchi et al., 1996, Schroeder et al., 1998, Atshaves et al., 1999), and facilitate cholesterol intracellular transport (Puglielli et al., 1995), esterification (Murphy and Schroeder, 1997) and oxidation (Chanderbhan et al., 1986, Yamamoto et al., 1991). In addition it has been shown to remodel lipid composition, structure and function of lipid rafts (Schroeder et al., 2007). Given the importance of this protein in cholesterol metabolism, it is conceivable that SCP would respond to changes in cholesterol levels. Indeed Kraemer and colleagues (Kraemer et al., 1995) showed an up-regulation of SCP in muscle cells treated with cholesterol.

#### **4.6.1: High fat/high cholesterol diet influences plasma cholesterol levels**

In the previous chapter, evidence was produced which showed that CD147 levels in primary neuronal cells were altered in a dose dependent manner following exposure to cholesterol (Chapter 3, section 3.4.2). In the current study, APPswe mice were fed a high fat/high cholesterol diet to provide an *in vivo* experimental model to assess the impact of a high cholesterol diet on CD147 protein expression, and to determine if there were any changes associated with alterations in SCP and APP metabolism.

To raise peripheral levels of cholesterol, mice were fed a diet containing 10% fat, 0.75% cholesterol and 0.3% cholate, with controls feed on normal chow diet (SF08-020,

AIN93M Extra added vitamins) for 10 weeks. This led to a ~2 fold increase in plasma cholesterol levels (**Fig.4.3**). Previous studies on AD transgenic models have used similar high fat/high cholesterol diets however with cholesterol content ranging from 1.25% to 5% ((Refolo et al., 2000b, Shie et al., 2002, Li et al., 2003a, Fitz et al., 2010).

The composition of the diet was the same as that used in a study undertaken by a previous PhD student in our laboratory (Florence Lim) following changes from the initial composition of the diet. The student initially used a high fat/ high cholesterol diet comprising of 10% fat, 1% Cholesterol and 0.5% cholate, which was fed to APOE KI mice. The mice did not adapt well to the high fat/ high cholesterol diet, they did not find it palatable, most likely due to the bitter taste of cholate. The problem was rectified promptly by the addition of 7.5g fructose per 100 g of animal chow to make the food sweeter and to counteract the bitterness of the cholate. The percentages of cholesterol and cholate were also reduced (10% fat, 0.75% Cholesterol and 0.3% cholate). It is also important to note that when fructose was added to this high fat/high cholesterol diet, the sucrose content was also decreased slightly from 10g/100g feed (as in control rodent chow) to 7.5g/100g feed. In the presence of cholate, cholesterol can be more readily absorbed by the animal and therefore needs be included in the diet. Despite the lower dietary cholesterol content, significant fold increases in plasma cholesterol (2-3 folds) were observed in these previous experiments, compared to plasma levels of mice on the control diet. The same diet conditions were used in the current study and resulted in similar increases in plasma cholesterol.

In previous studies, apart from the diet containing greater cholesterol content, the mice were maintained on the high fat/high cholesterol diets for a much longer period of time (4 months to 10 months). This may explain the slightly greater increase in serum

cholesterol levels (2-4 fold increase) than that observed in the current study. However, using such diets and treatment periods (7-10 months), some studies have shown similar increases to those shown in the current study (Shie et al., 2002, Mihovilovic et al., 2007, Fitz et al., 2010)). Despite the above-mentioned studies not showing dramatic increases in serum cholesterol, enhanced amyloid deposition was still evident, indicating that moderate increases in cholesterol can still lead to changes in pathology. As described below, despite the lower cholesterol content used and shorter duration of treatment in the current study, changes in A $\beta$  levels were observed.

Interestingly, the increase in plasma cholesterol in female mice was greater than that observed in male mice. Male and female mice exhibited a similar weight gain, suggesting that the amount of food ingested by the male and female mice was similar, thus it is unlikely that the male to female differences in serum cholesterol levels are due to the females eating significantly more than the males. Previous studies have reported sex differences in cholesterol metabolism and homeostasis. In a model of severe hypercholesterolaemia, where the peroxisome proliferator-activated receptor (PPAR $\alpha$ ) important for lipid metabolism and homeostasis was ablated, differences between female and male mice were observed where female mice showed higher cholesterol levels and deposited fat earlier than male mice (Costet et al., 1998). Another study provided evidence for a role for oestrogen, such that in the absence of this hormone (through ablation of aromatase), serum cholesterol levels were increased only in female mice. In contrast, under conditions of cholesterol loading, male mice showed reduced serum but increased hepatic cholesterol and this was associated with changes in expression of cholesterol transporters (Hewitt et al., 2004). Although differences in the severity of AD pathology have been reported in male and female AD transgenic mice

models (Barrier et al., 2010, Carroll et al., 2010, Oikawa et al., 2010, Rosario et al., 2010), whether differences in cholesterol metabolism contribute to this remains unclear.

#### **4.6.3: Increased cholesterol levels do not alter brain CD147 levels *in vivo*.**

To determine if the increases in serum cholesterol in those mice fed the high fat/high cholesterol diet were associated with changes in peripheral or cerebral CD147 levels, CD147 protein levels were measured in tissue homogenates by Western immunoblotting. The expression of CD147 in brain tissue has been widely reported (Nahalkova et al., 2010, Xie et al., 2010, Agrawal and Yong, 2011). Expression of CD147 has also been reported in many peripheral tissues including the lung, cervix, kidney and liver (Han et al., 2010, Kong et al., 2011, Wu et al., 2011, Zeng et al., 2011) and a soluble form has been indentified in human serum (Moonsom et al., 2010).

The current study found that cerebral CD147 expression levels did not change significantly after 10 weeks on the high fat/high cholesterol diet, however, the male mice showed a trend towards higher CD147 levels and the female mice showed a trend towards lower CD147 levels in the brain after being on the high fat/ high cholesterol diet. In kidney tissue however, there were significant reductions in CD147 protein levels in the male mice and a trend towards lower levels in the female mice fed the high fat/high cholesterol diet. Whilst no significant changes in CD147 levels were observed in the liver, there was a trend toward a decrease in males fed the high fat/high cholesterol diet. Together, these results suggest that systemic increases in cholesterol do impact on the kidney. High dietary cholesterol may also alter cerebral CD147 levels and CD147 protein levels in other peripheral tissues, in particular if levels of soluble CD147 are altered in the mice serum/plasma. Soluble CD147 can be detected in conditioned

media from human tumour cell cultures (Tang et al., 2004, Hanata et al., 2007), supernatant of human lipid loaded macrophages (Yue et al., 2009). A quantitative ELISA assay to measure CD147 in human serum, has only recently been reported (Moonsom et al., 2010). Currently, there is a lack of suitable assays to measure soluble CD147 in rodent serum, and as is shown in **Fig 5.4**, specific antibodies and assays are required to detect CD147 from different species. Within the group of mice fed the high fat, high cholesterol diet, plasma cholesterol levels were found to be negatively correlated with brain CD147 levels, strengthening the notion of possible cholesterol mediated changes in brain CD147 levels. If these experiments were repeated with greater numbers of mice to increase the statistical strength of the results, or perhaps if mice were kept on these diets for a much longer period, it is possible that many of the trends seen here would be significant differences in such expanded or extended studies.

#### **4.6.4: A high fat/high cholesterol diet does not appear to affect SCP-2 transcript levels**

As mentioned above, CD147 transcription can be regulated by SCP-2. *In vitro* evidence also indicates that cholesterol can alter SCP-2 transcription (Kraemer et al., 1995). There is yet no *in vivo* evidence that cholesterol mediated changes in SCP-2 occurs. To the best of my knowledge this is the first study to investigate whether dietary cholesterol can alter SCP-2 transcription. Thus, one aim of the work in this chapter was to determine whether the high fat/high cholesterol diet would increase SCP transcription. The results in **Fig 5.10** show that the high fat/ high cholesterol diet did not alter brain SCP transcription. A previous, *in vitro* study has investigated the effects of cholesterol on SCP transcription. In this study, smooth muscle cells harvested from rat thoracic aortas were treated with cholesterol (Kraemer et al., 1995) and it was found that under these conditions transcription of SCP was increased. Apart from the differences in

experimental models (*in vitro* vs *in vivo*), the study by Kraemer et al. also used cationised LDL cholesterol, a positively charged LDL cholesterol which promotes a sterile inflammatory response in muscle and is a method used to measure cholesterol efflux (Tayler et al.). Under *in vitro* conditions, concentrations of specific lipoproteins can be more readily controlled, in contrast to *in vivo* where increases in LDL and other lipoproteins occur as a result of increased dietary cholesterol. The use of the type of LDL (native vs cationised) may also influence transcription (although there is no direct evidence of this as the Kraemer et al., study did not compare native versus cationised LDL).

The particular isoform of SCP protein that may be up-regulated may also impact on CD147 transcription. The SCP-2 gene is part of a fusion gene that contains two initiation sites encoding a 15.4 kDa (pro-SCP-2) and a 58.9 kDa (SCP-x) protein (Ohba et al., 1994, Ohba et al., 1995). The 58.9 kDa SCP-x protein undergoes a post-translational cleavage process to yield a mature 12.9 kDa SCP-2 which has been shown to translocate to the nucleus and activate CD147 transcription (Ko and Puglielli, 2007). In contrast, expression of pro-SCP-2 has been shown to abolish activity of 12.9 kDa SCP-2 and inhibit CD147 transcription, resulting in an increase in A $\beta$  production. In their study, Kraemer et al. assessed protein and mRNA levels of both 13 KDa SCP-2 (~12.9 kDa) and 58 KDa SCP-x (58.9 kDa) and showed that expression of SCP-2 mRNA and protein, but not SCP-x, were increased (Kraemer et al., 1995) which would most likely lead to increased CD147 expression.

It is conceivable that the high/ fat high cholesterol diet could alter CD147 levels, independent of any effects on SCP-2 expression. In addition to enhancing amyloid deposition, high fat/ high cholesterol diets fed to wild-type or transgenic mice have also

been associated with increases in cytokines/mediators and gliosis consistent with neuroinflammation (Thirumangalakudi et al., 2008) and increases in oxidative stress (Homma et al., 2004, Oliveros et al., 2004, Torreggiani et al., 2009). Changes in CD147 expression have been reported in many pathological conditions, involving inflammation, including rheumatoid arthritis (Tomita et al., 2002, Zhu et al., 2006, Yang et al., 2008, Damsker et al., 2009) and atherosclerosis (Spinale et al., 2000, Choi et al., 2002, Yoon et al., 2005, Siwik et al., 2008) where it has roles such as the facilitation of chemokine-mediated recruitment of inflammatory cells or tissue repair through activation of MMPs (chapter 1, (Kanyenda et al., 2011)). Although a specific role for CD147 in neuroinflammation has yet to be established, the presence of CD147 mRNA transcripts in microglia (Inoue et al., 1999) and astrocytes (Meeuwsen et al., 2003), suggest a similar role in the brain. CD147 expression and particularly its interaction with CypA is known to protect against neuronal oxidative stress (Boulos et al., 2007). The inflammation and oxidative stress evident in AD model transgenic mice may be exacerbated by the high fat/ high cholesterol diet, subsequently impacting on CD147 expression. In this scenario, the observed decreasing trend in levels of CD147 may be suggestive of a consequence of exacerbated AD pathology.

#### **4.6.5: CD147 influences on A $\beta$ production**

Considering the roles that CD147 is currently believed to play in APP metabolism, in which it is thought to be capable of reducing A $\beta$  levels, it was expected that an increase in CD147 levels would correlate with reduced A $\beta$  load under conditions of the high-cholesterol/ high fat diet. To assess this, levels of APP and its metabolites, including A $\beta$  and the APP- C-terminal fragments C83 and C99 were assessed in brain tissues from mice fed the control chow diet or the high fat/ high cholesterol diet. As expected in



APP<sup>swe</sup> transgenic mice, significant increases in FL-APP levels were observed and decreases in one of the APP-C terminal fragments (C83) were also detected, although only in the male mice. With respect to these particular APP-C83 results, the levels were particularly low in two of the mice, which most likely reduced the average to provide the overall significantly lower levels. Indeed, overall there was a large animal-to-animal variation in APP-C99 and C83 levels. All mice used in this study were confirmed to have the APP-transgene (by PCR, data not shown) and to express human APP protein (as confirmed by immunoblotting with human APP specific antibodies WO2 and 6E10, data not shown). Thus the variation in C-terminal fragments and later in the A $\beta$  peptide measurements were not due to some mice being non-transgenic.

Variations were also observed in brain A $\beta$ 40 and A $\beta$ 42 levels as values spanned from <1 to 20 nmol/g levels in A $\beta$ 42 levels and <1 to 60 nmol/g in A $\beta$ 40 levels. The APP<sup>swe</sup> mice used in these experiments were relatively young mice (4.5 months). At this age, although A $\beta$ 40 and A $\beta$ 42 levels would begin to increase, plaque deposition would not be evident (plaque deposition occurs between 12-14 months of age). As the major aim of this study was to determine the effects of the high fat/ high cholesterol diet on CD147, the mouse age was chosen so that plaque/ AD pathology would not yet be evident. If the mice already had established AD pathology, any effects of the high fat/high cholesterol diet may have been masked by this pathology. The study was also aiming to examine changes in the initiating stages of the disease. As a result of the age of the mice, since AD pathology should not have been present, the variation in A $\beta$  levels cannot be attributed to variations in A $\beta$  deposition.

To normalise for animal variations in cerebral A $\beta$ 40 and A $\beta$ 42 levels, the ratio of A $\beta$ 42/40 was calculated for each animal and represented as a scatter plot in (**Fig. 4.14**).

This not only accounted for the large variations in the data but also provided a better indicator of whether the high fat high cholesterol diet increased levels of the more pathological A $\beta$ 42 species. Although not significant, there was a trend towards higher A $\beta$ 42/40 ratios (particularly in female mice). Although to a lesser degree (as explained above with differences in diets used), these results are consistent with previous reports in cholesterol fed transgenic APP<sup>swe</sup> mice, where cerebral amyloid load and A $\beta$  levels are increased (Refolo et al., 2000b, Refolo et al., 2001, Shie et al., 2002, George et al., 2004).

A trend towards lower CD147 levels and increases in A $\beta$ 42 levels, following a period on a high fat/high cholesterol diet would be consistent with the notion that CD147 negatively regulates A $\beta$  levels. The results presented in this chapter cannot determine if this is a consequence of increases in A $\beta$ , a scenario in which progressive increases in A $\beta$  would down-regulate CD147 levels, thereby allowing further accumulation of A $\beta$ . This could occur either through a growing inability of CD147 to regulate  $\gamma$ -secretase activity or less inducement of enzymes that can degrade A $\beta$  such as MMPs (Vetrivel et al., 2008b). The measurement of CD147 protein, relevant enzyme activities and A $\beta$  levels in similar cholesterol fed mice at different ages could be performed in future studies to determine if changes in CD147 expression occur as A $\beta$  accumulates. However, further studies aimed at deciphering how CD147 may (or may not) be involved in the early pathogenesis stages of AD would most likely be the most interesting.

## 4.7: Conclusions

The results from this *in vivo* study have confirmed that a high fat/high cholesterol diet results in elevated circulating plasma cholesterol levels as evidenced by the elevated levels in both males and female fed on this diet. Although no significant increase in A $\beta$ 42/40 ratios were observed, a trend towards an increase in all mice fed on the high fat/high cholesterol diet was observed. The major finding observed in this study was a significant reduction in kidney CD147 protein levels in males combined with trends towards decreasing CD147 levels in brain, liver and kidney tissues from females fed the high fat/high cholesterol diet, compared to the control diet. In addition to changes in CD147 levels, the current study also identified significant increases in brain FL-APP levels and a significant reduction in APP-C83 fragments. Although there were no changes in SCP transcript levels, changes in SCP protein isoforms (*pro*-SCP and SCP-*x*) cannot be ruled out. Whether the onset of AD results in changes in CD147 protein levels and if there is a correlation with AD pathology is addressed in chapter 5.

## CHAPTER 5

### CD147 protein expression and localisation in AD brain tissue.

#### 5.1: Introduction

The findings in chapters 3 and 4 describe the regulation of CD147 expression *in vitro* and *in vivo*. Together with evidence supporting a role for CD147 in regulating A $\beta$  levels, either through regulating  $\gamma$ -secretase activity (Zhou et al., 2005) or A $\beta$  degradation (Vetrivel et al., 2008b) warrants investigation of its expression in AD brain. In this chapter, expression levels of CD147 were assessed in brain tissue from controls, AD and Non-AD type dementia {dementia with Lewy Bodies (LBD) and frontal temporal dementia (FTD)} cases.

The CD147 protein is expressed in many tissues including the brain (Seulberger et al., 1990, Fan et al., 1998). The protein is expressed in a number of brain regions, including the frontal cortex and thalamus, and is particularly abundant in the hippocampus (Fan et al., 1998). CD147 expression has been reported in normal brain (in the vascular endothelium) and has been shown to be highly and widely expressed in gliomas, consistent with its role in tumour progression (Sameshima et al., 2000, Sameshima et al., 2003, Gu et al., 2009). Correlations between CD147 expression and BBB function have also been reported (Sameshima et al., 2000, Sameshima et al., 2003). Despite the number of studies describing CD147 expression in human brain, only one study has compared expression in the frontal cortex and thalamus from AD and control brain tissue (Nahalkova et al., 2010). The findings were inconclusive, as only a small number of samples were assessed (3 controls and 3 AD brains).

In this chapter I assessed CD147 protein expression analysis in a larger number of samples by immunohistochemistry (AD; n=17 and Controls; n=5), western blot (AD; n=14 and controls; n=4) and extended this analysis to hippocampal tissue. In addition, CD147 expression analysis was assessed in tissue from non-AD type dementias (LBD and FTD) to determine if any changes in expression is a result of general neurodegeneration. Furthermore, given evidence suggesting that CD147 expression regulates  $\gamma$ -secretase activity (Zhou et al., 2005) and although not a core component, interacts with the complex (Zhou et al., 2005, Winkler et al., 2009), expression of the  $\gamma$ -secretase core components, presenilins (PS1), nicastrin, and pen-2 were assessed and correlated with CD147 protein levels.

## **5.2: Aims**

1) To determine if CD147 protein levels are altered in the frontal cortex or hippocampus of AD brain.

Assess tissue expression and localisation of CD147 protein in the frontal cortex from AD cases and compare with control and non-AD type dementia (LBD and FTD) cases.

2) To determine if there is a correlation of CD147 protein levels with A $\beta$  and that of the core components of the  $\gamma$ -secretase complex.

Assess protein levels of A $\beta$ 42 and the PS1, NCT, aph1 and pen2 in frontal cortex and hippocampus from control, AD and non-AD type dementia (LBD and FTD) cases.

### 5.3: Materials and methods

#### 5.3.1: Sourcing and preparation of tissues

Tissue collection and analysis was approved by Hollywood Private Hospital and Edith Cowan University human ethics committees. Western Australian Brain Bank Network (WABBN) supplied us with the frozen and formalin fixed frontal cortex and hippocampal tissues. Paraffin embedded tissue sections from formalin fixed tissues from ABBN were prepared in our laboratory (**Table 5.1**). Frozen hippocampal and frontal cortical tissues from controls ( $n=4$ ; 4 males, no females), lewy body disease (LBD) ( $n=5$ ; 3 males, 2 females =), frontal temporal dementia (FTD) ( $n=5$ ; 3 males, 2 females) and Alzheimer's disease (AD) ( $n=14$ ; 7 males, 10 females) were homogenised as described in section 2.3.3 prior to total protein estimation and expression analysis as described in sections 2.4.4 and 2.5 of the methodology chapter (chapter 2).

**Table 5.1:** List of IDs, pathology, age and sex of test samples

<b>ID</b>	<b>Pathology</b>	<b>Age</b>	<b>Sex</b>
<b>WABBN</b>			
R10A 08A	Alzheimers	74	M
R09A 33E	Alzheimers	86	M
R09A 13L	Alzheimers	57	M
R07A 32R	Alzheimers	64	M
R07A 29L	Alzheimers	60	F
R07A 27H	Alzheimers	55	F
R07A 21T	Alzheimers	91	F
R07A 09T	Alzheimers	92	F
R07A 06A	Alzheimers	76	F
R06A 20F	Alzheimers	100	F
R06A 16K	Alzheimers	93	F
R06A 06B	Alzheimers	58	F
R05A 22L	Alzheimers	76	M
R05A 20H	Alzheimers	80	F
R05A 02T	Alzheimers	83	M
R04A 36F	Alzheimers	84	F
R04A 29P	Alzheimers	73	M
R10A 11F	Frontotemporal	78	F
R09A 19A	Frontotemporal	58	M
R08A 19B	Frontotemporal	63	M
R07A 38F	Frontotemporal	60	M
R06A 18N	Frontotemporal	63	F
R09A 35J	Lewy Body Disease	79	F
R09A 32N	Lewy Body Disease	82	M
R09A 02M	Lewy Body Disease	88	F
R08A 15R	Lewy Body Disease	78	M
R07A 28X	Lewy Body Disease	77	M
R09A 11H	Control	47	M
R07A 34X	Control	67	M
R07A 33H	Control	66	M
R07A 25D	Control	46	M

### 5.3.2: Western blot analysis

CD147 protein levels were determined by SDS-PAGE gel electrophoresis in frozen hippocampal and cortical tissues as described in section 2.5 using anti goat EMMPRIN SC-9754 primary (Santa Cruz) specific for EMMPRIN of human origin, anti-Nicastrin (Sigma), anti-Presenilin (Kindly provided by Dr Paul Mathews, NYU), anti- PEN2 (Sigma),  $\beta$ -Actin (AB8229)(Abcam – Australia) and anti goat HRP secondary antibodies. The CD147 (~55kDa), nicastrin (~78kDa), presenilin (~ 30kDa) and PEN2 (~12kDa) and  $\beta$ -actin (~42kDa) protein bands were quantified using BioRad densitometry. Analysis of variance (ANOVA) with post-hoc analysis and Pearson's correlation analysis were used to determine significant differences in levels of the proteins of interest among the test groups using SPSS software.

### 5.3.3: Immunohistochemistry analysis

In addition to western immunoblotting, CD147 protein levels were also determined by immunohistochemistry in formalin fixed and paraffin embedded tissue sections (4-5 $\mu$ ) from all cases analysed in this study. Sections were stained by EMMPRIN MAB2623 primary antibody (Chemicon, USA) as described in section 2.18. Stained sections were examined under light microscope (Olympus BX 51) fitted with Olympus DP71 Digital Camera. Two sets of pictures of each stained section were taken at the same light intensity and magnification. The first set was taken at x10 and the second set at x40 magnifications. Image analysis to generate raw data was performed using ImageJ software (NIH). Images were first changed to HSB type for haematoxylin stained tissue analysis, then binary pictures generated to discriminate background staining and stained tissues. Particle analysis was performed and generated raw data values were converted using the following formula: **1/sample mean OD x 10000**.



## 5.4: Results

### 5.4.1: CD147 protein expression levels are not altered in brain tissue from Alzheimer's disease (AD) cases.

In mouse brain, CD147 expression has been located in the hippocampus and upper layers of the cortex (Naruhashi et al., 1997, Higgins and Jacobsen, 2003, Richardson et al., 2003) where depletion in AD models results in increased A $\beta$  deposition (Zhou et al., 2007, Vetrivel et al., 2008b). In human brain, expression of CD147 has been shown in the frontal cortex and thalamus (Sameshima et al., 2000, Nahalkova et al., 2009). Only one study has investigated expression of CD147 in control and AD brain, however no conclusive changes were observed due to the limited number of samples (Nahalkova et al., 2010). Here, I analyse a larger cohort of cases and also compare expression in AD brain tissue to that from controls and non-AD type dementias.

CD147 tissue expression and localisation was assessed using immunohistochemistry with a human specific EMMPRIN MAB2623 primary antibody (Chemicon, USA). Prior to immunohistochemical analysis, specificity of the CD147 was assessed (**Fig 5.1**). Analysis was performed on a control and AD case. Melanoma and glioma tissue samples which are known to express high levels of CD147 (Liang et al., 2009, Han et al., 2010, Matsudaira et al., 2010, Kong et al., 2011, Wu et al., 2011) were used as positive controls. As expected, intensive staining was observed in the glioma (**Fig 5.1, Bi**) and melanoma (**Fig 5.1, Ci**) tissues. Staining was absent in tissue sections that were exposed to secondary antibody only, in the absence of primary antibody (**Fig 5.1, Ai- ii**), indicating that the staining seen in the glioma or melanoma tissues is not background staining (**Fig 5.1, Bi, Ci**). Staining was also evident in hippocampal and frontal cortex tissue of the control (**Fig 5.1, Bii, and Cii**) and AD (**Fig 5.1, Biii, and**

**Ciii**). Although staining was evident throughout the tissue, it was particularly prominent in the vascular endo-thelial cells (arrows). Diffuse cytoplasmic staining with accentuation along the cell membrane was also observed. Of note is that staining appeared to be more intense in the AD brain tissue, compared with control (**Fig 5.1**, compare **Bii** and **Cii**, with **Biii** and **Ciii**). Whether this held true in a larger sample size, was assessed next.

Immunohistochemical analysis for CD147 was assessed in control, AD, FTD and LBD brain tissue. Representative figures of hippocampus and frontal cortex for each case at low (x10) and higher magnification (x40) are shown in Figures 5.2 and 5.4, respectively. As described above staining was evident throughout the tissue, it was particularly prominent in blood vessels/capillaries (arrows). Diffuse cytoplasmic staining with accentuation along the cell membrane was also observed. A similar staining pattern has been observed in other studies of brain tissue (Sameshima et al., 2000, Sameshima et al., 2003, Gu et al., 2009). Qualitatively, it appeared that compared to control tissue, overall staining and in particular the capillaries were more prominent in the AD, FTD or LBD frontal cortex or hippocampal tissue (Figures 5.2 and 5.4, compare B-D with A). Overall quantitation of staining using ImageJ software (NIH) (which measures both cytoplasmic and vascular staining) revealed similar levels of CD147 expression in control, AD, FTD and DLB tissue samples (**Fig. 5.3** and **5.5**). No regional differences were observed when levels were compared in the hippocampus and frontal cortex (**Fig. 5.6**).

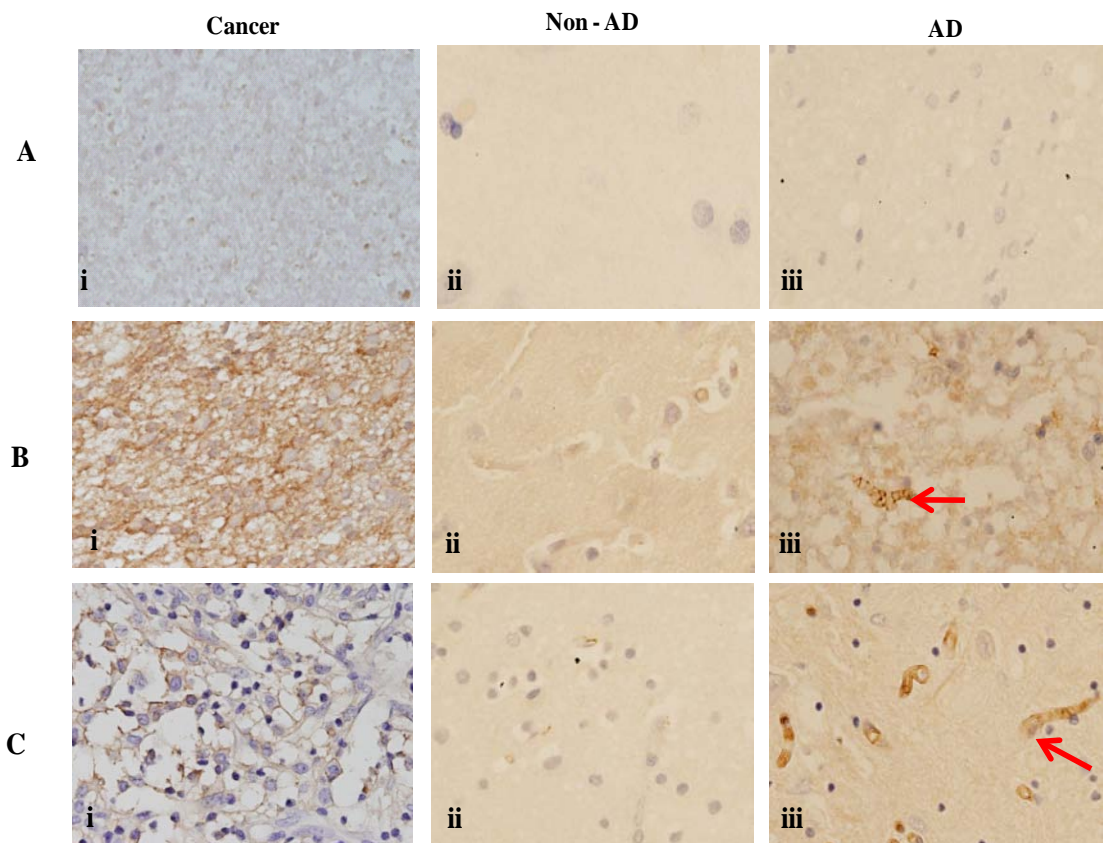


**Figure 5.1: Immunostaining for CD147 in melanoma, glioma and brain tissue.**

Cancer (i), brain tissue from a control (ii), and AD case (iii) underwent immunostaining with and without primary antibody. No or minimal background staining was observed in the antibody control tissues (A; i, ii and iii). CD147 staining was observed in frontal cortex (Bii) and hippocampal (Cii) tissues from the control sample. Intensive CD147 staining was observed in the glioma (Bi), melanoma (Ci) tissues, and frontal cortex (Bii) and hippocampal (Cii) tissues from the AD sample.

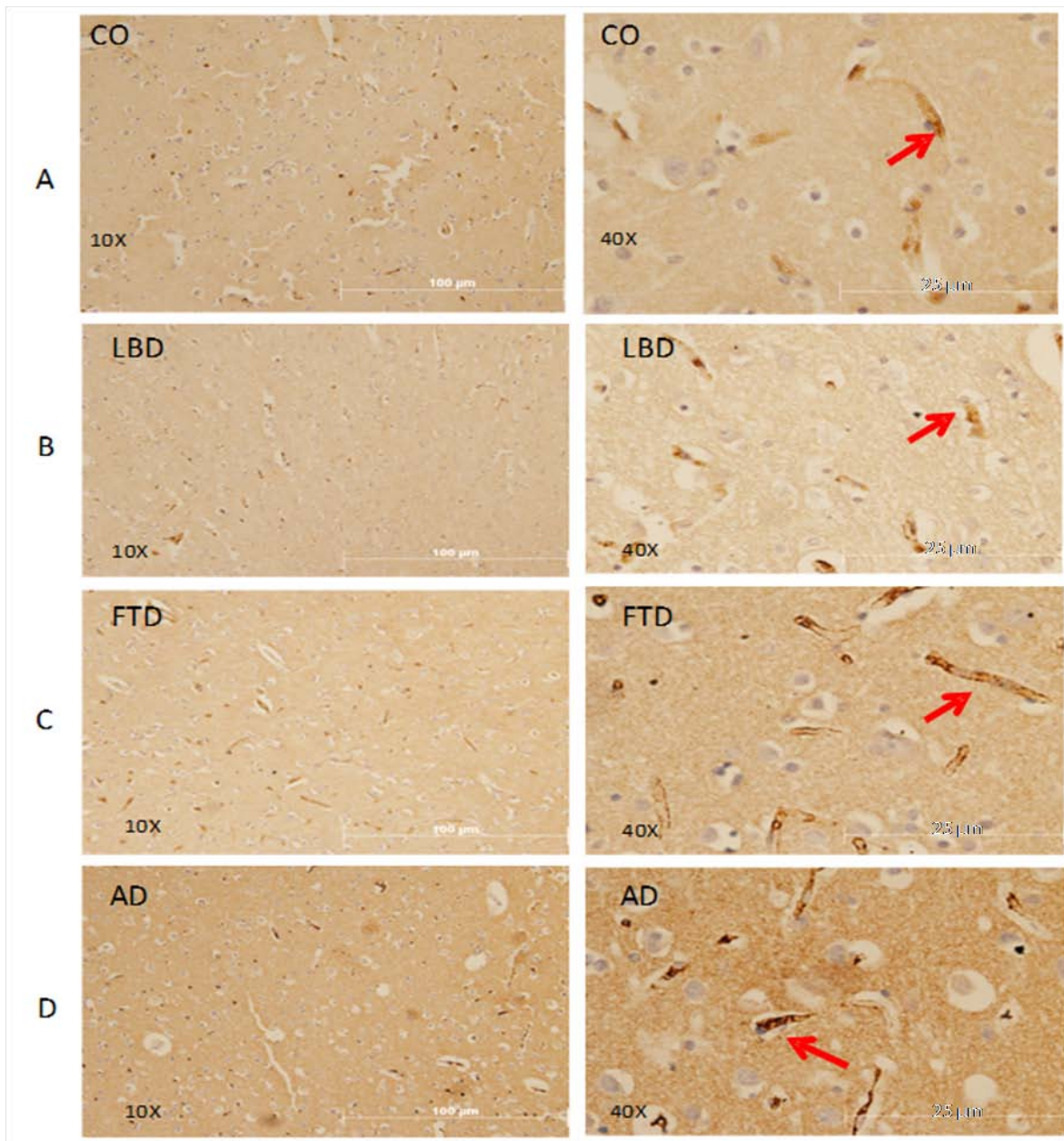


**Figure 5.2: CD147 immunostaining in the hippocampus from control, LBD, FTD and AD brain tissue.** Representative immunostained images at x10 (first column) or x40 magnification (second column) of hippocampal tissue from controls (A), LBD (B), FTD (C), and AD (D). Scale bar represents 100 μm at 10x and 25μm at 40x magnifications respectively. Qualitatively, compared to control tissue (A), staining of the vascular endo-thelial cells (red arrows) was more prominent in the AD, FTD or LBD tissue (B-D).

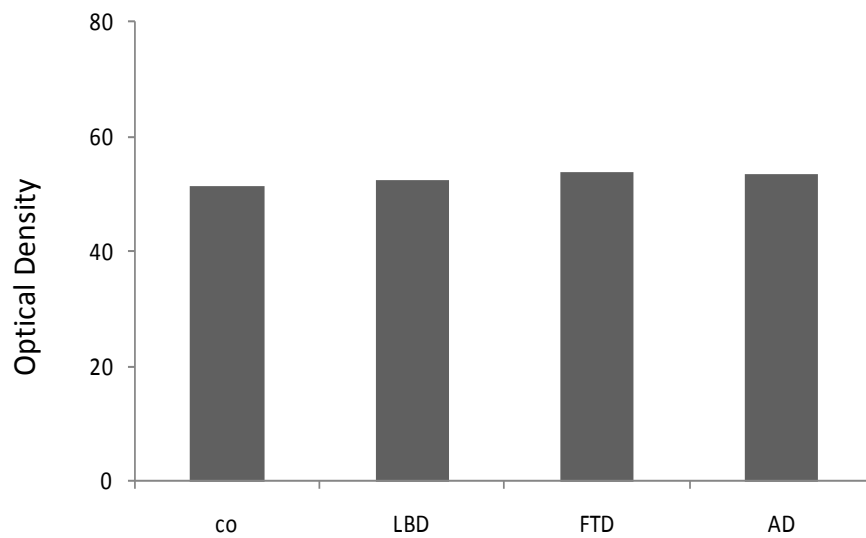


**Figure 5.3: Quantitation of CD147 immunostaining from hippocampus of control, LBD, FTD and AD cases.**

Cytoplasmic and vascular endothelial CD147 expression in the hippocampus tissue was assessed in all tissues and data is represented as mean  $\pm$  SD. Groups represent controls (n=4), LBD (n=5), FTD (n=5), AD (n=17). Compared to controls results indicate no significant differences in CD147 expression.



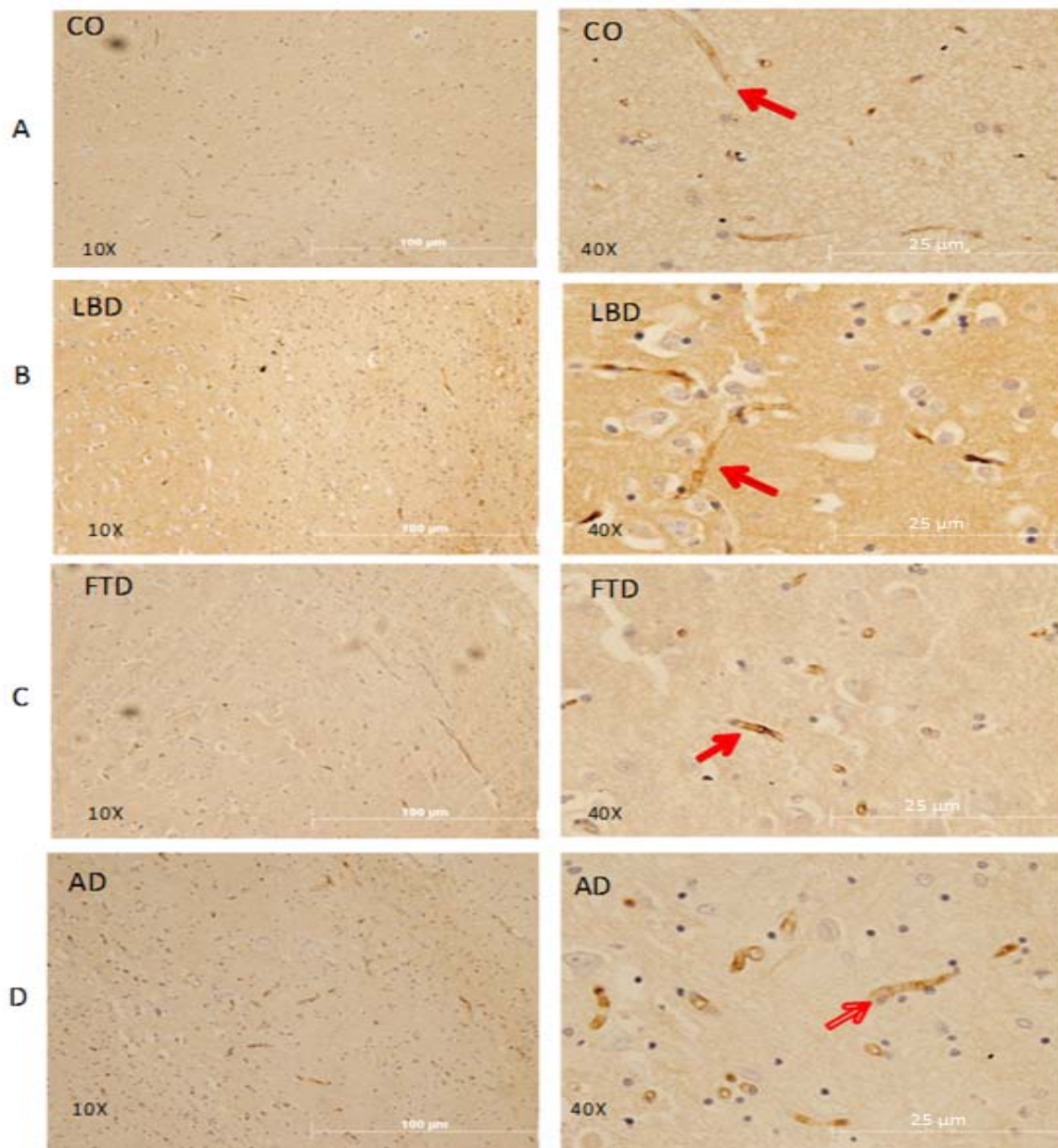


**Figure 5.4: CD147 immunostaining in the frontal cortex from control, LBD, FTD and AD brain tissue.**

Representative immunostained images at x10 (first column) or x40 magnification (second column) of hippocampal tissue from controls (A), LBD (B), FTD (C), and AD (D). Scale bar represents 100 μm at 10x and 25μm at 40x magnifications respectively. Qualitatively, compared to control tissue (A), staining of the vascular endo-thelial cells (red arrows) was more prominent in the AD, FTD or LBD tissue (B-D)

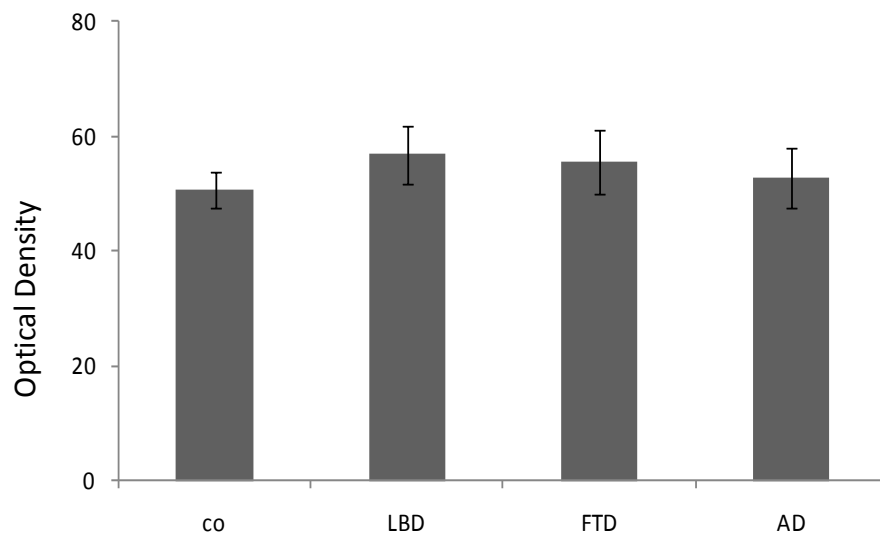


**Figure 5.5: Quantitation of CD147 immunostaining from frontal cortex of control, LBD, FTD and AD cases.**

Cytoplasmic and vascular endothelial CD147 staining in the frontal cortex was measured in all tissues and data is represented as mean  $\pm$  SD. Groups represent controls (n=4), LBD (n=5), FTD (n=5), AD (n=17). Compared to controls results indicate no significant differences of CD147 expression in LBD, FTD and AD, however there is a slight trend towards an increase observed in LBD and FTD.

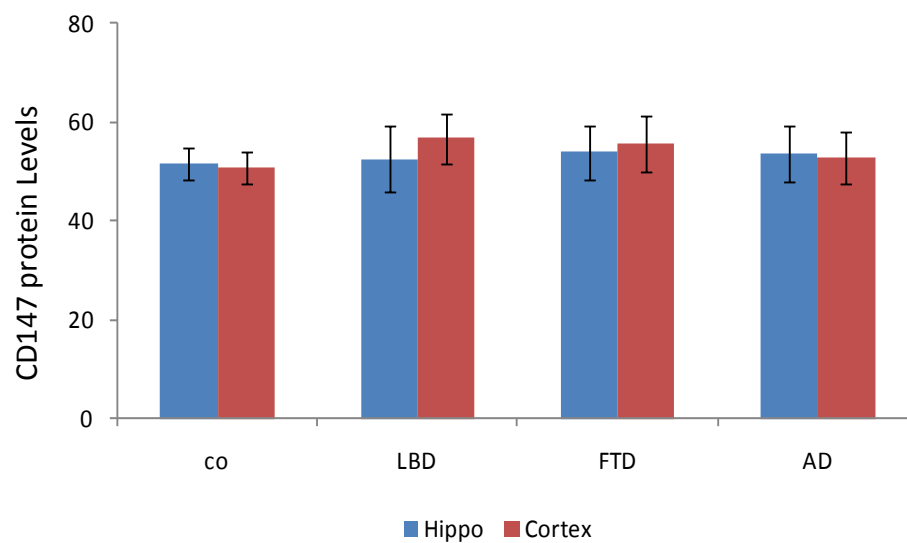


**Figure 5.6: A comparison of CD147 immunostaining in hippocampus and frontal cortex from control, LBD, FTD and AD cases.**

Cytoplasmic and vascular endothelial CD147 expression in hippocampal and frontal cortex tissue was assessed in all tissues and is represented as mean  $\pm$  SD. Groups represent control (n=4), LBD (n=5), FTD (n=5), AD (n=17).



In order to more accurately quantitate total CD147 levels, brain homogenates from all cases underwent western blotting with EMMPRIN SC-9754 primary antibody (Santa Cruz). A ~ 55 kDa band representing CD147 was observed in the hippocampus and frontal cortex from all brain tissue samples (**Fig 5.7A and C**). Quantitation of the protein band, revealed no significant differences in total CD147 levels in hippocampal tissue from control, AD, LBD or FTD brain samples (**Fig 5.7B**). However a trend towards an increase was observed in hippocampus from AD brains. Similarly, no significant differences were observed in the frontal cortex from control, AD, FTD and LBD cases (**Fig.5.7C and D**).

**Note: This page left blank on purpose**

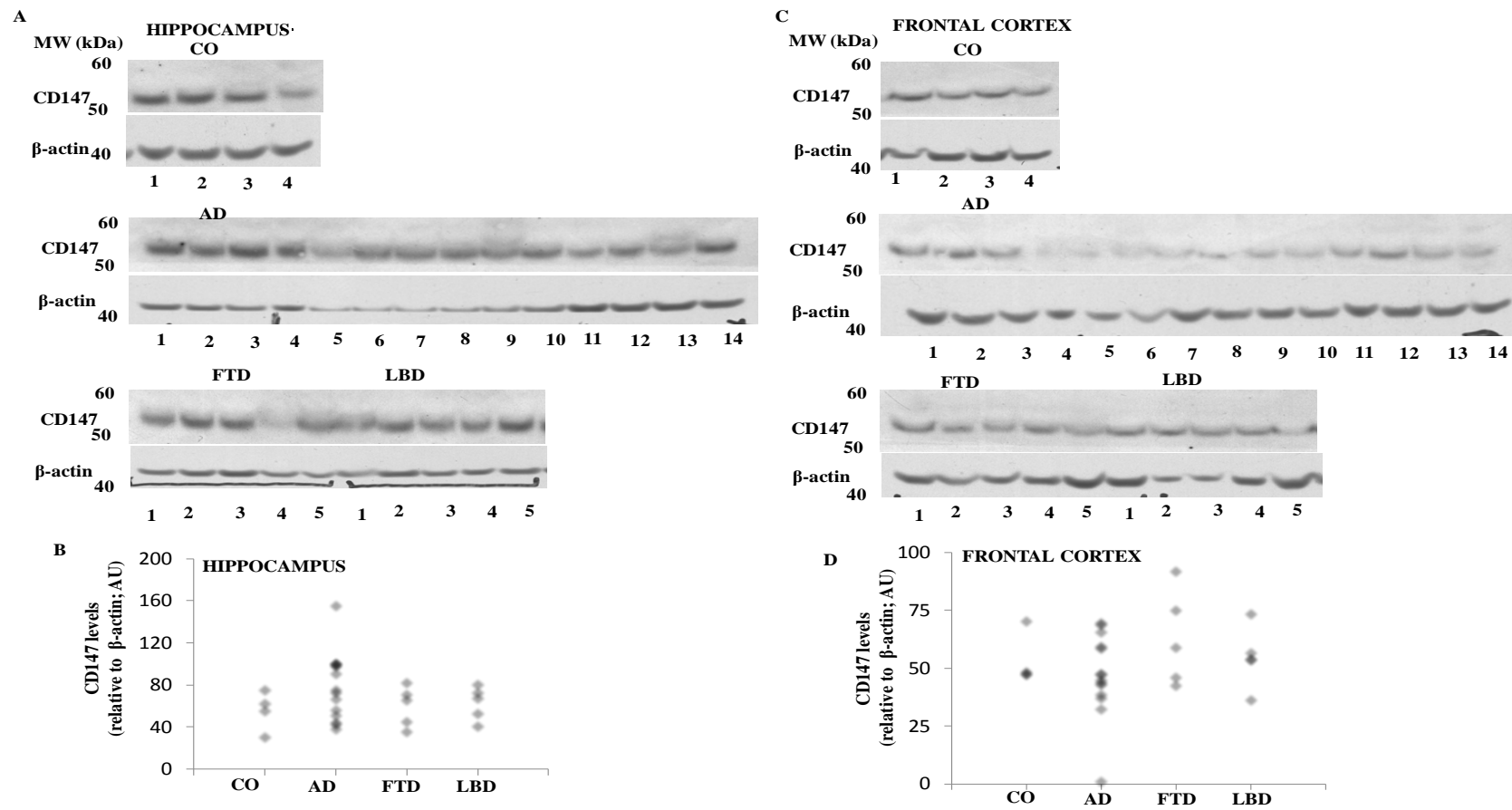


**Figure 5.7: CD147 levels in hippocampus and frontal cortex.**

**Figure 5.7: CD147 levels in hippocampus and frontal cortex.**

Western immunoblot analysis of CD147 protein levels in hippocampus (A and B) and frontal cortex (C and D). (A and C) Western blots of brain homogenates run in singles showing the ~55 kDa CD147 protein levels and corresponding  $\beta$ -actin levels as a loading control in hippocampus (A) and frontal cortex (C) in controls, LBD, FTD and AD. (B and D) Scatter plots representing CD147 levels in hippocampus and frontal cortex from controls, LBD, FTD and AD brain tissue. Individual points represent a specific sample value (as quantitated from adjacent blots) with the sample mean represented by horizontal line. Compared to controls, data shows no significant differences of CD147 expression in both hippocampus and frontal cortex in LBD, FTD and AD.

#### **5.4.2: Associations of CD147 protein expression with levels of A $\beta$ 42 and core protein components of $\gamma$ -secretase.**

Although there was no overall changes in CD147 expression levels (see section above), as might be expected, there were large variations between samples, despite similar  $\beta$ -actin levels. The close association of CD147 expression with A $\beta$  levels and  $\gamma$ -secretase activity (Zhou et al., 2005) (Zhou et al., 2005, Winkler et al., 2009), prompted the investigation of whether there was an association between CD147 levels and levels of A $\beta$ 42, and expression of the  $\gamma$ -secretase core components in the brain tissue. Thus levels of A $\beta$ 42, PS1, NCT and Pen2 were measured in the brain tissue samples.

Levels of A $\beta$ 42 were measured in the hippocampus and frontal cortex of control, FTD, LBD and AD brain tissue using ELISA. The results are shown in Figures 5.8 and 5.9. As expected compared to control tissue, A $\beta$ 42 levels were not altered in FTD brain tissue whilst levels were significantly increased in AD brain tissue ( $p<0.001$ ) in hippocampus and ( $p=0.02$ ) in the frontal cortex. Although there was large variation, compared to controls, levels were increased ( $p=0.004$ ) in brain tissue from LBD dementia patients. A comparison of A $\beta$ 42 levels showed high levels in the frontal cortex (Fig.5.10).

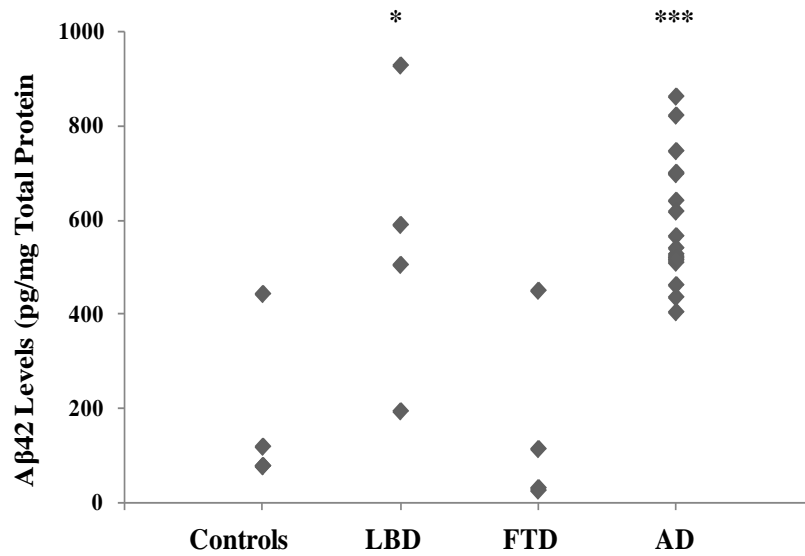


**Figure 5.8: Aβ42 levels in hippocampus.**

Aβ42 levels in brain tissue from the hippocampus of controls, lewy body disease (LBD), frontal temporal dementia (FTD) and Alzheimer's disease (AD). Scatter plots representing Aβ42 levels in hippocampus from controls, LBD, FTD and AD brain tissue. Individual points represent a specific sample value with the sample mean represented by horizontal line. Compared to the controls data shows that Aβ42 levels are significantly increased in hippocampus from LBD and AD ( $***p < 0.001$  and  $*p < 0.05$  respectively) with AD showing the highest levels.

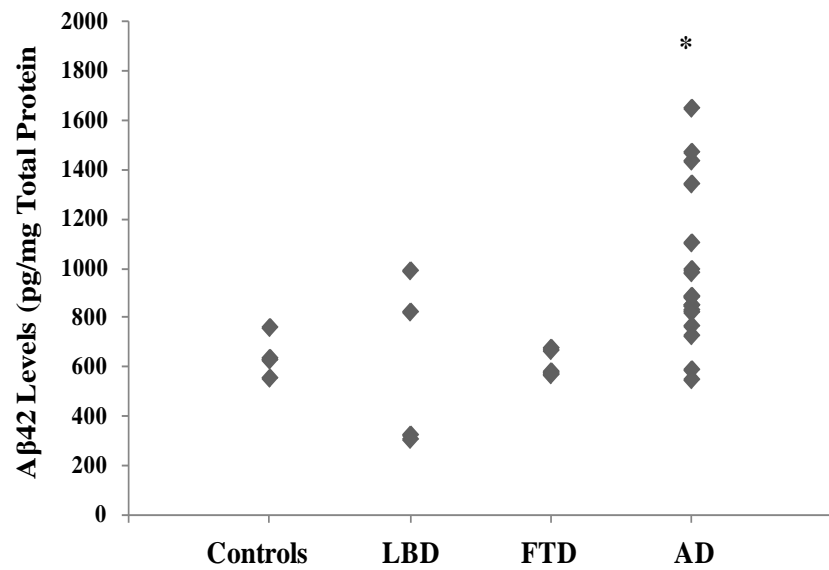


**Figure 5.9: Aβ42 levels in frontal cortex.**

Aβ42 levels in brain tissue from the frontal cortex of controls, lewy body disease (LBD), frontal temporal dementia (FTD) and Alzheimer's disease (AD). Scatter plots representing Aβ42 levels in frontal cortex from controls, LBD, FTD and AD brain tissue. Individual points represent a specific sample value with the sample mean represented by horizontal line. Compared to the controls data shows that Aβ42 levels are significantly increased in hippocampus from AD (\* $p < 0.05$ ).

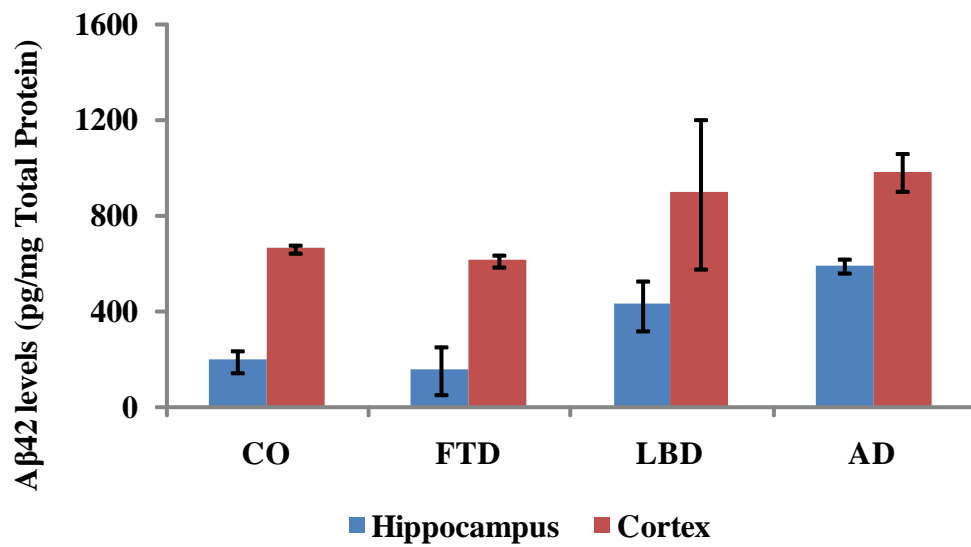


**Figure 5.10: Comparison of A $\beta$ 42 levels between hippocampus and frontal cortex.**

A $\beta$ 42 levels in hippocampus and frontal cortex from controls, lewy body disease (LBD), frontal temporal dementia (FTD) and Alzheimer's disease (AD). Data is presented as  $\pm$ SEM and indicate that frontal cortex has high A $\beta$ 42 expression compared to hippocampus.



Levels of the core protein components of  $\gamma$ -secretase including nicastrin, PS1 and PEN-2 were assessed in the hippocampus and frontal cortex from all brain samples via western immunoblotting.

Nicastrin, a type 1 transmembrane glycoprotein (Yu et al., 2000), plays a role in the assembly and intracellular trafficking of the  $\gamma$ -secretase complex (see chapter 1) (Shah et al., 2005, Zhang et al., 2005). Compared to controls, nicastrin levels were not altered in hippocampal (**Fig.5.11A and B**) and frontal cortex (**Fig.5.11C and D**) tissues from AD, FTD or LBD. However, though not significant, an increasing trend was observed in both hippocampus and frontal cortex tissues from AD.

The presenilins are regarded as the core catalytic component of  $\gamma$ -secretase (L'Hernault and Arduengo, 1992, Levitan and Petersen, 1995, Martins et al., 1995, Xia et al., 1997) (Herreman et al., 1999)-(Palacino et al., 2000). Levels of PS1 were measured as recent evidence suggests that PS1 containing  $\gamma$ -secretase complexes are more active than PS2 containing complexes (Stromberg et al., 2005, Hedskog et al., 2011, Yonemura et al., 2011). Levels of PS1 were not significantly altered in hippocampal tissue from AD, FTD or LBD compared to controls (**Fig.5.12A and B**). However a trend towards and increase was observed in hippocampus tissue. A comparison between AD and LBD, showed significant difference of PS1 ( $p < 0.031$ ) in hippocampus tissue. In the frontal cortex, compared to controls, PS1 levels were not altered in tissue from AD subjects (**Fig.5.12C and D**) but an increasing trend was observed in AD and LBD.

The Presenilin Enhancer 2 (PEN-2) is a ~12 kDa protein and has a critical role in the  $\gamma$ -secretase complex as described in chapter 1, where it facilitates end proteolysis of the presenilins (Crystal et al., 2003, Prokop et al., 2004, Steiner et al., 2002, Luo et al., 2003, Takasugi et al., 2003, Hasegawa et al., 2004). Levels of this protein were

significantly increased in hippocampal tissue from AD tissue ( $p=0.014$ ) compared to controls (**Fig.5.13A and B**). In the frontal cortex, PEN2 levels showed no significant change in FTD, LBD or AD tissue, although a trend towards an increase was observed (**Fig.5.13C and D**).

Overall, these results show that compared to control brain tissue A $\beta$ 42 levels were increased in AD tissue. In addition levels of components of the  $\gamma$ -secretase enzyme including, PS1 and PEN-2 were altered. To determine if there were associations between CD147 levels and levels of A $\beta$ 42 and the  $\gamma$ -secretase components, a bivariate Pearson's correlation analysis was performed (**Table 5.2**).

Strong significant positive correlations between CD147 and PS1 in hippocampus from controls ( $p=0.028$ ), AD ( $p=0.002$ ) and LBD ( $p=0.003$ ); CD147 and NCT in AD ( $p=0.0001$ ) and CD147 and PEN2 in controls ( $p=0.035$ ) were observed. However, in the frontal cortex, significant correlations were observed in LBD (PS1,  $p=0.034$ ; PEN2,  $p=0.003$  respectively) and FTD (PEN2,  $p=0.042$ ). Interestingly, there were similar correlations observed in LBD samples, which may reflect the presence of AD pathology in this type of dementia (Griffin et al., 2006, Maetzler et al., 2009). However, as there were only five samples obtained of LBD tissue, the significant correlation may need to be confirmed in a larger sample. There was no correlation between CD147 and A $\beta$ 42 in AD brains.

**Table 5.2:** CD147 correlations with nicastrin, presenilin1 and presenilin enhancer 2 in hippocampus and frontal cortex from AD, LBD and FTD brains.

		HIPPOCAMPUS				FRONTAL CORTEX			
		A $\beta$ 42	NCT	PS1	PEN2	A $\beta$ 42	NCT	PS1	PEN2
<b>CD147</b>	<b>CO</b>	-.017	.723	.972	.965	-.167	-.259	.764	-.629
		0.983	0.277	0.028*	0.035*	0.833	0.741	0.236	0.371
	<b>AD</b>	.405	.824	.760	.207	.211	.468	.386	.443
		0.151	0.0001**	0.002**	0.478	0.470	0.091	0.173	0.113
	<b>LBD</b>	.615	.763	.982	.582	-.402	.025	.906	.983
		0.385	0.134	0.003**	0.304	0.598	0.968	0.034*	0.003**
	<b>FTD</b>	-.091	-.030	-.922	.491	.711	-.729	-.766	.958
		0.909	0.970	p.078	0.509	0.178	0.271	0.234	0.042*

*P-value* calculated by bivariate Pearson's correlation analysis. \* Correlation is significant at the 0.05 level. \*\* Correlation is significant at the 0.01 level (2-tailed).

**Note: This page left blank on purpose**

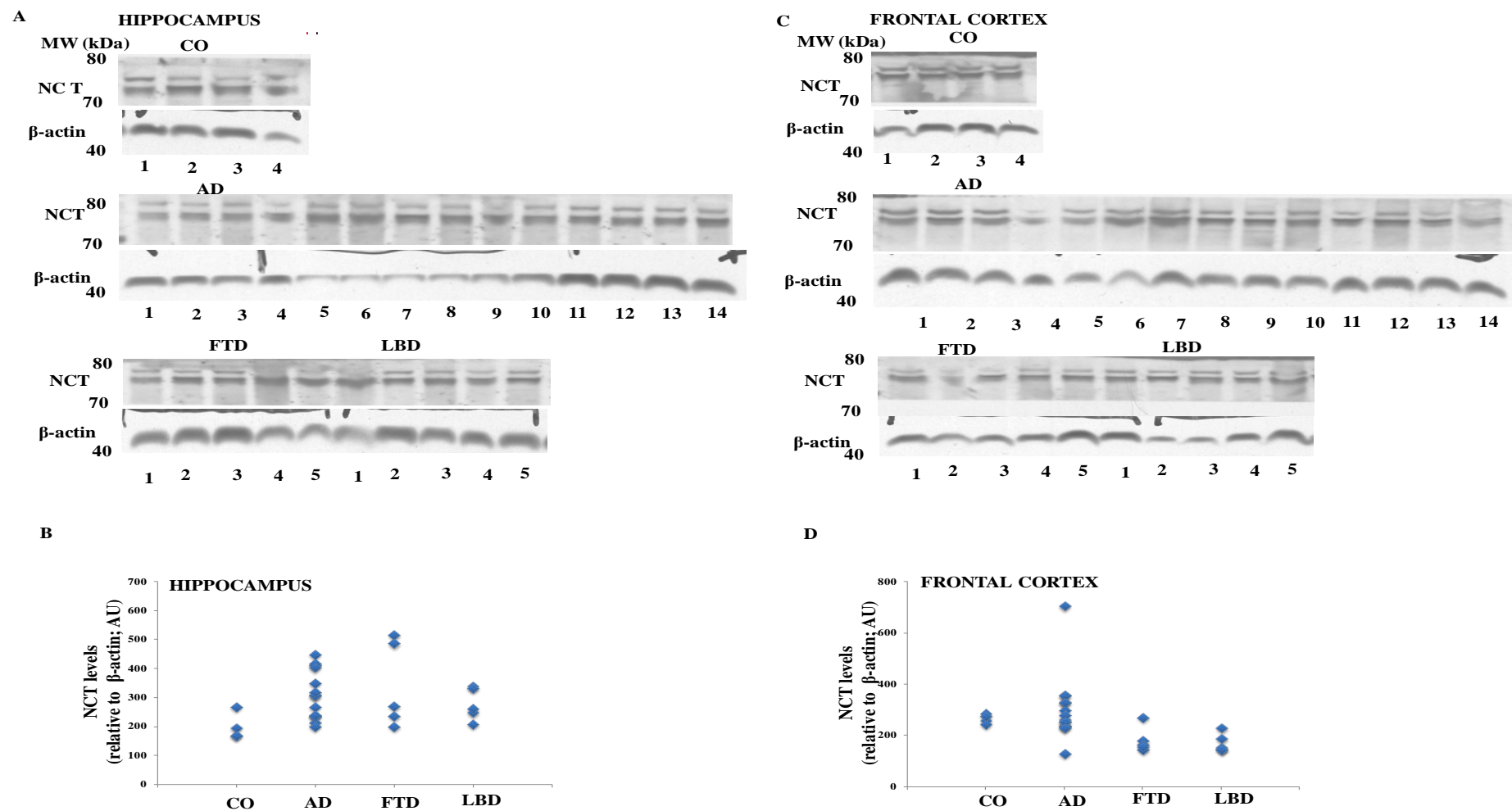


**Figure 5.11: Nicastrin levels in hippocampus and frontal cortex.**

**Figure 5.11: Nicastrin levels in hippocampus and frontal cortex.**

Western blots and data analysis of nicastrin in hippocampus (A and B) and frontal cortex (C and D). (A and C) Western blots of brain homogenates run in singles showing the ~75 kDa nicastrin protein levels and corresponding  $\beta$ -actin levels as a loading control in hippocampus (A) and frontal cortex (C) in controls, LBD, FTD and AD. (B and D) Scatter plots representing nicastrin levels in hippocampus and frontal cortex from controls, LBD, FTD and AD brain tissue. Individual points represent a specific sample value (as quantitated from adjacent blots) with the sample mean represented by horizontal line. Compared to the controls, there was no difference in nicastrin levels observed in hippocampus and frontal cortex from LBD, FTD and AD respectively. However an increasing trend was observed in hippocampus and frontal cortex tissues from AD.

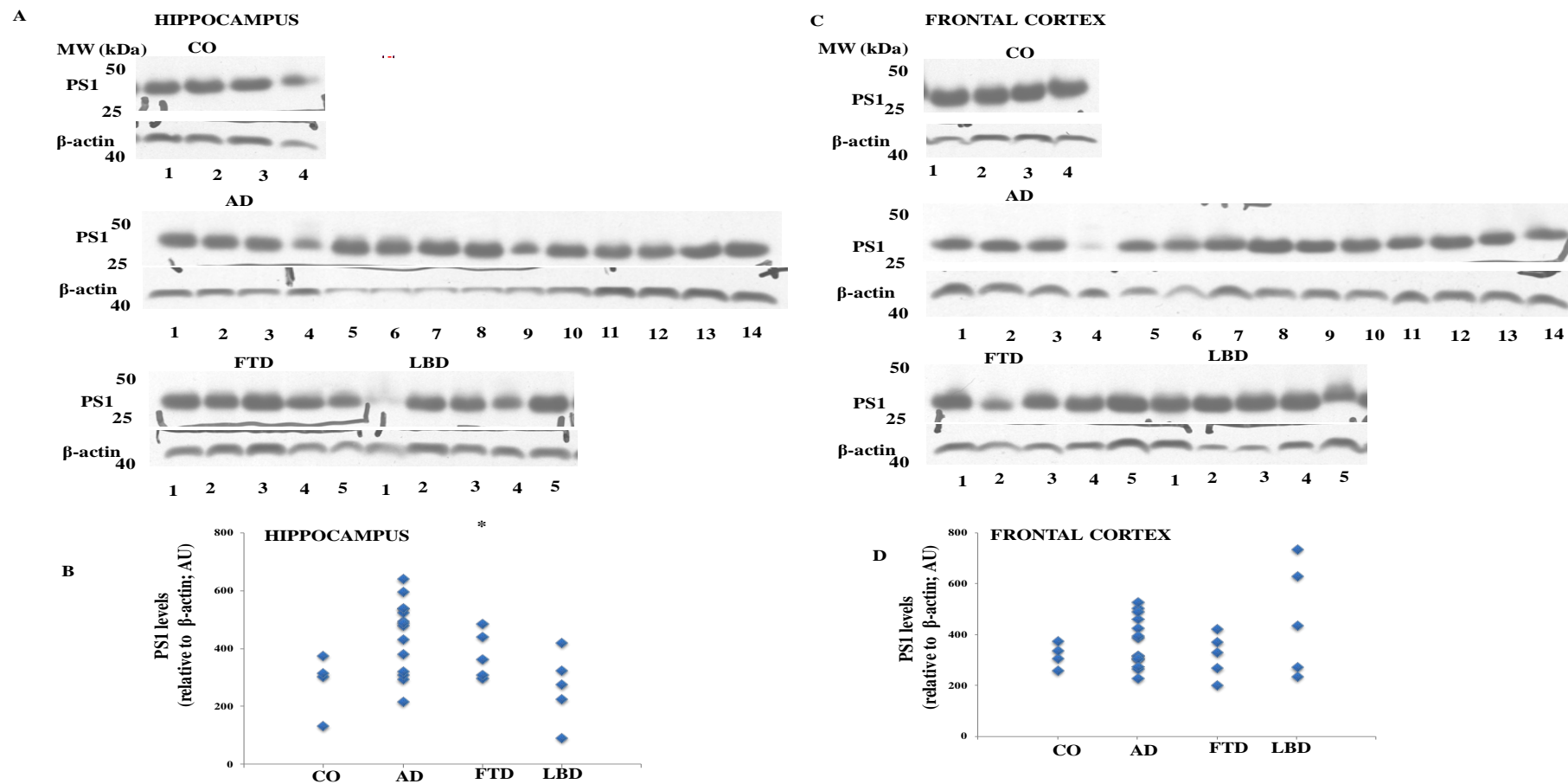


**Figure 5.12: PS 1 levels in hippocampus and frontal cortex.**

Western blots and data analysis of PS1 levels in hippocampus (A and B) and frontal cortex (C and D). (A and C) Western blots of brain homogenates run in singles showing the ~38 kDa PS1 protein levels and corresponding  $\beta$ -actin levels as a loading control in hippocampus (A) and frontal cortex (C) in controls, LBD, FTD and AD. (B and D) Scatter plots representing PS1 levels in hippocampus and frontal cortex from controls, LBD, FTD and AD brain tissue. Individual points represent a specific sample value (as quantitated from adjacent blots) with the sample mean represented by horizontal line. Compared to the control group, there is no significant difference in PS1 levels in hippocampus and frontal cortex. However in hippocampus there was significant difference in PS1 between AD and LBD ( $*p < 0.05$ ) with an increasing trend observed in frontal cortex from LBD.



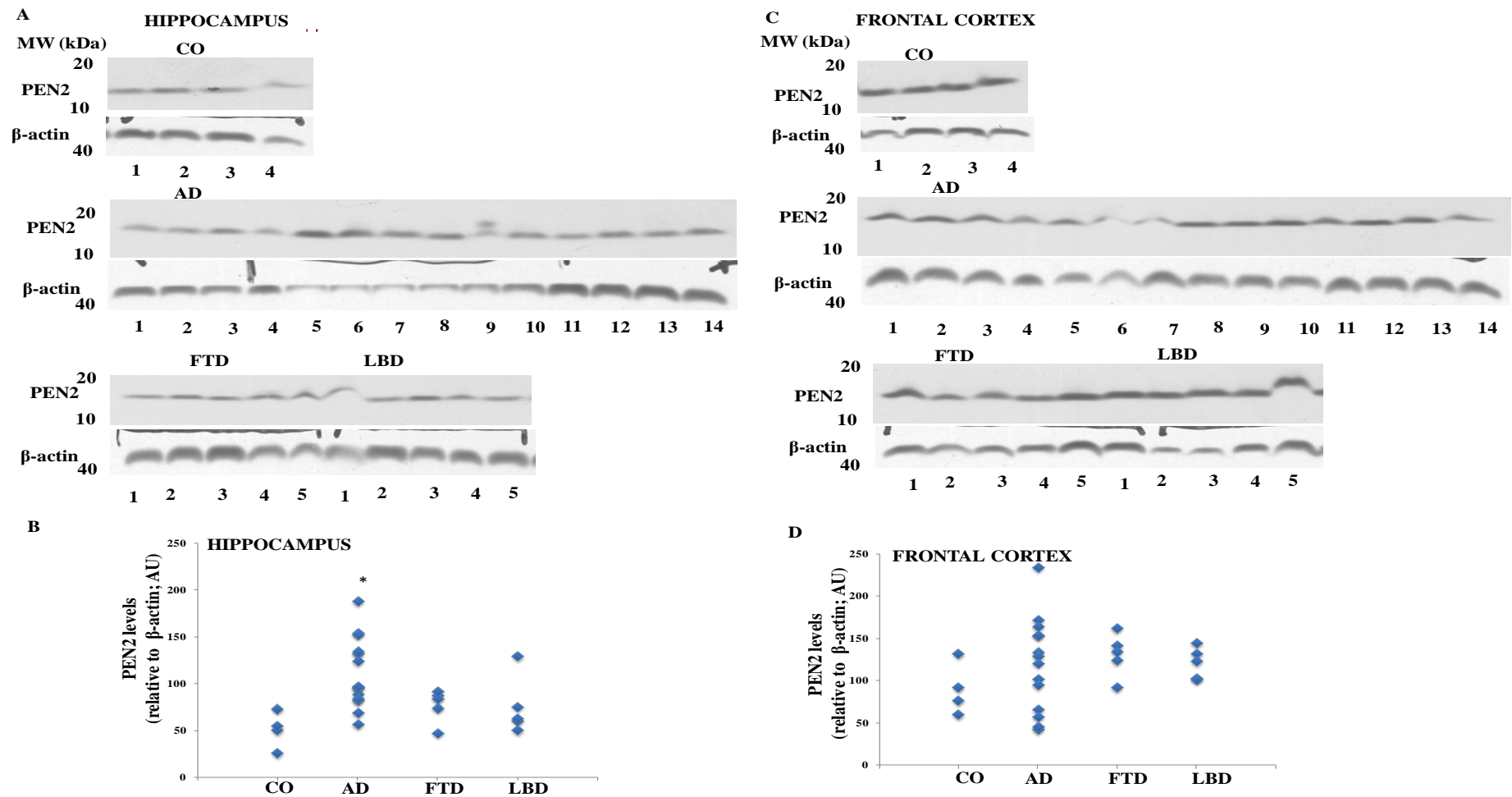


Figure 5.13: PEN2 levels in hippocampus and frontal cortex.

**Figure 5.13: PEN2 levels in hippocampus and frontal cortex.**

Western blots analysis of PEN2 protein levels in the hippocampus (A and B)) and frontal cortex (C and D). (A and C) Western blots of brain homogenates run in singles showing the ~12 kDa CD147 protein levels and corresponding  $\beta$ -actin levels as a loading control in hippocampus (A) and frontal cortex (C) in controls, LBD, FTD and AD. (B and D) Scatter plots representing PEN2 levels in hippocampus and frontal cortex from controls, LBD, FTD and AD brain tissue. Individual points represent a specific sample value (as quantitated from adjacent blots) with the sample mean represented by horizontal line. Compared to the controls, PEN2 levels are significantly increased in hippocampus of AD patients ( $*p<0.05$ ). A trend towards an increase is seen in the in frontal cortex from AD, FTD and LBD.

### **5.5: Summary of results:**

This chapter has shown the expression and localisation profile of CD147 in the frontal cortex and hippocampus of control, AD and non-AD type dementia subjects. The results have shown cytoplasmic and particularly strong staining pattern surrounding the vascular endothelial cells which qualitatively appear to increase in intensity in AD brain tissue. Similar staining intensity was also observed in LBD and FTD brain tissue. Quantitatively measuring CD147 levels revealed no significant changes, however trends were observed. Highly significant positive correlations between CD147 and PS1 and CD147 and NCT were observed in hippocampal tissue from AD samples, suggesting tight associations between CD147 and core components of the  $\gamma$ -secretase complex.

### **5.6: Discussion**

The expression of CD147 has been shown to impact on neuro-protection and modulating A $\beta$  levels. Apart from *in vitro* over-expression and knock-down studies in proof-of-concept studies, the effects of CD147 transcription/expression on AD pathology have not been explored. Indeed, whether CD147 transcription or protein expression is altered in AD has not been fully examined. Only one study has investigated CD147 protein expression levels in different regions in a small number of control and AD brain samples (Nahalkova et al., 2010). The numbers used (3 control and 3 AD brains) were too small to show significant differences, however qualitative analysis of immunostained tissue sections revealed that CD147 staining was more intensive in the neurons and capillaries in both frontal cortex and thalamus of AD brain compared to control brain. In this chapter a more detailed, qualitative and quantitative

analysis in a larger number of tissue samples (4 controls and 17 AD brains) was undertaken to determine if CD147 protein expression is significantly altered in AD. In addition, CD147 expression analysis was assessed in tissue from non-AD type dementias (LBD and FTD) to determine if any changes in expression is a result of general neurodegeneration.

In mouse brain, CD147 expression has been located in the hippocampus and upper layers of the cortex (Naruhashi et al., 1997, Higgins and Jacobsen, 2003, Richardson et al., 2003). In human brain, expression of CD147 has been shown in the frontal cortex and thalamus (Sameshima et al., 2000, Nahalkova et al., 2009). The results presented in this thesis also show prominent CD147 expression in the hippocampus (See Fig 5.1 and 5.2). Analysis of brain tissue by immunohistochemistry revealed a similar tissue localisation as reported by previous studies of human brain (Nahalkova et al., 2010) in both the hippocampus and frontal cortex. Immunostaining with an antibody specific to human CD147 showed that staining was evident throughout the tissue with diffuse cytoplasmic staining with accentuation along the cell membrane was also observed. Staining was particularly prominent in capillaries and blood vessels (Fig 5.2 and 5.4 at x40 magnification). This is in line with previous reports that have located CD147 expression to the vascular endothelium and have suggested a role in BBB function (Sameshima et al., 2000, Sameshima et al., 2003, Gu et al., 2009). Indeed an MRI and immunohistochemical study of brain tumours has correlated CD147 expression in vascular endothelial cells with blood-brain barrier function (Sameshima et al., 2003). BBB function is known to be compromised in AD and other neurodegenerative diseases (Caserta et al., 1998, Clifford et al., 2007, Nagele et al., 2011) whether it correlates with vascular endothelial expression of CD147 levels in these disease states may provide insight into a possible marker of BBB dysfunction.

It was noted that compared to control brain tissue, there was a strong CD147 staining of the blood vessels or capillaries in AD (Fig 5.2 and 5.4 at x40 magnification). CD147 is known to play a role in cerebral injury after ischemic stroke by stimulating endothelial cells to secrete matrix metalloproteases (MMPs) (Liebetrau et al., 2005). The blood vessels are the structures in the brain that contain ECM proteins known to be substrates for MMPs and take part in micro vascular damage. Abnormalities in brain vascular system and brain hypofusion are features of AD and are consistent with the vascular hypothesis of AD development (de la Torre, 2004) and although not to the extent of vascular dementia or AD, can also occur in other neurodegenerative diseases (Grammas, 2011). Indeed, CD147 staining within capillaries and blood vessels appeared to be increased in FTD and LBD compared to controls in the current study (Fig 5.2, B and D).

As a more quantitative analysis of CD147 expression, brain homogenates underwent western immunoblotting. The study by Nahalkova et al., (2010) investigated CD147 expression in the cortex and thalamus of 3 controls and 3 AD brain samples. Overall there was no significant changes as the number of sample assessed were small and there were variations in expression levels (increased, unchanged, and decreased). In the current study, a greater number of control and AD samples were assessed to increase the statistical power of observing changes in CD147 levels. In addition to the frontal cortex, the hippocampus, where expression has been reported to be highest in rodent brain (Lee et al., 2003a, Lee et al., 2003b) was also assessed. Quantitation by western immunoblotting of CD147 protein levels in the frontal cortex and hippocampus revealed no significant changes in mean protein values in AD brain compared to control brain, however there was an increasing trend observed in the hippocampus from AD.

Considering the reported roles of CD147 in modulating A $\beta$  levels and interactions with core components of the  $\gamma$ -secretase complex, and that CD147 has been shown to partially co-localise with components of the complex, PS1, nicastrin and Pen-2 (Nahalkova et al., 2010), correlations with levels of these proteins in the brain samples were assessed. Correlations would be indicative of potentially functional involvement of this protein in the pathological changes happening in AD brain.

As expected A $\beta$ 42 levels were increased in the hippocampus and frontal cortex of the AD brain. Levels were also increased in both regions of brain tissue obtain from subjects with LBD. In addition to the wide-spread distribution of lewy bodies, subjects with LBD also show a variable burden of amyloid deposition and neurofibrillary tangles, a characteristic of AD (Gomperts et al., 2008, Armstrong and Cairns, 2000, 2009). Although not to the extent of AD, A $\beta$ 42 is the predominant species deposited (Mann et al., 1998). In the current study, results have shown that A $\beta$ 42 does not correlate with CD147 which is consistent with the findings of Vetrivel (Vetrivel et al., 2008b).

### **5.6.3: PEN2 are increased in Alzheimer's disease (AD)**

Nicastrin is a type 1 transmembrane glycoprotein and a component of the  $\gamma$ -secretase enzyme complex (Yu et al., 2000). In addition NCT plays a role in the assembly of the  $\gamma$ -secretase complex within the endoplasmic reticulum and its intracellular trafficking to the cell surface (Shah et al., 2005, Zhang et al., 2005). NCT also acts as a scaffold for the assembly of the  $\gamma$ -secretase enzyme complex that binds with APH-1 to form the first sub-complex (Morais et al., 2003, Periz and Fortini, 2004). Since  $\gamma$ -secretase enzyme is responsible for the production of A $\beta$ , the current study investigated if NCT is altered in

hippocampus and frontal cortex tissues from controls, LBD, FTD and AD. Although not significant, our results have shown an increasing trend in nicastrin levels both in hippocampus and frontal Cortex from AD (**Fig.5.11C and D**). In addition to AD, increasing trends were also observed in hippocampus from FTD. Taken together these findings are suggestive of an increased  $\gamma$ -secretase enzyme activity during A $\beta$  generation as NCT plays a role in its assembly. This is consistent with findings from other studies which reported increased NCT levels in Tg2576 mice (Chu et al., 2012, Gwon et al., 2012).

The Presenilins (PS1 and PS2) are also transmembrane proteins (Sherrington et al., 1995, Lehmann et al., 1997) which facilitates APP metabolism and processing and mutations in PS1 increase the production of the longer more pathological A $\beta$  species (Martins et al., 1995, Xia et al., 1997). In addition to Nicastrin, the current study also investigated PS1 expression levels in hippocampus and frontal cortex from controls, LBD, FTD and AD. Although not significant, increasing trends of PS1 levels in hippocampus and frontal cortex from FTD and AD were observed (**Fig.5.12A and B**). Interestingly though was the finding of a significant difference in PS1 levels between AD and LBD in hippocampus. This difference may have been influenced by one LBD sample that showed the lowest PS1 expression hence pulling down the mean of this group. The increasing trend in PS1 levels observed in AD in the current study are consistent to those reported in previous studies (Kodam et al., 2010, Chu et al., 2012) and is an indication of increased APP metabolism through the amyloidogenic pathway. This may also suggest a possible relationship between CD147 and PS1 expression levels in hippocampus. Since both CD147 and PS1 are transmembrane proteins, there may be possible interactions taking place during their biological functions at cellular levels, since CD147 is a multifunctional protein. There is therefore a need to investigate

further any possible interactions, not only between CD147 and PS1, but also with other members of the  $\gamma$ -secretase complex which will help explain further how CD147 and the  $\gamma$ -secretase complex interact to facilitate APP metabolism.

Interaction of PEN-2 with other proteins results in the stability of the  $\gamma$ -secretase complex (Crystal et al., 2003, Prokop et al., 2004) and is required for stabilization of the presenilin N- and C-terminal fragments within the  $\gamma$ -secretase complex in addition to contributing to NCT maturation. Reports have also shown that knocking down PEN-2 expression results in marked decrease in A $\beta$  production, suggesting that PEN-2 is essential for  $\gamma$ -secretase activity (Steiner et al., 2002, Luo et al., 2003, Takasugi et al., 2003). In addition to NCT and PS1 the current study also investigated PEN2 levels in hippocampus and frontal cortex from controls, LBD, FTD and AD. Our results have shown a significant increase of PEN2 levels in hippocampus from AD and an increasing trend in frontal cortex from AD, FTD and LBD (**Fig.5.13A and B, and Fig. 5.13C and D**). These findings are also consistent to those reported in other studies where increased PS1, NCT and PEN2 levels were observed (Kodam et al., 2010, Chu et al., 2012). The increased PEN2 levels observed in the hippocampus from AD may also be attributed to increased  $\gamma$ -secretase activity as PEN2 is responsible for its stability. Since PEN2 levels are increased in AD and we have also observed an increasing trend in CD147 level in hippocampus from AD, taken together these findings indicate a close relationship between PEN2 and CD147 that needs to be investigated further.

It was interesting to observe that CD147, NCT, and PS1 levels showed an increasing profile in hippocampus and decreasing profile in some disease status in the cortex. I anticipated finding significant levels of these  $\gamma$ -secretase complex components in LBD and FTD that have similar manifestations as AD but this was not the case. These



findings are consistent with other studies that have reported mean differences between AD and age matched controls but with no statistical differences (Schonlein et al., 1993, Patel et al., 2006, Vetrivel et al., 2008a). In addition, our findings from hippocampal tissues are correct as it has also been reported that over expression of one member does not affect the whole complex (Edbauer et al., 2003, Kimberly et al., 2003, Takasugi et al., 2003) and that elevation of  $\gamma$ -secretase activity can only be achieved by over expressing all the components (Li et al., De Strooper, 2003). The cited studies support our findings where NCT, PS1, and currently CD147 showed increasing trends in addition to a significant increase in PEN2

I have also reported decreasing trends in NCT, PS1 and PEN2 levels in the cortex which is consistent with TPM 21 findings by Vetrivel and colleagues. These findings confirm that  $\gamma$ -secretase complex components, including CD147, are reduced in the cortex and provide additional proof that CD147 is not elevated in cortex from AD brains as reported by Nahlakova et al (2010). Our data has shown increased PS1 and PEN2 levels with increasing trends of CD147 and NCT, in addition to a positive correlation between CD147 and NCT and PS1 levels in the hippocampus. These findings may indicate that a balance between CD147 and  $\gamma$ -secretase may be responsible for modulating A $\beta$  levels in brains.

## **5.7: Conclusion**

I report for the first time that CD147 is not altered in AD. However the observed increasing trends in CD147, PS1, nicastrin and significant increase and PEN2 levels in hippocampus from AD is an indication of increased  $\gamma$ -secretase activity. I also report for the first time that CD147 correlates with PS1 and NCT but not A $\beta$ 42 in hippocampus

from AD brains. Finally the findings confirm that CD147 is not part of the  $\gamma$ -secretase complex but rather that it may influence the  $\gamma$ -secretase complex activity indirectly by interacting with NCT, PS1, ALPH-1 and PEN 2 as it is a multifunctional protein.

## CHAPTER 6

### **Polymorphisms in the CD147 promoter region may influence Alzheimer's disease (AD) pathology.**

#### **6.1: Introduction**

The CD147 protein description and classification (Biswas and Vonderhaar, 1987, Fossum et al., 1991, Miyauchi et al., 1991, Kasinrerker et al., 1992, Biswas et al., 1995), its role in MMPs production (Biswas et al., 1995, Guo et al., 1997) and its involvement in the development of the nervous system, spatial learning and memory, sensory inputs and retinal functions (Naruhashi et al., 1997, Muramatsu and Miyauchi, 2003, Zhou et al., 2005) have been reported. In addition its involvement in the development of cancer, tumour progression and AD pathogenesis (Nabeshima et al., 2006a, Winkler, 2008, Nahalkova et al., 2010), in particular regulating A $\beta$  levels (Zhou et al., 2005, Vetrivel et al., 2008b) have also been reported.

CD147 expression is facilitated by Sterol carrier protein 2 (SCP-2). The properties of SCP-2 have been discussed in Chapter 1 of this thesis, where I have described SCP-2 as part of a fusion gene with two initiation sites coding for a 15.4 kDa (pro-SCP-2) and a 58.9 kDa (SCP-x) proteins (Ohba et al., 1994, Ohba et al., 1995). In addition to its involvement in cholesterol trafficking and metabolism, SCP-x undergoes a post-translational process yielding a mature 12.9 kDa DNA binding fragment in the nucleus where it regulates CD147 transcription (Ko and Puglielli, 2007). This fragment is controlled by *pro*-SCP-2 which acts as a competitive regulator for CD147 transcription

(Ko and Puglielli, 2007). SCP-2 was initially identified as a sterol carrier and a non-specific lipid-binding protein. However, subsequent studies have shown that SCP-2 binds fatty acid and cholesterol and facilitates their translocation between membrane systems both *in vitro* and *in vivo*. It has been established that SCP-2 is responsible for a rapid protein-mediated translocation of cholesterol in cells and tissues and that it alters cholesterol metabolism in the liver and plasma (Baum et al., 1997, Zanlungo et al., 2000).

The expression of *pro*-SCP-2 abolishes the transcriptional activity of 12.9kDa SCP-2 which thereby shuts down CD147 transcription. The loss of CD147 expression (Ko and Puglielli, 2007) and deletion of CD147 in female knock- out mice (Zhou et al., 2006) lead to the increased production of A $\beta$ . In addition findings in chapter 3 of this thesis have shown that cholesterol loading affects CD147 expression in rat primary cortical neuronal cultures. Taken together these findings suggest that both cholesterol and SCP-2 play a role in CD147 expression, which in turn has an impact on A $\beta$  peptide levels. The findings in chapters 3 and 4 describe the regulation of CD147 expression *in vitro* and *in vivo*. In addition findings in chapter 5 reveal CD147 expression in brain tissue from controls, AD and Non-AD type dementia (dementia with Lewy Bodies (LBD) and frontal temporal dementia (FTD)) cases and its association with the  $\gamma$ -secretase complex components. Taken together the *in vitro* and *in vivo* evidence supporting a role for CD147 in regulating A $\beta$  levels, (either through regulating  $\gamma$ -secretase activity (Zhou et al., 2005) or A $\beta$  degradation (Vetrivel et al., 2008b) warrants further investigation of its genotypic association with AD. It is not known if any polymorphisms in the CD147 promoter region (where SCP-2 binds to initiate its transcription) influence AD development and pathology. Thus in this chapter I investigated the presence of single

nucleotide polymorphisms (SNPs) within the CD147 promoter region, where SCP-2 binds to initiate its transcription, that may be involved in AD pathology.

## **6.2: Aims**

- a) To confirm SCP-2 binding of CD147 DNA.
- b) To identify novel SNPs within the SCP-2 binding site on the CD147 promoter in addition to the already characterised SNPs reported in NCBI
- c) To determine an association between the identified SNPs and AD pathology.

## **6.3: Material and methods**

The generation and purification of SCP-2 protein was performed as described in *sections 2.4.2 and 2.4.3* of the methodology chapter. SCP-2 protein was generated using chemically competent KRX E.coli cell line transformed with *pro*-SCP and SCP-x DNA (1µl) and subcultured on Kanamycin agar plates over night. Following several steps of the transformation procedure protein expression was induced by the addition of 1mM IPTG and 0.1% Rhamnose. After approximately 18 hours of incubation the cell suspension was subjected to three passages of homogenization using a French press, followed by centrifugation at 10000g for 10 minutes. Inclusion bodies containing the desired protein were recovered from the homogenate as a pellet. The lysate was retained and further processed to recover recombinant proteins localized to the cytoplasm.

The purification of *pro*-SCP and SCP-x cytoplasmic protein was achieved through immobilized metal ion affinity chromatography (IMAC) as described in *section 2.4.3* of the methodology chapter. In brief the lysate was treated with 1ml of Ni-NTA agarose

beads (Qiagen) and gently mixed at 4°C for 1 hour, centrifuged at 2000g for 5 minutes, and the supernatant removed. Four millilitres of wash solution was then mixed with the remaining beads, followed by centrifugation at 2000g for 5 minutes repeated 4 times. Protein was eluted by addition of 1ml of elution buffer to the beads, centrifuged for 5 minutes at 2000g and the supernatant collected. The protein solution was transferred to dialysis tubing and dialysed against three 2 litre volumes of dialysis buffer solution at 4°C, over a 24 hour period. The protein solution was then removed from the cellulose tubing, combined with glycerol (10%), filter sterilised (0.2µM) and stored at -80°C. Protein recovery was confirmed by western blot whereas SCP-2 binding of the CD147 DNA was confirmed by electrophoretic mobility shift assay (EMSA) following the manufacturer's instruction.

The DNA binding properties of mature SCP-2 on an electrophoretic mobility shift assay (EMSA) following incubation of affinity-purified 12.9-kDa SCP-2 with PCR products corresponding to the CD147 promoter region has been described (Ko and Puglielli, 2007) (**Fig. 6.1**). KO and Puglielli generated probes corresponding to nucleotides -492 to -392, -392 to -242, -245 to -95 and -94 to 10 and used them to determine their binding capacity for the CD147 promoter DNA. They reported no binding observed with PCR products corresponding to nucleotides -492 to -392 and -94 to 10. However there was a strong mobility shift with the probe corresponding nucleotides to -245 to -95 with a weak shift with the probe corresponding to nucleotides -392 to -242 when incubated with the transcriptionally active fragment of SCP-2 suggesting the existence affinity binding sites for SCP-2 on the CD147 promoter as shown in Figure 6.1. The 471 bp EMMPRIN DNA used for EMSA as described by Liang et al. (Liang et al., 2002) was kindly provided by Dr. Sherif Boulos of Australia Neuromuscular Research Institute (ANRI – Australia).

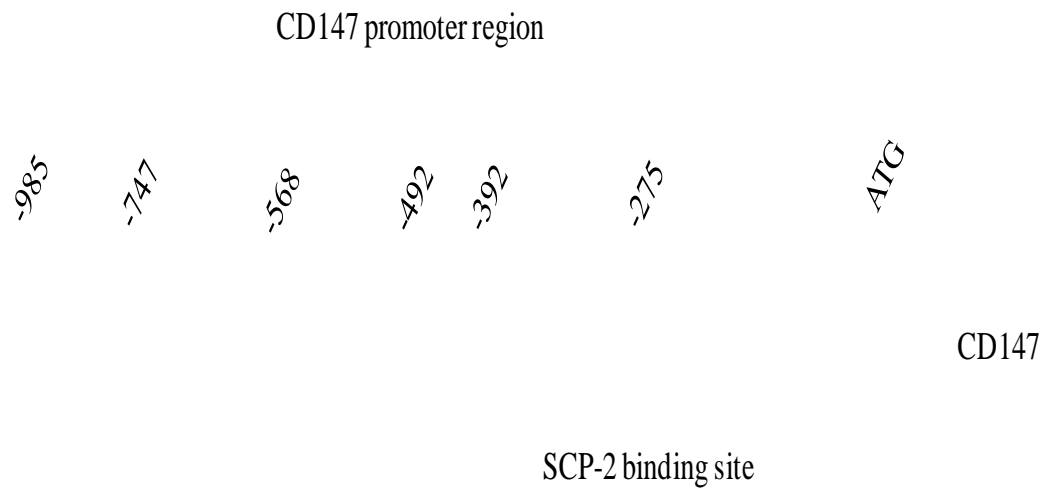


**Fig.6.1: The schematic view of the 5'-Untranslated region of CD147**

CD147 promoter region showing SCP-2 binding site between nucleotides -392 and -95

*(adapted from (Ko and Puglielli, 2007))*

Human genomic DNA samples (health controls;  $n=100$  and AD cases,  $n=100$ ) were sourced from the Australian Imaging Biomarker and Lifestyle (AIBL) study (Perth and Melbourne – Australia). A larger 709 bp fragment that covers the whole region sequenced by KO and Puglielli (Ko and Puglielli, 2007) as well as regions up and down stream of this region (**Fig.6.3**). To generate the 709bp fragment a slowdown PCR was performed as described by Frey et al. (Frey et al., 2008). Approximately 30-50ng of genomic DNA was amplified by PCR in a reaction containing 400nM each primer (forward 5' **AGGCTCTGGGAGTACAGACG** and reverse 5' **CCGGGAGGAACCTCTAGTC**), 1.6µl MgCl<sub>2</sub>, 0.2 µl Taq polymerase, 4 µl 10x PCR buffer (Phusion), 1.5 µl 7-Deaza-dGTP, 2 µl dNTPS and 9.7 µl dH<sub>2</sub>O. The thermal cycle conditions are as follows:

- 1 cycle of 95°C for 5min., setting heating ramp to 2.5°C<sup>-1</sup> and the cooling ramp rate for reaching annealing temperature to 1.5°C<sub>s</sub><sup>-1</sup>
- 48 cycles of 95°C x 30sec denaturation.
  - 30sec annealing with a progressively lowered temperature from 70-53°C at a rate of 1°C every third cycle and a primer extension of 40 sec at 72°C.
- 15 cycles of 58°C, 4°C hold.

The 709bp product, which covers up- and down-stream of the putative SCP binding region (-392 to -95 nucleotides; (Ko and Puglielli, 2007), was verified by agarose electrophoresis and viewed under UV on a Biorad Gel doc prior to sequencing.

Sequencing of the amplified region of the CD147 promoter was undertaken at Applied Genetic Diagnostics (APG), Department of Pathology-University of Melbourne. The



provided 709bp product was verified by agarose electrophoresis before pre-sequencing cleanup using EXOSAP-IT (GE Healthcare) and a sequencing reaction with 5µM forward primer and Big Dye V3.1 terminators (Applied Biosystems). The Qiagen DyeEx kit was used to clean up the product before capillary electrophoresis on an ABI3130xl Genetic Analyser with POP7 polymer. The product was amplified by PCR and sequenced by capillary electrophoresis on an ABI 3130xl Genetic Analyser and compared to the reference sequence NG\_007468.1 using Mutation Surveyor Software® (Soft Genetics). Results were confirmed by repeat sequencing.

Linkage Disequilibrium was estimated by  $D'$  and  $r^2$  as implemented in Haploview V4.2 software (Barrett et al., 2005). Allelic and haplotypic associations with clinical classification were undertaken using chi-squared ( $\chi^2$ ) tests as implemented in Haploview. Corrections for multiple testing were considered if mandatory, 1000 permutations as implemented in Haploview. Genotype associations were then analyzed using IBM SPSS® Statistics version 19. Analysis of association with categorical variables (i.e. clinical classification) was undertaken using  $\chi^2$  analysis, whilst continuous variables were analyzed using either the Student's T-test or One Way ANOVA, where appropriate.

## **6.4: Results.**

### **6.4.1: SCP- $\alpha$ and *pro*-SCP bind CD147 DNA *in vitro***

The two isoforms of SCP-2 protein (*pro*-SCP and SCP- $\alpha$ ) were generated and purified as described in the methodology. In order to confirm its purity and production the protein was run on western blot and stained with *His* antibody. A positive 15kDa band

(**Fig.6.2A**) was identified and provided proof that the protein had been successfully produced and purified. For SCP to initiate transcription it has to bind to the CD147 promoter region. Just like in the study by Ko and Puglielli (Ko and Puglielli, 2007) I also used the electrophoretic mobility shift assay (EMSA) to determine the SCP-2 binding of the CD147 DNA and to confirm that the generated SCP isoforms were also binding CD147 DNA. I used yeast extract protein (lane 2), SCP-x and pro-SCP (lanes 3 and 4 respectively), CD147 protein (lane 5) and yeast extract protein plus CD147 (lane 6) as my controls. Compared to yeast extract protein (lanes 2 and 5), SCP protein minus CD147 DNA (lanes 3 and 4) and CD147 protein (lane 5), results showed positive CD147 DNA binding as evidenced by reduced mobility of SCP protein isoforms (lanes 7 and 8) on the gel (**Fig.6.2B**).

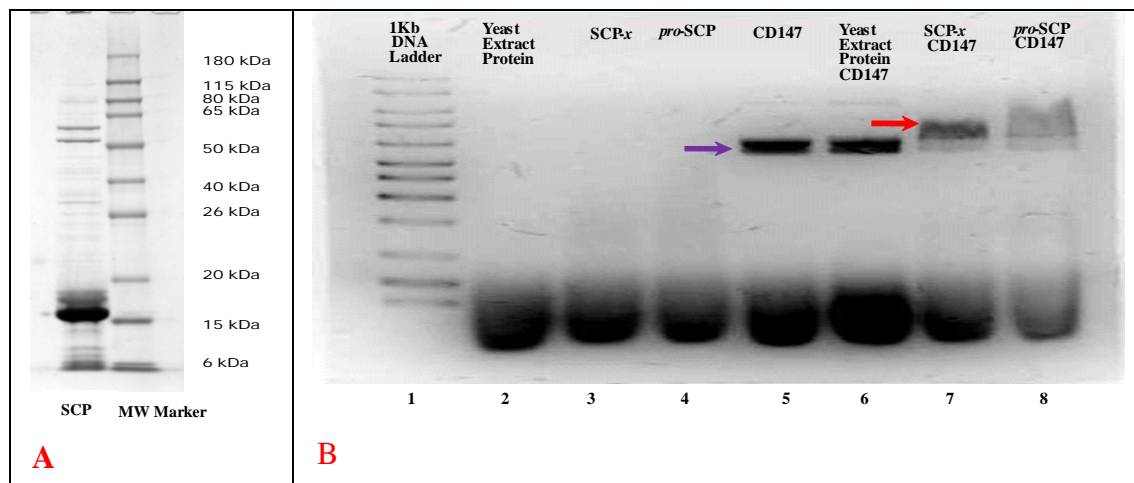


**Figure 6.2: Purified SCP-2 protein and electrophoretic mobility shift assay of SCP protein.**

Purified SCP protein separated by SDS-PAGE gel electrophoretic method (A). Electrophoretic mobility shift assay (EMSA) (B) showing SCP isoforms binding CD147 DNA. Compared to yeast extract protein (lanes 2 and 5), SCP protein minus CD147 DNA (lanes 3 and 4) and CD147 protein (lane 5), results show positive SCP protein binding (lanes 7 and 8) of CD147 DNA as evidenced by reduced mobility of the SCP protein bands with SCP-x showing strong binding (red arrow).

#### **6.4.2: CD147 promoter is a GC-rich region requiring special PCR technique to amplify.**

CD147 promoter region was amplified in human genomic DNA by polymerase chain reaction (PCR) as described above. Although PCR amplification of DNA has previously been reported (Mullis and Faloona, 1987, Saiki et al., 1988, Huh et al., 2011, Kang et al., 2011, Ramana et al., 2011), amplification of the GC-rich sequences have not been easy because they are refractory to amplification due to the formation of secondary intermolecular structures reported (Varadaraj and Skinner, 1994, Schwientek et al., 2011). CD147 promoter region, as a regulatory domain, is a GC-rich region (**Fig.6.3**) requiring a special PCR method to amplify (Jung et al., 2002, Deng et al., 2010, Jensen et al., 2010, Wei et al., 2010). Thus preliminary amplification of the region was performed using the slowdown PCR as described in (Frey et al., 2008) in order to ascertain that the GC-rich region was successfully amplified (**Fig 6.4**). Results have shown that compared to negative control (master mix minus DNA, lane 1) the promoter region was successfully amplified in the PCR products from 6 human brain test samples (lanes 2 – 7). Having established that CD147 promoter can be successfully amplified in human genomic DNA, the region was amplified in 200 DNA samples (n=100, controls and AD cases respectively) from the AIBL study cohort with the resultant product sent to Melbourne for sequencing as described above.

(Chr19:571680)

CAGCGAGACCACTTTACTTGTACGGAAGGGGGCTGCCTGCGTGGGATGCAA  
TCTCCAGAGCACACGGGACAAAGGAAGGGAGCTTCTGTTCTCTGTCCTTTC  
CCTGTTGGCTGGGGTTGGACGCCCACAATCTAAGCTGATCCCGGTTGGCTAA  
AACTTAAACCTTTTTTAAATAGGGTAAACGCGCCACCTGCGAGGAAAGAA  
GAAGGGGGTAAGGTTGATTGACAACCTTTAGACCTGGAAGTTGAGTTTCTGA  
AGAGGAACTTACTTGTCCCAACCAAATGGTGCACAGGACGTTTATACTAAG  
AAATTATTCATTTTCTGAGATCCAGATTCAAGTGCCCTTTAAGTATTTTTATT  
TGGGCGGAGGAGGTCACCTCCTCCACCTAATTTATTAATACGTTTCATATAT  
ATATATATATATGTACATTTTTAAAGGCAGAGATGTGCGTCTCGCCATGTTG  
CCGCGTCTGGTCTCGAGCTCCCGGGCTCAAGCGATCTTCCCGCCTCGACCTC  
CCA***AGGCTCTGGGAGTACAGACG***TGAGCCACAGC**G**GCCGGCCCGTGTTTAA  
CTCAGATAAAATCTGGGTAACACACTTTCAACGCTTCAACCCCCCT**C**GGGCGC  
ACCGCTCTGCGCTCATT**G**CAACTTTGAAAGCAGGAAGGAAGAAAT**G**CGCAG  
GCTCCAGCCGCGTCCCCGCAGGCCCCACTCCCGTTTCCTAGCAACGCCGGGT  
CACGTGCGCCGCGCCCGGATTCCGTAGCGTGAGCCTGCCGGAGCCGGCGC  
GTACATGCGAGCGTGTGCGCGCGTGCGCAGGC**G**GGGCGACCGGCGTCCCCG  
GCGCTCGCCCCGCCCCGAGATGACGCCGTGCGTGCGCGCGCCCG**G**TCCGC  
GCCTCCGCCGCT**N**TTTTATAGCGGCCGCG**N**GGCGGCGGCGGC**A**GCGGTTGG  
AGGTTGTAGGACCGGCGAGGAAT**A**GGAA**T**C**ATG**GCGGCTGCGCTGTTTCGTG  
CTGCTGGGATTCGCGCTGCTGGGC**A**CCACGGAGCCTCCGGGGCTGGTGAG  
GAGCGGGTAGGGGGCGGGGGTGCGGTCCTGCAGGGGCCGGAATGGAGGC  
CGCGGTGCCGACCCGAAGCCGACGGGAGCCTGGGGCCTCGGCGCGGGGCG  
GCCT**G**GGGTGCGAAAG**G**CCCGCCCCGGGGGCTTCCCGCGCCAGCATGGAGC  
TT**G**GGGGTGAAGTCCCAGGG**T**TTGAGGGGG**ACTAGAGGTTCTCCCGG**CG  
CGGCCTGCCGGGCTCCCCCGGGCGCT (Chr19:572934)

### Figure 6.3: Sequence of the CD147 promoter region

Promoter region showing the GC-rich cis-elements, NCBI annotated SNPs (in red), and the region where SCP binds to initiate CD147 transcription (underlined). In this thesis a total of 709bp was sequenced using primers (blue italics) to determine known SNPs and ascertain the presence of novel SNPs.

**A**

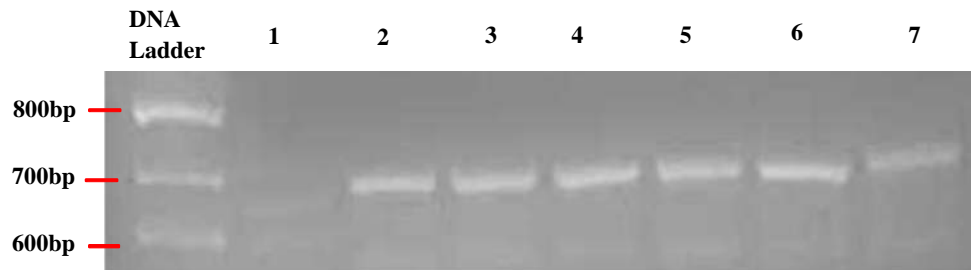


**Figure 6.4: Slowdown PCR amplification of the CD147 promoter region**

Amplification of 709bp PCR product from the CD147 promoter region. Compared to negative control (master mix minus DNA, lane 1), results indicate successful amplification of the CD147 GC-rich promoter in human genomic DNA PCR products from 6 human brain test samples (lanes 2 - 7) by slowdown PCR method.

#### **6.4.3: CD147 promoter contains two novel SNPs not previously reported.**

The CD147 promoter region sequenced in this thesis contains 16 SNPs that have been previously reported in NCBI with varying minor allele frequencies. Analysis of sequencing data failed to observe any sequence variation at 9 of these sites (potentially monomorphic in the cohort studied), whilst the remaining 7 SNPs already reported in NCBI were successfully identified, these being: rs4919859, rs145461969, rs11551906, rs28915407, rs142683396, rs28915408, and rs2072307. In addition to the previously reported SNPs results from the current study have identified two new novel SNPs that have not been previously reported. A comparison of minor allele frequencies in the current study is made to those reported in European populations from NCBI in Table 6.1.

**Table 6.1: Comparison of minor allele frequencies reported in European populations from NCBI and in the current study**

SNP	Position	MAF – NCBI*	MAF – Current Study
rs4919859	chr19:572317	0.333, 0.350	0.385
rs145461969	chr19:572550	NA, NA	0.0025
rs000001(c.-61A>G)**	chr19:572574	Not reported	0.0025
rs000002 (37C>G)**	chr19:572672	Not reported	0.0025
rs11551906	chr19:572680	NA, NA	0.02
rs28915407	chr19:572811	0.087, NA	0.02
rs142683396	chr19:572823	NA, NA	0.002
rs28915408	chr19:572860	0.022, NA	0.032
rs2072307	chr19:572878	0.022, NA	0.102

\*European population (PGA\_CEPH-PANEL, HapMap-CEU): NA, not available in given population. Not reported, SNP has not been previously reported in NCBI database.

\*\*Novel SNP



The first of these, an A to G transition located 61 base pairs upstream (-61A>G) of the transcription initiation site, was identified in a single heterozygous healthy control individual and is subsequently referred to in this thesis as rs00000001. A second novel SNP, a C to G transversion located 37 base pairs downstream (37C>G) of the transcription initiation site, was identified in a single heterozygous AD individual and is subsequently referred to in this thesis as rs00000002. These SNPs need to be investigated further to determine if they have any influence on the development and pathology of AD or other neurodegenerative diseases. The 9 SNPs identified with minor allele frequency (MAF) greater than 0 were determined via Haploview and are presented with a plot of the relative D' levels between each marker below (**Fig.6.5**). After identifying the SNPs, I then wanted to know if any of them is associated with AD. Results of this analysis are presented in the sections below.

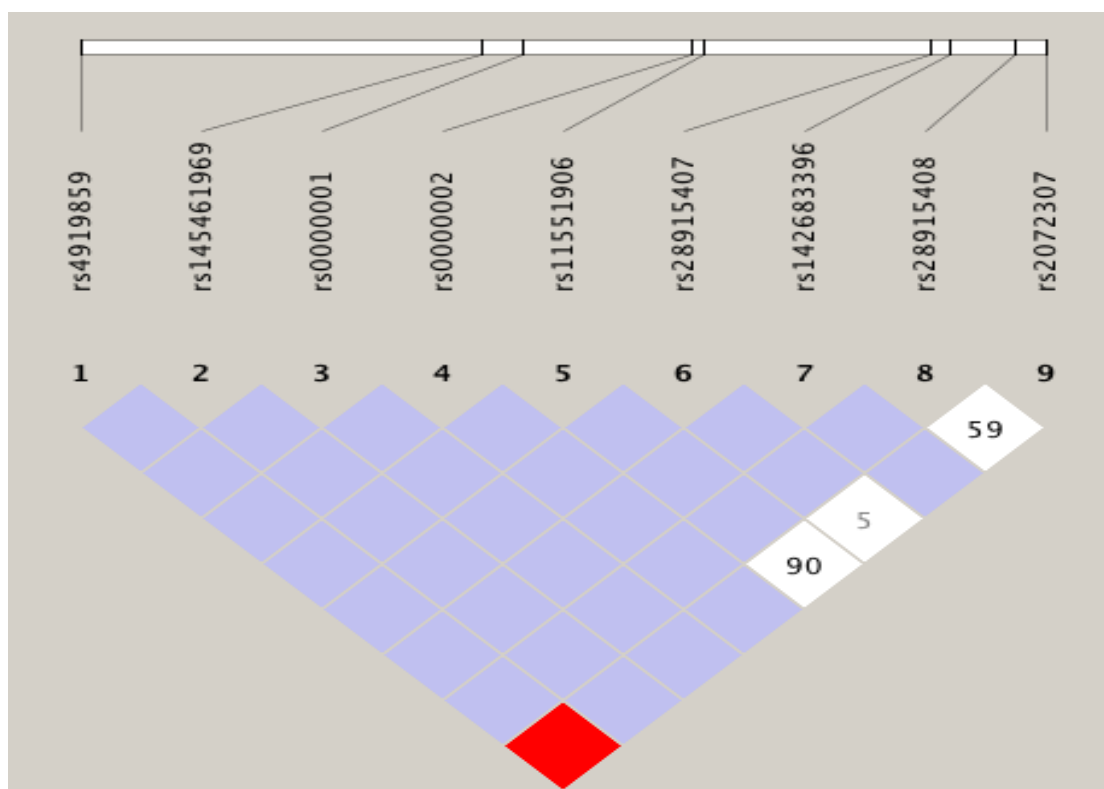


**Figure 6.5: Linkage disequilibrium for CD147 Single Nucleotide Polymorphisms in the AIBL cohort sample.**

Each of the 9 SNPs identified with MAF greater than 0 are presented with a plot of the relative D' levels between each marker below, as determined via Haploview.

#### **6.4.4: CD147 promoter SNPs are not associated with AD.**

SCP-2 binding to CD147 promoter has been reported (Ko and Puglielli, 2007) . However genetic variations within this region may alter SCP-2 binding which in turn may lead to alteration in CD147 expression leading to increased AD risk and pathology. As such, ascertaining the frequency of known genetic variations as well as the discovery of novel genetic variations within this region would be of interest. In the current study a sample of 100 AD and 100 healthy controls from the AIBL cohort were utilised. Allelic and haplotypic associations were analysed using Haploview V4.2 software (Barrett et al., 2005) and genotype associations were analyzed using IBM SPSS® Statistics version 19 as described in section 6.3 of this chapter. Results from these experiments have shown no allelic (**Table 6.2**), genotypic (**Table 6.3**) and haplotypic (**Tables 6.4**) association with AD.

**Table 6.2: Allelic Frequencies**

<b>SNP (major/minor)</b>	<b>Risk Allele</b>	<b>CTRL MAF</b>	<b>AD MAF</b>	<b>chisq</b>	<b><i>p-value</i></b>
rs4919859 (G/C)	-	0.385	0.385	0.0	1.0
rs145461969 (G/T)	G	0.005	0.000	1.003	0.3167
rs0000001 (A/G)	A	0.005	0.000	1.003	0.3167
rs0000002 (C/G)	G	0.000	0.005	1.003	0.3167
rs11551906 (A/G)	G	0.015	0.025	0.51	0.4751
rs28915407 (G/T)	G	0.03	0.01	2.041	0.1531
rs142683396 (G/A)	A	0.000	0.005	1.003	0.3167
rs28915408 (G/A)	G	0.04	0.025	0.716	0.3976
rs2072307 (T/C)	T	0.11	0.095	0.245	0.6209

SNPs and minor (MAF) allele frequencies in controls and AD patients. P-values (range: 0.3167 – 1.0) for the 9 SNPs were calculated using chi-squared ( $\chi^2$ ) tests as implemented in Haploview and indicating no association with AD

**Table 6.3: Genotype association**

SNP	Genotype	Controls	AD	Chiq	<i>p-value*</i>
rs4919859	GG	39	38	.089	.957
	GC	45	47		
	CC	16	15		
rs145461969	GG	99	100	.316	1.00
	GT	1	0		
rs00000001	AA	99	100	.316	1.0
	AG	1	0		
rs00000002	CC	100	99	.316	1.0
	CG	0	1		
rs11551906	AA	98	95	3.713	.156
	AG	1	5		
	GC	1	0		
rs28915407	GG	94	98	2.083	.149
	GT	6	2		
rs142683396	GG	100	99	1.005	.316
	GA	0	1		
rs28915408	GG	92	95	.740	.390
	GA	8	5		
rs2072307	TT	80	82	.387	.824
	TC	18	17		
	CC	2	1		

Genotype associations of the 9 SNPs in controls and AD cases were analyzed using IBM SPSS® Statistics version 19. P-values (range: 0.149 – 1.0) were calculated using chi-squared ( $\chi^2$ ) tests as implemented in Haploview and indicating no association with AD

**Table 6.4: Manual Haplotype Associations**

Haplotype	Freq	AD Freq	Ctrl Freq	chisq	<i>p-value</i>
GGACAGGGT	0.438	0.461,	0.416	0.819	0.3654
CGACAGGGT	0.378	0.375,	0.380	0.01	0.922
GGACAGGGC	0.102	0.094,	0.109	0.245	0.6204

Haplotypic frequencies in health controls and AD patients and p-values (range: 0.3654 – 0.922) calculated using chi-squared ( $\chi^2$ ) tests as implemented in Haploview and indicating no association with AD.

#### **6.4.5: CD147 promoter SNPs are not associated with A $\beta$ , cholesterol and ApoE levels.**

Many potential risk factors for AD have been described which include, low levels of sex steroids (Pericak-Vance et al., 1991, Poirier et al., 1993, Strittmatter et al., 1993, Haskell et al., 1997, Lambert et al., 1998, Short et al., 2001), increased levels of gonadotropins (Smith et al., 1998, Bowen et al., 2000, Short et al., 2001), head injury, physical inactivity, stroke, diabetes, hypertension, and hypercholesterolemia. In addition age and possession of the  $\epsilon 4$  allele of the Apolipoprotein E gene (APOE  $\epsilon 4$ ) are some of the major risk factors for most of the population (Martins et al., 2006). Thus the current study investigated associations between the CD147 promoter SNPs and plasma A $\beta 40$ , A $\beta 42$ , cholesterol and ApoE levels. No association analysis of the new identified SNPs was done as they appear in only 1 health control and AD case respectively. However an association analysis of the other SNPs showed that these SNPs are not associated with A $\beta 40$ , A $\beta 42$ , cholesterol and ApoE levels (**Table 6.5**).

**Table 6.5: SNPs association with A $\beta$ , cholesterol and ApoE Levels**

SNP	Genotype	n	Mean	Std. Dev	p-value
Aβ40					
rs4919859	GG	77	114.3451	79.03767	.982
	GC	92	112.3340	70.09841	
	CC	31	111.8019	77.30048	
rs11551906	AA	193	114.0789	78.27700	.477
	AG	6	91.2300	29.46459	
rs28915407	GG	192	113.2423	78.37106	.847
	GT	8	107.8288	47.42792	
rs28915408	GG	187	109.4164	71.81514	.143
	GA	13	164.9454	126.60262	
rs2072307	TT	162	109.4405	73.89005	.371
	TC	35	126.8474	90.85050	
	CC	3	145.3800	77.30048	
Aβ42					
rs4919859	GG	77	38.4395	18.64391	.526
	GC	92	37.9095	17.18257	
	CC	31	34.0903	22.06179	
rs11551906	AA	193	37.7050	18.80707	.581
	AG	6	33.4433	6.20001	
rs28915407	GG	192	37.4291	18.84739	.731
	GT	8	39.7400	7.93448	
rs28915408	GG	187	37.0856	17.76225	.208
	GA	13	43.7931	27.53798	
rs2072307	TT	162	36.3743	17.55477	.193
	TC	35	42.2791	22.26998	
	CC	3	43.9700	18.99478	
Cholesterol					
rs4919859	GG	77	5.3727	1.05539	.437
	GC	91	5.4967	1.02604	
	CC	31	5.2258	1.12041	
rs11551906	AA	192	5.4156	1.05531	.168
	AG	6	4.8167	0.41673	
rs28915407	GG	191	5.4230	1.06252	.280
	GT	8	5.0125	0.66641	
rs28915408	GG	186	5.3995	1.06418	.721
	GA	13	5.5077	0.87793	
rs2072307	TT	161	5.4379	1.04319	.686
	TC	35	5.2686	1.08784	
	CC	3	5.3333	1.36137	
ApoE					
rs4919859	GG	77	14.5928	2.92177	.255
	GC	87	15.1154	2.52136	
	CC	30	15.4358	2.20916	
rs11551906	AA	187	14.9600	2.64031	.906
	AG	6	14.8298	3.44908	
rs28915407	GG	186	14.9972	2.65860	.316
	GT	8	14.0350	2.43816	
rs28915408	GG	181	14.9955	2.68765	.459
	GA	13	14.4298	2.08612	
rs2072307	TT	156	14.8645	2.56049	.532
	TC	35	15.2719	3.11273	
	CC	3	14.9576	0.93808	

Association analysis CD147 SNPs (n>1 in  $\geq 2$  genotypes) with A $\beta$ 40, A $\beta$ 42, cholesterol and ApoE levels were undertaken using  $\chi^2$  analysis, whilst continuous variables were analyzed using IBM SPSS® Statistics version 19 with either the Student's T-test or One Way ANOVA, where appropriate. P-values (range: 0.143 – 0.982) showing no association of the SNPs with A $\beta$ 40, A $\beta$ 42, cholesterol and ApoE levels



#### **6.4.5: CD147 promoter SNP rs11551906 is associated with AD pathology.**

Imaging techniques using radio labelled positron emission tomography (PET) tracers that bind to A $\beta$  peptides in amyloid plaques are currently being used to assess relative brain amyloid plaque pathology in AD (Lee et al., 2003a, Mistur et al., 2009, Mosconi et al., 2009, Jagust et al., 2010, Kadir et al., 2011). The AIBL study performed PET scans on a subset of the study participants and the current study did a genotype association analysis of the CD147 promoter SNPs with the standard uptake value ratios (SUVR) of the radio labelled tracer (Pittsburgh Compound B, PiB) used in the AIBL study. Results have shown a positive association with rs11551906 SNP ( $*p<0.05$ ) (**Table 6.6**) indicating that presence of the minor allele of this SNP is associated with increase cerebral amyloid burden.

**Table 6.6: Genotype association with SUVR**

SNP	GENOTYPE	n	MEAN	SD	<i>p-value</i>
rs11551906	AA	40	1.7850	.56186	<b>.010*</b>
	AG	2	2.1300	.08485	
rs28915407	GG	39	1.8364	.55135	.141
	GT	3	1.3467	.40377	
rs28915408	GG	39	1.7936	.54587	.745
	GA	3	1.9033	.77106	

Genotypic association of the 3 SNPs with SUVR in AD patients were analyzed using IBM SPSS® Statistics version 19. P-values (range: 0.010 – 0.745) *p-values* indicating a significant association of **rs11551906** with SUVR (\* $p < 0.05$ )

## 6.5: Summary of results

Overall the results presented in this chapter show that SCP-2 binds CD147 DNA and based on previous studies this is likely to be within the promoter region, specifically in the region -392 to -95 as identified by Ko and Puglielli (Ko and Puglielli, 2007). Sequencing of a 709bp fragment covering this region identified 2 novel SNPs within the CD147 promoter that have not been reported before in NCBI. There was neither an association between the 9 identified polymorphic SNPs and AD risk or with changes in plasma cholesterol, A $\beta$ 40, A $\beta$ 42 and ApoE levels. However, a significant association between the rs11551906 minor allele and elevated cerebral amyloid burden, as determined by PiB-PET SUVR, ( $*p<0.05$ ) was observed.

## 6.6: Discussion

### 6.6.1: SNPs association with AD

Genetic mutations or polymorphisms linked to AD development and severity (Prince et al., 2003, Greeve et al., 2004, Frey et al., 2008, Ringman et al., 2010) and AD risk factors such as sex steroids (Pericak-Vance et al., 1991, Poirier et al., 1993, Strittmatter et al., 1993, Haskell et al., 1997, Lambert et al., 1998, Short et al., 2001), gonadotrophins (Smith et al., 1998, Bowen et al., 2000, Short et al., 2001) and possession of the APOE  $\epsilon$ 4 allele (Martins et al., 2006) have been reported. The current study investigated SNPs in the CD147 promoter region, where SCP-2 binds to stimulate CD147 transcription and determined their association with AD. Allelic (**Table 6.2**), genotypic (**Tables 6.3**) and Haplotypic (**Table 6.4**), association analysis were undertaken and showed no association with AD. These findings cannot completely rule out the possible association of the identified SNPs with AD as only a small subset of samples were utilised for sequencing experiments. Due to the small sample size the

possibility remains that there was not sufficient power to identify any associations. Further, as the focus of this study was on the promoter region of CD147 it cannot be ruled out that an untyped variant downstream from the sequenced region, within the coding region of the gene, may impart risk for AD. Previous studies have associated differences in CD147 expression with A $\beta$  levels (Zhou et al., 2005, Vetrivel et al., 2008b) and deficits in memory and behaviour functions (Naruhashi et al., 1997) where a number of behavioural tasks were carried out in mice lacking CD147. Compared to wild-type and heterogeneous (Basigin +/-) mice, the CD147 null mice (Basigin -/-) performed worse in memory and learning tasks (e.g. Y-maze and water finding tasks). In addition CD147 null mice were less sensitive to light, pain, and induced electric shock, reflecting the importance of CD147 in sensory functions. As such, genetic variation within the CD147 promoter may likewise be associated with AD biomarkers and abnormal limbic system function.

To address the above question the current study investigated any associations between these SNPs and plasma A $\beta$ 40, A $\beta$ 42, cholesterol and ApoE levels. Due to previous links between CD147 expression and the aforementioned biomarkers it was anticipated that some association with these parameters linked to AD pathology would be observed. However, there were no associations revealed for the identified SNPs with levels of A $\beta$ 40, A $\beta$ 42, cholesterol and ApoE in plasma (**Table 6.4**) despite these being amongst the most potent reported AD risk factors (Martins et al., 2006) (Jarvik et al., 1995, Igbavboa et al., 1996). The findings may suggest that genetic variations in the CD147 promoter do not play a role in AD pathology as seen in those in the APP and ApoE genes. However, it may also be hypothesised that CD147 promoter mutations play a role in AD pathology only when SCP-2 binds the promoter region that may result in increased A $\beta$  generation as reported by Ko and Puglielli (Ko and Puglielli, 2007).

Further, this study did not investigate any proximal or distal regulatory elements, which may also impact on CD147 expression levels and in turn impact upon regulation of A $\beta$  generation. However these hypotheses need to be proved further in future studies.

#### **6.6.2: SUVR is associated with rs11551906**

The uses of PET scans that utilise tracers that bind to A $\beta$  peptides in amyloid plaques to assess relative brain amyloid plaque pathology in AD have been reported (Lee et al., 2003a, Mistur et al., 2009, Mosconi et al., 2009, Jagust et al., 2010, Kadir et al., 2011). The AIBL study also used a similar technique on the study subjects as reported in the previous studies. A subset of 42 individuals from the 200 AIBL subjects sequenced in this thesis underwent PiB-PET scans and genotype association analysis of SNPs within the sequenced CD147 promoter region with PiB-PET derived SUVR. Only 3 SNPs from those identified could be analysed due to the frequency of identified genotypes. Out of the 3 SNPs only 1 (rs11551906) is associated with SUVR (**Table 6.5**) indicating its association with increase cerebral amyloid burden.

CD147 knock down studies reported increased A $\beta$  levels (Zhou et al., 2005, Vetrivel et al., 2008b) and that SCP-2 binding of CD147 promoter facilitates CD147 transcription (Ko and Puglielli, 2007). Expression of *pro*-SCP-2 has been shown to abolish activity of 12.9 kDa SCP-2 and inhibit CD147 transcription, resulting in an increase in A $\beta$  production (Ko and Puglielli, 2007). Furthermore the current study has shown that rs11551906 is associated with SUVR. Taken together these findings may suggest that this SNP interferes with SCP-2 binding to the CD147 promoter or facilitates *pro*-SCP-2 expression which in turn shuts down CD147 transcription resulting in increased A $\beta$  generation. This may explain why this SNP is associated with SUVR. It is not known if

the other SNPs would also show an association if a larger cohort is used, thus a follow-up study is required to better answer this question.

### **6.6.3: Novel SNPs within the CD147 promoter**

In addition to the already NCBI reported SNPs (**Table 6.1**), the main aim for sequencing the CD147 promoter region described in this thesis was to identify novel SNPs that may be associated with AD development and pathology. At the time of writing the NCBI database identifies 16 SNPs within the region sequenced and only one of these (rs28915404 an -/G deletion-insertion variation) located within the putative SCP binding region. However, no additional SNPs were identified in the region where SCP-2 binds to initiate CD147 transcription that later influences A $\beta$  levels *in vivo*. Interestingly though was the discovery of the 2 novel SNPs within the promoter region but outside the region where SCP-2 binds. These were an A to G transition located 61 base pairs upstream (-61A>G) of the transcription initiation site and a C to G transversion located 37 base pairs downstream (37C>G) of the transcription initiation site. These novel genetic variations were identified in a single heterozygous healthy control individual and a single heterozygous AD individual, respectively. It is not known if -61A>G SNP may provide some protection whereas 37C>G SNP may be a risk factor for AD, however a comprehensive study using a larger and well characterized sample cohort has to be undertaken to prove this hypothesis.

Taken together that GC-rich sequences are difficult to amplify (Varadaraj and Skinner, 1994, Schwientek et al., 2011) and that CD147 promoter is a GC-rich region (**Fig.6.3**) requiring special PCR method to amplify (Jung et al., 2002, Deng et al., 2010, Jensen et al., 2010, Wei et al., 2010), warrants a robust sequencing of the entire CD147 promoter

to identify other novel SNPs that have not been identified yet. This will also further help in the investigation of the roles such SNPs may play in disease pathology including the 2 currently reported in this thesis despite being identified in one health control and AD patient only.

## **6.7: Conclusion**

I report for the first time that the CD147 promoter region sequenced in this study contains 2 novel SNPs that have not been reported before in NCBI. I also report for the first time that out of the 9 SNPs identified in this region only one (rs11551906) is associated with AD biomarker SUVR.

## CHAPTER 7

### General discussion

#### 7.1: The link between CD147 protein and AD pathology.

There are several theories regarding AD development and pathogenesis with the amyloid cascade hypothesis being the most widely accepted and studied one. The amyloid cascade hypothesis proposes that the aggregation and deposition of  $\beta$ -amyloid ( $A\beta$ ) is the initial pathological event in AD, which leads to the formation of amyloid plaques and then to NFT, neuronal cell death, and ultimately dementia. However, the reasons for  $A\beta$  aggregation and additional factor(s) involved in the amyloid cascade are not properly understood and need to be established. Oxidative stress, inflammatory processes, reduced  $A\beta$  clearance, dys-regulated lipid metabolism, reduced oxygen levels and hormonal changes have all been suggested, either directly or indirectly, to initiate or to promote the initial stages of  $A\beta$  aggregation. For example, age-related losses of oestrogen in women and testosterone in men are risk factors for AD, possibly due to hormone influences on  $A\beta$  production and degradation, neuron viability, and oestrogen signalling mechanisms (Li et al., 2000b, Pike et al., 2009).

Possibly the majority of studies on factors that may influence risk of AD have emanated from the early genetic studies which found links between AD and possession of apolipoprotein E4 alleles (Holtzman et al., 2012). This was soon followed by studies that found links between cardiovascular diseases and AD (Sahathevan et al., 2012). There is now also substantial evidence that conditions such as stroke, hypertension, diabetes and lipid disorders are independently associated with an increased risk of AD



and vascular cognitive impairment. As part of these studies, cholesterol and diet have been extensively studied. Due to this research, elevated cholesterol levels and high fat diets have now been associated with increased A $\beta$  production and have been classified as AD risk factors.

The brain represents only about 2 percent of your body weight, but actually has about 20 percent of your body's cholesterol. Cholesterol is important for normal brain function - it is important for synaptic function and is also an essential component of cell membranes in the brain. Defects in cholesterol metabolism are associated with serious neurological and mental dysfunctions (Tint et al., 1994). Alterations in general cholesterol metabolism have been implicated in AD pathogenesis (Jarvik et al., 1995, Igbavboa et al., 1996) as evidenced by reported higher plasma cholesterol levels in people who subsequently develop AD compared to people who don't (Notkola et al., 1998). Some early longitudinal studies of cholesterol-reducing drugs (statins) found that statins such as lovastatin or simvastatin could reduce the risk of developing AD (Miida et al., 2005).

By competitive inhibition of hydroxymethyl co-enzyme A-reductase, statins reduce the production of cholesterol and isoprenoid intermediates including geranyl and farnesyl pyrophosphate. *In vitro* studies also found that statin-induced depletion of cellular cholesterol reduces A $\beta$  production and secretion (Simons et al., 1998a), whereas cholesterol supplementation results in increased production of A $\beta$ 40/42, suggesting that intracellular cholesterol levels can influence APP processing. The reason for this may be that membrane cholesterol content influences the activity of  $\gamma$ -secretase, the APP cleavage enzyme found in cholesterol rich microdomains of the cell membrane, and that is unusual due to its intra-membrane cleavage site. More recent reviews of the clinical

statin data, however, have found that statins have no effect on incidence of AD (McGuinness et al., 2009), or alternatively that the results are just too variable to make any conclusions (Shepardson et al., 2011a, b). The variability in the results of statin studies has been put down to differences in the blood-brain barrier permeability among statins, the stage of AD at which statins were administered, and/or drug pleiotropic metabolic effects. Nevertheless, the interest in cholesterol metabolism and the effect of cholesterol on A $\beta$  production has prompted much research into lipids and AD. From this research, a high fat diet has now also been implicated in the aetiology and development of AD as evidenced by the findings that AD incidence is higher in countries with high-fat/high-calorie diets (Kalmijn et al., 1997), and that the risks for cardiovascular diseases such as elevated blood cholesterol and triacylglycerol (triglyceride) levels, obesity, diabetes, lack of exercise and hypertension are also risks for developing AD (Fillit et al., 2008).

Other interesting studies have reported changes in A $\beta$  peptide generation due to cellular CD147 alterations, an indication of a possible link between CD147 and A $\beta$ . CD147 is a member of the immunoglobulin superfamily, it was first identified as a tumour surface protein capable of inducing matrix metalloproteinase (MMP) expression in fibroblasts, and thus it is also known as EMMPRIN (extracellular matrix metalloproteinase inducer). CD147 is a transmembrane glycoprotein, and increased expression of CD147 occurs in many tumours, however the protein is also critical in foetal development and retinal function and it has been shown to play a role in thymic T cell development, as well as many neurological processes ranging from the development of the nervous system to involvement in spatial learning (Iacono et al., 2007).

Cancer studies of CD147-null animals found that a lack of CD147 leads to a dramatic reduction in accumulation of the monocarboxylate (lactate) transporters (MCT)-1 and -4 proteins, which indicated a role for CD147 in targeting these transporters to the plasma membrane. Continued association of these proteins is required for function, and high levels of these proteins are found on aggressive tumour cells, both of these characteristics are potentially necessary to meet the high glycolytic needs of transformed (cancer) cells (Iacono et al., 2007). Other studies more relevant to AD have reported that CD147 expression levels influence A $\beta$  generation and that a lack of CD147 can cause cognition defects similar to those seen in AD (Zhu et al., 2006, Zhou et al., 2007). CD147 has been shown to be a regulatory co-factor for the  $\gamma$ -secretase complex and that depletion of CD147 from the  $\gamma$ -secretase complex through RNA interference in cell lines results in an increase in A $\beta$  production (Zhou et al., 2005).

These results suggested that CD147 levels could modulate A $\beta$  generation. However, other studies have found that the levels and localization of CD147 in fibroblasts, as well as the postnatal expression and distribution of CD147 in the brain, are distinct from those of integral  $\gamma$ -secretase subunits. It has also been found that membranes isolated from CD147-depleted cells fail to elevate A $\beta$  production in *in vitro*  $\gamma$ -secretase assays (Vetrivel et al., 2008). Instead, Vetrivel et al. found that CD147's influence on A $\beta$  levels was more likely due to extracellular degradation by matrix metalloproteinases (MMPs), the levels of which have been previously reported to be stimulated by CD147 (Vetrivel et al., 2008b). From other studies of  $\gamma$ -secretase, it appears only a small fraction of the cellular pool of CD147 or p23 (also known as TMP21, involved in vesicular trafficking between the ER and Golgi) remains complexed with  $\gamma$ -secretase at steady state, and the precise mechanisms by which these proteins modulate  $\gamma$ -secretase activity remain obscure.

A major role for CD147 in the brain is supported by studies that have demonstrated neurological abnormalities such as spatial learning and memory deficits in CD147 null mice (Naruhashi et al., 1997, Higgins and Jacobsen, 2003, Richardson et al., 2003). However, there is still little literature on CD147 effects on neuronal health and A $\beta$  production and/or clearance, whereas many studies have been carried out to establish its involvement in cancer metastasis.

The recent CD147 studies that have attracted the attention of researchers in the AD field are those which have looked into the regulation of CD147 as a potential strategy to reduce the risk of AD via the modulation of  $\gamma$ -secretase activity, or via the modulation of extracellular enzymes (possibly MMPs) that can degrade extracellular A $\beta$  (Zhou et al., 2007, Vetrivel et al., 2008b). In addition to the siRNA CD147 knock down studies in transgenic mice which have shown CD147 reduction causes a dose-dependent increase in A $\beta$  production (Zhou et al., 2005), CD147's involvement in AD pathology is also supported by studies which have shown increased levels of the protein in the frontal cortex of AD affected individuals (Nahalkova et al., 2009, 2010).

The current study has attempted to characterise further the ways in which CD147 may contribute to AD development and pathogenesis, and the results of these studies are outlined in chapters 3 – 6 of this thesis. In summary CD147 protein levels were measured in rat primary neuronal cultures in the presence and/or absence of endogenous cholesterol and A $\beta$ 42 peptide, whilst CD147 neuronal protection against oxidative stress and A $\beta$  toxicity was also investigated, as reported in chapter 3. In addition to these *in vitro* experiments, the current study has also measured CD147 levels in brain tissues from APPswe transgenic mice fed on normal chow or a high fat/high cholesterol diet to

investigate the impact of diet on CD147 protein expression. The findings of these studies are reported in chapter 4. CD147 levels in human brains from control, frontal temporal dementia, Lewy body disease, and Alzheimer's disease cases were measured to characterise any differences in CD147 levels between aged control brains and brains with the various neurodegenerative disorders. The findings of these experiments are reported in chapter 5. In chapter 6, sequencing studies were carried out to investigate known and any novel polymorphisms in the CD147 gene promoter region, which may also contribute to the development and/or pathology of AD. The findings from all these experiments listed are discussed in detail below.

## **7.2: Cholesterol and A $\beta$ 42 loading increases CD147 protein expression *in vitro***

Brain cholesterol can be produced by glial cells, although in adult brains, most brain cholesterol is believed to be recycled. Neurons, which are especially enriched with cholesterol, are believed to obtain their cholesterol by uptake of apoE/cholesterol complexes via receptors of the LDLR family. Neurological and mental dysfunctions due to defects in cholesterol metabolism have been reported (Tint et al., 1994). There is now significant *in vitro* evidence to indicate a role of cholesterol in AD pathology and recent clinical findings also support the notion that progressive deterioration of cholesterol homeostasis is a central player in AD pathophysiology. Firstly, polymorphisms in several proteins and enzymes involved in cholesterol or lipoprotein transport and metabolism have been linked to the risk of AD. Secondly, enzymatic production of A $\beta$  is affected by membrane cholesterol levels, thought to be due to effects on  $\gamma$ -secretase. However, studies that have led to this conclusion have often been studies of statin effects, and more recent studies have suggested that due to the high number of pleiotropic effects of statins, novel molecular mechanisms that account for

the beneficial effect of statins on AD might be discovered in the future. Thirdly, cholesterol has been shown to affect APP maturation (Galbete et al., 2000a), and alterations to cholesterol metabolism are likely to affect this step in APP metabolism.

To maintain cholesterol homeostasis in the brain, some excretion occurs following enzymatic conversion of cholesterol to the oxysterol 24-OH cholesterol. Another oxysterol found in the brain is 27-OH cholesterol, although this is believed to derive mostly from the circulation. The brain levels of these oxysterols influence expression of many enzymes involved in lipid homeostasis in the brain such as the sterol regulatory element binding proteins (SERBP), apoE (via the liver X receptor) and ABCA1 and ABCG1 (ATP binding cassette transporters, cholesterol efflux transporters) (Martins et al., 2009). CSF 24-OH cholesterol has been found to be higher in AD individuals, and cholesterol efflux appears to be elevated and related to the increased risk for AD (Papassotiropoulos et al., 2002, Koldamova et al., 2003).

In chapter 3 of this thesis the studies demonstrate that cholesterol and A $\beta$ 42 loading in rat primary cortical neuronal cultures altered CD147 and FL-APP expression levels. In primary cultures of rat neurons, cholesterol loading increased CD147 protein levels (**Fig.3.1**) and reduced FL-APP protein levels (**Fig. 3.2**). These findings suggest that CD147 protein expression can increase under conditions of hypercholesterolemia. It is possible that a similar scenario happens in human brains in relation to AD development/pathogenesis. Further investigations are required to establish the detailed mechanism(s) through which cholesterol exerts its influence on CD147 protein expression levels at the cellular level.

In order to determine the cause of the higher CD147 expression, cell viability was investigated by measuring LDH release into the culture supernatants. A significant increase in LDH release (**Fig. 3.3**) was found, indicating that the cholesterol loading caused stress to the neuronal cultures. It is therefore likely that cellular stress was responsible for the observed increased CD147 expression. Our findings are consistent with findings from previous studies that have reported that protein production can be affected in cells undergoing environmental stress (Yao and Tabas, 2001, Matsuda et al., 2002, Nilsson and Sunnerhagen, 2011).

The results in this chapter have also shown a reduction in FL-APP levels in response to cholesterol loading, at high concentrations of cholesterol. In a study by Galbete and colleagues (Galbete et al., 2000b), it was shown that increased cholesterol levels cause a decrease in the secretion of the  $\alpha$ -secretase-cleaved form of soluble APP by interfering with glycosylation in the protein maturation pathway. It was concluded that although APP was probably being inserted in the membrane, a proportion was not being glycosylated, and was not being cleaved by  $\alpha$ -secretase (Galbete et al., 2000b). At much higher concentrations of cholesterol, cellular toxicity is likely to have reduced APP production in the cells, which is what we have observed. The findings suggest that increased cholesterol levels can affect APP production and maturation, and the other results of this section of chapter 3 shows that cholesterol loading can induce cell oxidative stress in rat primary cortical neuronal cultures as evidenced by the elevated LDH release, and result in the over-expression of CD147 protein. The observed increased CD147 protein levels in the presence of increased cholesterol loading are most likely due to cell stress induced by exogenous cholesterol. These findings support the notion that CD147 is a marker of inflammation. In this case it could be hypothesized that increased cholesterol levels, which in turn activated the apoptotic pathway, triggered the inflammatory process.

### 7.3: A $\beta$ 42 induced oxidative stress increases CD147 protein expression *in vitro*

As mentioned previously, CD147 levels have been shown to influence levels of A $\beta$ , either by modulating  $\gamma$ -secretase activity, or by stimulating the production of the MMPs, which have been shown to degrade A $\beta$ . CD147 has also been shown to protect neuronal cells against oxidative stress and injury (Boulos et al., 2007), and the A $\beta$ 42 addition experiments in chapter 3 were designed to provide further evidence that oxidative stress leads to increased CD147 protein production. As can be seen from the results, there was a significant increase in CD147 expression (**Fig.3.6**, chapter 3) and significantly reduced FL-APP (**Fig.3.7** chapter 3) levels in the neuronal cells following exposure to high extracellular levels of A $\beta$ 42 peptide. LDH release (**Fig.3.5**, chapter 3) also increased in the neuronal cultures treated with A $\beta$ 42, indicating cellular oxidative stress was being induced by the peptides. These experiments involved the addition of high concentrations of A $\beta$ 42, and the LDH release results indicate that cellular toxicity occurs at even the lowest A $\beta$ 42 level used (1  $\mu$ M, Fig. 3.5). The FL-APP bands on the Western blot suggest that APP maturation is affected at the lower A $\beta$ 42 concentrations, and that FL-APP production is significantly reduced at higher levels of A $\beta$ 42. The effects at the higher levels of A $\beta$ 42 (~ 5 – 15  $\mu$ M) are most likely due to cytotoxicity (**Fig. 3.7**), as LDH levels were 4 - 5 fold above control (untreated) levels at these A $\beta$ 42 concentrations. The levels of CD147 did not show any significant change till higher concentrations were utilised, at which point the increase in CD147 protein levels was highly significant. Other studies have provided evidence that CD147 is a regulatory component of the  $\gamma$ -secretase complex (Zhou et al. 2005, 2007), by showing that depletion of CD147 from the  $\gamma$ -secretase complex through RNA interference in cell lines results in an increase in A $\beta$  production without affecting expression levels of the other  $\gamma$ -secretase components. However, as follow-up studies have indicated, instead of



regulating A $\beta$  production, CD147 may play a role in its degradation and clearance (Vetrivel et al., 2008b), it may be that the high A $\beta$  concentrations have induced an increase in CD147 production, in an effort to remove the A $\beta$  and reduce the oxidative stress. Nevertheless, the A $\beta$ 42 concentrations that appear to be required to induce the increase in CD147 (5-15  $\mu$ M) are not physiologically relevant, thus the increase in CD147 may be simply due to cytotoxicity. It also needs to be remembered that the CD147 neuronal protection may require the presence of cyclophilin A (CyPA) as reported by Boulous et al (2007).

The discovery that CD147 is a signalling receptor for CyPA has provided a novel function for CD147 (Yurchenko et al., 2002). Activation of the CD147 receptor by CyPA has been shown to stimulate the phosphorylation of ERK1/2, which activates the anti-apoptotic proteins Bcl-2 (Riccio et al., 1999) and Bag-1 (Perkins et al., 2003) and phosphorylation-mediated inactivation of pro-apoptotic proteins such as Bim (Biswas and Greene, 2002) and Bad (Bonni et al., 1999, Zhu et al., 2002). These downstream pro-survival signalling events may be one mechanism through which CyPA/CD147 interaction protects neurons from toxic insults. To investigate the involvement of CyPA in protection against A $\beta$ 42, a different *in vitro* assay system was devised, as discussed in the next section.

#### **7.4: Adenoviral mediated CD147 over expression protects neuronal cell against A $\beta$ 42 induced oxidative stress only in the presence of CyPA *in vitro***

Researchers have studied the effect of reducing CD147 levels – for example the RNAi *in vitro* studies mentioned in the previous section and *in vivo* studies which have reported neurological abnormalities such as spatial learning deficits and memory

deficits in CD147 null mice (neurological problems that also occur in mouse models of AD) (Naruhashi et al., 1997, Higgins and Jacobsen, 2003, Richardson et al., 2003). Other *in vitro* studies have shown that CD147 is a component of the  $\gamma$ -secretase complex and that depletion of CD147 results in elevated A $\beta$  levels (Zhou et al., 2005, 2007), possibly due to effects on the  $\gamma$ -secretase complex. However other studies which have also shown that depletion of CD147 increases extracellular A $\beta$  levels, found that the levels and localisation of CD147 in fibroblasts, as well as the postnatal expression and distribution of CD147 in the brain, are distinct from those of integral  $\gamma$ -secretase subunits (Vetrivel et al., 2008b).

In other experiments, CyPA-CD147 protein interaction has been reported to protect neurons *in vitro* from oxidative stress (induced by cumene hydroperoxide) and ischemia (induced by oxygen glucose deprivation) through the ERK1/2 pathways (Boulos et al., 2007). Oxidative stress can be induced by elevated A $\beta$  levels and is thought to play a role in AD pathogenesis. It may be that CyPA-CD147 protein interaction may reduce A $\beta$ -induced oxidative stress, thus protecting cells. This provides another reason for low levels of CD147 being detrimental to neuronal health, and suggests that inducing higher levels of CD147 may protect against AD-related neuropathology. Other studies which suggest higher levels of CD147 may be advantageous are those which have shown that CD147 is capable of inducing matrix metalloproteases (MMPs), enzymes capable of degrading A $\beta$  peptides.

In order to characterise further the possible protective effect of CD147 against oxidative stress, CD147 protein was over-expressed using recombinant adenoviruses *in vitro*. Rat primary neuronal cultures and SH-SY5Y human neuroblastoma cultures were transduced with recombinant adenoviruses (AdRSV-Empty as a control and AdRSV-

CD147) to over-express CD147 protein. Cells were exposed to A $\beta$ 42, with or without prior exposure to CyPA. The purpose of these studies was to examine the effect of increased levels of CD147, as well as the possible involvement of CyPA, on neuronal protection against A $\beta$ 42-induced oxidative stress.

In the first stage of this work, it was shown that CD147 protein was successfully over-expressed in rat primary (**Fig.3.9**) and SH-SY5Y neuronal (**Fig.3.12**) cultures. The results of the next stage of the experiments suggest that neuronal cultures exposed to CyPA prior to A $\beta$ 42 exposure are protected from A $\beta$ 42-induced oxidative stress (**Fig.3.10** and **Fig.3.11**). The results also show that adenoviral mediated CD147 over-expression alone does not achieve the protective effect seen when the protein is used in combination with CypA (**Fig.3.11** and **Fig.3.13**). These results are consistent with those reported by Boulos et al. (Boulos et al., 2007) where it was shown that the CyPA/CD147 combination can protect neurons against oxidative stress and ischemia. Our results are also consistent with the notion that CD147 protein requires interaction with other proteins to achieve its cellular role. This is supported by a study which has reported that the functional effect of CD147 at the cellular level is integrin-dependent and requires the physical association of integrins with CD147 (Berdichevski et al., 1997). It is interesting to note that CD147- associated  $\alpha$ 6 $\beta$ 1 integrins bind A $\beta$  peptides and initiate a signal transduction cascade in microglial cells (Bamberger et al., 2003). This is yet another association that may explain how CD147 protein may be involved in A $\beta$  metabolism (Vetrivel et al., 2008b).

In summary, the results presented in chapter 3 show that exposure to high cholesterol or high A $\beta$ 42 loading may induce CD147 protein expression and support the theory that these agents cause oxidative stress and can be neurotoxic, as evidenced by elevated

LDH release. The studies also support the hypothesis that the CD147/CyPA combination may be of major significance in the protection against oxidative stress. CD147 protein is quite abundant in regions of the brain affected early in AD, such as the CA1 region of the hippocampus. It could therefore be argued that CD147 is well-placed to play a role in reducing AD pathology indirectly by reducing oxidative stress when in combination with CyPA protein.

In order to characterise further the influence of cholesterol on CD147 protein expression reported above, the current study also investigated its levels in the AD model APP<sup>swe</sup> transgenic mice fed on either a normal chow or a high fat/ high cholesterol diet. Results from these *in vivo* experiments are discussed below.

#### **7.5: CD147 levels are not altered by high fat/high cholesterol diet *in vivo***

Transgenic and non-transgenic animal models of AD fed high fat/ high cholesterol diets exhibit increased AD pathology – in particular increased A $\beta$  deposition (Sparks et al., 1994b, Refolo et al., 2000b, Shie et al., 2002). A comparatively longer duration on a high cholesterol diet leads to more severe accumulation of A $\beta$  in rabbit brains (Sparks et al., 1994a). Furthermore, TgAPP<sup>swe</sup> mice fed a high fat/high cholesterol diet for 10 months have increased A $\beta$  deposition compared to standard chow-fed control mice, and the A $\beta$  deposition levels correlate inversely with HDL levels (Shie et al., 2002). A $\beta$ <sub>40</sub> and A $\beta$ <sub>42</sub> appear to accumulate initially in the lipid rafts of aging AD model Tg2576 mice brains (Kawarabayashi et al., 2004). Interestingly, after dimeric A $\beta$  accumulates in the lipid rafts of the Tg2576 brain, apolipoprotein E (ApoE) and then phosphorylated tau accumulate, suggesting A $\beta$  aggregation and accumulation is the initial pathology to

develop, and emphasizing the importance of trying to prevent A $\beta$  accumulation (Kawarabayashi et al., 2004).

In chapter 4, studies were carried out to assess the impact of a high cholesterol/high fat diet on CD147 expression in AD-model transgenic mice. Results presented in this chapter have first confirmed that a high fat/high cholesterol diet affects body weight. All experimental mice gained weight by the end of the study; however this was more evident in the APP<sup>swe</sup> mice fed a high fat/high cholesterol diet (**Fig.4.2**, chapter 4). It was also noted that males gained more body weight than females suggesting that the males were eating more than the females. Secondly, compared to controls, results also confirmed that a high cholesterol diet affects circulating plasma cholesterol *in vivo* as evidenced by a significant increase in circulating cholesterol levels in the mice fed the high cholesterol diet (**Fig.4.3**, chapter 4). Interestingly, female mice exhibited a 2-fold cholesterol increase compared to the males indicating a gender-based difference in cholesterol metabolism. These results are consistent with the findings from previous studies that have also reported sex differences in cholesterol metabolism and homeostasis, where female mice have tended to show higher cholesterol levels and to deposit fat earlier than male mice (Costet et al., 1998). Other studies have reported that, following high cholesterol diets, male mice show reduced serum but increased hepatic cholesterol and that these changes are associated with changes in expression of cholesterol transporters (Hewitt et al., 2004). Similarly, sex based differences have also been reported in the severity of AD pathology in male and female AD transgenic mice models (Barrier et al., 2010, Carroll et al., 2010, Oikawa et al., 2010, Rosario et al., 2010).

Lastly the results from this chapter have shown that mice fed on high fat/high cholesterol diet showed an increasing trend in brain CD147 protein levels in males with females expressing the reduced levels (**Fig. 4.5**, chapter 4) and that CD147 correlates with plasma cholesterol. Furthermore, although not significant, A $\beta$ 42/40 ratios showed increasing trends in mice on a high fat/high cholesterol diet. These findings are also consistent with other studies that have reported increased A $\beta$  levels in conditions of high cholesterol (Sparks et al., 1994b, Refolo et al., 2000b, Shie et al., 2002) and depleted CD147 protein (Zhou et al., 2007) levels. Taken together these findings suggest that the increasing trend of CD147 in males may be due to higher intake of the diet as they also showed a higher weight gain. The females may have shown reduced levels due to not eating the diet more as evidenced by their body weight as compared to males on the same diet. It can therefore be concluded that high cholesterol diet has some influence on CD147 expression *in vivo*. To further understand the mechanism through which CD147 may be influenced by a high cholesterol diet, the current study also investigated the influence of this diet on SCP, a protein which stimulates CD147 transcription. The outcomes of these *in vivo* experiments are discussed below.

#### **7.6: High fat/high cholesterol diet did not affect SCP-2 levels *in vivo***

The importance of cholesterol homeostasis in brain function and its devastating effects when its metabolism and circulating levels are altered have been reported before, as discussed earlier in this thesis (Tint et al., 1994, Jarvik et al., 1995, Igbavboa et al., 1996, Notkola et al., 1998). Most studies have investigated the association between a high fat/high cholesterol diet and AD in relation to A $\beta$  generation and cognitive function. However there has been very little research done on the influence of diet on SCP-2 protein expression levels. Recently a study by Ko and Puglielli reported that

SCP-2 influences CD147 transcription (Ko and Puglielli, 2007). Since SCP-2 regulates cholesterol transport to the cell membrane and that increased cholesterol loading results in increased CD147 protein levels *in vitro*, the current study investigated the effects of a high fat/high cholesterol diet on SCP-2 protein levels in APP<sup>swe</sup> transgenic mice.

SCP-2 levels were measured in APP<sup>swe</sup> mice fed a normal chow and a high fat/high cholesterol diet by RT-PCR. Results are presented in chapter 4 of this thesis (**Fig. 4.8**, chapter 4) and show that SCP-2 was successfully amplified and that a high fat/high cholesterol diet did not alter SCP-2 mRNA levels (**Fig. 4.9**, chapter 4). These results are different from those reported by Kraemer et al., who showed that expression of SCP-2, but not SCP-x, was increased in conditions of increased cholesterol loading in muscle cells (Kraemer et al., 1995). The difference may be attributed to the type of cholesterol used, the tissue in which SCP-2 was measured and the type of experiment under which SCP-2 protein was determined. In the next stage of these studies, the effect of a high cholesterol/high fat on SCP-2 mRNA levels in the brain were examined *in vivo*, using the AD model APP<sup>swe</sup> mice. Our results showed that a high cholesterol/high fat diet did not alter SCP-2 levels. In the *in vitro* studies by Kraemer et al., (1995) cationized cholesterol was used. This could not be used *in vivo* as it influences cholesterol efflux from muscle tissues. These differences in the experimental design and methodology may explain the differences between the SCP-2 levels reported here and those reported by Kraemer et al. In addition, it is likely that SCP-2 mRNA/protein levels in different tissues are not the same, and due to the systemic changes to lipid metabolism that a high cholesterol diet is likely to bring about, a more comprehensive study of SCP-2 levels in several tissues including the brain will be needed to determine whether such differences exist. There is therefore a need for further study to establish conclusively whether

CD147 expression alters in muscle, brain, liver, or any other tissue in the presence of increasing cholesterol levels in the diet.

In the next stage of this thesis, CD147 levels in the hippocampus and frontal cortex of health controls, Lewy Body dementia (LB), fronto-temporal dementia (FTD) and AD were investigated. In addition, possible associations of single nucleotide polymorphisms (SNPs) within the CD147 promoter region (where SCP-2 binds to initiate CD147 transcription) and AD pathology were also investigated. Results from these experiments are discussed below.

#### **7.7: CD147 protein levels are not altered in Alzheimer's disease (AD)**

Some evidence has been reported to indicate a role for CD147 in the pathogenesis of AD and that CD147 may have neuroprotective actions (Boulos et al., 2007). CD147 protein has been detected in the hippocampus, especially in the CA1 region, a brain region that plays a key role in memory and learning and that is most vulnerable in AD (Hrabovszky et al., 2000, Rao, 2001). Recently, elevated CD147 levels have been reported in AD/dementia (Nahalkova et al., 2009, 2010). This is in addition to its possible influence on A $\beta$  production via the  $\gamma$ -secretase enzyme (Zhou et al., 2005, 2006, 2007) and the potential influence on extracellular A $\beta$  degradation through MMP induction (Vetrivel et al., 2008b). Taken together these reports indicate that CD147 may play an important role in APP processing and/or A $\beta$  clearance. However there is little information concerning CD147 distribution in the various cells of the brain, thus the current study measured CD147 expression levels in hippocampal and frontal cortex tissue from lewy body disease, frontal temporal dementia and Alzheimer's disease cases and compared to age-matched control brain tissue.



The immunohistochemistry and Western blot analysis results presented in chapter 5 of this thesis show that CD147 protein is not elevated in AD (**Fig.5.2 and 5.7**). However, although not significant, there were trends towards higher CD147 levels observed in the hippocampus and frontal cortex of AD, FTD and LBD brains (**Fig.5.2, 5.5.4 and 5.7**). Increased A $\beta$  peptide accumulation that leads to senile plaque deposition in Lewy body disease pathology and dementia (Gomperts et al., 2008, Armstrong and Cairns, 2009, Foster et al., 2010) has been reported before. The current study has also shown significant A $\beta$  levels in AD and LBD which is consistent with findings from the previous studies mentioned above. The observed positive correlation between CD147 and NCT and PS1 levels in hippocampus from AD brains and PS1 from LBD (**Table 5.1**) is suggestive that CD147 interacts with the  $\gamma$ -secretase complex components. Although not significant, the trend towards higher levels of CD147, nicastrin and PS1 levels and the significant increase of PEN2 levels observed in hippocampus from AD cases, with a trend towards an increase in CD147 levels in the frontal cortex of AD cases, is an indication of increased  $\gamma$ -secretase activity in dementia that is likely to lead to increased A $\beta$  production and accumulation and provides further evidence that CD147 is involved to some extent in AD pathogenesis.

As discussed in chapter 5, findings of the current study agree with Nahalkova and colleagues who reported elevated CD147 levels in AD patients (Nahalkova et al., 2009, 2010). However Nahalkova reported increased CD147 levels in the cortex while our findings have shown only trends towards an increase in CD147 levels in the hippocampus and frontal cortex. These differences may be due to the different sample sizes used. Nahalkova's findings may have been compromised due to a small sample size ( $n=3$ ) which did not give his study a required statistical power. The current findings

of CD147 expression in the AD are possibly more reliable due to the bigger sample size (AD,  $n=14$ ) for Western blot and ( $n=17$ ) for immunohistochemistry. For statistical analysis to be applied, this was a big enough sample size to give the study the required power. As a recent study has provided evidence that CD147 may not influence A $\beta$  production by being an integral part of the  $\gamma$ -secretase complex (Vetrivel et al., 2008b), an increase in expression of CD147 in the hippocampus and frontal cortex in AD may be more the result of increased A $\beta$  accumulation which initiates oxidative stress. Thus higher levels of CD147 may be a reaction to this oxidative stress, either in an attempt to reduce stress by inducing production of degradative enzymes (MMPs), or possibly as a result of cellular toxicity and death (apoptosis). Members of the monocarboxylate transporter (MCT) family of proteins, MCT1 and MCT4, require CD147 as a chaperone for their expression at the plasma membrane, CD147 has also been associated with integrin,  $\gamma$ -secretase, caveolin-1, and cyclophilins, as mentioned earlier in this thesis (Iacono et al., 2007). This variety of potential functional roles for CD147 makes it very difficult to come to simple conclusions concerning its likely role in AD. Many more studies will be required to understand the functions of CD147, the roles this protein has in lipid and cholesterol metabolism, and the involvement of any of these roles in AD.

### **7.8: Incidence of known CD147 SNPs and discovery of 2 novel CD147 SNPs**

In order to examine other potential aspects of CD147 involvement in AD pathology, the current study also investigated the incidence of known SNPs and the possibility of novel SNPs in the promoter region of CD147. This was carried out on human genomic DNA samples obtained from both control and AD-affected cases. Results presented in chapter 6 of this thesis have shown no association between SNPs in the sequenced region and AD. This further supports the notion that CD147 is not directly associated with AD

pathology but rather interacts with several proteins whose outcomes may be linked to factors associated to AD development and pathology. There does appear to be some association between possession of the rs11551906 minor allele with elevated cerebral amyloid burden, warranting further investigation in future studies. Interestingly though was the discovery of the 2 novel SNPs within the promoter region, outside the region where SCP-2 binds. These were an A to G transition located 61 base pairs upstream (-61A>G) of the transcription initiation site and a C to G transversion located 37 base pairs downstream (37C>G) of the transcription initiation site. These novel genetic variations were identified in a single heterozygous healthy control individual and a single heterozygous AD individual, respectively. It is not known if -61A>G SNP may provide some protection whereas 37C>G SNP may be a risk factor for AD. However, a comprehensive study using a larger and well characterized sample cohort has to be undertaken to investigate this hypothesis.

## **7.9: Future directions**

The work presented in this thesis has provided further evidence that CD147 is a multifunctional protein whose roles and expression may be influenced by other factors including cholesterol, oxidative stress and SCP-2. The relationships between CD147 and these factors, as well as others such as MMPs,  $\gamma$ -secretase and MCT proteins, all require further investigation. As many of the proposed functions of this protein have been linked to AD pathogenesis, further research into this protein may yield important information concerning the development and potential prevention of AD pathology. Some of the proposed future studies include, but are not limited to the following:

- A larger sample size of AD cases with similar disease severity as classified by the Braack Staging method, together with age-matched control cases, should be

assembled in order to compare more effectively CD147 expression levels in AD and age-matched control brains.

- It may be beneficial to sequence a larger portion of CD147 promoter region in a well characterized cohort in order to identify other possible CD147 promoter-related SNPs that may be associated with AD pathology.
- The effects of the newly discovered -61A>G and 37C>G CD147 SNPs on AD pathology and on the transcription/translation of CD147 protein should be investigated, to help characterise further the role(s) of CD147.

## **7.10: Conclusions**

This study has reported that **(a)** increasing cholesterol and A $\beta$ 42 loading affect cell viability, induce CD147 expression and that adenoviral mediated CD147 expression protects neuronal cultures against A $\beta$ 42 induced oxidative stress and injury only in the presence of CyPA. **(b)** that there is an association between high fat / high cholesterol diet and plasma cholesterol with a trend towards increasing cerebral CD147 levels and a positive correlation between CD147 and plasma cholesterol levels. **(c)** that CD147 protein levels are not significantly elevated in AD. In addition, we report that **(d)** SNPs within the CD147 promoter region are not associated with AD and finally **(e)** that two novel SNPs (-61A>G and 37C>G) within the CD147 promoter region (not listed in the NCBI) have been identified.

## Chapter 8

### References

- Abdi A, Sadraie H, Dargahi L, Khalaj L, Ahmadiani A (2011) Apoptosis inhibition can be threatening in Abeta-induced neuroinflammation, through promoting cell proliferation. *Neurochem Res* 36:39-48.
- Agrawal SM, Yong VW (2011) The many faces of EMMPRIN - roles in neuroinflammation. *Biochim Biophys Acta* 1812:213-219.
- Alfano M, Poli G (2005) Role of cytokines and chemokines in the regulation of innate immunity and HIV infection. *Mol Immunol* 42:161-182.
- Allain F, Vanpouille C, Carpentier M, Slomianny MC, Durieux S, Spik G (2002) Interaction with glycosaminoglycans is required for cyclophilin B to trigger integrin-mediated adhesion of peripheral blood T lymphocytes to extracellular matrix. *Proc Natl Acad Sci U S A* 99:2714-2719.
- Altruda F, Cervella P, Gaeta ML, Daniele A, Giancotti F, Tarone G, Stefanuto G, Silengo L (1989) Cloning of cDNA for a novel mouse membrane glycoprotein (gp42): shared identity to histocompatibility antigens, immunoglobulins and neural-cell adhesion molecules. *Gene* 85:445-451.
- Ames A (2000) CNS energy metabolism as related to function. *Brain Res Brain Res Rev* 34:42-68.
- Anandatheerthavarada HK, Biswas G, Robin MA, Avadhani NG (2003) Mitochondrial targeting and a novel transmembrane arrest of Alzheimer's amyloid precursor protein impairs mitochondrial function in neuronal cells. *J Cell Biol* 161:41-54.
- Anderton BH (2002) Ageing of the brain. *Mech Ageing Dev* 123:811-817.
- Ansari H, Greco G, Luban J (2002) Cyclophilin A peptidyl-prolyl isomerase activity promotes ZPR1 nuclear export. *Mol Cell Biol* 22:6993-7003.
- Aras MA, Hartnett KA, Aizenman E (2008) Assessment of cell viability in primary neuronal cultures. *Curr Protoc Neurosci Chapter 7:Unit 7* 18.
- Arckens L, Van der Gucht E, Van den Bergh G, Massie A, Leysen I, Vandenbussche E, Eysel UT, Huybrechts R, Vandesande F (2003) Differential display implicates cyclophilin A in adult cortical plasticity. *Eur J Neurosci* 18:61-75.
- Area-Gomez E, de Groof AJ, Boldogh I, Bird TD, Gibson GE, Koehler CM, Yu WH, Duff KE, Yaffe MP, Pon LA, Schon EA (2009) Presenilins are enriched in endoplasmic reticulum membranes associated with mitochondria. *Am J Pathol* 175:1810-1816.
- Armstrong RA, Cairns NJ (2009) Size frequency distribution of the beta-amyloid (abeta) deposits in dementia with Lewy bodies with associated Alzheimer's disease pathology. *Neurol Sci* 30:471-477.
- Atshaves BP, McIntosh AL, Martin GG, Landrock D, Payne HR, Bhuvanendran S, Landrock KK, Lyuksyutova OI, Johnson JD, Macfarlane RD, Kier AB, Schroeder F (2009) Overexpression of sterol carrier protein-2 differentially alters hepatic cholesterol accumulation in cholesterol-fed mice. *J Lipid Res* 50:1429-1447.
- Atshaves BP, Petrescu AD, Starodub O, Roths JB, Kier AB, Schroeder F (1999) Expression and intracellular processing of the 58 kDa sterol carrier protein-2/3-

- oxoacyl-CoA thiolase in transfected mouse L-cell fibroblasts. *J Lipid Res* 40:610-622.
- Avila G, Sandoval A, Felix R (2004) Intramembrane charge movement associated with endogenous K<sup>+</sup> channel activity in HEK-293 cells. *Cell Mol Neurobiol* 24:317-330.
- Backstrom JR, Lim GP, Cullen MJ, Tokes ZA (1996) Matrix metalloproteinase-9 (MMP-9) is synthesized in neurons of the human hippocampus and is capable of degrading the amyloid-beta peptide (1-40). *J Neurosci* 16:7910-7919.
- Bales KR, Dodart JC, DeMattos RB, Holtzman DM, Paul SM (2002) Apolipoprotein E, amyloid, and Alzheimer disease. *Mol Interv* 2:363-375, 339.
- Bamberger ME, Harris ME, McDonald DR, Husemann J, Landreth GE (2003) A cell surface receptor complex for fibrillar beta-amyloid mediates microglial activation. *J Neurosci* 23:2665-2674.
- Barrett JC, Fry B, Maller J, Daly MJ (2005) Haploview: analysis and visualization of LD and haplotype maps. *Bioinformatics* 21:263-265.
- Barrier L, Ingrand S, Fauconneau B, Page G (2010) Gender-dependent accumulation of ceramides in the cerebral cortex of the APP(SL)/PS1Ki mouse model of Alzheimer's disease. *Neurobiol Aging* 31:1843-1853.
- Barron AM, Verdile G, Martins RN (2006) The role of gonadotropins in Alzheimer's disease: potential neurodegenerative mechanisms. *Endocrine* 29:257-269.
- Baum CL, Reschly EJ, Gayen AK, Groh ME, Schadick K (1997) Sterol carrier protein-2 overexpression enhances sterol cycling and inhibits cholesterol ester synthesis and high density lipoprotein cholesterol secretion. *J Biol Chem* 272:6490-6498.
- Baum L, Seger R, Woodgett JR, Kawabata S, Maruyama K, Koyama M, Silver J, Saitoh T (1995) Overexpressed tau protein in cultured cells is phosphorylated without formation of PHF: implication of phosphoprotein phosphatase involvement. *Brain Res Mol Brain Res* 34:1-17.
- Baun MM (1993) "Closed-system, in-line endotracheal suctioning". *Crit Care Nurse* 13:16-17; author reply 17-18.
- Bayer TA, Wirths O, Majtenyi K, Hartmann T, Multhaup G, Beyreuther K, Czech C (2001) Key factors in Alzheimer's disease: beta-amyloid precursor protein processing, metabolism and intraneuronal transport. *Brain Pathol* 11:1-11.
- Behr D, Elle C, Underwood J, Davis JB, Ward R, Karran E, Masters CL, Beyreuther K, Multhaup G (1999) Proteolytic fragments of Alzheimer's disease-associated presenilin 1 are present in synaptic organelles and growth cone membranes of rat brain. *J Neurochem* 72:1564-1573.
- Behl C, Davis JB, Lesley R, Schubert D (1994) Hydrogen peroxide mediates amyloid beta protein toxicity. *Cell* 77:817-827.
- Beisiegel U, Weber W, Ihrke G, Herz J, Stanley KK (1989) The LDL-receptor-related protein, LRP, is an apolipoprotein E-binding protein. *Nature* 341:162-164.
- Belton RJ, Jr., Chen L, Mesquita FS, Nowak RA (2008) Basigin-2 is a cell surface receptor for soluble basigin ligand. *J Biol Chem* 283:17805-17814.
- Bentahir M, Nyabi O, Verhamme J, Tolia A, Horre K, Wiltfang J, Esselmann H, De Strooper B (2006) Presenilin clinical mutations can affect gamma-secretase activity by different mechanisms. *J Neurochem* 96:732-742.
- Berditchevski F, Tolia KF, Wong K, Carpenter CL, Hemler ME (1997) A novel link between integrins, transmembrane-4 superfamily proteins (CD63 and CD81), and phosphatidylinositol 4-kinase. *J Biol Chem* 272:2595-2598.
- Bertram L, McQueen MB, Mullin K, Blacker D, Tanzi RE (2007) Systematic meta-analyses of Alzheimer disease genetic association studies: the AlzGene database. *Nat Genet* 39:17-23.

- Bhaskar K, Miller M, Chludzinski A, Herrup K, Zagorski M, Lamb BT (2009) The PI3K-Akt-mTOR pathway regulates Abeta oligomer induced neuronal cell cycle events. *Mol Neurodegener* 4:14.
- Bigi R, Cortigiani L, Desideri A (2003) Exercise electrocardiography after acute coronary syndromes: still the first testing modality? *Clin Cardiol* 26:390-395.
- Billich A, Winkler G, Aschauer H, Rot A, Peichl P (1997) Presence of cyclophilin A in synovial fluids of patients with rheumatoid arthritis. *J Exp Med* 185:975-980.
- Bissette G, Smith WH, Dole KC, Crain B, Ghanbari H, Miller B, Nemeroff CB (1991) Alterations in Alzheimer's disease-associated protein in Alzheimer's disease frontal and temporal cortex. *Arch Gen Psychiatry* 48:1009-1012.
- Biswas C (1982) Tumor cell stimulation of collagenase production by fibroblasts. *Biochem Biophys Res Commun* 109:1026-1034.
- Biswas C (1984) Collagenase stimulation in cocultures of human fibroblasts and human tumor cells. *Cancer Lett* 24:201-207.
- Biswas J, Shanmugam MP, Gopal L (1995) Malignant melanoma of the choroid in association with oculodermal melanocytosis: a case report. *Indian J Ophthalmol* 43:140-141.
- Biswas R, Vonderhaar BK (1987) Role of serum in the prolactin responsiveness of MCF-7 human breast cancer cells in long-term tissue culture. *Cancer Res* 47:3509-3514.
- Biswas SC, Greene LA (2002) Nerve growth factor (NGF) down-regulates the Bcl-2 homology 3 (BH3) domain-only protein Bim and suppresses its proapoptotic activity by phosphorylation. *J Biol Chem* 277:49511-49516.
- Black RA, Rauch CT, Kozlosky CJ, Peschon JJ, Slack JL, Wolfson MF, Castner BJ, Stocking KL, Reddy P, Srinivasan S, Nelson N, Boiani N, Schooley KA, Gerhart M, Davis R, Fitzner JN, Johnson RS, Paxton RJ, March CJ, Cerretti DP (1997) A metalloproteinase disintegrin that releases tumour-necrosis factor- $\alpha$  from cells. *Nature* 385:729-733.
- Bonni A, Brunet A, West AE, Datta SR, Takasu MA, Greenberg ME (1999) Cell survival promoted by the Ras-MAPK signaling pathway by transcription-dependent and -independent mechanisms. *Science* 286:1358-1362.
- Borchelt DR, Thinakaran G, Eckman CB, Lee MK, Davenport F, Ratovitsky T, Prada CM, Kim G, Seekins S, Yager D, Slunt HH, Wang R, Seeger M, Levey AI, Gandy SE, Copeland NG, Jenkins NA, Price DL, Younkin SG, Sisodia SS (1996) Familial Alzheimer's disease-linked presenilin 1 variants elevate Abeta1-42/1-40 ratio in vitro and in vivo. *Neuron* 17:1005-1013.
- Borroni B, Volpi R, Martini G, Del Bono R, Archetti S, Colciaghi F, Akkawi NM, Di Luca M, Romanelli G, Caimi L, Padovani A (2002) Peripheral blood abnormalities in Alzheimer disease: evidence for early endothelial dysfunction. *Alzheimer Dis Assoc Disord* 16:150-155.
- Boulos S, Meloni BP, Arthur PG, Bojarski C, Knuckey NW (2006) Assessment of CMV, RSV and SYN1 promoters and the woodchuck post-transcriptional regulatory element in adenovirus vectors for transgene expression in cortical neuronal cultures. *Brain Res* 1102:27-38.
- Boulos S, Meloni BP, Arthur PG, Majda B, Bojarski C, Knuckey NW (2007) Evidence that intracellular cyclophilin A and cyclophilin A/CD147 receptor-mediated ERK1/2 signalling can protect neurons against in vitro oxidative and ischemic injury. *Neurobiol Dis* 25:54-64.
- Bowen RL, Isley JP, Atkinson RL (2000) An association of elevated serum gonadotropin concentrations and Alzheimer disease? *J Neuroendocrinol* 12:351-354.

- Boyle PA, Buchman AS, Wilson RS, Kelly JF, Bennett DA (2010) The APOE epsilon4 allele is associated with incident mild cognitive impairment among community-dwelling older persons. *Neuroepidemiology* 34:43-49.
- Braak H, Braak E (1997) Staging of Alzheimer-related cortical destruction. *Int Psychogeriatr* 9 Suppl 1:257-261; discussion 269-272.
- Breitner JC, Jarvik GP, Plassman BL, Saunders AM, Welsh KA (1998) Risk of Alzheimer disease with the epsilon4 allele for apolipoprotein E in a population-based study of men aged 62-73 years. *Alzheimer Dis Assoc Disord* 12:40-44.
- Brown CR, Cui DY, Hung GG, Chiang HL (2001) Cyclophilin A mediates Vid22p function in the import of fructose-1,6-bisphosphatase into Vid vesicles. *J Biol Chem* 276:48017-48026.
- Brown MS, Goldstein JL (1997) The SREBP pathway: regulation of cholesterol metabolism by proteolysis of a membrane-bound transcription factor. *Cell* 89:331-340.
- Bruno MA, Mufson EJ, Wu J, Cuello AC (2009) Increased matrix metalloproteinase 9 activity in mild cognitive impairment. *J Neuropathol Exp Neurol* 68:1309-1318.
- Bu G (2009) Apolipoprotein E and its receptors in Alzheimer's disease: pathways, pathogenesis and therapy. *Nat Rev Neurosci* 10:333-344.
- Butterfield DA (2002) Amyloid beta-peptide (1-42)-induced oxidative stress and neurotoxicity: implications for neurodegeneration in Alzheimer's disease brain. A review. *Free Radic Res* 36:1307-1313.
- Butterfield DA, Castegna A, Lauderback CM, Drake J (2002) Evidence that amyloid beta-peptide-induced lipid peroxidation and its sequelae in Alzheimer's disease brain contribute to neuronal death. *Neurobiol Aging* 23:655-664.
- Butterfield DA, Drake J, Pocernich C, Castegna A (2001) Evidence of oxidative damage in Alzheimer's disease brain: central role for amyloid  $\beta$ -peptide. *Trends in Molecular Medicine* 7:548-554.
- Buxbaum JD, Koo EH, Greengard P (1993) Protein phosphorylation inhibits production of Alzheimer amyloid beta/A4 peptide. *Proc Natl Acad Sci U S A* 90:9195-9198.
- Cahill L, McGaugh JL (1998) Mechanisms of emotional arousal and lasting declarative memory. *Trends Neurosci* 21:294-299.
- Carney JM, Smith CD, Carney AM, Butterfield DA (1994) Aging- and oxygen-induced modifications in brain biochemistry and behavior. *Ann N Y Acad Sci* 738:44-53.
- Carroll JC, Rosario ER, Kreimer S, Villamagna A, Gentzschein E, Stanczyk FZ, Pike CJ (2010) Sex differences in beta-amyloid accumulation in 3xTg-AD mice: role of neonatal sex steroid hormone exposure. *Brain Res* 1366:233-245.
- Caselli RJ, Dueck AC, Osborne D, Sabbagh MN, Connor DJ, Ahern GL, Baxter LC, Rapcsak SZ, Shi J, Woodruff BK, Locke DE, Snyder CH, Alexander GE, Rademakers R, Reiman EM (2009) Longitudinal modeling of age-related memory decline and the APOE epsilon4 effect. *N Engl J Med* 361:255-263.
- Caserta MT, Caccioppo D, Lapin GD, Ragin A, Groothuis DR (1998) Blood-brain barrier integrity in Alzheimer's disease patients and elderly control subjects. *J Neuropsychiatry Clin Neurosci* 10:78-84.
- Casley CS, Canevari L, Land JM, Clark JB, Sharpe MA (2002) Beta-amyloid inhibits integrated mitochondrial respiration and key enzyme activities. *J Neurochem* 80:91-100.
- Caspersen C, Wang N, Yao J, Sosunov A, Chen X, Lustbader JW, Xu HW, Stern D, McKhann G, Yan SD (2005) Mitochondrial A $\beta$ : a potential focal point for neuronal metabolic dysfunction in Alzheimer's disease. *FASEB J* 19:2040-2041.



- Cervantes S, Gonzalez-Duarte R, Marfany G (2001) Homodimerization of presenilin N-terminal fragments is affected by mutations linked to Alzheimer's disease. *FEBS Lett* 505:81-86.
- Chan AC, Chow CK, Chiu D (1999) Interaction of antioxidants and their implication in genetic anemia. *Proc Soc Exp Biol Med* 222:274-282.
- Chanderbhan RF, Kharroubi AT, Noland BJ, Scallen TJ, Vahouny GV (1986) Sterol carrier protein2: further evidence for its role in adrenal steroidogenesis. *Endocr Res* 12:351-370.
- Chapman PF, Falinska AM, Knevetz SG, Ramsay MF (2001) Genes, models and Alzheimer's disease. *Trends Genet* 17:254-261.
- Chen J, Crabbe A, Van Duppen V, Vankelecom H (2006) The notch signaling system is present in the postnatal pituitary: marked expression and regulatory activity in the newly discovered side population. *Mol Endocrinol* 20:3293-3307.
- Chen L, Nakai M, Belton RJ, Jr., Nowak RA (2007) Expression of extracellular matrix metalloproteinase inducer and matrix metalloproteinases during mouse embryonic development. *Reproduction* 133:405-414.
- Cheng H, Vetrivel KS, Gong P, Meckler X, Parent A, Thinakaran G (2007) Mechanisms of disease: new therapeutic strategies for Alzheimer's disease--targeting APP processing in lipid rafts. *Nat Clin Pract Neurol* 3:374-382.
- Chiu R, Rey O, Zheng JQ, Twiss JL, Song J, Pang S, Yokoyama KK (2003) Effects of altered expression and localization of cyclophilin A on differentiation of p19 embryonic carcinoma cells. *Cell Mol Neurobiol* 23:929-943.
- Chklovskaya E, Nissen C, Landmann L, Rahner C, Pfister O, Wodnar-Filipowicz A (2001) Cell-surface trafficking and release of flt3 ligand from T lymphocytes is induced by common cytokine receptor gamma-chain signaling and inhibited by cyclosporin A. *Blood* 97:1027-1034.
- Choi EY, Kim D, Hong BK, Kwon HM, Song YG, Byun KH, Park HY, Whang KC, Kim HS (2002) Upregulation of extracellular matrix metalloproteinase inducer (EMMPRIN) and gelatinases in human atherosclerosis infected with *Chlamydia pneumoniae*: the potential role of *Chlamydia pneumoniae* infection in the progression of atherosclerosis. *Exp Mol Med* 34:391-400.
- Chu J, Giannopoulos PF, Ceballos-Diaz C, Golde TE, Pratico D (2012) Adeno-associated virus-mediated brain delivery of 5-lipoxygenase modulates the AD-like phenotype of APP mice. *Mol Neurodegener* 7:1.
- Citron M, Diehl TS, Capell A, Haass C, Teplow DB, Selkoe DJ (1996) Inhibition of amyloid beta-protein production in neural cells by the serine protease inhibitor AEBSF. *Neuron* 17:171-179.
- Clifford PM, Zarrabi S, Siu G, Kinsler KJ, Kosciuk MC, Venkataraman V, D'Andrea MR, Dinsmore S, Nagele RG (2007) Abeta peptides can enter the brain through a defective blood-brain barrier and bind selectively to neurons. *Brain Res* 1142:223-236.
- Colciaghi F, Borroni B, Pastorino L, Marcello E, Zimmermann M, Cattabeni F, Padovani A, Di Luca M (2002) [alpha]-Secretase ADAM10 as well as [alpha]APPs is reduced in platelets and CSF of Alzheimer disease patients. *Mol Med* 8:67-74.
- Cole GM, Beech W, Frautschy SA, Sigel J, Glasgow C, Ard MD (1999) Lipoprotein effects on Abeta accumulation and degradation by microglia in vitro. *J Neurosci Res* 57:504-520.
- Colgan J, Asmal M, Yu B, Luban J (2005) Cyclophilin A-deficient mice are resistant to immunosuppression by cyclosporine. *J Immunol* 174:6030-6038.

- Colles SM, Woodford JK, Moncecchi D, Myers-Payne SC, McLean LR, Billheimer JT, Schroeder F (1995) Cholesterol interaction with recombinant human sterol carrier protein-2. *Lipids* 30:795-803.
- Coolen MW, van Loo KM, van Bakel NN, Ellenbroek BA, Cools AR, Martens GJ (2006) Reduced Aph-1b expression causes tissue- and substrate-specific changes in gamma-secretase activity in rats with a complex phenotype. *FASEB J* 20:175-177.
- Costet P, Legendre C, More J, Edgar A, Galtier P, Pineau T (1998) Peroxisome proliferator-activated receptor alpha-isoform deficiency leads to progressive dyslipidemia with sexually dimorphic obesity and steatosis. *J Biol Chem* 273:29577-29585.
- Crouch PJ, Blake R, Duce JA, Ciccotosto GD, Li QX, Barnham KJ, Curtain CC, Cherny RA, Cappai R, Dyrks T, Masters CL, Trounce IA (2005) Copper-dependent inhibition of human cytochrome c oxidase by a dimeric conformer of amyloid-beta1-42. *J Neurosci* 25:672-679.
- Crystal AS, Morais VA, Pierson TC, Pijak DS, Carlin D, Lee VM, Doms RW (2003) Membrane topology of gamma-secretase component PEN-2. *J Biol Chem* 278:20117-20123.
- Curtain CC, Ali F, Volitakis I, Cherny RA, Norton RS, Beyreuther K, Barrow CJ, Masters CL, Bush AI, Barnham KJ (2001) Alzheimer's disease amyloid-beta binds copper and zinc to generate an allosterically ordered membrane-penetrating structure containing superoxide dismutase-like subunits. *J Biol Chem* 276:20466-20473.
- Curtin KD, Meinertzhagen IA, Wyman RJ (2005) Basigin (EMMPRIN/CD147) interacts with integrin to affect cellular architecture. *J Cell Sci* 118:2649-2660.
- Damsker JM, Okwumabua I, Pushkarsky T, Arora K, Bukrinsky MI, Constant SL (2009) Targeting the chemotactic function of CD147 reduces collagen-induced arthritis. *Immunology* 126:55-62.
- Das HK, McPherson J, Bruns GA, Karathanasis SK, Breslow JL (1985) Isolation, characterization, and mapping to chromosome 19 of the human apolipoprotein E gene. *J Biol Chem* 260:6240-6247.
- Davidson Y, Gibbons L, Pritchard A, Hardicre J, Wren J, Tian J, Shi J, Stopford C, Julien C, Thompson J, Payton A, Thaker U, Hayes AJ, Iwatsubo T, Pickering-Brown SM, Pendleton N, Horan MA, Burns A, Purandare N, Lendon CL, Neary D, Snowden JS, Mann DM (2006) Genetic associations between cathepsin D exon 2 C-->T polymorphism and Alzheimer's disease, and pathological correlations with genotype. *J Neurol Neurosurg Psychiatry* 77:515-517.
- Davies CA, Mann DM, Sumpter PQ, Yates PO (1987 ) A quantitative morphometric analysis of the neuronal and synaptic content of the frontal and temporal cortex in patients with Alzheimer's disease. *J Neurol Sci* 78:151-164.
- De Fusco M, Marconi R, Silvestri L, Atorino L, Rampoldi L, Morgante L, Ballabio A, Aridon P, G. C (2003) Haploinsufficiency of ATP1A2 encoding the Na<sup>+</sup>/K<sup>+</sup> pump alpha2 subunit associated with familial hemiplegic migraine type 2. *Nat Genet* 33:192-196.
- de la Torre JC (2004) Alzheimer's disease is a vasocognopathy: a new term to describe its nature. *Neurol Res* 26:517-524.
- De Strooper B (2003) Aph-1, Pen-2, and Nicastrin with Presenilin generate an active gamma-Secretase complex. *Neuron* 38:9-12.
- De Strooper B (2007) Loss-of-function presenilin mutations in Alzheimer disease. Talking Point on the role of presenilin mutations in Alzheimer disease. *EMBO Rep* 8:141-146.

- De Strooper B, Annaert W, Cupers P, Saftig P, Craessaerts K, Mumm JS, Schroeter EH, Schrijvers V, Wolfe MS, Ray WJ, Goate A, Kopan R (1999) A presenilin-1-dependent gamma-secretase-like protease mediates release of Notch intracellular domain. *Nature* 398:518-522.
- Dejaegere T, Serneels L, Schafer MK, Van Biervliet J, Horre K, Depboylu C, Alvarez-Fischer D, Herreman A, Willem M, Haass C, Hoglinger GU, D'Hooge R, De Strooper B (2008) Deficiency of Aph1B/C-gamma-secretase disturbs Nrg1 cleavage and sensorimotor gating that can be reversed with antipsychotic treatment. *Proc Natl Acad Sci U S A* 105:9775-9780.
- Demuro A, Parker I, Stutzmann GE (2010) Calcium signaling and amyloid toxicity in Alzheimer disease. *J Biol Chem* 285:12463-12468.
- Deng J, Wei M, Yu B, Chen Y (2010) Efficient amplification of genes involved in microbial secondary metabolism by an improved genome walking method. *Appl Microbiol Biotechnol* 87:757-764.
- Denihan A, Wilson G, Cunningham C, Coakley D, Lawlor BA (2000) CT measurement of medial temporal lobe atrophy in Alzheimer's disease, vascular dementia, depression and paraphrenia. *Int J Geriatr Psychiatry* 15:306-312.
- Denzel A, Otto F, Girod A, Pepperkok R, Watson R, Rosewell I, Bergeron JJ, Solari RC, Owen MJ (2000) The p24 family member p23 is required for early embryonic development. *Curr Biol* 10:55-58.
- Devi L, Prabhu BM, Galati DF, Avadhani NG, Anandatheerthavarada HK (2006) Accumulation of amyloid precursor protein in the mitochondrial import channels of human Alzheimer's disease brain is associated with mitochondrial dysfunction. *J Neurosci* 26:9057-9068.
- Dickstein DL, Walsh J, Brautigam H, Stockton SD, Jr., Gandy S, Hof PR (2010) Role of vascular risk factors and vascular dysfunction in Alzheimer's disease. *Mt Sinai J Med* 77:82-102.
- Dietschy JM, Turley SD (2004) Thematic review series: brain Lipids. Cholesterol metabolism in the central nervous system during early development and in the mature animal. *J Lipid Res* 45:1375-1397.
- Dong J, Atwood CS, Anderson VE, Siedlak SL, Smith MA, Perry G, Carey PR (2003) Metal binding and oxidation of amyloid-beta within isolated senile plaque cores: Raman microscopic evidence. *Biochemistry* 42:2768-2773.
- Dyrks T, Dyrks E, Hartmann T, Masters CL, Beyreuther K (1992) Amyloidogenicity of bA4 and bA4-bearing APP fragments by metal catalysed oxidation. *J Biol Chem* 267:18210-18217.
- Edbauer D, Winkler E, Haass C, Steiner H (2002) Presenilin and nicastrin regulate each other and determine amyloid beta-peptide production via complex formation. *Proc Natl Acad Sci U S A* 99:8666-8671.
- Edbauer D, Winkler E, Regula JT, Pesold B, Steiner H, Haass C (2003) Reconstitution of gamma-secretase activity. *Nat Cell Biol* 5:486-488.
- Egensperger R, Kosel S, von Eitzen U, Graeber MB (1998) Microglial activation in Alzheimer disease: Association with APOE genotype. *Brain Pathol* 8:439-447.
- Eikelenboom P, van Exel E, Hoozemans JJ, Veerhuis R, Rozemuller AJ, van Gool WA (2010) Neuroinflammation - an early event in both the history and pathogenesis of Alzheimer's disease. *Neurodegener Dis* 7:38-41.
- Erecinska M, Cherian S, Silver IA (2004) Energy metabolism in mammalian brain during development. *Prog Neurobiol* 73:397-445.
- Esler WP, Kimberly WT, Ostaszewski BL, Diehl TS, Moore CL, Tsai JY, Rahmati T, Xia W, Selkoe DJ, Wolfe MS (2000) Transition-state analogue inhibitors of gamma-secretase bind directly to presenilin-1. *Nat Cell Biol* 2:428-434.

- Esler WP, Wolfe MS (2001) A portrait of Alzheimer secretases--new features and familiar faces. *Science* 293:1449-1454.
- Fadool JM, Linser PJ (1993) Differential glycosylation of the 5A11/HT7 antigen by neural retina and epithelial tissues in the chicken. *J Neurochem* 60:1354-1364.
- Fan QW, Yuasa S, Kuno N, Senda T, Kobayashi M, Muramatsu T, Kadomatsu K (1998) Expression of basigin, a member of the immunoglobulin superfamily, in the mouse central nervous system. *Neurosci Res* 30:53-63.
- Farmery MR, Tjernberg LO, Pursglove SE, Bergman A, Winblad B, Naslund J (2003) Partial purification and characterization of gamma-secretase from post-mortem human brain. *J Biol Chem* 278:24277-24284.
- Feng B, Zhang D, Kuriakose G, Devlin CM, Kockx M, Tabas I (2003) Niemann-Pick C heterozygosity confers resistance to lesional necrosis and macrophage apoptosis in murine atherosclerosis. *Proc Natl Acad Sci U S A* 100:10423-10428.
- Feng X, Xia Q, Yuan L, Yang X, Wang K (2010) Impaired mitochondrial function and oxidative stress in rat cortical neurons: implications for gadolinium-induced neurotoxicity. *Neurotoxicology* 31:391-398.
- Festoff BW, Suo Z, Citron BA (2001) Plasticity and stabilization of neuromuscular and CNS synapses: interactions between thrombin protease signaling pathways and tissue transglutaminase. *Int Rev Cytol* 211:153-177.
- Fillit H, Nash DT, Rundek T, Zuckerman A (2008) Cardiovascular risk factors and dementia. *Am J Geriatr Pharmacother* 6:100-118.
- Fiskum G, Murphy AN, Beal MF (1999) Mitochondria in neurodegeneration: acute ischemia and chronic neurodegenerative diseases. *J Cereb Blood Flow Metab* 19:351-369.
- Fitz NF, Cronican A, Pham T, Fogg A, Fauq AH, Chapman R, Lefterov I, Koldamova R (2010) Liver X receptor agonist treatment ameliorates amyloid pathology and memory deficits caused by high-fat diet in APP23 mice. *J Neurosci* 30:6862-6872.
- Foda HD, Rollo EE, Drews M, Conner C, Appelt K, Shalinsky DR, Zucker S (2001) Ventilator-induced lung injury upregulates and activates gelatinases and EMMPRIN: attenuation by the synthetic matrix metalloproteinase inhibitor, Prinomastat (AG3340). *Am J Respir Cell Mol Biol* 25:717-724.
- Fonte J, Miklossy J, Atwood C, Martins R (2001) The severity of cortical Alzheimer's type changes is positively correlated with increased amyloid-beta Levels: Resolubilization of amyloid-beta with transition metal ion chelators. *J Alzheimers Dis* 3:209-219.
- Fortna RR, Crystal AS, Morais VA, Pijak DS, Lee VM, Doms RW (2004) Membrane topology and nicastrin-enhanced endoproteolysis of APh-1, a component of the gamma-secretase complex. *J Biol Chem* 279:3685-3693.
- Fossum S, Mallett S, Barclay AN (1991) The MRC OX-47 antigen is a member of the immunoglobulin superfamily with an unusual transmembrane sequence. *Eur J Immunol* 21:671-679.
- Foster ER, Campbell MC, Burack MA, Hartlein J, Flores HP, Cairns NJ, Hershey T, Perlmuter JS (2010) Amyloid imaging of Lewy body-associated disorders. *Mov Disord* 25:2516-2523.
- Frey UH, Bachmann HS, Peters J, Siffert W (2008) PCR-amplification of GC-rich regions: 'slowdown PCR'. *Nat Protoc* 3:1312-1317.
- Fuentealba RA, Farias G, Scheu J, Bronfman M, Marzolo MP, Inestrosa NC (2004) Signal transduction during amyloid-beta-peptide neurotoxicity: role in Alzheimer disease. *Brain Res Brain Res Rev* 47:275-289.
- Gabbita SP, Lovell MA, Markesbery WR (1998) Increased nuclear DNA oxidation in the brain in Alzheimer's disease. *J Neurochem* 71:2034-2040.

- Gabison EE, Mourah S, Steinfels E, Yan L, Hoang-Xuan T, Watsky MA, De Wever B, Calvo F, Mauviel A, Menashi S (2005) Differential expression of extracellular matrix metalloproteinase inducer (CD147) in normal and ulcerated corneas: role in epithelio-stromal interactions and matrix metalloproteinase induction. *Am J Pathol* 166:209-219.
- Galbete J, T R-M, E P, P M, R B, G F (2000a) Cholesterol decreases secretion of the secreted form of amyloid precursor protein by interfering with glycosylation in the protein secretory pathway. *Biochem J* 348:307-313.
- Galbete JL, Martin TR, Peressini E, Modena P, Bianchi R, Forloni G (2000b) Cholesterol decreases secretion of the secreted form of amyloid precursor protein by interfering with glycosylation in the protein secretory pathway. *Biochem J* 348 Pt 2:307-313.
- Gallala HD, Breiden B, Sandhoff K (2011) Regulation of the NPC2 protein-mediated cholesterol trafficking by membrane lipids. *J Neurochem* 116:702-707.
- Gandhi GK, Cruz NF, Ball KK, Theus SA, Dienel GA (2009) Selective astrocytic gap junctional trafficking of molecules involved in the glycolytic pathway: impact on cellular brain imaging. *J Neurochem* 110:857-869.
- George AJ, Holsinger RM, McLean CA, Laughton KM, Beyreuther K, Evin G, Masters CL, Li QX (2004) APP intracellular domain is increased and soluble Abeta is reduced with diet-induced hypercholesterolemia in a transgenic mouse model of Alzheimer disease. *Neurobiol Dis* 16:124-132.
- Gilman S (1997) Alzheimer's disease. *Perspect Biol Med* 40:230-245.
- Giulian D, Haverkamp LJ, Yu JH, Karshin W, Tom D, Li J, Kirkpatrick J, Kuo YM, Roher AE (1996) Specific domains of beta-amyloid from Alzheimer plaque elicit neuron killing in human microglia. *J Neurosci* 6021-6037
- Goedert M (1993) Tau protein and the neurofibrillary pathology of Alzheimer's disease. *Trends Neurosci* 16:460-465.
- Goedert M, Spillantini MG (2006a) A century of Alzheimer's disease. *Science* 314:777-781.
- Goedert M, Spillantini MG (2006b) Frontotemporal lobar degeneration through loss of progranulin function. *Brain* 129:2808-2810.
- Goldner FM, Patrick JW (1996) Neuronal localization of the cyclophilin A protein in the adult rat brain. *J Comp Neurol* 372:283-293.
- Gomperts SN, Rentz DM, Moran E, Becker JA, Locascio JJ, Klunk WE, Mathis CA, Elmaleh DR, Shoup T, Fischman AJ, Hyman BT, Growdon JH, Johnson KA (2008) Imaging amyloid deposition in Lewy body diseases. *Neurology* 71:903-910.
- Goutte C, Tsunozaki M, Hale VA, Priess JR (2002) APH-1 is a multipass membrane protein essential for the Notch signaling pathway in *Caenorhabditis elegans* embryos. *Proc Natl Acad Sci U S A* 99:775-779.
- Grammas P (2011) Neurovascular dysfunction, inflammation and endothelial activation: implications for the pathogenesis of Alzheimer's disease. *J Neuroinflammation* 8:26.
- Greeve I, Kretschmar D, Tschape JA, Beyn A, Brellinger C, Schweizer M, Nitsch RM, Reifegerste R (2004) Age-dependent neurodegeneration and Alzheimer-amyloid plaque formation in transgenic *Drosophila*. *J Neurosci* 24:3899-3906.
- Griffin WS, Liu L, Li Y, Mrak RE, Barger SW (2006) Interleukin-1 mediates Alzheimer and Lewy body pathologies. *J Neuroinflammation* 3:5.
- Grunberg J, Walter J, Eckman C, Capell A, Schindzielorz A, Younkin S, Mehta N, Hardy J, Haass C (1998) Truncated presenilin 2 derived from differentially spliced mRNA does not affect the ratio of amyloid beta-peptide 1-42/1-40. *Neuroreport* 9:3293-3299.

- Gu J, Zhang C, Chen R, Pan J, Wang Y, Ming M, Gui W, Wang D (2009) Clinical implications and prognostic value of EMMPRIN/CD147 and MMP2 expression in pediatric gliomas. *Eur J Pediatr* 168:705-710.
- Gu Y, Chen F, Sanjo N, Kawarai T, Hasegawa H, Duthie M, Li W, Ruan X, Luthra A, Mount HT, Tandon A, Fraser PE, St George-Hyslop P (2003) APH-1 interacts with mature and immature forms of presenilins and nicastrin and may play a role in maturation of presenilin.nicastrin complexes. *J Biol Chem* 278:7374-7380.
- Guo H, Zucker S, Gordon MK, Toole BP, Biswas C (1997) Stimulation of matrix metalloproteinase production by recombinant extracellular matrix metalloproteinase inducer from transfected Chinese hamster ovary cells. *J Biol Chem* 272:24-27.
- Guo JH, Cheng HP, Yu L, Zhao S (2006) Natural antisense transcripts of Alzheimer's disease associated genes. *DNA Seq* 17:170-173.
- Guo X, Wu X, Ren L, Liu G, Li L (2011) Epigenetic mechanisms of amyloid-beta production in anisomycin-treated SH-SY5Y cells. *Neuroscience* 194:272-281.
- Gwon AR, Park JS, Arumugam TV, Kwon YK, Chan SL, Kim SH, Baik SH, Yang S, Yun YK, Choi Y, Kim S, Tang SC, Hyun DH, Cheng A, Dann CE, 3rd, Bernier M, Lee J, Markesbery WR, Mattson MP, Jo DG (2012) Oxidative lipid modification of nicastrin enhances amyloidogenic gamma-secretase activity in Alzheimer's disease. *Aging Cell*.
- Halestrap AP, Price NT (1999) The proton-linked monocarboxylate transporter (MCT) family: structure, function and regulation. *Biochem J* 343 Pt 2:281-299.
- Han ZD, He HC, Bi XC, Qin WJ, Dai QS, Zou J, Ye YK, Liang YX, Zeng GH, Zhu G, Chen ZN, Zhong WD (2010) Expression and clinical significance of CD147 in genitourinary carcinomas. *J Surg Res* 160:260-267.
- Hanata K, Yamaguchi N, Yoshikawa K, Mezaki Y, Miura M, Suzuki S, Senoo H, Ishikawa K (2007) Soluble EMMPRIN (extra-cellular matrix metalloproteinase inducer) stimulates the migration of HEp-2 human laryngeal carcinoma cells, accompanied by increased MMP-2 production in fibroblasts. *Arch Histol Cytol* 70:267-277.
- Hansson CA, Frykman S, Farmery MR, Tjernberg LO, Nilsberth C, Pursglove SE, Ito A, Winblad B, Cowburn RF, Thyberg J, Ankarcrona M (2004) Nicastrin, presenilin, APH-1, and PEN-2 form active gamma-secretase complexes in mitochondria. *J Biol Chem* 279:51654-51660.
- Hansson EM, Stromberg K, Bergstedt S, Yu G, Naslund J, Lundkvist J, Lendahl U (2005) Aph-1 interacts at the cell surface with proteins in the active gamma-secretase complex and membrane-tethered Notch. *J Neurochem* 92:1010-1020.
- Hara MR, Kovacs JJ, Whalen EJ, Rajagopal S, Strachan RT, Grant W, Towers AJ, Williams B, Lam CM, Xiao K, Shenoy SK, Gregory SG, Ahn S, Duckett DR, Lefkowitz RJ (2011) A stress response pathway regulates DNA damage through beta2-adrenoreceptors and beta-arrestin-1. *Nature* 477:349-353.
- Hardy JA, Higgins GA (1992) Alzheimer's disease: the amyloid cascade hypothesis. *Science* 256:184-185.
- Harold D, Abraham R, Hollingworth P, Sims R, Gerrish A, Hamshere ML, Pahwa JS, Moskvina V, Dowzell K, Williams A, Jones N, Thomas C, Stretton A, Morgan AR, Lovestone S, Powell J, Proitsi P, Lupton MK, Brayne C, Rubinsztein DC, Gill M, Lawlor B, Lynch A, Morgan K, Brown KS, Passmore PA, Craig D, McGuinness B, Todd S, Holmes C, Mann D, Smith AD, Love S, Kehoe PG, Hardy J, Mead S, Fox N, Rossor M, Collinge J, Maier W, Jessen F, Schurmann B, van den Bussche H, Heuser I, Kornhuber J, Wiltfang J, Dichgans M, Frolich L, Hampel H, Hull M, Rujescu D, Goate AM, Kauwe JS, Cruchaga C, Nowotny P, Morris JC, Mayo K, Sleegers K, Bettens K, Engelborghs S, De Deyn PP, Van

- Broeckhoven C, Livingston G, Bass NJ, Gurling H, McQuillin A, Gwilliam R, Deloukas P, Al-Chalabi A, Shaw CE, Tsolaki M, Singleton AB, Guerreiro R, Muhleisen TW, Nothen MM, Moebus S, Jockel KH, Klopp N, Wichmann HE, Carrasquillo MM, Pankratz VS, Younkin SG, Holmans PA, O'Donovan M, Owen MJ, Williams J (2009) Genome-wide association study identifies variants at CLU and PICALM associated with Alzheimer's disease. *Nat Genet* 41:1088-1093.
- Hartmann H, Eckert A, Muller WE (1994) Disturbances of the neuronal calcium homeostasis in the aging nervous system. *Life Sci* 2011-2018.
- Hartmann T, Bergsdorf C, Sandbrink R, Tienari PJ, Multhaup G, Ida N, Bieger S, Dyrks T, Weidemann A, Masters CL, Beyreuther K (1996) Alzheimer's disease betaA4 protein release and amyloid precursor protein sorting are regulated by alternative splicing. *J Biol Chem* 271:13208-13214.
- Hasaneen NA, Zucker S, Cao J, Chiarelli C, Panettieri RA, Foda HD (2005) Cyclic mechanical strain-induced proliferation and migration of human airway smooth muscle cells: role of EMMPRIN and MMPs. *FASEB J* 19:1507-1509.
- Hasegawa H, Sanjo N, Chen F, Gu YJ, Shier C, Petit A, Kawarai T, Katayama T, Schmidt SD, Mathews PM, Schmitt-Ulms G, Fraser PE, St George-Hyslop P (2004) Both the sequence and length of the C terminus of PEN-2 are critical for intermolecular interactions and function of presenilin complexes. *J Biol Chem* 279:46455-46463.
- Hashimoto Y, Jiang H, Niikura T, Ito Y, Hagiwara A, Umezawa K, Abe Y, Murayama Y, Nishimoto I (2000) Neuronal apoptosis by apolipoprotein E4 through low-density lipoprotein receptor-related protein and heterotrimeric GTPases. *J Neurosci* 20:8401-8409.
- Haskell SG, Richardson ED, Horwitz RI (1997) The effect of estrogen replacement therapy on cognitive function in women: a critical review of the literature. *J Clin Epidemiol* 50:1249-1264.
- Havel RJ (1998) Receptor and non-receptor mediated uptake of chylomicron remnants by the liver. *Atherosclerosis* 141 Suppl 1:S1-7.
- He TC, Zhou S, da Costa LT, Yu J, Kinzler KW, Vogelstein B (1998) A simplified system for generating recombinant adenoviruses. *Proc Natl Acad Sci U S A* 95:2509-2514.
- Hedskog L, Petersen CA, Svensson AI, Welanders H, Tjernberg LO, Karlstrom H, Ankarcrona M (2011) gamma-Secretase complexes containing caspase-cleaved presenilin-1 increase intracellular Abeta(42) /Abeta(40) ratio. *J Cell Mol Med* 15:2150-2163.
- Helisalmi S, Hiltunen M, Mannermaa A, Koivisto AM, Lehtovirta M, Alafuzoff I, Ryyanen M, Soininen H (2000) Is the presenilin-1 E318G missense mutation a risk factor for Alzheimer's disease? *Neurosci Lett* 278:65-68.
- Hemar A, Mulle C (2011) [Alzheimer's disease, amyloid peptide and synaptic dysfunction]. *Med Sci (Paris)* 27:733-736.
- Heppner KJ, Matrisian LM, Jensen RA, Rodgers WH (1996) Expression of most matrix metalloproteinase family members in breast cancer represents a tumor-induced host response. *Am J Pathol* 149:273-282.
- Herremans A, Hartmann D, Annaert W, Saftig P, Craessaerts K, Serneels L, Umans L, Schrijvers V, Checler F, Vanderstichele H, Baekelandt V, Dressel R, Cupers P, Huylebroeck D, Zwijsen A, Van Leuven F, De Strooper B (1999) Presenilin 2 deficiency causes a mild pulmonary phenotype and no changes in amyloid precursor protein processing but enhances the embryonic lethal phenotype of presenilin 1 deficiency. *Proc Natl Acad Sci U S A* 96:11872-11877.

- Hewitt KN, Pratis K, Jones ME, Simpson ER (2004) Estrogen replacement reverses the hepatic steatosis phenotype in the male aromatase knockout mouse. *Endocrinology* 145:1842-1848.
- Higgins GA, Jacobsen H (2003) Transgenic mouse models of Alzheimer's disease: phenotype and application. *Behav Pharmacol* 14:419-438.
- Hirai A, Kino T, Tokinaga K, Tahara K, Tamura Y, Yoshida S (1994) Regulation of sterol carrier protein 2 (SCP-2) gene expression in rat peritoneal macrophages during foam cell formation. A key role for free cholesterol content. *J Clin Invest* 94:2215-2223.
- Holsinger RM, McLean CA, Beyreuther K, Masters CL, Evin G (2002) Increased expression of the amyloid precursor beta-secretase in Alzheimer's disease. *Ann Neurol* 51:783-786.
- Holtzman DM, Herz J, Bu G (2012) Apolipoprotein e and apolipoprotein e receptors: normal biology and roles in Alzheimer disease. *Cold Spring Harb Perspect Med* 2:a006312.
- Holtzman DM, Pitas RE, Kilbridge J, Nathan B, Mahley RW, Bu G, Schwartz AL (1995) Low density lipoprotein receptor-related protein mediates apolipoprotein E-dependent neurite outgrowth in a central nervous system-derived neuronal cell line. *Proc Natl Acad Sci U S A* 92:9480-9484.
- Homma Y, Kondo Y, Kaneko M, Kitamura T, Nyu WT, Yanagisawa M, Yamamoto Y, Kakizoe T (2004) Promotion of carcinogenesis and oxidative stress by dietary cholesterol in rat prostate. *Carcinogenesis* 25:1011-1014.
- Hone E, Martins IJ, Fonte J, Martins RN (2003) Apolipoprotein E influences amyloid-beta clearance from the murine periphery. *J Alzheimers Dis* 5:1-8.
- Hooijmans CR, Graven C, Dederen PJ, Tanila H, van Groen T, Kiliaan AJ (2007) Amyloid beta deposition is related to decreased glucose transporter-1 levels and hippocampal atrophy in brains of aged APP/PS1 mice. *Brain Res* 1181:93-103.
- Hook VY, Tezapsidis N, Hwang SR, Sei C, Byrne M, Yasothornsrikul S (1999) Alpha1-antichymotrypsin-like proteins I and II purified from bovine adrenal medulla are enriched in chromaffin granules and inhibit the proenkephalin processing enzyme "prohormone thiol protease". *J Neurochem* 73:59-69.
- Hovland AR, La Rosa FG, Hovland PG, Cole WC, Kumar A, Prasad JE, Prasad KN (1999) Cyclosporin A regulates the levels of cyclophilin A in neuroblastoma cells in culture. *Neurochem Int* 35:229-235.
- Howland DS, Trusko SP, Savage MJ, Reaume AG, Lang DM, Hirsch JD, Maeda N, Siman R, Greenberg BD, Scott RW, Flood DG (1998) Modulation of secreted beta-amyloid precursor protein and amyloid beta-peptide in brain by cholesterol. *J Biol Chem* 273:16576-16582.
- Hrabovszky E, Shughrue PJ, Merchenthaler I, Hajszan T, Carpenter CD, Liposits Z, Petersen SL (2000) Detection of estrogen receptor-beta messenger ribonucleic acid and 125I-estrogen binding sites in luteinizing hormone-releasing hormone neurons of the rat brain. *Endocrinology* 141:3506-3509.
- Hu J, LaDu MJ, Van Eldik LJ (1998) Apolipoprotein E attenuates beta-amyloid-induced astrocyte activation. *J Neurochem* 71:1626-1634.
- Huang GC, Chen JJ, Liu CP, Zhou JM (2002) Chaperone and antichaperone activities of trigger factor. *Eur J Biochem* 269:4516-4523.
- Huang X, Atwood CS, Hartshorn MA, Multhaup G, Goldstein LE, Scarpa RC, Cuajungco MP, Gray DN, Lim J, Moir RD, Tanzi RE, Bush AI (1999) The A beta peptide of Alzheimer's disease directly produces hydrogen peroxide through metal ion reduction. *Biochemistry* 38:7609-7616.
- Huh JY, Park G, Jang SJ, Moon DS, Park YJ (2011) A rapid long PCR-direct sequencing analysis for ABO genotyping. *Ann Clin Lab Sci* 41:340-345.



- Hurtado DE, Molina-Porcel L, Iba M, Aboagye AK, Paul SM, Trojanowski JQ, Lee VM (2010) A $\beta$  accelerates the spatiotemporal progression of tau pathology and augments tau amyloidosis in an Alzheimer mouse model. *Am J Pathol* 177:1977-1988.
- Hussain I, Powell D, Howlett DR, Tew DG, Meek TD, Chapman C, Gloger IS, Murphy KE, Southan CD, Ryan DM, Smith TS, Simmons DL, Walsh FS, Dingwall C, Christie G (1999) Identification of a novel aspartic protease (Asp 2) as beta-secretase. *Mol Cell Neurosci* 14:419-427.
- Hyman BT, Van Hoesen GW, Damasio AR, Barnes CL (1984) Alzheimer's disease: cell-specific pathology isolates the hippocampal formation. *Science* 225:1168 - 1170.
- Iacono KT, Brown AL, Greene MI, Saouaf SJ (2007) CD147 immunoglobulin superfamily receptor function and role in pathology. *Exp Mol Pathol* 83:283-295.
- Igakura T, Kadomatsu K, Kaname T, Muramatsu H, Fan QW, Miyauchi T, Toyama Y, Kuno N, Yuasa S, Takahashi M, Senda T, Taguchi O, Yamamura K, Arimura K, Muramatsu T (1998) A null mutation in basigin, an immunoglobulin superfamily member, indicates its important roles in peri-implantation development and spermatogenesis. *Dev Biol* 194:152-165.
- Igbavboa U, Avdulov NA, Schroeder F, Wood WG (1996) Increasing age alters transbilayer fluidity and cholesterol asymmetry in synaptic plasma membranes of mice. *J Neurochem* 66:1717-1725.
- Inoue H, Sawada M, Ryo A, Tanahashi H, Wakatsuki T, Hada A, Kondoh N, Nakagaki K, Takahashi K, Suzumura A, Yamamoto M, Tabira T (1999) Serial analysis of gene expression in a microglial cell line. *Glia* 28:265-271.
- Ionov ID, Pushinskaya, II (2010) Amyloid-beta production in aged guinea pigs: atropine-induced enhancement is reversed by naloxone. *Neurosci Lett* 480:83-86.
- Iwatsubo T, Odaka A, Suzuki N, Mizusawa H, Nukina N, Ihara Y (1994) Visualization of A $\beta$  42(43) and A $\beta$  40 in senile plaques with end-specific A $\beta$  monoclonals: evidence that an initially deposited species is A $\beta$  42(43). *Neuron* 13:45-53.
- Jagust WJ, Bandy D, Chen K, Foster NL, Landau SM, Mathis CA, Price JC, Reiman EM, Skovronsky D, Koeppe RA (2010) The Alzheimer's Disease Neuroimaging Initiative positron emission tomography core. *Alzheimers Dement* 6:221-229.
- Jankowsky JL, Slunt HH, Gonzales V, Jenkins NA, Copeland NG, Borchelt DR (2004) APP processing and amyloid deposition in mice haplo-insufficient for presenilin 1. *Neurobiol Aging* 25:885-892.
- Janus C, Pearson J, McLaurin J, Mathews PM, Jiang Y, Schmidt SD, Chishti MA, Horne P, Heslin D, French J, Mount HT, Nixon RA, Mercken M, Bergeron C, Fraser PE, St George-Hyslop P, Westaway D (2000) A $\beta$  peptide immunization reduces behavioural impairment and plaques in a model of Alzheimer's disease. *Nature* 408:979-982.
- Jarvik GP, Wijsman EM, Kukull WA, Schellenberg GD, Yu C, Larson EB (1995) Interactions of apolipoprotein E genotype, total cholesterol level, age, and sex in prediction of Alzheimer's disease: a case-control study. *Neurology* 45:1092-1096.
- Jensen MA, Fukushima M, Davis RW (2010) DMSO and betaine greatly improve amplification of GC-rich constructs in de novo synthesis. *PLoS One* 5:e11024.
- Ji ZS, Brecht WJ, Miranda RD, Hussain MM, Innerarity TL, Mahley RW (1993) Role of heparan sulfate proteoglycans in the binding and uptake of apolipoprotein E-enriched remnant lipoproteins by cultured cells. *J Biol Chem* 268:10160-10167.

- Jin ZG, Melaragno MG, Liao DF, Yan C, Haendeler J, Suh YA, Lambeth JD, Berk BC (2000) Cyclophilin A is a secreted growth factor induced by oxidative stress. *Circ Res* 87:789-796.
- Jorissen E, Prox J, Bernreuther C, Weber S, Schwanbeck R, Serneels L, Snellinx A, Craessaerts K, Thathiah A, Tesseur I, Bartsch U, Weskamp G, Blobel CP, Glatzel M, De Strooper B, Saftig P (2010) The disintegrin/metalloproteinase ADAM10 is essential for the establishment of the brain cortex. *J Neurosci* 30:4833-4844.
- Jung A, Ruckert S, Frank P, Brabletz T, Kirchner T (2002) 7-Deaza-2'-deoxyguanosine allows PCR and sequencing reactions from CpG islands. *Mol Pathol* 55:55-57.
- Kadir A, Marutle A, Gonzalez D, Scholl M, Almkvist O, Mousavi M, Mustafiz T, Darreh-Shori T, Nennesmo I, Nordberg A (2011) Positron emission tomography imaging and clinical progression in relation to molecular pathology in the first Pittsburgh Compound B positron emission tomography patient with Alzheimer's disease. *Brain* 134:301-317.
- Kalmijn S, Launer LJ, Ott A, Witteman JC, Hofman A, Breteler MM (1997) Dietary fat intake and the risk of incident dementia in the Rotterdam Study. *Ann Neurol* 42:776-782.
- Kan R, Wang B, Zhang C, Jin F, Yang Z, Ji S, Lu Z, Zheng C, Wang L (2005) Genetic association of BACE1 gene polymorphism C786G with late-onset Alzheimer's disease in Chinese. *J Mol Neurosci* 25:127-131.
- Kang JH, Yu KH, Park JY, An CM, Jun JC, Lee SJ (2011) Allele-specific PCR genotyping of the HSP70 gene polymorphism discriminating the green and red color variants sea cucumber (*Apostichopus japonicus*). *J Genet Genomics* 38:351-355.
- Kanyenda LJ, Verdile G, Boulos S, Krishnaswamy S, Taddei K, Meloni BP, Mastaglia FL, Martins RN (2011) The dynamics of CD147 in Alzheimer's disease development and pathology. *J Alzheimers Dis* 26:593-605.
- Kasinerk W, Fiebigler E, Stefanova I, Baumrucker T, Knapp W, Stockinger H (1992) Human leukocyte activation antigen M6, a member of the Ig superfamily, is the species homologue of rat OX-47, mouse basigin, and chicken HT7 molecule. *J Immunol* 149:847-854.
- Kataoka H, DeCastro R, Zucker S, Biswas C (1993) Tumor cell-derived collagenase-stimulatory factor increases expression of interstitial collagenase, stromelysin, and 72-kDa gelatinase. *Cancer Res* 53:3154-3158.
- Kawarabayashi T, Shoji M, Younkin LH, Wen-Lang L, Dickson DW, Murakami T, Matsubara E, Abe K, Ashe KH, Younkin SG (2004) Dimeric Amyloid  $\beta$  protein rapidly accumulates in lipid rafts followed by Apolipoprotein E and phosphorylated Tau accumulation in the Tg2576 mouse model of Alzheimer's Disease. *The Journal of Neuroscience* 24:3801-3809.
- Kim SH, Sisodia SS (2005) Evidence that the "NF" motif in transmembrane domain 4 of presenilin 1 is critical for binding with PEN-2. *J Biol Chem* 280:41953-41966.
- Kim WS, Hill AF, Fitzgerald ML, Freeman MW, Evin G, Garner B (2011) Wild Type and Tangier Disease ABCA1 Mutants Modulate Cellular Amyloid-beta Production Independent of Cholesterol Efflux Activity. *J Alzheimers Dis*.
- Kimberly WT, LaVoie MJ, Ostaszewski BL, Ye W, Wolfe MS, Selkoe DJ (2003) Gamma-secretase is a membrane protein complex comprised of presenilin, nicastrin, Aph-1, and Pen-2. *Proc Natl Acad Sci U S A* 100:6382-6387.
- Kirk P, Wilson MC, Heddle C, Brown MH, Barclay AN, Halestrap AP (2000) CD147 is tightly associated with lactate transporters MCT1 and MCT4 and facilitates their cell surface expression. *EMBO J* 19:3896-3904.

- Kleene R, Loers G, Langer J, Frobert Y, Buck F, Schachner M (2007) Prion protein regulates glutamate-dependent lactate transport of astrocytes. *J Neurosci* 27:12331-12340.
- Ko MH, Puglielli L (2007) The sterol carrier protein SCP-x/pro-SCP-2 gene has transcriptional activity and regulates the Alzheimer disease gamma-secretase. *J Biol Chem* 282:19742-19752.
- Kochi M, Ushio Y (1999) High-dose chemotherapy with autologous hematopoietic stem-cell rescue for patients with malignant brain tumors. *Crit Rev Neurosurg* 9:295-302.
- Kodam A, Maulik M, Peake K, Amritraj A, Vetrivel KS, Thinakaran G, Vance JE, Kar S (2010) Altered levels and distribution of amyloid precursor protein and its processing enzymes in Niemann-Pick type C1-deficient mouse brains. *Glia* 58:1267-1281.
- Koike H, Tomioka S, Sorimachi H, Saido TC, Maruyama K, Okuyama A, Fujisawa-Sehara A, Ohno S, Suzuki K, Ishiura S (1999) Membrane-anchored metalloprotease MDC9 has an alpha-secretase activity responsible for processing the amyloid precursor protein. *Biochem J* 343 Pt 2:371-375.
- Kojro E, G G, S L, W M, F F (2001) Low cholesterol stimulates the nonamyloidogenic pathway by its effect on the  $\gamma$ -secretase ADAM 10. *Proc Natl Acad Sci USA* 98:5815-5820.
- Koldamova RP, Lefterov IM, Ikonomic MD, Skoko J, Lefterov PI, Isanski BA, DeKosky ST, Lazo JS (2003) 22R-hydroxycholesterol and 9-cis-retinoic acid induce ATP-binding cassette transporter A1 expression and cholesterol efflux in brain cells and decrease amyloid beta secretion. *J Biol Chem* 278:13244-13256.
- Kong LM, Liao CG, Chen L, Yang HS, Zhang SH, Zhang Z, Bian HJ, Xing JL, Chen ZN (2011) Promoter hypomethylation up-regulates CD147 expression through increasing Sp1 binding and associates with poor prognosis in human hepatocellular carcinoma. *J Cell Mol Med* 15:1415-1428.
- Kong LM, Liao CG, Fei F, Guo X, Xing JL, Chen ZN (2010) Transcription factor Sp1 regulates expression of cancer-associated molecule CD147 in human lung cancer. *Cancer Sci* 101:1463-1470.
- Kontinen YT, Li TF, Mandelin J, Liljestrom M, Sorsa T, Santavirta S, Virtanen I (2000) Increased expression of extracellular matrix metalloproteinase inducer in rheumatoid synovium. *Arthritis Rheum* 43:275-280.
- Kontush A, Berndt C, Weber W, Akopyan V, Arlt S, Schippling S, Beisiegel U (2001) Amyloid-beta is an antioxidant for lipoproteins in cerebrospinal fluid and plasma. *Free Radic Biol Med* 30:119-128.
- Kopan R, Goate A (2002) Aph-2/Nicastrin: an essential component of gamma-secretase and regulator of Notch signaling and Presenilin localization. *Neuron* 33:321-324.
- Koponen J, Laakso K, Koskeniemi K, Kankainen M, Savijoki K, Nyman TA, de Vos WM, Tynkkynen S, Kalkkinen N, Varmanen P (2012) Effect of acid stress on protein expression and phosphorylation in *Lactobacillus rhamnosus* GG. *J Proteomics* 75:1357-1374.
- Kraemer R, Pomerantz KB, Kesav S, Scallen TJ, Hajjar DP (1995) Cholesterol enrichment enhances expression of sterol-carrier protein-2: implications for its function in intracellular cholesterol trafficking. *J Lipid Res* 36:2630-2638.
- Krishnaswamy S, Verdile G, Groth D, Kanyenda L, Martins RN (2009) The structure and function of Alzheimer's gamma secretase enzyme complex. *Crit Rev Clin Lab Sci* 46:282-301.
- Kuentzel SL, Ali SM, Altman RA, Greenberg BD, Raub TJ (1993) The Alzheimer beta-amyloid protein precursor/protease nexin-II is cleaved by secretase in a trans-

- Golgi secretory compartment in human neuroglioma cells. *Biochem J* 295 ( Pt 2):367-378.
- Kuhn PH, Wang H, Dislich B, Colombo A, Zeitschel U, Ellwart JW, Kremmer E, Rossner S, Lichtenthaler SF (2010) ADAM10 is the physiologically relevant, constitutive alpha-secretase of the amyloid precursor protein in primary neurons. *EMBO J* 29:3020-3032.
- L'Hernault SW, Arduengo PM (1992) Mutation of a putative sperm membrane protein in *Caenorhabditis elegans* prevents sperm differentiation but not its associated meiotic divisions. *J Cell Biol* 119:55-68.
- Lad RP, Smith MA, Hilt DC (1991) Molecular cloning and regional distribution of rat brain cyclophilin. *Brain Res Mol Brain Res* 9:239-244.
- Lai MT, Chen E, Crouthamel MC, DiMuzio-Mower J, Xu M, Huang Q, Price E, Register RB, Shi XP, Donoviel DB, Bernstein A, Hazuda D, Gardell SJ, Li YM (2003) Presenilin-1 and presenilin-2 exhibit distinct yet overlapping gamma-secretase activities. *J Biol Chem* 278:22475-22481.
- Lambert JC, Berr C, Pasquier F, Delacourte A, Frigard B, Cottel D, Perez-Tur J, Mouroux V, Mohr M, Cecyre D, Galasko D, Lendon C, Poirier J, Hardy J, Mann D, Amouyel P, Chartier-Harlin MC (1998) Pronounced impact of Th1/E47cs mutation compared with -491 AT mutation on neural APOE gene expression and risk of developing Alzheimer's disease. *Hum Mol Genet* 7:1511-1516.
- Lambert JC, Heath S, Even G, Campion D, Sleegers K, Hiltunen M, Combarros O, Zelenika D, Bullido MJ, Tavernier B, Letenneur L, Bettens K, Berr C, Pasquier F, Fievet N, Barberger-Gateau P, Engelborghs S, De Deyn P, Mateo I, Franck A, Helisalmi S, Porcellini E, Hanon O, de Pancorbo MM, Lendon C, Dufouil C, Jaillard C, Leveillard T, Alvarez V, Bosco P, Mancuso M, Panza F, Nacmias B, Bossu P, Piccardi P, Annoni G, Seripa D, Galimberti D, Hannequin D, Licastro F, Soininen H, Ritchie K, Blanche H, Dartigues JF, Tzourio C, Gut I, Van Broeckhoven C, Alperovitch A, Lathrop M, Amouyel P (2009) Genome-wide association study identifies variants at CLU and CR1 associated with Alzheimer's disease. *Nat Genet* 41:1094-1099.
- Lammich S, Kojro E, Postina R, Gilbert S, Pfeiffer R, Jasionowski M, Haass C, Fahrenholz F (1999) Constitutive and regulated alpha-secretase cleavage of Alzheimer's amyloid precursor protein by a disintegrin metalloprotease. *Proc Natl Acad Sci U S A* 96:3922-3927.
- Laudon H, Karlstrom H, Mathews PM, Farmery MR, Gandy SE, Lundkvist J, Lendahl U, Naslund J (2004a) Functional domains in presenilin 1: the Tyr-288 residue controls gamma-secretase activity and endoproteolysis. *J Biol Chem* 279:23925-23932.
- Laudon H, Mathews PM, Karlstrom H, Bergman A, Farmery MR, Nixon RA, Winblad B, Gandy SE, Lendahl U, Lundkvist J, Naslund J (2004b) Co-expressed presenilin 1 NTF and CTF form functional gamma-secretase complexes in cells devoid of full-length protein. *J Neurochem* 89:44-53.
- Lee BC, Mintun M, Buckner RL, Morris JC (2003a) Imaging of Alzheimer's disease. *J Neuroimaging* 13:199-214.
- Lee HK, Choi SS, Han KJ, Han EJ, Suh HW (2003b) Cycloheximide inhibits neurotoxic responses induced by kainic acid in mice. *Brain Res Bull* 61:99-107.
- Lee SF, Shah S, Li H, Yu C, Han W, Yu G (2002) Mammalian APH-1 interacts with presenilin and nicastrin and is required for intramembrane proteolysis of amyloid-beta precursor protein and Notch. *J Biol Chem* 277:45013-45019.
- Lee SW, Kwon KH, Kim MJ (1998) Comparison of lipid profiles in long-term CAPD and hemodialysis patients. *Perit Dial Int* 18:435-437.

- Lehmann S, Chiesa R, Harris DA (1997) Evidence for a six-transmembrane domain structure of presenilin 1. *J Biol Chem* 272:12047-12051.
- Leonard S, Arbogast D, Geyer D, Jones C, Sinensky M (1986) Localization of the gene encoding 3-hydroxy-3-methylglutaryl-coenzyme A synthase to human chromosome 5. *Proc Natl Acad Sci U S A* 83:2187-2189.
- Levitan D, Lee J, Song L, Manning R, Wong G, Parker E, Zhang L (2001) PS1 N- and C-terminal fragments form a complex that functions in APP processing and Notch signaling. *Proc Natl Acad Sci U S A* 98:12186-12190.
- Levitan DR, Petersen C (1995) Sperm limitation in the sea. *Trends Ecol Evol* 10:228-231.
- Lewczuk P, Popp J, Lelental N, Kolsch H, Maier W, Kornhuber J, Jessen F (2011) Cerebrospinal Fluid Soluble Amyloid-beta Protein Precursor as a Potential Novel Biomarkers of Alzheimer's Disease. *J Alzheimers Dis*.
- Li L, Cao D, Garber DW, Kim H, Fukuchi K (2003a) Association of aortic atherosclerosis with cerebral beta-amyloidosis and learning deficits in a mouse model of Alzheimer's disease. *Am J Pathol* 163:2155-2164.
- Li R, Huang L, Guo H, Toole BP (2001) Basigin (murine EMMPRIN) stimulates matrix metalloproteinase production by fibroblasts. *J Cell Physiol* 186:371-379.
- Li T, Li YM, Ahn K, Price DL, Sisodia SS, Wong PC Increased Expression of PS1 Is Sufficient to Elevate the Level and Activity of gamma-Secretase In Vivo. *PLoS One* 6:e28179.
- Li T, Ma G, Cai H, Price DL, Wong PC (2003b) Nicastrin is required for assembly of presenilin/gamma-secretase complexes to mediate Notch signaling and for processing and trafficking of beta-amyloid precursor protein in mammals. *J Neurosci* 23:3272-3277.
- Li W, Ghosh M, Eftekhari S, Yuan XM (2011) Lipid accumulation and lysosomal pathways contribute to dysfunction and apoptosis of human endothelial cells caused by 7-oxysterols. *Biochem Biophys Res Commun* 409:711-716.
- Li YM, Lai MT, Xu M, Huang Q, DiMuzio-Mower J, Sardana MK, Shi XP, Yin KC, Shafer JA, Gardell SJ (2000a) Presenilin 1 is linked with gamma-secretase activity in the detergent solubilized state. *Proc Natl Acad Sci U S A* 97:6138-6143.
- Li YM, Xu M, Lai MT, Huang Q, Castro JL, DiMuzio-Mower J, Harrison T, Lellis C, Nadin A, Neduvilil JG, Register RB, Sardana MK, Shearman MS, Smith AL, Shi XP, Yin KC, Shafer JA, Gardell SJ (2000b) Photoactivated gamma-secretase inhibitors directed to the active site covalently label presenilin 1. *Nature* 405:689-694.
- Liang L, Major T, Bocan T (2002) Characterization of the promoter of human extracellular matrix metalloproteinase inducer (EMMPRIN). *Gene* 282:75-86.
- Liang Q, Xiong H, Gao G, Xiong K, Wang X, Zhao Z, Zhang H, Li Y (2005) Inhibition of basigin expression in glioblastoma cell line via antisense RNA reduces tumor cell invasion and angiogenesis. *Cancer Biol Ther* 4:759-762.
- Liang YX, He HC, Han ZD, Bi XC, Dai QS, Ye YK, Qin WJ, Zeng GH, Zhu G, Xu CL, Zhong WD (2009) CD147 and VEGF expression in advanced renal cell carcinoma and their prognostic value. *Cancer Invest* 27:788-793.
- Liebetrau M, Burggraf D, Wunderlich N, Jager G, Linz W, Hamann GF (2005) ACE inhibition reduces activity of the plasminogen/plasmin and MMP systems in the brain of spontaneous hypertensive stroke-prone rats. *Neurosci Lett* 376:205-209.
- Lin H, Bhatia R, Lal R (2001) Amyloid beta protein forms ion channels: implications for Alzheimer's disease pathophysiology. *FASEB J* 15:2433-2444.
- Lingrel JB, Williams MT, Vorhees CV, Moseley AE (2007) Na,K-ATPase and the role of alpha isoforms in behavior. *J Bioenerg Biomembr* 39:385-389.

- Lipka G, Schulthess G, Thurnhofer H, Wacker H, Wehrli E, Zeman K, Weber FE, Hauser H (1995) Characterization of lipid exchange proteins isolated from small intestinal brush border membrane. *J Biol Chem* 270:5917-5925.
- Lippa CF, Nee LE, Mori H, St George-Hyslop P (1998) Abeta-42 deposition precedes other changes in PS-1 Alzheimer's disease. *Lancet* 352:1117-1118.
- Liu J, Farmer JD, Jr., Lane WS, Friedman J, Weissman I, Schreiber SL (1991) Calcineurin is a common target of cyclophilin-cyclosporin A and FKBP-FK506 complexes. *Cell* 66:807-815.
- Liu Q, Yang H, Zhang SF (2010) [Expression and significance of MIF and CD147 in non-small cell lung cancer]. *Sichuan Da Xue Xue Bao Yi Xue Ban* 41:85-90.
- Lo SM, McNamara J, Seashore MR, Mistry PK (2010) Misdiagnosis of Niemann-Pick disease type C as Gaucher disease. *J Inherit Metab Dis*.
- Lopez-Perez E, Zhang Y, Frank SJ, Creemers J, Seidah N, Checler F (2001) Constitutive alpha-secretase cleavage of the beta-amyloid precursor protein in the furin-deficient LoVo cell line: involvement of the pro-hormone convertase 7 and the disintegrin metalloprotease ADAM10. *J Neurochem* 76:1532-1539.
- Lorenzl S, Albers DS, Relkin N, Ngyuen T, Hilgenberg SL, Chirichigno J, Cudkowicz ME, Beal MF (2003) Increased plasma levels of matrix metalloproteinase-9 in patients with Alzheimer's disease. *Neurochem Int* 43:191-196.
- Lovell MA, Gabbita SP, Markesbery WR (1999) Increased DNA oxidation and decreased levels of repair products in Alzheimer's disease ventricular CSF. *J Neurochem* 72:771-776.
- Lu X, Liu J, Hou F, Liu Z, Cao X, Seo H, Gao B (2011) Cholesterol induces pancreatic beta cell apoptosis through oxidative stress pathway. *Cell Stress Chaperones* 16:539-548.
- Luo W, Wang W, Li B, Chen Y (2001) [Inhibitory effects of beta-carotene on hepatic cancer cell line SMMC-7721]. *Wei Sheng Yan Jiu* 30:213-214.
- Luo WJ, Wang H, Li H, Kim BS, Shah S, Lee HJ, Thinakaran G, Kim TW, Yu G, Xu H (2003) PEN-2 and APH-1 coordinately regulate proteolytic processing of presenilin 1. *J Biol Chem* 278:7850-7854.
- Lustbader JW, Cirilli M, Lin C, Xu HW, Takuma K, Wang N (2004a) ABAD directly links A $\beta$  to mitochondrial toxicity in Alzheimer's disease. *Science* 304:448-452.
- Lustbader JW, Cirilli M, Lin C, Xu HW, Takuma K, Wang N, Caspersen C, Chen X, Pollak S, Chaney M, Trinchese F, Liu S, Gunn-Moore F, Lue LF, Walker DG, Kuppasamy P, Zewier ZL, Arancio O, Stern D, Yan SS, Wu H (2004b) ABAD directly links Abeta to mitochondrial toxicity in Alzheimer's disease. *Science* 304:448-452.
- Ma G, Li T, Price DL, Wong PC (2005) APH-1a is the principal mammalian APH-1 isoform present in gamma-secretase complexes during embryonic development. *J Neurosci* 25:192-198.
- Ma J, Meng Y, Kwiatkowski DJ, Chen X, Peng H, Sun Q, Zha X, Wang F, Wang Y, Jing Y, Zhang S, Chen R, Wang L, Wu E, Cai G, Malinowska-Kolodziej I, Liao Q, Liu Y, Zhao Y, Xu K, Dai J, Han J, Wu L, Zhao RC, Shen H, Zhang H (2010) Mammalian target of rapamycin regulates murine and human cell differentiation through STAT3/p63/Jagged/Notch cascade. *J Clin Invest* 120:103-114.
- Maccioni RB, Munoz JP, Barbeito L (2001) The molecular bases of Alzheimer's disease and other neurodegenerative disorders. *Arch Med Res* 32:367-381.
- Maekawa F, Minehira K, Kadomatsu K, Pellerin L (2008) Basal and stimulated lactate fluxes in primary cultures of astrocytes are differentially controlled by distinct proteins. *J Neurochem* 107:789-798.

- Maetzler W, Liepelt I, Reimold M, Reischl G, Solbach C, Becker C, Schulte C, Leyhe T, Keller S, Melms A, Gasser T, Berg D (2009) Cortical PIB binding in Lewy body disease is associated with Alzheimer-like characteristics. *Neurobiol Dis* 34:107-112.
- Mahley RW, Nathan BP, Pitas RE (1996) Apolipoprotein E. Structure, function, and possible roles in Alzheimer's disease. *Ann N Y Acad Sci* 777:139-145.
- Manczak M, Anekonda TS, Henson E, Park BS, Quinn J, Reddy PH (2006) Mitochondria are a direct site of A beta accumulation in Alzheimer's disease neurons: implications for free radical generation and oxidative damage in disease progression. *Hum Mol Genet* 15:1437-1449.
- Mann DM, Brown SM, Owen F, Baba M, Iwatsubo T (1998) Amyloid beta protein (A beta) deposition in dementia with Lewy bodies: predominance of A beta 42(43) and paucity of A beta 40 compared with sporadic Alzheimer's disease. *Neuropathol Appl Neurobiol* 24:187-194.
- Marambaud P, Wen PH, Dutt A, Shioi J, Takashima A, Siman R, Robakis NK (2003) A CBP binding transcriptional repressor produced by the PS1/epsilon-cleavage of N-cadherin is inhibited by PS1 FAD mutations. *Cell* 114:635-645.
- Marjaux E, Hartmann D, De Strooper B (2004) Presenilins in memory, Alzheimer's disease, and therapy. *Neuron* 42:189-192.
- Markesbery WR, Lovell MA (1998) Four-hydroxynonenal, a product of lipid peroxidation, is increased in the brain in Alzheimer's disease. *Neurobiol Aging* 19:33-36.
- Martins IJ, Berger T, Sharman MJ, Verdile G, Fuller SJ, Martins RN (2009) Cholesterol metabolism and transport in the pathogenesis of Alzheimer's disease. *J Neurochem* 111:1275-1308.
- Martins IJ, Hone E, Foster JK, Sunram-Lea SI, Gnjec A, Fuller SJ, Nolan D, Gandy SE, Martins RN (2006) Apolipoprotein E, cholesterol metabolism, diabetes, and the convergence of risk factors for Alzheimer's disease and cardiovascular disease. *Mol Psychiatry* 11:721-736.
- Martins RN, Clarnette R, Fisher C, Broe GA, Brooks WS, Montgomery P, Gandy SE (1995) ApoE genotypes in Australia: roles in early and late onset Alzheimer's disease and Down's syndrome. *Neuroreport* 6:1513-1516.
- Martins RN, Harper CG, Stokes GB, Masters CL (1986) Increased cerebral glucose-6-phosphate dehydrogenase activity in Alzheimer's disease may reflect oxidative stress. *J Neurochem* 46:1042-1045.
- Masters CL, Beyreuther K (1995) Molecular neuropathology of Alzheimer's disease. *Arzneimittelforschung* 45:410-412.
- Mastrangelo P, Mathews PM, Chishti MA, Schmidt SD, Gu Y, Yang J, Mazzella MJ, Coomaraswamy J, Horne P, Strome B, Pelly H, Levesque G, Ebeling C, Jiang Y, Nixon RA, Rozmahel R, Fraser PE, St George-Hyslop P, Carlson GA, Westaway D (2005) Dissociated phenotypes in presenilin transgenic mice define functionally distinct gamma-secretases. *Proc Natl Acad Sci U S A* 102:8972-8977.
- Mathis CA, Wang Y, Klunk WE (2004) Imaging beta-amyloid plaques and neurofibrillary tangles in the aging human brain. *Curr Pharm Des* 10:1469-1492.
- Matsuda K, Yoshida K, Taya Y, Nakamura K, Nakamura Y, Arakawa H (2002) p53AIP1 regulates the mitochondrial apoptotic pathway. *Cancer Res* 62:2883-2889.
- Matsudaira H, Asakura T, Aoki K, Searashi Y, Matsuura T, Nakajima H, Tajiri H, Ohkawa K (2010) Target chemotherapy of anti-CD147 antibody-labeled liposome encapsulated GSH-DXR conjugate on CD147 highly expressed carcinoma cells. *Int J Oncol* 36:77-83.

- Mattson MP, Chan SL (2003) Neuronal and glial calcium signaling in Alzheimer's disease. *Cell Calcium* 34:385-397.
- Mattson MP, Tomaselli KJ, Rydel RE (1993) Calcium-destablizing and neurodegenerative effect of aggregate beta-amyloid peptide are attenuated by basic FGF. *Brain Res* 35-49.
- McGuinness B, Craig D, Bullock R, Passmore P (2009) Statins for the prevention of dementia. *Cochrane Database Syst Rev* CD003160.
- McLean MP, Puryear TK, Khan I, Azhar S, Billheimer JT, Orly J, Gibori G (1989) Estradiol regulation of sterol carrier protein-2 independent of cytochrome P450 side-chain cleavage expression in the rat corpus luteum. *Endocrinology* 125:1337-1344.
- Meeuwssen S, Persoon-Deen C, Bsibsi M, Ravid R, van Noort JM (2003) Cytokine, chemokine and growth factor gene profiling of cultured human astrocytes after exposure to proinflammatory stimuli. *Glia* 43:243-253.
- Mei S, Gu H, Yang X, Guo H, Liu Z, Cao W (2012) Prolonged Exposure to Insulin Induces Mitochondrion-Derived Oxidative Stress through Increasing Mitochondrial Cholesterol Content in Hepatocytes. *Endocrinology*.
- Meloni BP, Van Dyk D, Cole R, Knuckey NW (2005) Proteome analysis of cortical neuronal cultures following cycloheximide, heat stress and MK801 preconditioning. *Proteomics* 5:4743-4753.
- Mendis-Handagama SM, Watkins PA, Gelber SJ, Scallen TJ (1998) The effect of chronic luteinizing hormone treatment on adult rat Leydig cells. *Tissue Cell* 30:64-73.
- Metrailler-Ruchonnet I, Pagano A, Carnesecchi S, Khatib K, Herrera P, Donati Y, Bron C, Barazzone C (2010) Bcl-2 overexpression in type II epithelial cells does not prevent hyperoxia-induced acute lung injury in mice. *Am J Physiol Lung Cell Mol Physiol* 299:L312-322.
- Mihovilovic M, Robinette JB, DeKroon RM, Sullivan PM, Strittmatter WJ (2007) High-fat/high-cholesterol diet promotes a S1P receptor-mediated antiapoptotic activity for VLDL. *J Lipid Res* 48:806-815.
- Miida T, Takahashi A, Tanabe N, Ikeuchi T (2005) Can statin therapy really reduce the risk of Alzheimer's disease and slow its progression? *Curr Opin Lipidol* 16:619-623.
- Mistur R, Mosconi L, Santi SD, Guzman M, Li Y, Tsui W, de Leon MJ (2009) Current Challenges for the Early Detection of Alzheimer's Disease: Brain Imaging and CSF Studies. *J Clin Neurol* 5:153-166.
- Mitsuda N, Roses AD, Vittek MP (1997) Transcriptional regulation of the mouse presenilin-1 gene. *J Biol Chem* 272:23489-23497.
- Miyauchi T, Jimma F, Igakura T, Yu S, Ozawa M, Muramatsu T (1995) Structure of the mouse basigin gene, a unique member of the immunoglobulin superfamily. *J Biochem* 118:717-724.
- Miyauchi T, Kanekura T, Yamaoka A, Ozawa M, Miyazawa S, Muramatsu T (1990) Basigin, a new, broadly distributed member of the immunoglobulin superfamily, has strong homology with both the immunoglobulin V domain and the beta-chain of major histocompatibility complex class II antigen. *J Biochem* 107:316-323.
- Miyauchi T, Masuzawa Y, Muramatsu T (1991) The basigin group of the immunoglobulin superfamily: complete conservation of a segment in and around transmembrane domains of human and mouse basigin and chicken HT7 antigen. *J Biochem* 110:770-774.



- Moncecchi D, Murphy EJ, Prows DR, Schroeder F (1996) Sterol carrier protein-2 expression in mouse L-cell fibroblasts alters cholesterol uptake. *Biochim Biophys Acta* 1302:110-116.
- Moonsom S, Tayapiwatana C, Wongkham S, Kongtawelert P, Kasinrerk W (2010) A Competitive ELISA for quantifying serum CD147: reduction of soluble CD147 levels in cancer patient sera. *Hybridoma (Larchmt)* 29:45-52.
- Morais VA, Crystal AS, Pijak DS, Carlin D, Costa J, Lee VM, Doms RW (2003) The transmembrane domain region of nicastrin mediates direct interactions with APH-1 and the gamma-secretase complex. *J Biol Chem* 278:43284-43291.
- Morgan D, Diamond DM, Gottschall PE, Ugen KE, Dickey C, Hardy J, Duff K, Jantzen P, DiCarlo G, Wilcock D, Connor K, Hatcher J, Hope C, Gordon M, Arendash GW (2000) A beta peptide vaccination prevents memory loss in an animal model of Alzheimer's disease. *Nature* 408:982-985.
- Mori TA, Burke V, Puddey I, Irish A, Cowpland CA, Beilin L, Dogra G, Watts GF (2009) The effects of [omega]3 fatty acids and coenzyme Q10 on blood pressure and heart rate in chronic kidney disease: a randomized controlled trial. *J Hypertens* 27:1863-1872.
- Morris JC (1997) Clinical dementia rating: a reliable and valid diagnostic and staging measure for dementia of the Alzheimer type. *Int Psychogeriatr* 9 Suppl 1:173-176; discussion 177-178.
- Mosconi L, Mistur R, Switalski R, Tsui WH, Glodzik L, Li Y, Pirraglia E, De Santi S, Reisberg B, Wisniewski T, de Leon MJ (2009) FDG-PET changes in brain glucose metabolism from normal cognition to pathologically verified Alzheimer's disease. *Eur J Nucl Med Mol Imaging* 36:811-822.
- Moseley AE, Williams MT, Schaefer TL, Bohanan CS, Neumann JC, Behbehani MM, Vorhees CV, Lingrel JB (2007) Deficiency in Na,K-ATPase alpha isoform genes alters spatial learning, motor activity, and anxiety in mice. *J Neurosci* 27:616-626.
- Muller WE, Kirsch C, Eckert GP (2001) Membrane-disordering effects of beta-amyloid peptides. *Biochem Soc Trans* 29:617-623.
- Mullis KB, Faloona FA (1987) Specific synthesis of DNA in vitro via a polymerase-catalyzed chain reaction. *Methods Enzymol* 155:335-350.
- Muramatsu T, Miyauchi T (2003) Basigin (CD147): a multifunctional transmembrane protein involved in reproduction, neural function, inflammation and tumor invasion. *Histol Histopathol* 18:981-987.
- Murphy EJ, Schroeder F (1997) Sterol carrier protein-2 mediated cholesterol esterification in transfected L-cell fibroblasts. *Biochim Biophys Acta* 1345:283-292.
- Nabeshima K, Iwasaki H, Koga K, Hojo H, Suzumiya J, Kikuchi M (2006a) Emmprin (basigin/CD147): matrix metalloproteinase modulator and multifunctional cell recognition molecule that plays a critical role in cancer progression. *Pathol Int* 56:359-367.
- Nabeshima K, Iwasaki H, Nishio J, Koga K, Shishime M, Kikuchi M (2006b) Expression of emmprin and matrix metalloproteinases (MMPs) in peripheral nerve sheath tumors: emmprin and membrane-type (MT)1-MMP expressions are associated with malignant potential. *Anticancer Res* 26:1359-1367.
- Nagele RG, Clifford PM, Siu G, Levin EC, Acharya NK, Han M, Kosciuk MC, Venkataraman V, Zavareh S, Zarrabi S, Kinsler K, Thaker NG, Nagele EP, Dash J, Wang HY, Levitas A (2011) Brain-reactive autoantibodies prevalent in human sera increase intraneuronal amyloid-beta(1-42) deposition. *J Alzheimers Dis* 25:605-622.

- Nagerl UV, Eberhorn N, Cambridge SB, Bonhoeffer T (2004) Bidirectional activity-dependent morphological plasticity in hippocampal neurons. *Neuron* 44:759-767.
- Nahalkova J, Volkmann I, Aoki M, Winblad B, Bogdanovic N, Tjernberg LO, Behbahani H (2009) CD147, a gamma-secretase associated protein is upregulated in Alzheimer's disease brain and its cellular trafficking is affected by presenilin-2. *Neurochem Int*.
- Nahalkova J, Volkmann I, Aoki M, Winblad B, Bogdanovic N, Tjernberg LO, Behbahani H (2010) CD147, a gamma-secretase associated protein is upregulated in Alzheimer's disease brain and its cellular trafficking is affected by presenilin-2. *Neurochem Int* 56:67-76.
- Nahreini P, Hovland AR, Kumar B, Andreatta C, Edwards-Prasad J, Prasad KN (2001) Effects of altered cyclophilin A expression on growth and differentiation of human and mouse neuronal cells. *Cell Mol Neurobiol* 21:65-79.
- Nalivaeva NN, Fisk LR, Belyaev ND, Turner AJ (2008) Amyloid-degrading enzymes as therapeutic targets in Alzheimer's disease. *Curr Alzheimer Res* 5:212-224.
- Naruhashi K, Kadomatsu K, Igakura T, Fan QW, Kuno N, Muramatsu H, Miyauchi T, Hasegawa T, Itoh A, Muramatsu T, Nabeshima T (1997) Abnormalities of sensory and memory functions in mice lacking Bsg gene. *Biochem Biophys Res Commun* 236:733-737.
- Naslund J, Haroutunian V, Mohs R, Davis KL, Davies P, Greengard P, Buxbaum JD (2000) Correlation between elevated levels of amyloid beta-peptide in the brain and cognitive decline. *JAMA* 283:1571-1577.
- Nehme CL, Fayos BE, Bartles JR (1995) Distribution of the integral plasma membrane glycoprotein CE9 (MRC OX-47) among rat tissues and its induction by diverse stimuli of metabolic activation. *Biochem J* 310 ( Pt 2):693-698.
- Nicholls DG, Budd SL (2000) Mitochondria and neuronal survival. *Physiol Rev Neurosci* 80:315-360.
- Nie R, Xie S, Du B, Liu X, Deng B, Wang J (2009) Extracellular matrix metalloproteinase inducer (EMMPRIN) is increased in human left ventricle after acute myocardial infarction. *Arch Med Res* 40:605-611.
- Nilsson D, Sunnerhagen P (2011) Cellular stress induces cytoplasmic RNA granules in fission yeast. *RNA* 17:120-133.
- Nishimoto I, Okamoto T, Matsuura Y, Takahashi S, Murayama Y, Ogata E (1993) Alzheimer amyloid protein precursor complexes with brain GTP-binding protein G(o). *Nature* 362:75-79.
- Nixon RA (2004) Niemann-Pick Type C disease and Alzheimer's disease: the APP-endosome connection fattens up. *Am J Pathol* 164:757-761.
- Notkola IL, Sulkava R, Pekkanen J, Erkinjuntti T, Ehnholm C, Kivinen P, Tuomilehto J, Nissinen A (1998) Serum total cholesterol, apolipoprotein E epsilon 4 allele, and Alzheimer's disease. *Neuroepidemiology* 17:14-20.
- Ohba T, Holt JA, Billheimer JT, Strauss JF, 3rd (1995) Human sterol carrier protein x/sterol carrier protein 2 gene has two promoters. *Biochemistry* 34:10660-10668.
- Ohba T, Rennert H, Pfeifer SM, He Z, Yamamoto R, Holt JA, Billheimer JT, Strauss JF, 3rd (1994) The structure of the human sterol carrier protein X/sterol carrier protein 2 gene (SCP-2). *Genomics* 24:370-374.
- Oikawa N, Ogino K, Masumoto T, Yamaguchi H, Yanagisawa K (2010) Gender effect on the accumulation of hyperphosphorylated tau in the brain of locus-coeruleus-injured APP-transgenic mouse. *Neurosci Lett* 468:243-247.
- Okamoto M, Sakiyama J, Kurazono S, Mori S, Nakata Y, Nakaya N, Oohira A (2001) Developmentally regulated expression of brain-specific chondroitin sulfate

- proteoglycans, neurocan and phosphacan, in the postnatal rat hippocampus. *Cell Tissue Res* 306:217-229.
- Oksman M, Iivonen H, Högges E, Amtul Z, Penke B, Leenders I, Broersen L, Lutjohann D, Hartmann T, Tanila H (2006) Impact of different saturated fatty acid, polyunsaturated fatty acid and cholesterol containing diets on beta-amyloid accumulation in APP/PS1 transgenic mice. *Neurobiol Dis* 23:563-572.
- Olaisen B, Teisberg P, Gedde-Dahl T, Jr. (1982) The locus for apolipoprotein E (apoE) is linked to the complement component C3 (C3) locus on chromosome 19 in man. *Hum Genet* 62:233-236.
- Oliveros LB, Videla AM, Gimenez MS (2004) Effect of dietary fat saturation on lipid metabolism, arachidonic acid turnover and peritoneal macrophage oxidative stress in mice. *Braz J Med Biol Res* 37:311-320.
- Palacino JJ, Berechid BE, Alexander P, Eckman C, Younkin S, Nye JS, Wolozin B (2000) Regulation of amyloid precursor protein processing by presenilin 1 (PS1) and PS2 in PS1 knockout cells. *J Biol Chem* 275:215-222.
- Palmblad M, Westlind-Danielsson A, Bergquist J (2002) Oxidation of Methionine 35 Attenuates Formation of Amyloid -Peptide 1-40 Oligomers. *J Biol Chem* 277:19506-19510.
- Papassotiropoulos A, Lutjohann D, Bagli M, Locatelli S, Jessen F, Buschfort R, Ptak U, Bjorkhem I, von Bergmann K, Heun R (2002) 24S-hydroxycholesterol in cerebrospinal fluid is elevated in early stages of dementia. *J Psychiatr Res* 36:27-32.
- Patel S, O'Malley S, Connolly B, Liu W, Hargreaves R, Sur C, Gibson RE (2006) In vitro characterization of a gamma-secretase radiotracer in mammalian brain. *J Neurochem* 96:171-178.
- Peano A, Min AM, Beccati M, Menzano A, Pasquetti M, Gallo MG (2011) Use of western blot to study *Microsporum canis* antigenic proteins in canine dermatophytosis. *Mycoses* 54:223-229.
- Pereira C, Ferreira E, Cardoso SM, de Oliveira CR (2004) Cell degeneration induced by amyloid-beta peptides: implications for Alzheimer's disease. *J Mol Neurosci* 23:97-104.
- Perez JL, Carrero I, Gonzalo P, Arevalo-Serrano J, Sanz-Anquela JM, Ortega J, Rodriguez M, Gonzalo-Ruiz A (2010) Soluble oligomeric forms of beta-amyloid (A $\beta$ ) peptide stimulate A $\beta$  production via astrogliosis in the rat brain. *Exp Neurol* 223:410-421.
- Pericak-Vance MA, Bebout JL, Gaskell PC, Jr., Yamaoka LH, Hung WY, Alberts MJ, Walker AP, Bartlett RJ, Haynes CA, Welsh KA, et al. (1991) Linkage studies in familial Alzheimer disease: evidence for chromosome 19 linkage. *Am J Hum Genet* 48:1034-1050.
- Periz G, Fortini ME (2004) Functional reconstitution of gamma-secretase through coordinated expression of presenilin, nicastrin, Aph-1, and Pen-2. *J Neurosci Res* 77:309-322.
- Perkins D, Pereira EF, Aurelian L (2003) The herpes simplex virus type 2 R1 protein kinase (ICP10 PK) functions as a dominant regulator of apoptosis in hippocampal neurons involving activation of the ERK survival pathway and upregulation of the antiapoptotic protein Bag-1. *J Virol* 77:1292-1305.
- Perl DP (2010) Neuropathology of Alzheimer's disease. *Mt Sinai J Med* 77:32-42.
- Perry G, Castellani RJ, Smith MA, Harris PL, Kubat Z, Ghanbari K, Jones PK, Cordone G, Tabaton M, Wolozin B, Ghanbari H (2003) Oxidative damage in the olfactory system in Alzheimer's disease. *Acta Neuropathol* 106:552-556.
- Philips N, Smith J, Keller T, Gonzalez S (2003) Predominant effects of *Polypodium leucotomos* on membrane integrity, lipid peroxidation, and expression of elastin

- and matrixmetalloproteinase-1 in ultraviolet radiation exposed fibroblasts, and keratinocytes. *J Dermatol Sci* 32:1-9.
- Pike CJ, Carroll JC, Rosario ER, Barron AM (2009) Protective actions of sex steroid hormones in Alzheimer's disease. *Front Neuroendocrinol* 30:239-258.
- Pistol G, Matache C, Calugaru A, Stavaru C, Tanaseanu S, Ionescu R, Dumitrache S, Stefanescu M (2007) Roles of CD147 on T lymphocytes activation and MMP-9 secretion in systemic lupus erythematosus. *J Cell Mol Med* 11:339-348.
- Pitas RE, Boyles JK, Lee SH, Hui D, Weisgraber KH (1987) Lipoproteins and their receptors in the central nervous system. Characterization of the lipoproteins in cerebrospinal fluid and identification of apolipoprotein B,E(LDL) receptors in the brain. *J Biol Chem* 262:14352-14360.
- Placanica L, Tarassishin L, Yang G, Peethumongsin E, Kim SH, Zheng H, Sisodia SS, Li YM (2009) Pen2 and presenilin-1 modulate the dynamic equilibrium of presenilin-1 and presenilin-2 gamma-secretase complexes. *J Biol Chem* 284:2967-2977.
- Podlisny MB, Citron M, Amarante P, Sherrington R, Xia W, Zhang J, Diehl T, Levesque G, Fraser P, Haass C, Koo EH, Seubert P, St George-Hyslop P, Teplow DB, Selkoe DJ (1997) Presenilin proteins undergo heterogeneous endoproteolysis between Thr291 and Ala299 and occur as stable N- and C-terminal fragments in normal and Alzheimer brain tissue. *Neurobiol Dis* 3:325-337.
- Poirier J, Davignon J, Bouthillier D, Kogan S, Bertrand P, Gauthier S (1993) Apolipoprotein E polymorphism and Alzheimer's disease. *Lancet* 342:697-699.
- Ponte P, Gonzalez-DeWhitt P, Schilling J, Miller J, Hsu D, Greenberg B, Davis K, Wallace W, Lieberburg I, Fuller F (1988) A new A4 amyloid mRNA contains a domain homologous to serine proteinase inhibitors. *Nature* 331:525-527.
- Popp GM, Graebert KS, Pietrzik CU, Rosentreter SM, Lemansky P, Herzog V (1996) Growth regulation of rat thyrocytes (FRTL-5 cells) by the secreted ectodomain of beta-amyloid precursor-like proteins. *Endocrinology* 137:1975-1983.
- Prince JA, Feuk L, Gu HF, Johansson B, Gatz M, Blennow K, Brookes AJ (2003) Genetic variation in a haplotype block spanning IDE influences Alzheimer disease. *Hum Mutat* 22:363-371.
- Prokop S, Shirotani K, Edbauer D, Haass C, Steiner H (2004) Requirement of PEN-2 for stabilization of the presenilin N-/C-terminal fragment heterodimer within the gamma-secretase complex. *J Biol Chem* 279:23255-23261.
- Puglielli L, Rigotti A, Greco AV, Santos MJ, Nervi F (1995) Sterol carrier protein-2 is involved in cholesterol transfer from the endoplasmic reticulum to the plasma membrane in human fibroblasts. *J Biol Chem* 270:18723-18726.
- Qi-Takahara Y, Morishima-Kawashima M, Tanimura Y, Dolios G, Hirotani N, Horikoshi Y, Kametani F, Maeda M, Saido TC, Wang R, Ihara Y (2005) Longer forms of amyloid beta protein: implications for the mechanism of intramembrane cleavage by gamma-secretase. *J Neurosci* 25:436-445.
- Qian AR, Zhang W, Cao JP, Yang PF, Gao X, Wang Z, Xu HY, Weng YY, Shang P (2008) Downregulation of CD147 expression alters cytoskeleton architecture and inhibits gelatinase production and SAPK pathway in human hepatocellular carcinoma cells. *J Exp Clin Cancer Res* 27:50.
- Racchi M, R B, N S, P I, G F, R P (1997) Secretory processing of amyloid precursor protein is inhibited by increase in cellular cholesterol content. *Biochem J* 322:893-898.
- Rall SC, Jr., Weisgraber KH, Innerarity TL, Mahley RW (1982) Structural basis for receptor binding heterogeneity of apolipoprotein E from type III hyperlipoproteinemic subjects. *Proc Natl Acad Sci U S A* 79:4696-4700.

- Ramana MV, Balakrishna K, Murali HC, Batra HV (2011) Multiplex PCR-based strategy to detect contamination with mycotoxigenic *Fusarium* species in rice and finger millet collected from southern India. *J Sci Food Agric* 91:1666-1673.
- Rao KS (2001) Mental health around the world. *J Indian Med Assoc* 99:214-216, 218-219.
- Ray WJ, Yao M, Mumm J, Schroeter EH, Saftig P, Wolfe M, Selkoe DJ, Kopan R, Goate AM (1999) Cell surface presenilin-1 participates in the gamma-secretase-like proteolysis of Notch. *J Biol Chem* 274:36801-36807.
- Refolo LM, Malester B, LaFrancois J, Bryant-Thomas T, Wang R, Tint GS, Sambamurti K, Duff K, Pappolla MA (2000a) Hypercholesterolemia accelerates the Alzheimer's amyloid pathology in a transgenic mouse model. *Neurobiol Dis* 7:321-331.
- Refolo LM, Pappolla MA, LaFrancois J, Malester B, Schmidt SD, Thomas-Bryant T, Tint GS, Wang R, Mercken M, Petanceska SS, Duff KE (2001) A cholesterol-lowering drug reduces beta-amyloid pathology in a transgenic mouse model of Alzheimer's disease. *Neurobiol Dis* 8:890-899.
- Refolo LM, Pappolla MA, Malester B, LaFrancois J, Bryant-Thomas T, Wang R, Tint GS, Sambamurti K, Duff K (2000b) Hypercholesterolemia accelerates the Alzheimer's amyloid pathology in a transgenic mouse model. *Neurobiology of Disease* 321-331.
- Refolo LM, Sambamurti K, Efthimiopoulos S, Pappolla MA, Robakis NK (1995) Evidence that secretase cleavage of cell surface Alzheimer amyloid precursor occurs after normal endocytic internalization. *J Neurosci Res* 40:694-706.
- Reimers N, Zafrakas K, Assmann V, Egen C, Riethdorf L, Riethdorf S, Berger J, Ebel S, Janicke F, Sauter G, Pantel K (2004) Expression of extracellular matrix metalloproteinases inducer on micrometastatic and primary mammary carcinoma cells. *Clin Cancer Res* 10:3422-3428.
- Ren S, Hylemon P, Marques D, Hall E, Redford K, Gil G, Pandak WM (2004) Effect of increasing the expression of cholesterol transporters (StAR, MLN64, and SCP-2) on bile acid synthesis. *J Lipid Res* 45:2123-2131.
- Riccio A, Ahn S, Davenport CM, Blendy JA, Ginty DD (1999) Mediation by a CREB family transcription factor of NGF-dependent survival of sympathetic neurons. *Science* 286:2358-2361.
- Richardson JC, Kendal CE, Anderson R, Priest F, Gower E, Soden P, Gray R, Topps S, Howlett DR, Lavender D, Clarke NJ, Barnes JC, Haworth R, Stewart MG, Rupniak HT (2003) Ultrastructural and behavioural changes precede amyloid deposition in a transgenic model of Alzheimer's disease. *Neuroscience* 122:213-228.
- Ringman JM, Pope W, Salamon N (2010) Insensitivity of visual assessment of hippocampal atrophy in familial Alzheimer's disease. *J Neurol* 257:839-842.
- Roff CF, Pastuszyn A, Strauss JF, 3rd, Billheimer JT, Vanier MT, Brady RO, Scallen TJ, Pentchev PG (1992) Deficiencies in sex-regulated expression and levels of two hepatic sterol carrier proteins in a murine model of Niemann-Pick type C disease. *J Biol Chem* 267:15902-15908.
- Roheim PS, Carey M, Forte T, Vega GL (1979) Apolipoproteins in human cerebrospinal fluid. *Proc Natl Acad Sci U S A* 76:4646-4649.
- Romi F, Helgeland G, Gilhus NE (2012) Serum levels of matrix metalloproteinases: implications in clinical neurology. *Eur Neurol* 67:121-128.
- Rosario ER, Carroll J, Pike CJ (2010) Testosterone regulation of Alzheimer-like neuropathology in male 3xTg-AD mice involves both estrogen and androgen pathways. *Brain Res* 1359:281-290.

- Roses AD (1994) Apolipoprotein E is a relevant susceptibility gene that affects the rate of expression of Alzheimer's disease. *Neurobiol Aging* 15 Suppl 2:S165-167.
- Roses AD (1997) Apolipoprotein E, a gene with complex biological interactions in the aging brain. *Neurobiol Dis* 4:170-185.
- Rossor MN, Fox NC, Beck J, Campbell TC, Collinge J (1996) Incomplete penetrance of familial Alzheimer's disease in a pedigree with a novel presenilin-1 gene mutation. *Lancet* 347:1560.
- Rozmahel R, Mount HT, Chen F, Nguyen V, Huang J, Erdebil S, Liauw J, Yu G, Hasegawa H, Gu Y, Song YQ, Schmidt SD, Nixon RA, Mathews PM, Bergeron C, Fraser P, Westaway D, St George-Hyslop P (2002) Alleles at the Nicastrin locus modify presenilin 1- deficiency phenotype. *Proc Natl Acad Sci U S A* 99:14452-14457.
- Runz H, J R, I T, M dB, K B, R P (2002) Inhibition of intracellular cholesterol transport alters presenilin localization and amyloid precursor protein processing in neuronal cells. *Journal of Neuroscience* 22:1679-1689.
- Sahathevan R, Brodtmann A, Donnan GA (2012) Dementia, stroke, and vascular risk factors; a review. *Int J Stroke* 7:61-73.
- Saiki RK, Gelfand DH, Stoffel S, Scharf SJ, Higuchi R, Horn GT, Mullis KB, Erlich HA (1988) Primer-directed enzymatic amplification of DNA with a thermostable DNA polymerase. *Science* 239:487-491.
- Saito S, Araki W (2005) Expression profiles of two human A $\beta$ -1 genes and their roles in formation of presenilin complexes. *Biochem Biophys Res Commun* 327:18-22.
- Sakai J, Duncan EA, Rawson RB, Hua X, Brown MS, Goldstein JL (1996) Sterol-regulated release of SREBP-2 from cell membranes requires two sequential cleavages, one within a transmembrane segment. *Cell* 85:1037-1046.
- Salahudeen AK, Joshi M, Jenkins JK (2001) Apoptosis versus necrosis during cold storage and rewarming of human renal proximal tubular cells. *Transplantation* 72:798-804.
- Sameshima T, Nabeshima K, Toole BP, Inoue T, Yokogami K, Nakano S, Ohi T, Wakisaka S (2003) Correlation of emmprin expression in vascular endothelial cells with blood-brain-barrier function: a study using magnetic resonance imaging enhanced by Gd-DTPA and immunohistochemistry in brain tumors. *Virchows Arch* 442:577-584.
- Sameshima T, Nabeshima K, Toole BP, Yokogami K, Okada Y, Goya T, Kono M, Wakisaka S (2000) Expression of emmprin (CD147), a cell surface inducer of matrix metalloproteinases, in normal human brain and gliomas. *Int J Cancer* 88:21-27.
- Sanan DA, Weisgraber KH, Russell SJ, Mahley RW, Huang D, Saunders A, Schmechel D, Wisniewski T, Frangione B, Roses AD, et al. (1994) Apolipoprotein E associates with beta amyloid peptide of Alzheimer's disease to form novel monofibrils. Isoform apoE4 associates more efficiently than apoE3. *J Clin Invest* 94:860-869.
- Sanderson MP, Erickson SN, Gough PJ, Garton KJ, Wille PT, Raines EW, Dunbar AJ, Dempsey PJ (2005) ADAM10 mediates ectodomain shedding of the betacellulin precursor activated by p-aminophenylmercuric acetate and extracellular calcium influx. *J Biol Chem* 280:1826-1837.
- Sawane MV, Kaore SB, Gaikwad RD, Patil PM, Patankar SS, Deshkar AM (2002) Seminal LDH-C4 isoenzyme and sperm mitochondrial activity: a study in male partners of infertile couples. *Indian J Med Sci* 56:560-566.

- Sayre LM, Zelasko DA, Harris PL, Perry G, Salomon RG, Smith MA (1997) 4-Hydroxynonenal-derived advanced lipid peroxidation end products are increased in Alzheimer's disease. *J Neurochem* 68:2092-2097.
- Schlosshauer B, Bauch H, Frank R (1995) Neurothelin: amino acid sequence, cell surface dynamics and actin colocalization. *Eur J Cell Biol* 68:159-166.
- Schmechel A, Strauss M, Schlicksupp A, Pipkorn R, Haass C, Bayer TA, Multhaup G (2004) Human BACE forms dimers and colocalizes with APP. *J Biol Chem* 279:39710-39717.
- Schneider A, Schulz-Schaeffer W, Hartmann T, Schulz JB, Simons M (2006) Cholesterol depletion reduces aggregation of amyloid-beta peptide in hippocampal neurons. *Neurobiol Dis* 23:573-577.
- Schon EA, Area-Gomez E (2010) Is Alzheimer's disease a disorder of mitochondria-associated membranes? *J Alzheimers Dis* 20 Suppl 2:S281-292.
- Schonlein C, Probst A, Huber G (1993) Characterization of proteases with the specificity to cleave at the secretase-site of beta-APP. *Neurosci Lett* 161:33-36.
- Schroeder F, Atshaves BP, McIntosh AL, Gallegos AM, Storey SM, Parr RD, Jefferson JR, Ball JM, Kier AB (2007) Sterol carrier protein-2: new roles in regulating lipid rafts and signaling. *Biochim Biophys Acta* 1771:700-718.
- Schroeder RJ, Ahmed SN, Zhu Y, London E, Brown DA (1998) Cholesterol and sphingolipid enhance the Triton X-100 insolubility of glycosylphosphatidylinositol-anchored proteins by promoting the formation of detergent-insoluble ordered membrane domains. *J Biol Chem* 273:1150-1157.
- Schroeter EH, Ilagan MX, Brunkan AL, Hecimovic S, Li YM, Xu M, Lewis HD, Saxena MT, De Strooper B, Coonrod A, Tomita T, Iwatsubo T, Moore CL, Goate A, Wolfe MS, Shearman M, Kopan R (2003) A presenilin dimer at the core of the gamma-secretase enzyme: insights from parallel analysis of Notch 1 and APP proteolysis. *Proc Natl Acad Sci U S A* 100:13075-13080.
- Schwientek P, Szczepanowski R, Ruckert C, Stoye J, Puhler A (2011) Sequencing of high G+C microbial genomes using the ultrafast pyrosequencing technology. *J Biotechnol* 155:68-77.
- Seeger M, Nordstedt C, Petanceska S, Kovacs DM, Gouras GK, Hahne S, Fraser P, Levesque L, Czernik AJ, George-Hyslop PS, Sisodia SS, Thinakaran G, Tanzi RE, Greengard P, Gandy S (1997) Evidence for phosphorylation and oligomeric assembly of presenilin 1. *Proc Natl Acad Sci U S A* 94:5090-5094.
- Seiffert D, Bradley JD, Rominger CM, Rominger DH, Yang F, Meredith JE, Jr., Wang Q, Roach AH, Thompson LA, Spitz SM, Higaki JN, Prakash SR, Combs AP, Copeland RA, Arneric SP, Hartig PR, Robertson DW, Cordell B, Stern AM, Olson RE, Zaczek R (2000) Presenilin-1 and -2 are molecular targets for gamma-secretase inhibitors. *J Biol Chem* 275:34086-34091.
- Seko Y, Fujimura T, Taka H, Mineki R, Murayama K, Nagai R (2004) Hypoxia followed by reoxygenation induces secretion of cyclophilin A from cultured rat cardiac myocytes. *Biochem Biophys Res Commun* 317:162-168.
- Serneels L, De Jaegere T, Craessaerts K, Horre K, Jorissen E, Tousseyn T, Hebert S, Coolen M, Martens G, Zwijsen A, Annaert W, Hartmann D, De Strooper B (2005) Differential contribution of the three Aph1 genes to gamma-secretase activity in vivo. *Proc Natl Acad Sci U S A* 102:1719-1724.
- Serneels L, Van Biervliet J, Craessaerts K, De Jaegere T, Horre K, Van Houtvin T, Esselmann H, Paul S, Schafer MK, Berezovska O, Hyman BT, Sprangers B, Sciot R, Moons L, Jucker M, Yang Z, May PC, Karran E, Wiltfang J, D'Hooge R, De Strooper B (2009) gamma-Secretase heterogeneity in the Aph1 subunit: relevance for Alzheimer's disease. *Science* 324:639-642.

- Seshadri S, Fitzpatrick AL, Ikram MA, DeStefano AL, Gudnason V, Boada M, Bis JC, Smith AV, Carassquillo MM, Lambert JC, Harold D, Schrijvers EM, Ramirez-Lorca R, Debette S, Longstreth WT, Jr., Janssens AC, Pankratz VS, Dartigues JF, Hollingworth P, Aspelund T, Hernandez I, Beiser A, Kuller LH, Koudstaal PJ, Dickson DW, Tzourio C, Abraham R, Antunez C, Du Y, Rotter JJ, Aulchenko YS, Harris TB, Petersen RC, Berr C, Owen MJ, Lopez-Arrieta J, Varadarajan BN, Becker JT, Rivadeneira F, Nalls MA, Graff-Radford NR, Champion D, Auerbach S, Rice K, Hofman A, Jonsson PV, Schmidt H, Lathrop M, Mosley TH, Au R, Psaty BM, Uitterlinden AG, Farrer LA, Lumley T, Ruiz A, Williams J, Amouyel P, Yoonkin SG, Wolf PA, Launer LJ, Lopez OL, van Duijn CM, Breteler MM (2010) Genome-wide analysis of genetic loci associated with Alzheimer disease. *JAMA* 303:1832-1840.
- Seulberger H, Lottspeich F, Risau W (1990) The inducible blood--brain barrier specific molecule HT7 is a novel immunoglobulin-like cell surface glycoprotein. *EMBO J* 9:2151-2158.
- Sexena N, Bhatia M, Yoshi YK, Garg PK, Tandon RK (2001) Utility of P300 auditory event related potential in detecting cognitive dysfunction in patients with cirrhosis of the liver. *Neurol India* 49:350-354.
- Shackel NA, McGuinness PH, Abbott CA, Gorrell MD, McCaughan GW (2002) Insights into the pathobiology of hepatitis C virus-associated cirrhosis: analysis of intrahepatic differential gene expression. *Am J Pathol* 160:641-654.
- Shah S, Lee SF, Tabuchi K, Hao YH, Yu C, LaPlant Q, Ball H, Dann CE, 3rd, Sudhof T, Yu G (2005) Nicastrin functions as a gamma-secretase-substrate receptor. *Cell* 122:435-447.
- Sharman MJ, Morici M, Hone E, Berger T, Taddei K, Martins IJ, Lim WL, Singh S, Wenk MR, Ghiso J, Buxbaum JD, Gandy S, Martins RN (2010) APOE genotype results in differential effects on the peripheral clearance of amyloid-beta42 in APOE knock-in and knock-out mice. *J Alzheimers Dis* 21:403-409.
- Shen J, Bronson RT, Chen DF, Xia W, Selkoe DJ, Tonegawa S (1997) Skeletal and CNS defects in Presenilin-1-deficient mice. *Cell* 89:629-639.
- Shepardson NE, Shankar GM, Selkoe DJ (2011a) Cholesterol level and statin use in Alzheimer disease: I. Review of epidemiological and preclinical studies. *Arch Neurol* 68:1239-1244.
- Shepardson NE, Shankar GM, Selkoe DJ (2011b) Cholesterol level and statin use in Alzheimer disease: II. Review of human trials and recommendations. *Arch Neurol* 68:1385-1392.
- Sherrington R, Froelich S, Sorbi S, Champion D, Chi H, Rogaeva EA, Levesque G, Rogaev EI, Lin C, Liang Y, Ikeda M, Mar L, Brice A, Agid Y, Percy ME, Clerget-Darpoux F, Piacentini S, Marcon G, Nacmias B, Amaducci L, Frebourg T, Lannfelt L, Rommens JM, St George-Hyslop PH (1996) Alzheimer's disease associated with mutations in presenilin 2 is rare and variably penetrant. *Hum Mol Genet* 5:985-988.
- Sherrington R, Rogaev EI, Liang Y, Rogaeva EA, Levesque G, Ikeda M, Chi H, Lin C, Li G, Holman K, et al. (1995) Cloning of a gene bearing missense mutations in early-onset familial Alzheimer's disease. *Nature* 375:754-760.
- Sherry B, Yarlett N, Strupp A, Cerami A (1992) Identification of cyclophilin as a proinflammatory secretory product of lipopolysaccharide-activated macrophages. *Proc Natl Acad Sci U S A* 89:3511-3515.
- Shie F-S, Jin L-W, Cook DG, Leverenz JB, LeBoeuf RC (2002) Diet-induced hypercholesterolemia enhances brain A $\beta$  accumulation in transgenic mice. *NeuroReport* 13:455-459.



- Shirozu M, Tada H, Tashiro K, Nakamura T, Lopez ND, Nazarea M, Hamada T, Sato T, Nakano T, Honjo T (1996) Characterization of novel secreted and membrane proteins isolated by the signal sequence trap method. *Genomics* 37:273-280.
- Short RA, Bowen RL, O'Brien PC, Graff-Radford NR (2001) Elevated gonadotropin levels in patients with Alzheimer disease. *Mayo Clin Proc* 76:906-909.
- Simons LA, Sullivan D, Simons J, Celermajer DS (1998a) Effects of atorvastatin monotherapy and simvastatin plus cholestyramine on arterial endothelial function in patients with severe primary hypercholesterolaemia. *Atherosclerosis* 137:197-203.
- Simons M, P K, B DS, Beyrether K, CG D, K S (1998b) Cholesterol depletion inhibits the generation beta-amyloid in hippocampal neurons. *Proc Natl Acad Sci USA* 95:6460-6464.
- Sisodia SS, Price DL (1995) Role of the beta-amyloid protein in Alzheimer's disease. *FASEB J* 9:366-370.
- Siwik DA, Kuster GM, Brahmabhatt JV, Zaidi Z, Malik J, Ooi H, Ghorayeb G (2008) EMMPRIN mediates beta-adrenergic receptor-stimulated matrix metalloproteinase activity in cardiac myocytes. *J Mol Cell Cardiol* 44:210-217.
- Small DH, Mok SS, Bornstein JC (2001) Alzheimer's disease and A $\beta$  toxicity: from top to bottom. *Nature Rev Neurosci* 2:595-598.
- Smith AD, Jobst KA, Navaratnam DS, Shen ZX, Priddle JD, McDonald B, King E, Esiri MM (1991) Anomalous acetylcholinesterase in lumbar CSF in Alzheimer's disease. *Lancet* 338:1538.
- Smith DH, Nakamura M, McIntosh TK, Wang J, Rodriguez A, Chen XH, Raghupathi R, Saatman KE, Clemens J, Schmidt ML, Lee VM, Trojanowski JQ (1998) Brain trauma induces massive hippocampal neuron death linked to a surge in beta-amyloid levels in mice overexpressing mutant amyloid precursor protein. *Am J Pathol* 153:1005-1010.
- Song J, Lu YC, Yokoyama K, Rossi J, Chiu R (2004) Cyclophilin A is required for retinoic acid-induced neuronal differentiation in p19 cells. *J Biol Chem* 279:24414-24419.
- Sparks DL (1997) Coronary artery disease, hypertension, ApoE, and cholesterol: a link to Alzheimer's disease? *Ann N Y Acad Sci* 826:128-146.
- Sparks DL, Connor DJ, Browne PJ, Lopez JE, Sabbagh MN (2002) HMG-CoA reductase inhibitors (statins) in the treatment of Alzheimer's disease and why it would be ill-advise to use one that crosses the blood-brain barrier. *J Nutr Health Aging* 6:324-331.
- Sparks DL, Hunsaker JC, 3rd, Scheff SW, Kryscio RJ, Henson JL, Markesbery WR (1990) Cortical senile plaques in coronary artery disease, aging and Alzheimer's disease. *Neurobiol Aging* 11:601-607.
- Sparks DL, Scheff SW, Hunsaker III JC, Liu H, Landers T, Gross DR (1994a) Induction of Alzheimer-like  $\beta$ -Amyloid immunoreactivity in the brains of rabbits with dietary cholesterol. *Experimental Neurology* 88-94.
- Sparks DL, Scheff SW, Hunsaker JC, 3rd, Liu H, Landers T, Gross DR (1994b) Induction of Alzheimer-like beta-amyloid immunoreactivity in the brains of rabbits with dietary cholesterol. *Exp Neurol* 126:88-94.
- Spillantini MG, Murrell JR, Goedert M, Farlow M, Klug A, Ghetti B (2006) Mutations in the tau gene (MAPT) in FTDP-17: the family with Multiple System Tauopathy with Presenile Dementia (MSTD). *J Alzheimers Dis* 9:373-380.
- Spinale FG, Coker ML, Heung LJ, Bond BR, Gunasinghe HR, Etoh T, Goldberg AT, Zellner JL, Crumbley AJ (2000) A matrix metalloproteinase induction/activation system exists in the human left ventricular myocardium and is upregulated in heart failure. *Circulation* 102:1944-1949.

- Steiner H, Duff K, Capell A, Romig H, Grim MG, Lincoln S, Hardy J, Yu X, Picciano M, Fechteler K, Citron M, Kopan R, Pesold B, Keck S, Baader M, Tomita T, Iwatsubo T, Baumeister R, Haass C (1999) A loss of function mutation of presenilin-2 interferes with amyloid beta-peptide production and notch signaling. *J Biol Chem* 274:28669-28673.
- Steiner H, Winkler E, Edbauer D, Prokop S, Basset G, Yamasaki A, Kostka M, Haass C (2002) PEN-2 is an integral component of the gamma-secretase complex required for coordinated expression of presenilin and nicastrin. *J Biol Chem* 277:39062-39065.
- Stevens JC, Beck J, Lukic A, Ryan N, Abbs S, Collinge J, Fox NC, Mead S (2011) Familial Alzheimer's disease and inherited prion disease in the UK are poorly ascertained. *J Neurol Neurosurg Psychiatry* 82:1054-1057.
- Strittmatter WJ, Saunders AM, Schmechel D, Pericak-Vance M, Enghild J, Salvesen GS, Roses AD (1993) Apolipoprotein E: high-avidity binding to beta-amyloid and increased frequency of type 4 allele in late-onset familial Alzheimer disease. *Proc Natl Acad Sci U S A* 90:1977-1981.
- Stromberg K, Hansson EM, Laudon H, Bergstedt S, Naslund J, Lundkvist J, Lendahl U (2005) gamma-Secretase complexes containing N- and C-terminal fragments of different presenilin origin retain normal gamma-secretase activity. *J Neurochem* 95:880-890.
- Sun J, Hemler ME (2001) Regulation of MMP-1 and MMP-2 production through CD147/extracellular matrix metalloproteinase inducer interactions. *Cancer Res* 61:2276-2281.
- Takami M, Nagashima Y, Sano Y, Ishihara S, Morishima-Kawashima M, Funamoto S, Ihara Y (2009) gamma-Secretase: successive tripeptide and tetrapeptide release from the transmembrane domain of beta-carboxyl terminal fragment. *J Neurosci* 29:13042-13052.
- Takasugi N, Tomita T, Hayashi I, Tsuruoka M, Niimura M, Takahashi Y, Thinakaran G, Iwatsubo T (2003) The role of presenilin cofactors in the gamma-secretase complex. *Nature* 422:438-441.
- Tang Y, Kesavan P, Nakada MT, Yan L (2004) Tumor-stroma interaction: positive feedback regulation of extracellular matrix metalloproteinase inducer (EMMPRIN) expression and matrix metalloproteinase-dependent generation of soluble EMMPRIN. *Mol Cancer Res* 2:73-80.
- Tang Y, Nakada MT, Kesavan P, McCabe F, Millar H, Rafferty P, Bugelski P, Yan L (2005) Extracellular matrix metalloproteinase inducer stimulates tumor angiogenesis by elevating vascular endothelial cell growth factor and matrix metalloproteinases. *Cancer Res* 65:3193-3199.
- Taylor H, Fraser T, Miners JS, Kehoe PG, Love S (2010) Oxidative balance in Alzheimer's disease: relationship to APOE, Braak tangle stage, and the concentrations of soluble and insoluble amyloid-beta. *J Alzheimers Dis* 22:1363-1373.
- Tegeder I, Schumacher A, John S, Geiger H, Geisslinger G, Bang H, Brune K (1997) Elevated serum cyclophilin levels in patients with severe sepsis. *J Clin Immunol* 17:380-386.
- Thinakaran G, Borchelt DR, Lee MK, Slunt HH, Spitzer L, Kim G, Ratovitsky T, Davenport F, Nordstedt C, Seeger M, Hardy J, Levey AI, Gandy SE, Jenkins NA, Copeland NG, Price DL, Sisodia SS (1996) Endoproteolysis of presenilin 1 and accumulation of processed derivatives in vivo. *Neuron* 17:181-190.
- Thirumangalakudi L, Prakasam A, Zhang R, Bimonte-Nelson H, Sambamurti K, Kindy MS, Bhat NR (2008) High cholesterol-induced neuroinflammation and amyloid

- precursor protein processing correlate with loss of working memory in mice. *J Neurochem* 106:475-485.
- Tint GS, Irons M, Elias ER, Batta AK, Frieden R, Chen TS, Salen G (1994) Defective cholesterol biosynthesis associated with the Smith-Lemli-Opitz syndrome. *N Engl J Med* 330:107-113.
- Tomita T, Nakase T, Kaneko M, Shi K, Takahi K, Ochi T, Yoshikawa H (2002) Expression of extracellular matrix metalloproteinase inducer and enhancement of the production of matrix metalloproteinases in rheumatoid arthritis. *Arthritis Rheum* 46:373-378.
- Torreggiani M, Liu H, Wu J, Zheng F, Cai W, Striker G, Vlassara H (2009) Advanced glycation end product receptor-1 transgenic mice are resistant to inflammation, oxidative stress, and post-injury intimal hyperplasia. *Am J Pathol* 175:1722-1732.
- Trachtenberg A, Pushkarsky T, Heine S, Constant S, Brichacek B, Bukrinsky M (2011) The level of CD147 expression correlates with cyclophilin-induced signalling and chemotaxis. *BMC Res Notes* 4:396.
- Trzeciak WH, Simpson ER, Scallen TJ, Vahouny GV, Waterman MR (1987) Studies on the synthesis of sterol carrier protein-2 in rat adrenocortical cells in monolayer culture. Regulation by ACTH and dibutyryl cyclic 3',5'-AMP. *J Biol Chem* 262:3713-3717.
- Turner PR, O'Connor K, Tate WP, Abraham WC (2003) Roles of amyloid precursor protein and its fragments in regulating neural activity, plasticity and memory. *Prog Neurobiol* 70:1-32.
- Urban S, Lee JR, Freeman M (2001) Drosophila rhomboid-1 defines a family of putative intramembrane serine proteases. *Cell* 107:173-182.
- Utermann G, Langenbeck U, Beisiegel U, Weber W (1980) Genetics of the apolipoprotein E system in man. *Am J Hum Genet* 32:339-347.
- van Heusden GP, Bos K, Raetz CR, Wirtz KW (1990) Chinese hamster ovary cells deficient in peroxisomes lack the nonspecific lipid transfer protein (sterol carrier protein 2). *J Biol Chem* 265:4105-4110.
- Varadaraj K, Skinner DM (1994) Cytoplasmic localization of transcripts of a complex G+C-rich crab satellite DNA. *Chromosoma* 103:423-431.
- Vassar R (2004) BACE1: the beta-secretase enzyme in Alzheimer's disease. *J Mol Neurosci* 23:105-114.
- Vassar R, Bennett BD, Babu-Khan S, Kahn S, Mendiaz EA, Denis P, Teplow DB, Ross S, Amarante P, Loeloff R, Luo Y, Fisher S, Fuller J, Edenson S, Lile J, Jarosinski MA, Biere AL, Curran E, Burgess T, Louis JC, Collins F, Treanor J, Rogers G, Citron M (1999) Beta-secretase cleavage of Alzheimer's amyloid precursor protein by the transmembrane aspartic protease BACE. *Science* 286:735-741.
- Vaya J, Schipper HM (2007) Oxysterols, cholesterol homeostasis, and Alzheimer disease. *J Neurochem* 102:1727-1737.
- Verdier Y, Zarandi M, Penke B (2004) Amyloid beta-peptide interactions with neuronal and glial cell plasma membrane: binding sites and implications for Alzheimer's disease. *J Pept Sci* 10:229-248.
- Verdile G, Fuller S, Atwood CS, Laws SM, Gandy SE, Martins RN (2004) The role of beta amyloid in Alzheimer's disease: still a cause of everything or the only one who got caught? *Pharmacol Res* 50:397-409.
- Verdile G, Gandy SE, Martins RN (2007) The role of presenilin and its interacting proteins in the biogenesis of Alzheimer's beta amyloid. *Neurochem Res* 32:609-623.

- Vetrivel KS, Gong P, Bowen JW, Cheng H, Chen Y, Carter M, Nguyen PD, Placanica L, Wieland FT, Li YM, Kounnas MZ, Thinakaran G (2007) Dual roles of the transmembrane protein p23/TMP21 in the modulation of amyloid precursor protein metabolism. *Mol Neurodegener* 2:4.
- Vetrivel KS, Kodam A, Gong P, Chen Y, Parent AT, Kar S, Thinakaran G (2008a) Localization and regional distribution of p23/TMP21 in the brain. *Neurobiol Dis* 32:37-49.
- Vetrivel KS, Zhang X, Meckler X, Cheng H, Lee S, Gong P, Lopes KO, Chen Y, Iwata N, Yin KJ, Lee JM, Parent AT, Saido TC, Li YM, Sisodia SS, Thinakaran G (2008b) Evidence that CD147 modulation of beta-amyloid (A $\beta$ ) levels is mediated by extracellular degradation of secreted A $\beta$ . *J Biol Chem* 283:19489-19498.
- Wahrle S, Das P, Nyborg AC, McLendon C, Shoji M, Kawarabayashi T, Younkin LH, Younkin SG, Golde TE (2002) Cholesterol-dependent gamma-secretase activity in buoyant cholesterol-rich membrane microdomains. *Neurobiol Dis* 9:11-23.
- Waldow T, Witt W, Buzin A, Ulmer A, Matschke K (2009) Prevention of ischemia/reperfusion-induced accumulation of matrix metalloproteinases in rat lung by preconditioning with nitric oxide. *J Surg Res* 152:198-208.
- Wang DS, Iwata N, Hama E, Saido TC, Dickson DW (2003) Oxidized neprilysin in aging and Alzheimer's disease brains. *Biochem Biophys Res Commun* 310:236-241.
- Wang X, Sato R, Brown MS, Hua X, Goldstein JL (1994) SREBP-1, a membrane-bound transcription factor released by sterol-regulated proteolysis. *Cell* 77:53-62.
- Wei M, Deng J, Feng K, Yu B, Chen Y (2010) Universal method facilitating the amplification of extremely GC-rich DNA fragments from genomic DNA. *Anal Chem* 82:6303-6307.
- Wei W, Norton DD, Wang X, Kusiak JW (2002) A $\beta$  17-42 in Alzheimer's disease activates JNK and caspase-8 leading to neuronal apoptosis. *Brain* 125:2036-2043.
- Weisgraber KH, Innerarity TL, Mahley RW (1982) Abnormal lipoprotein receptor-binding activity of the human E apoprotein due to cysteine-arginine interchange at a single site. *J Biol Chem* 257:2518-2521.
- Weller RO, Massey A, Kuo YM, Roher AE (2000) Cerebral amyloid angiopathy: accumulation of A beta in interstitial fluid drainage pathways in Alzheimer's disease. *Ann N Y Acad Sci* 903:110-117.
- Whitehouse PJ, Price DL, Struble RG, Clark AW, Coyle JT, Delon MR, Whitehouse PJ (1982) Alzheimer's disease and senile dementia: loss of neurons in the basal forebrain. *Science* 215:1237-1242.
- Wilhelmus MM, Otte-Holler I, Davis J, Van Nostrand WE, de Waal RM, Verbeek MM (2005) Apolipoprotein E genotype regulates amyloid-beta cytotoxicity. *J Neurosci* 25:3621-3627.
- Wilson MC, Meredith D, Fox JE, Manoharan C, Davies AJ, Halestrap AP (2005) Basigin (CD147) is the target for organomercurial inhibition of monocarboxylate transporter isoforms 1 and 4: the ancillary protein for the insensitive MCT2 is EMBIGIN (gp70). *J Biol Chem* 280:27213-27221.
- Wilson MC, Meredith D, Halestrap AP (2002) Fluorescence resonance energy transfer studies on the interaction between the lactate transporter MCT1 and CD147 provide information on the topology and stoichiometry of the complex in situ. *J Biol Chem* 277:3666-3672.
- Winkler DA (2008) Network models in drug discovery and regenerative medicine. *Biotechnol Annu Rev* 14:143-170.

- Winkler E, Hobson S, Fukumori A, Dumpelfeld B, Luebbbers T, Baumann K, Haass C, Hopf C, Steiner H (2009) Purification, pharmacological modulation, and biochemical characterization of interactors of endogenous human gamma-secretase. *Biochemistry* 48:1183-1197.
- Wirtz KW (1997) Phospholipid transfer proteins revisited. *Biochem J* 324 ( Pt 2):353-360.
- Wolfe MS (2007) When loss is gain: reduced presenilin proteolytic function leads to increased Abeta42/Abeta40. *Talking Point on the role of presenilin mutations in Alzheimer disease. EMBO Rep* 8:136-140.
- Wolfe MS, Xia W, Ostaszewski BL, Diehl TS, Kimberly WT, Selkoe DJ (1999) Two transmembrane aspartates in presenilin-1 required for presenilin endoproteolysis and gamma-secretase activity. *Nature* 398:513-517.
- Wu CW, Liao PC, Lin C, Kuo CJ, Chen ST, Chen HI, Kuo YM (2003) Brain region-dependent increases in beta-amyloid and apolipoprotein E levels in hypercholesterolemic rabbits. *J Neural Transm* 110:641-649.
- Wu HY, Hudry E, Hashimoto T, Kuchibhotla K, Rozkalne A, Fan Z, Spires-Jones T, Xie H, Arbel-Ornath M, Grosskreutz CL, Bacskai BJ, Hyman BT (2010) Amyloid beta induces the morphological neurodegenerative triad of spine loss, dendritic simplification, and neuritic dystrophies through calcineurin activation. *J Neurosci* 30:2636-2649.
- Wu Y, Zhou X, Zheng PS (2011) Involvement of CD147 isoform4 in the proliferation of SiHa cells: a possible molecular mechanism of cervical cancer. *Oncol Rep* 26:717-724.
- Xia W, Zhang J, Kholodenko D, Citron M, Podlisny MB, Teplov DB, Haass C, Seubert P, Koo EH, Selkoe DJ (1997) Enhanced production and oligomerization of the 42-residue amyloid beta-protein by Chinese hamster ovary cells stably expressing mutant presenilins. *J Biol Chem* 272:7977-7982.
- Xie M, Jiao T, Chen Y, Xu C, Li J, Jiang X, Zhang F (2010) EMMPRIN (basigin/CD147) is involved in the morphogenesis of tooth germ in mouse molars. *Histochem Cell Biol* 133:585-594.
- Xu Q, Leiva MC, Fischkoff SA, Handschumacher RE, Lyttle CR (1992) Leukocyte chemotactic activity of cyclophilin. *J Biol Chem* 267:11968-11971.
- Yaar M, Zhai S, Pilch PF, Doyle SM, Eisenhauer PB, Fine RE, Gilchrist BA (1997) Binding of beta-amyloid to the p75 neurotrophin receptor induces apoptosis. A possible mechanism for Alzheimer's disease. *J Clin Invest* 100:2333-2340.
- Yamamoto R, Kallen CB, Babalola GO, Rennert H, Billheimer JT, Strauss JF, 3rd (1991) Cloning and expression of a cDNA encoding human sterol carrier protein 2. *Proc Natl Acad Sci U S A* 88:463-467.
- Yang AJ, Knauer M, Burdick DA, Glabe C (1995) Intracellular A beta 1-42 aggregates stimulate the accumulation of stable, insoluble amyloidogenic fragments of the amyloid precursor protein in transfected cells. *J Biol Chem* 270:14786-14792.
- Yang F, Chen X, Su J (2008) [The role of CD147 in the proliferation, activation and chemotaxis of Jurkat cell induced by cyclophilin A]. *Zhonghua Xue Ye Xue Za Zhi* 29:793-796.
- Yao PM, Tabas I (2001) Free cholesterol loading of macrophages is associated with widespread mitochondrial dysfunction and activation of the mitochondrial apoptosis pathway. *J Biol Chem* 276:42468-42476.
- Yarden Y, Sliwkowski MX (2001) Untangling the ErbB signalling network. *Nat Rev Mol Cell Biol* 2:127-137.
- Yelin R, Dahary D, Sorek R, Levanon EY, Goldstein O, Shoshan A, Diber A, Biton S, Tamir Y, Khosravi R, Nemzer S, Pinner E, Walach S, Bernstein J, Savitsky K,

- Rotman G (2003) Widespread occurrence of antisense transcription in the human genome. *Nat Biotechnol* 21:379-386.
- Ying L, Gervay-Hague J (2005) One-bead-one-inhibitor-one-substrate screening of neuraminidase activity. *Chembiochem* 6:1857-1865.
- Yonemura Y, Futai E, Yagishita S, Suo S, Tomita T, Iwatsubo T, Ishiura S (2011) Comparison of presenilin 1 and presenilin 2 gamma-secretase activities using a yeast reconstitution system. *J Biol Chem* 286:44569-44575.
- Yoon YW, Kwon HM, Hwang KC, Choi EY, Hong BK, Kim D, Kim HS, Cho SH, Song KS, Sangiorgi G (2005) Upstream regulation of matrix metalloproteinase by EMMPRIN; extracellular matrix metalloproteinase inducer in advanced atherosclerotic plaque. *Atherosclerosis* 180:37-44.
- Yu G, Chen F, Levesque G, Nishimura M, Zhang DM, Levesque L, Rogaeva E, Xu D, Liang Y, Duthie M, St George-Hyslop PH, Fraser PE (1998) The presenilin 1 protein is a component of a high molecular weight intracellular complex that contains beta-catenin. *J Biol Chem* 273:16470-16475.
- Yu G, Nishimura M, Arawaka S, Levitan D, Zhang L, Tandon A, Song YQ, Rogaeva E, Chen F, Kawarai T, Supala A, Levesque L, Yu H, Yang DS, Holmes E, Milman P, Liang Y, Zhang DM, Xu DH, Sato C, Rogaev E, Smith M, Janus C, Zhang Y, Aebbersold R, Farrer LS, Sorbi S, Bruni A, Fraser P, St George-Hyslop P (2000) Nicastrin modulates presenilin-mediated notch/glp-1 signal transduction and betaAPP processing. *Nature* 407:48-54.
- Yue HH, Leng N, Wu ZB, Li HM, Li XY, Zhu P (2009) Expression of CD147 on phorbol-12-myristate-13-acetate (PMA)-treated U937 cells differentiating into foam cells. *Arch Biochem Biophys* 485:30-34.
- Yurchenko V, O'Connor M, Dai WW, Guo H, Toole B, Sherry B, Bukrinsky M (2001) CD147 is a signaling receptor for cyclophilin B. *Biochem Biophys Res Commun* 288:786-788.
- Yurchenko V, Pushkarsky T, Li JH, Dai WW, Sherry B, Bukrinsky M (2005) Regulation of CD147 cell surface expression: involvement of the proline residue in the CD147 transmembrane domain. *J Biol Chem* 280:17013-17019.
- Yurchenko V, Zybarth G, O'Connor M, Dai WW, Franchin G, Hao T, Guo H, Hung HC, Toole B, Gallay P, Sherry B, Bukrinsky M (2002) Active site residues of cyclophilin A are crucial for its signaling activity via CD147. *J Biol Chem* 277:22959-22965.
- Zanlungo S, Amigo L, Mendoza H, Miquel JF, Vio C, Glick JM, Rodriguez A, Kozarsky K, Quinones V, Rigotti A, Nervi F (2000) Sterol carrier protein 2 gene transfer changes lipid metabolism and enterohepatic sterol circulation in mice. *Gastroenterology* 119:1708-1719.
- Zeng HZ, Qu YQ, Liang AB, Deng AM, Zhang WJ, Xiu B, Wang H (2011) Expression of CD147 in advanced non-small cell lung cancer correlated with cisplatin-based chemotherapy resistance. *Neoplasma* 58:449-454.
- Zeng M, Smith SK, Siegel F, Shi Z, Van Kampen KR, Elmets CA, Tang DC (2001) AdEasy system made easier by selecting the viral backbone plasmid preceding homologous recombination. *Biotechniques* 31:260-262.
- Zhang C, Browne A, Kim DY, Tanzi RE (2010a) Familial Alzheimer's disease mutations in presenilin 1 do not alter levels of the secreted amyloid-beta protein precursor generated by beta-secretase cleavage. *Curr Alzheimer Res* 7:21-26.
- Zhang L, Yu H, Zhao X, Lin X, Tan C, Cao G, Wang Z (2010b) Neuroprotective effects of salidroside against beta-amyloid-induced oxidative stress in SH-SY5Y human neuroblastoma cells. *Neurochem Int* 57:547-555.
- Zhang YW, Luo WJ, Wang H, Lin P, Vetrivel KS, Liao F, Li F, Wong PC, Farquhar MG, Thinakaran G, Xu H (2005) Nicastrin is critical for stability and trafficking

- but not association of other presenilin/gamma-secretase components. *J Biol Chem* 280:17020-17026.
- Zhou Q, Homma KJ, Poo MM (2004) Shrinkage of dendritic spines associated with long-term depression of hippocampal synapses. *Neuron* 44:749-757.
- Zhou S, Zhou H, Walian PJ, Jap BK (2005) CD147 is a regulatory subunit of the gamma-secretase complex in Alzheimer's disease amyloid beta-peptide production. *Proc Natl Acad Sci U S A* 102:7499-7504.
- Zhou S, Zhou H, Walian PJ, Jap BK (2006) The discovery and role of CD147 as a subunit of gamma-secretase complex. *Drug News Perspect* 19:133-138.
- Zhou S, Zhou H, Walian PJ, Jap BK (2007) Regulation of gamma-secretase activity in Alzheimer's disease. *Biochemistry* 46:2553-2563.
- Zhu P, Ding J, Zhou J, Dong WJ, Fan CM, Chen ZN (2005) Expression of CD147 on monocytes/macrophages in rheumatoid arthritis: its potential role in monocyte accumulation and matrix metalloproteinase production. *Arthritis Res Ther* 7:R1023-1033.
- Zhu P, Lu N, Shi ZG, Zhou J, Wu ZB, Yang Y, Ding J, Chen ZN (2006) CD147 overexpression on synoviocytes in rheumatoid arthritis enhances matrix metalloproteinase production and invasiveness of synoviocytes. *Arthritis Res Ther* 8:R44.
- Zhu Y, Yang GY, Ahlemeyer B, Pang L, Che XM, Culmsee C, Klumpp S, Kriegstein J (2002) Transforming growth factor-beta 1 increases bad phosphorylation and protects neurons against damage. *J Neurosci* 22:3898-3909.